Biological Characterisation of Tissue-Engineered Vascular Grafts

Paula Engbers-Buijtenhuijs

Druk: PrintPartners Ipskamp, Enschede, The Netherlands, 2005.

Omslag: Immuno fluorescentie microscopie van actine filamenten in gladde spiercellen

Ontwerp: Richard Rieksen* / Paula Engbers

* Medisch Fotograaf, Laboratorium voor Pathologie Oost Nederland, Enschede

Biological Characterisation of Tissue-Engineered Vascular Grafts

ISBN: 90-365-2163-7

BIOLOGICAL CHARACTERISATION

OF TISSUE-ENGINEERED

VASCULAR GRAFTS

PROEFSCHRIFT

ter verkrijging van
de graad van doctor aan de Universiteit Twente,
op gezag van de rector magnificus,
prof. dr. W.H.M. Zijm,
volgens besluit van het College voor Promoties
in het openbaar te verdedigen
op vrijdag 1 april 2005 om 13.15 uur

door

Paula Engbers-Buijtenhuijs

geboren op 4 februari 1977

te Ermelo

Dit proefschrift is goedgekeurd door:

Promotoren:	prof. dr. I. Vermes
	prof. dr. J. Feijen
Assistent-promotor:	dr. A.A. Poot

De weg is het doel

J.O. Koss

Members of the committee:

Chairman:	prof. dr. A. Bliek	University of Twente
Promotors:	prof. dr. I. Vermes	University of Twente / Medisch Spectrum Twente
	prof. dr. J. Feijen	University of Twente
Assistant promotor:	dr. A.A. Poot	University of Twente
Referent:	dr. R.H. Geelkerken	Medisch Spectrum Twente
Members:	prof. dr. C.A. van Blitterswijk	University of Twente
	prof. dr. W. Kruijer	University of Twente
	prof. dr. C. Haanen	UMC St. Radboud, Nijmegen
	prof. dr. V.W.M. van Hinsbergh	VU Amsterdam / ICARVU

The study described in this thesis was supported by Medisch Spectrum Twente, Hospital Group

This publication was sponsored by:

Medisch Spectrum Twente, Hospital Group
Dutch Society for Biomaterials and Tissue Engineering (NBTE)
Beckman Coulter Nederland B.V.

Biological Characterisation of Vascular Grafts, P. Engbers-Buijtenhuijs
Thesis University of Twente, Enschede, The Netherlands
With references - With summary in English and Dutch

Table of Contents

List of Abbreviations

AIF	apoptosis-inducing factor
Apaf-1	apoptotic protease activating factor
α-SMA	alpha-smooth muscle actin
BMCs	bone marrow cells
BSA	bovine serum albumin
CARDs	caspase-associated recruitment domains
Caspases	cysteine dependent aspartic acid cleaving proteases
CHX	cycloheximide
CPT	camptothecin
CV	coefficients of variation
d	day(s)
DDs	death domains
DEDs	death effector domains
DiOC6	3,3’-dihexyloxacarbocyanine iodide
DMEM	Dulbecco’s modified Eagle’s Medium
DTT	dithiothreitol
ECM	extra-cellular matrix
ECs	endothelial cells
EDC	N-(3-dimethylaminopropyl)-N'-ethylcarbodiimide hydrochloride
EDTA	ethylene diamine tetra acetic acid
ELISA	enzyme-linked immuno sorbent assay
eNOS	endothelial nitric oxide synthase
e-PTFE	expanded polytetrafluoroethylene
ER	endoplasmic reticulum
FasR	Fas receptor
FLICA	fluorochrome-labelled inhibitor of caspases
FSC	forward scatter
GAPDH	glyceraldehyde phosphate dehydrogenase
g-TCPS	gelatin-coated tissue culture poly(styrene)
h	hour(s)
HAc	acetic acid
HEPES	N-[2-hydroxyethyl] piperazide-N’-[2-ethanesulphonic acid]
HL60	human promyelocytic leukemic cells
HUVEC	human umbilical vein endothelial cells
IAP	inhibitor of apoptosis proteins
ID	inner diameter
J230	Jeffamine230, poly(propylene glycol)-bis-(2-aminopropyl ether)

mAb	monoclonal antibody
min	minute(s)
M-MLV	Moloney Murine Leukemia Virus
NHS	N-hydroxysuccinimide
OD	outer diameter
PBGD	porphobilinogen deaminase
PBS	phosphate buffered saline
PDGF	platelet derived growth factor
PGA	polyglycolic acid
PI	propidium iodide
PS	phosphatidyl serine
RAM-FITC	rabbit anti mouse fluoresceine isothiocyanate
RT	room temperature
RT-PCR	reversed transcriptase polymerase chain reaction
s	second(s)
SEM	standard error of the mean
SMCs	smooth muscle cells
SSC	side scatter
TE	tissue-engineered
TGF-β	transforming growth factor-β
TNBS	2, 4, 6-trinitrobenzene sulphonic acid
TNF-α	tumor necrosis factor-α
TNFR	tumor necrosis factor receptor
tTG	tissue transglutaminase
tPA	human tissue plasminogen activator
TUNEL	terminal deoxynucleotidyl transferase (TdT) mediated dUTP-biotin nick end labelling
wk(s)	week(s)
y	year(s)

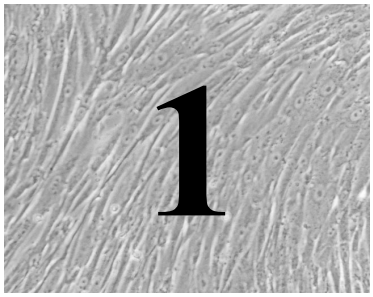

1

General Introduction and Objectives

Introduction

Atherosclerosis and related vascular diseases are the major causes of morbidity and mortality in western society and are characterised by progressive narrowing and occlusion of blood vessels [1]. Surgical treatment of atherosclerosis involves the replacement of a damaged blood vessel or inserting a vascular stent. For large-diameter applications (inner diameter > 6 mm), synthetic vascular prostheses such as Dacron® and Teflon® grafts [2] are commonly used in vascular surgery. These grafts remain patent for more than 10 yrs after implantation. In contrast, small-diameter synthetic grafts (inner diameter < 6 mm) placed in low-flow vascular regions, fail rapidly due to early thrombotic occlusion. Currently, autologous veins and arteries are used for small-diameter vascular reconstructions [3]. The use of these autologous blood vessels has certain limitations such as limited availability of suitable grafts and failure of vein grafts when exposed to increased flow and pressure in the arterial circulation [3]. Research to produce functional small-diameter blood vessel replacements has been directed to the field of tissue engineering. Vascular tissue engineering deals with preparing functional small-diameter blood vessels *in vitro* by applying the principles of engineering and life sciences. Most strategies aim at creating vascular grafts by closely mimicking the three-layered structure of a natural blood vessel [4]. The middle layer of a natural blood vessel, the media, is very important in terms of mechanical properties as it contains predominantly smooth muscle cells (SMCs), collagen and elastin fibres. Several research groups have reported on the production of a tissue-engineered (TE) blood vessel by seeding and culturing of vascular cells in biodegradable scaffolds [5-7]. The phenotype of SMCs (cell proliferation, differentiation, apoptosis and patterns of gene expression of extracellular matrix proteins) cultured in three-dimensional engineered scaffolds is dependent on the chemistry of the scaffold material, the presence of growth factors and cytokines and the culture conditions [8, 9]. Pulsatile flow conditions mimicking the *in vivo* conditions of human arteries promote both the development of TE constructs with appropriate mechanical strength [6] and modulation of appropriate cellular functions [10].

Objective

The objective of this study is to produce a TE autologous vascular prosthesis, exclusively composed of biological materials and vascular cells, which is blood-compatible and can be used as a graft in vascular surgery especially for small-diameter applications. Our approach to make such an artificial blood vessel is that it should consist of the three-layered structure of a natural blood vessel; the intima, the media and the adventitia. The first step towards tissue

engineering of such a small-diameter vascular graft is to obtain the media of the artificial blood vessel by seeding and culturing of human vascular SMCs in biodegradable tubular scaffolds composed of insoluble collagen and insoluble elastin. To enhance tissue formation, culturing of the cell-seeded scaffolds is carried out in a bioreactor in which pulsatile flow conditions and arterial pressures can be simulated. The spatial SMC distribution over the porous scaffolds and the phenotype of the cells present in the scaffolds are investigated in order to optimise the TE construct.

Outline of this thesis

In this thesis, seeding and culturing of human vascular SMCs in porous scaffolds composed of insoluble collagen and insoluble elastin and the biological characterisation of the TE constructs are described.

Chapter 2 gives a literature overview of SMC functions and the role of SMCs in the development of vascular diseases. The use of vascular prostheses, the field of tissue engineering of small-diameter blood vessels and the requirements for vascular grafts are discussed. The balance between cell proliferation and apoptosis mediates tissue homeostasis in natural viable tissues as well as functional TE constructs [8]. Therefore, different methods to evaluate the balance between cell proliferation and apoptosis of adherent cell types are described, with emphasis on the use of these methods for evaluation of tissue homeostasis in TE constructs.

Chapter 3 deals with the first steps towards tissue engineering of small-diameter blood vessels. SMCs were isolated from human umbilical veins and the identity and purity of the obtained cultures were analysed by staining the cells with specific monoclonal antibodies. SMCs were then seeded on flat porous scaffolds composed of insoluble collagen and insoluble elastin. In order to improve the stability of the scaffolds, they were crosslinked by two different methods. Water-soluble N-(3-dimetylaminopropyl)-N'-ethylcarbodiimide hydrochloride (EDC) in combination with N-hydroxysuccinimide (NHS) or poly(propylene glycol)-bis-(2-aminopropyl ether) (Jeffamine 230, J230) in the presence of EDC/NHS were used for this purpose. The cells were subsequently cultured under static conditions for different periods of time and their ability to grow and proliferate on/in these scaffolds was investigated.

Cell seeding is a critical step in the process to produce an adequate TE construct. In *chapter 4* the effects of several cell seeding procedures on the spatial SMC distribution in the porous scaffolds composed of insoluble collagen and insoluble elastin are presented. The aim was to

produce a homogeneous structure of collagen and elastin fibres interspersed with SMCs. In addition, effects of crosslinking of the scaffolds with EDC/NHS or J230/EDC/NHS on the spatial cell distribution were investigated.

A new method to analyse markers of both cell proliferation and apoptosis in one single assay to follow growth behaviour of cultured cells is described in *chapter 5*. mRNA expressions of cyclin E (marker of proliferation) and tissue transglutaminase (tTG, marker of apoptosis) were quantified by a real-time reversed transcriptase polymerase chain reaction. The aim was to develop a suitable method to evaluate tissue homeostasis in TE constructs.

Chapter 6 deals with the use of fluorochrome-labelled inhibitor of caspases (FLICA) and propidium iodide (PI) to measure the amount of cells present in different stages of the apoptotic cascade and to evaluate cell death kinetics. This technique was used to measure the rate of apoptotic cell death in cultured cells in suspension compared to cultured adherent cells.

A new and sensitive method to analyse apoptosis induced by loss of contact of adherent cells with the extracellular matrix (a phenomenon designated 'anoikis' or homelessness) is described in c*hapter 7.* A time resolved fluorometric assay with Europium-labelled Annexin V was developed for this purpose.

The development of a pulsatile flow bioreactor for tissue engineering of small-diameter blood vessels is described in *chapter 8*. In this system, pulsatile flow and fluctuations of pressure inside the cultured vessels, simulating conditions of the human carotid artery in terms of wall shear rate, pulsatile flow and arterial pressure, were used to stimulate tissue formation. The flow dynamics of the system were characterized and compared to those occurring *in vivo.*

The development of a TE construct mimicking the structure of a natural blood vessel using the pulsatile flow bioreactor is described in *chapter 9*. SMCs were seeded and cultured in porous tubular scaffolds composed of insoluble collagen and insoluble elastin under dynamic conditions. SMC proliferation, distribution of SMCs over the scaffolds and collagen and elastin gene expression were analysed. In addition, effects of crosslinking of the scaffolds with EDC/NHS or J230/EDC/NHS on cell numbers and spatial cell distribution were investigated.

Chapter 10 concludes this thesis with a summary, discussion and future perspectives. Most of the work described in this thesis has been published [11, 12, 13] or will be submitted for publication [14-16].

References

1. Libby, P. Inflammation in atherosclerosis. Nature 2002; 420: 868-874.
2. Faries, P.L., LoGerfo, F.W., Arora, S., Hook, S., Pulling, M.C., Akbari, C.M., Campbell, D.M., and Pomposelli, Jr.R.G. A comparative study of alternative conduits for lower extremity revascularization: all-autologous conduit versus prosthetic grafts. J.Vasc.Surg 2000; 32: 1080-1090.
3. Bos, G.W., Poot, A.A., Beugeling, T., van Aken, W.G., and Feijen, J. Small-diameter vascular graft prostheses: current status. Arch.Physiol Biochem. 1998; 106: 100-115.
4. Langer, R. and Vacanti, J.P. Tissue Engineering. Science 1993; 260: 920-926.
5. L'Heureux, N., Paquet, S., Labbe, R., Germain, L., and Auger, F.A. A completely biological tissue-engineered human blood vessel. FASEB J. 1998; 12: 47-56.
6. Niklason, L.E., Gao, J., Abbott, W.M., Hirschi, K.K., Houser, S., Marini, R., and Langer, R. Functional arteries grown in vitro. Science 1999; 284: 489-493.
7. Watanabe, M., Shin'oka, T., Tohyama, S., Hibino, N., Konuma, T., Matsumura, G., Kosaka, Y., Ishida, T., Imai, Y., Yamakawa, M., Ikada, Y., and Morita, S. Tissue-engineered vascular autograft: inferior vena cava replacement in a dog model. Tissue Eng. 2001; 7: 429-439.
8. Wendt, D., Marsano, A., Jakob, M., Heberer, M., and Martin, I. Oscillating perfusion of cell suspensions through three-dimensional scaffolds enhances cell seeding efficiency and uniformity. Biotechnol.Bioeng. 2003; 84: 205-214.
9. Martin, I., Wendt, D., and Heberer, M. The role of bioreactors in tissue engineering. Trends Biotechnol. 2004; 22: 80-86.
10. Seliktar, D., Black, R.A., Vito, R.P., and Nerem, R.M. Dynamic mechanical conditioning of collagen-gel blood vessel constructs induces remodeling in vitro. Ann.Biomed.Eng 2000; 28: 351-362.
11. Buijtenhuijs, P., Buttafoco, L., Poot, A.A., Daamen, W.F., van Kuppevelt, T.H., Dijkstra, P.J., de Vos, R.A.I., Sterk, L.M.Th., Geelkerken, R.H., Feijen, J., and Vermes, I. Tissue engineering of blood vessels: Characterisation of smooth muscle cells for culturing on collagen and elastin based scaffolds. Biotechnol.Appl.Biochem. 2004; 39: 141-149.
12. Wolbers, F., Buijtenhuijs, P., Haanen, C., and Vermes, I. Apoptotic cell death kinetics in vitro depend on the cell types and the inducers used. Apoptosis 2004; 9: 385-392.
13. Engbers-Buijtenhuijs, P., Kamphuis, M., van der Sluijs Veer, G., Haanen, C., Poot, A.A., Feijen, J., and Vermes, I. A novel time resolved fluorometric assay of anoikis using europium-labelled annexin V in cultured adherent cells. Apoptosis 2005; 10: 429-437.
14. Engbers-Buijtenhuijs, P., Buttafoco, L., Poot, A.A., Geelkerken, R.H., Feijen, J., and Vermes, I. Analysis of the balance between proliferation and apoptosis of cultured vascular smooth muscle cells for tissue engineering applications. Tissue Eng. 2005; submitted.
15. Buttafoco, L., Engbers-Buijtenhuijs, P., Poot, A.A., Dijkstra, P.J., Vermes, I., and Feijen, J. Development of a bioreactor for tissue engineering of small-diameter blood vessels: Design of a pulsatile flow system. Thesis University of Twente, chapter 6, The Netherlands 2005.
16. Engbers-Buijtenhuijs, P., Buttafoco, L., Poot, A.A., Geelkerken, R.H., de Vos, R.A.I., Sterk, L.M.T., Feijen, J., and Vermes, I. Biological characterisation of vascular grafts cultured in a bioreactor. Biomaterials 2005; submitted.

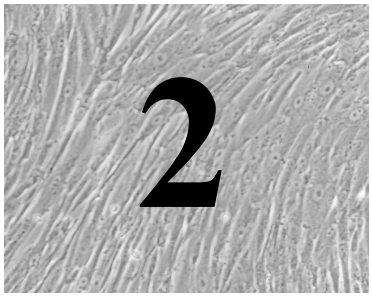

2

Tissue Engineering of Small-diameter Blood Vessels: A Literature Survey

2.1 Composition of native blood vessels

The three-layered structure

The walls of mature healthy blood vessels are composed of three distinct layers which vary in prominence in different vessel types. These layers can be distinguished by unique structural and functional properties and are named the tunica interna, the tunica media and the tunica externa (as shown in figure 1). The tunica interna or intima is the inner layer of a blood vessel and is composed of a confluent monolayer of endothelial cells (ECs). The endothelium is a selective barrier, allowing the passage of water and small ions but retaining larger molecules and blood cells to varying degrees [1]. The ECs lie on a sub-endothelial membrane, often referred to as the basement membrane or internal elastic membrane, which provides flexibility and stability for the adherent ECs. ECs are important in several physiological processes including blood coagulation, blood clotting, fibrinolysis, inflammation and complement activation by the secretion and/or activation of biologically active substances (hormones, cytokines and other (macro) molecules) or by expression of adhesion molecules on their plasma membrane. In addition, ECs secrete factors, which maintain the tone of smooth muscle and the phenotype of the smooth muscle cells (SMCs). The media is the middle layer in a blood vessel wall and is composed predominantly of SMCs reinforced by organised layers of elastic tissue and a small amount of collagen. This layer contributes to the ability of the blood vessel to resist cyclic mechanical loading by the pulsatile blood flow and changes in blood pressure. An external elastic membrane provides additional structural support to this layer. The tunica externa or adventitia, the outer layer of blood vessels, consists predominantly of fibroblasts and collagen and elastin fibres. Within the adventitia of the larger vessels, small blood vessels (the vasa vasorum) are present which penetrate into the media to supply it with blood. These small blood vessels are not seen in thinner vessel walls, which obtain their oxygen and nutrients by diffusion from the lumen. The adventitia also carries autonomic nerves, which innervate the smooth muscle of the media. Fibres of the adventitia typically blend with those of adjacent tissues, stabilising and anchoring the blood vessel [1].

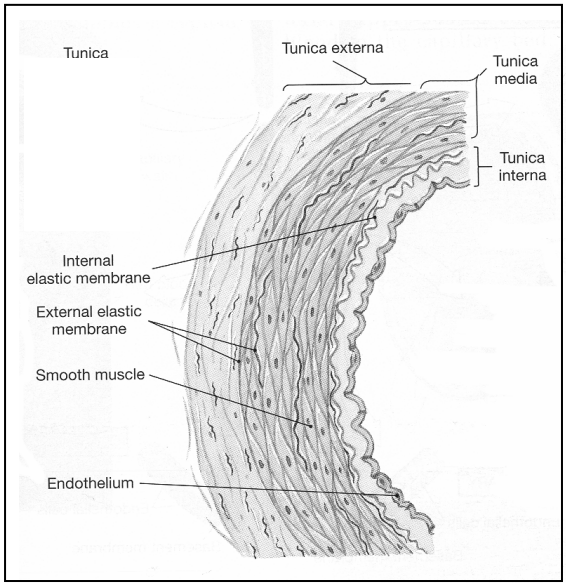

Figure 1: Schematic overview of the major histologically-distinct regions of a blood vessel wall. A monolayer lining of ECs, a multi layer of SMCs in between the internal and external elastic membrane, and a surrounding loosely organised structure form the tunica interna, tunica media and tunica externa respectively [1].

Muscular arteries

Blood from the left ventricle of the heart is pumped into large-diameter vessels with a high content of elastic tissue in their walls which smoothes the systolic pressure wave. These vessels are called the large elastic arteries and reflect the aorta and its large branches such as the common carotid, sub-clavian and renal arteries. Compared to vessel walls of the large elastic arteries, vessel walls of muscular arteries are more muscular and become proportionally more muscular with increasing distance from the heart. These vessels gradually decrease in size (to ~ 4 mm in diameter) as they branch within tissues until they form arterioles. The arterioles then branch into a system of very fine vessels termed capillaries. The media of a muscular artery is composed almost entirely of SMCs with 3 to 30 adherent cell layers dependent on the size of the vessel [1]. Because of the presence of SMCs, the muscular arteries are highly contractile. Their degree of contraction or relaxation is controlled by the autonomic nervous system as well as by endothelium-derived vaso-active substances. A few fine elastic fibres are scattered among the SMCs but are not organised into sheets as in elastic arteries. SMCs are usually arranged circumferentially perpendicular to the long axis of the vessel [2].

2.2 Smooth muscle cells

Morphology

The media of the wall of a muscular artery is mainly composed of SMCs. In contrast to skeletal muscle cells, SMCs are considerably smaller (2 to 10 μm in diameter and 50 to 400 μm long) and each cell has a single, centrally located nucleus. Each cell is surrounded by an external lamina to which the cell membrane adheres: groups of cells are typically arranged in sheets [3]. The major function of an adult healthy SMC is contraction and its cytoplasm is largely filled with filaments participating in the contractile process [4]. Smooth muscle filaments do not appear to form myofibrils and are not arranged in the sarcomere pattern found in skeletal muscle [5]. The amount of organelles such as free ribosomes, rough endoplasmic reticulum (ER), and Golgi complexes present within SMCs varies according to the tissue of origin and appears to depend on the cell's particular function. SMCs, apart from being able to contract are able to divide and/or to synthesise extra-cellular matrix (ECM) [4].

Phenotypes

SMCs can appear in a range of different phenotypic states. At one end of the spectrum cells can express a predominantly contractile (physiological) state in which they maintain the vascular tone of the blood vessel. At the other end of the spectrum cells can express a modulated state in which the cells are predominantly mitotic and/or synthetic. Normally, adult medial SMCs are of the contractile phenotype. This function is reflected structurally by occupation of 75-80% of the cell cytoplasm by contractile filaments. Organelles such as rough ER, Golgi apparatus and free ribosomes are few in numbers. A modulation of the phenotype can occur in situations of vascular reorganisation, for example in atherosclerotic lesions, myo-intimal thickenings or in arteries subjected to balloon catheterisation [4]. Cells undergo a marked structural change, in which the presence of myofilament bundles diminishes in the cytoplasm and the presence of rough ER, Golgi apparatus and free ribosomes increases (see table I). The events initiating the phenotypic modulation are not fully understood, but alteration of the composition of the ECM [6, 7] and continuous mechanical loading [8, 9] can alter the structural and metabolic characteristics of SMCs and increase their responsiveness to growth regulatory molecules.

Table I: Characteristics of different phenotypic states of SMCs.

Contractile phenotypic state	*Modulated phenotypic state*
Predominantly contractile	Predominantly mitotic and/or synthetic
Contractile filaments present	Contractile filaments have disappeared
Few organelles present	Large number of organelles present
Small cells	Large cells
Low secretion of proteins	Increased secretion of proteins
Not responsive to growth factors	Responsive to growth factors

ECM synthesis

SMCs provide the structural scaffolding of vascular tissue [10]. They produce proteins of the ECM which are important for spatial organisation and mechanical stability [2, 11-14]. The ECM is a complex ordered aggregate composed of two main classes of macromolecules; polysaccharide glycosaminoglycans and fibrillar proteins. Most if not all of these macromolecules have the ability to self-aggregate to form fibrillar meshworks or other structures appropriate for specific tissue function [15]. These macromolecules profoundly influence the biology of the cell including migration, proliferation, state of differentiation, development, metabolic responses, and expression of adhesion molecules, receptors and cell specific proteins [2]. Fibrillar proteins determine the tensile properties of support tissues. These proteins are divided into 4 major classes: collagen and elastin, which are mainly structural, and fibronectin, and laminin, which are mainly adhesive. The collagens comprise a large family of proteins which strengthen and organise the ECM. SMCs synthesise a great variety of collagen types, including types I, III, IV and V [14]. Elastin is a hydrophobic protein, which assembles into filaments and sheets by cross-linking and is the main component of elastic fibres, which are responsible for the elasticity of the tissue [16, 17]. Fibronectin and laminin are multifunctional and important glycoproteins. Functional importance stems from their ability to adhere to several different tissue components. Fibronectin and laminin contain sites which bind collagen and elastin as well as cell adhesion molecules, allowing cell adhesion to the ECM [2, 14, 18, 19].

Cell adhesion

Cell-cell and cell-ECM interactions are mediated by specific cell surface receptors, including members of the integrin family [14, 18, 20]. Integrins are a family of glycosylated, heterodimeric transmembrane adhesion receptors that consist of a non-covalently bound α- and β-sub-unit.

Several sub-units have been identified and the combination of the α- and β-sub-unit determines the ligand specificity of the integrins. For example α5β1 and α3β1 integrins mediate SMC adhesion to fibronectin [21]. α2β1 and α1β1 integrins mediate SMC adhesion to type I collagen and laminin [18]. SMCs can directly bind to the collagen substrate but can also indirectly bind via fibronectin. The fibronectin-receptor in SMC membranes possesses a cytosolic domain binding to actin, a transmembrane domain, and an extracellular domain binding to collagen via fibronectin (as shown in figure 2) [15, 22]. Because fibronectin receptors are linked to intracellular actin, the orientation of the internal cytoskeleton of a cell influences the orientation of the ECM [2]. Fibronectin is produced by vascular cells and is also present in relatively high concentrations in serum. The integrin expression of cells is dynamic and changes during different cellular processes. Besides its role in the maintainance of tissue structure and orientation, the integrin expression is involved in the regulation of cell proliferation [23], differentiation, phenotypic modulation [24, 25] and cell activation [14, 18, 26].

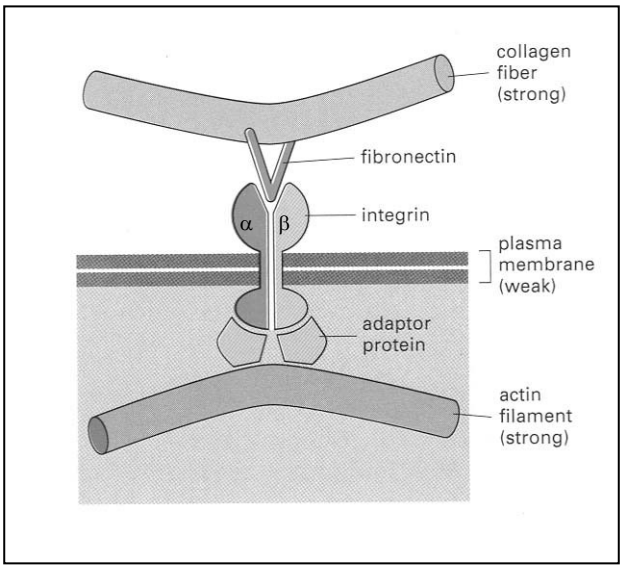

Figure 2: The transmembrane linkage from the ECM to the cytoskeleton of SMCs mediated by integrin and fibronectin. The integrin molecule is anchored inside the cell to the cytoskeleton (actin filaments) and externally via fibronectin to collagen fibres of the ECM [22].

2.3 Vascular diseases

Mechanism of atherosclerosis

SMCs play an important role in the development of vascular diseases [27]. Atherosclerosis, in the form of coronary artery or peripheral vascular disease, is the largest cause of morbidity and mortality in the United States and Europe [28-30]. This disease is characterised by progressive narrowing and occlusion of blood vessels. The development of atherosclerosis is

divided into several stages (as shown in figure 3) [31]. The pathogenesis starts with the damage or activation of the endothelium caused by chemical, mechanical, immunological, or infectious processes including elevated and modified levels of lipoproteins, free radicals, plasma homocysteine, hypertension, activated T-lymphocytes or infectious micro-organisms [27, 32]. One of the consequences associated with EC dysfunction is increased adherence of thrombocytes, monocytes/macrophages and T-lymphocytes. Monocytes/macrophages and T-lymphocytes then migrate between the endothelium and localise sub-endothelially. The macrophages become large foam cells because of lipid accumulation and together with the T-lymphocytes and SMCs they form a fatty streak or early atheroma (figure 3a) [33]. This first stage is accompanied by increased deposition of collagen and the artery enlarges in an outward, abluminal direction to accommodate the expansion of the intima. Stabilisation of the early atheroma can occur (figure 3c) but if inflammatory conditions prevail and risk factors persist, the lipid core can grow, forming an intermediate lesion or vulnerable plaque (figure 3b) [33]. Proteinases secreted by the activated leukocytes can degrade the ECM, while pro-inflammatory cytokines can limit the synthesis of new collagen. These changes can decrease the thickness of the fibrous cap and render it susceptible to rupture. When the plaque ruptures, blood comes in contact with the plaque and coagulates. Platelets activated by thrombin generated from the coagulation cascade and by contact with the intimal compartment initiate thrombus formation (figure 3d) [33]. On the other hand, lowering plasma lipid concentration after early atheroma or vulnerable plaque formation can reduce the lipid content of the plaque and may attenuate the intimal inflammatory response, yielding a more stable plaque with a thick fibrous cap and a preserved lumen (figure c) [33]. In case of a thrombus, it may eventually resorb as a result of endogenous or therapeutic thrombolysis. However, narrowing of the lumen has occurred because of several processes. A wound healing response triggered by thrombin generated during blood coagulation can stimulate SMC proliferation. Platelet derived growth factor (PDGF) released from activated platelets can stimulate SMC migration and transforming growth factor-β (TGF-β) also released from activated platelets, can stimulate interstitial collagen production. This increased migration, proliferation and ECM synthesis by SMCs thicken the intima and cause a constriction of the lumen (figure 3e). Both thrombus formation and constriction of the lumen can cause several clinical manifestations (figures 3e and 3f) [27, 33-36].

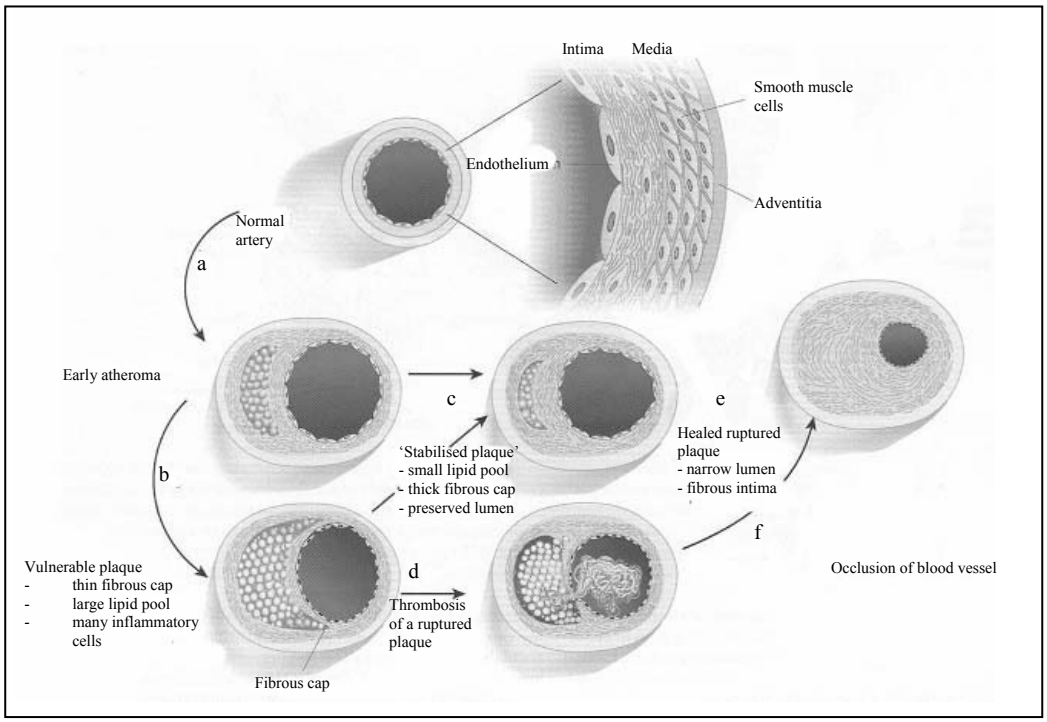

Figure 3: Several stages of atherosclerotic plaque formation (see text for a detailed description).

Clinical manifestations

Atherosclerosis itself is not merely a disease in its own right, but a process that is the principal contributor to the pathogenesis of several clinical manifestations. In small-diameter arteries atheromatous plaques lead to a reduced size of the lumen of the vessel so that blood flow is decreased (figure 3e). Clinical manifestations happen particularly in situations of increased cardiac demand, leading to ischaemia, commonly provoking symptoms such as angina pectoris and/or malfunctions of peripheral organs such as liver, kidney and pancreas [37]. Thrombus formation (figure 3d) also reduces the lumen of the vessel and may block it completely, resulting in death of the tissue supplied by the vessel (infarction). The myocardium of the left ventricle is particularly vulnerable to infarction, as is the brain (stroke) and the feet and toes (gangrene). Enlarged atheromatous plaques (figure 3b) can loose elastic fibres and smooth muscle cells from the underlying media. In the large elastic arteries such as the aorta, these specialised components become replaced by non-contractile, inelastic collagen and the vessel dilates to form an aneurysm. The danger of an aneurysm is that the vessel wall is greatly weakened and is prone to burst. Finally, atheromatous plaques or thrombi may detach from the wall of blood vessels, resulting in pulmonary or systemic arterial embolism [2, 27, 33, 35-37].

2.4 Vascular prostheses

The high mortality, the widespread suffering, and the huge economic impact of atherosclerosis demand integrated medical approaches and therapies. Surgical treatment of atherosclerosis deals with the replacement of a damaged blood vessel or by inserting a vascular stent. For large-diameter applications (> 6 mm), synthetic vascular prostheses such as Dacron® [poly(ethylene terephthalate)] grafts and Teflon® [expanded poly(tetrafluoroethylene)] grafts [38, 39] are commonly used in vascular surgery. These grafts remain patent for more than 10 yrs after implantation. However, these synthetic materials represent a suitable alternative only for high-flow low-resistance conditions in large-diameter arteries. Small-diameter vascular grafts made of these synthetic materials occlude rapidly upon implantation due to early thrombosis. Until today, drug-eluting stents are used to reduce restenosis in patients with focal, small-diameter artery stenoses [40-42]. Moreover, autologous saphenous veins or mammary arteries are used to replace small-diameter blood vessels [30, 43]. Both are flexible, viable, non-thrombogenic and biocompatible. Unfortunately, in around 30% of patients who undergo vascular reconstructions, a saphenous vein is unavailable [38] and a mammary artery may not always have the proper size or length [30]. Moreover, a saphenous vein may develop an aneurysm when transplanted to a high-pressure arterial site. To improve grafts to bypass diseased medium- and small-diameter blood vessels, several strategies have been pursued like endothelialization of vascular grafts with autologous ECs prior to implantation [43-46]. Initially, low numbers of primarily harvested autologous ECs, difficulties regarding cell culturing to increase the cell numbers, inadequate EC adhesion and/or growth and cell detachment after restoration of the blood circulation formed major obstacles in the development of functional small-diameter vascular prostheses [47]. However, new techniques for EC lining of expanded polytetrafluoroethylene (ePTFE) grafts [46, 48] and the use of heparinized collagen pre-loaded with basic fibroblast growth factor [49-51] provide strong evidence that autologous EC lining distinctly improves the patency of small-diameter vascular grafts.

Endothelialization of synthetic vascular grafts is an example of tissue engineering. The field of tissue engineering has further been explored to produce a functional small-diameter blood vessel replacement.

2.5 Tissue engineering

Principles of tissue engineering

Tissue engineering is an interdisciplinary field that applies the principles of engineering and life sciences towards the development of biological substitutes that restore, maintain or improve tissue function [52]. One strategy to create these biological substitutes is to use cells seeded in three-dimensional porous scaffolds. For tissue engineering of small-diameter blood vessels, several approaches have been described in which different natural polymers such as collagen [53-56] or biodegradable synthetic polymers [52, 57-61] were used. The polymer constitutes a temporary template, on which vascular cells can adhere and grow, with adequate mechanical properties to prevent failure of the constructs during dynamic culturing. The ideal engineered scaffold should degrade and resorb at a controlled rate to match cell proliferation, ECM production and tissue ingrowth *in vitro* and/*or in vivo*. After culturing of the TE constructs, the resulting tissue should mimic the biomechanical characteristics of the natural tissue [52]. All studies were aiming at creating a structure closely resembling the three-layered structure of a natural artery which may serve as a cell transplant device or a model to study vascular biology [52, 62, 63]. By mimicking the natural blood vessel structure, the graft should have the potential to become clinically useful with a patency rate of 90% at 30 d as observed with autologous vein grafts [57, 64]. The graft should possess sufficient strength not to burst with changes in blood pressure, a vessel wall that is elastic and able to withstand cyclic loading, matching compliance of the graft with the adjacent host vessel, and a lining of the lumen that is anti-thrombotic [28]. Moreover, as viable structures, tissue-engineered (TE) blood vessels should represent a responsive and self-renewing tissue with the inherent potential of healing and remodelling according to the requirements of their specific environment [65].

Process of tissue engineering

Several essential steps are involved in the process to develop a TE blood vessel mimicking a natural artery including harvesting of desired cells, expansion of cell number in culture, development of a porous biodegradable and biocompatible scaffold, cell seeding in the scaffolds, and culturing in an environment that induces tissue formation [66]. Human vascular cells can be isolated from several sources including umbilical cord arteries and veins [67], saphenous veins [4] and mammary arteries [68]. Cell expansion has been carried out for decades to study cell biology. Cell seeding in appropriate scaffolds plays an important role in determining the initial cell number and distribution which are critical factors for tissue development [69]. A high number of initially seeded cells can improve structural stability and

biochemical composition of the engineered tissue. Furthermore, uniform cell distribution in the TE construct associated with intimate cell-cell interactions, is desirable for both normal functions and phenotypic expression of vascular cells [70]. In the past, several vascular cell models [53, 71, 72] and animal models [73-76] have been used to evaluate the effects of chemical and mechanical stimuli on cell proliferation [77], phenotype modulation [78], alignment [79], migration and ECM production in TE scaffolds. However, the proper phenotype of cells, sufficient mechanical properties of the constructs for implantation and/or proper cell organisation and development of the desired ECM structure are often lacking in cell culture models [80]. These characteristics are more easily accomplished in animal models, but, in this case, it is not possible to study the effects of distinct factors (*e.g.* growth factors, hormones and cytokines) or to control the hemodynamics. With the development of bioreactors, dynamic culture conditions simulating the *in vivo* situation in terms of hemodynamic forces to which a blood vessel wall is exposed can be created and the effects of distinct factors can be studied.

2.6 The use of bioreactors in tissue engineering of small-diameter blood vessels

Advantages of the use of bioreactors

Bioreactors are generally defined as devices in which biological and/or biochemical processes develop under closely monitored and tightly controlled environmental and operating conditions [81]. For tissue engineering of blood vessels, numerous research groups have designed their own bioreactors. First bioreactors have been developed to induce laminar flow [70, 82] and thus to enhance mass transfer of nutrients, oxygen and metabolic waste products [82]. Other bioreactors [57, 80, 83-86] have been manufactured to mimic the physiological conditions of the human vasculature and to investigate the role of single mechanical factors. The effects of either steady or pulsatile luminal perfusion [55, 57, 79, 80, 83, 84, 87-89], cyclic mechanical strain [85, 86, 90, 91], pulse rate [92] or pulse pressure [93, 94] on the development of the TE construct during culturing have been investigated using these systems. All these studies demonstrated that an environment resembling *in vivo* conditions may promote both the development of constructs with sufficient mechanical strength to be implanted and the modulation of appropriate cellular functions. Continuous mechanical loading has at least three different effects on SMCs, i: acceleration of the orientation of SMCs, ii: acceleration of the production of collagen fibre bundles and iii: induction of the phenotypic modulation of SMCs from a synthetic to a contractile state [8]. However, the optimal bioreactor set up and culture conditions for the development of a functional arterial graft remain to be elucidated [95]. Optimising a bioreactor set up must address a careful balance between mass transfer rates, retention of cells and newly

synthesised ECM components within the construct, fluid-induced shear stresses and cyclic mechanical strain [70, 82 81].

Progress in tissue engineering using bioreactors

L'Heureux *et al*. [55] were the first who described a completely biological TE blood vessel cultured in a bioreactor. Human SMCs were cultured and a sheet of SMCs was wound around a tubular support to produce the media of the vessel. A sheet of fibroblasts was wrapped around the artificial media to serve as a vascular adventitia and ECs were seeded in the lumen of the TE blood vessel after a period of culturing. The vessel had a burst strength comparable to human vessels and after implantation in mongrel dogs 50% of the vessels remained patent for 1 wk. The construct should be produced from animal cells in order to assess the long-term value of this vascular graft in an autologous system. Moreover, the limiting factor in this process was the long time period of over 3 months needed for the production, which restricts the use of the graft in vascular surgery.

Niklason [57] described an interesting approach in which bovine vascular cells were cultured for up to 2 months on a biodegradable mesh of polyglycolic acid (PGA) wrapped around silicone rubber tubing in a pulsatile perfusion system. After implantation of these grafts in miniature swine, appropriate flow was demonstrated and all grafts remained patent for 2 wks postoperatively. Similar results were reported by Shum-Tim [60] who replaced abdominal aortic segments with vascular cell-seeded biodegradable PGA constructs in lambs.

Watanabe *et al* [96] constructed TE autografts by seeding a mixed cell population obtained from femoral veins of mongrel dogs onto biodegradable polymer scaffolds composed of PGA and a copolymer of L-lactide and caprolactone. After 1 wk, the inferior vena cava's of the same dogs were replaced with the graft. Follow up was 3-6 months. Neither occlusion nor aneurysm formation was found and ECs were present on the luminal surface.

However, till today, only one group have reported successful transplantation of a TE blood vessel into 25 patients at present [97, 98]. Either cultured vascular cells, isolated from an autologous peripheral vein, or autologous bone marrow cells were used to seed medium-sized tubular scaffolds (outer diameter of 10 to 24 mm) prepared from a copolymer of ε-caprolactone and lactic acid (molar ratio of 50:50). The copolymer was synthesised by ring-opening polymerisation and the scaffolds were over 80% porous with pore sizes of 100 to 200 μm. Three different procedures were used to construct the TE grafts. In the first procedure scaffolds were reinforced with PGA and approximately 3 months before cardiac surgery,

autologous veins were harvested from the patients and vascular cells were isolated and cultured. One week before the operation, cells were seeded onto the scaffolds and kept in culture till the day of surgery. In the second and third procedure scaffolds were reinforced with poly-L-lactic acid and at the same time of the beginning of cardiac surgery, bone marrow cells (BMCs) were aspirated from the patient under general anesthesia. These BMCs were directly seeded onto the biodegradable scaffold (procedure II) or mononuclear BMCs were obtained after centrifugation and seeded (procedure III) [99]. The seeded biodegradable scaffolds were then kept in culture for approximately 2-4 h until use. Diseased pulmonary arteries of 25 young patients (age between 3 and 14 yrs) were replaced with the obtained TE constructs. Anticoagulant therapies were administered to all patients for at least 3 months. Postoperative examinations revealed no dilation or rupture of the grafts, and there were no thrombogenic complications. The grafts were patent, no unwanted calcification was found and the patients were doing well.

2.7 Role of tissue homeostasis in vascular diseases and tissue engineering

In natural viable tissues as well as functional TE constructs tissue homeostasis is mediated by the balance between cell proliferation and programmed cell death (apoptosis) [70]. Alterations in cell death signalling by growth factors, hormones or cytokines, or expression of specific genes that govern apoptosis or proliferation lead to disturbed homeostasis and are involved in the pathogenesis of many vascular diseases [70, 100].

Several recent studies have demonstrated that both cell proliferation and apoptosis are major events occurring during atherosclerotic plaque development [35, 36, 101, 102]. The induction of apoptosis in ECs is a potential reaction of these cells to exposure of circulating harmful factors and may be involved in the development of atherosclerosis (see section 2.3) [103-105]. Apoptotic cells within atherosclerotic plaques are typically macrophages, SMCs and T-lymphocytes and the frequency of death varies in the different regions of the lesion. SMC apoptosis can exert major changes in arterial architecture, regulated by several pro and anti-apoptotic agents and by cell-cell and cell-matrix interactions via specific integrin-mediated signalling (see section 2.2) [35, 106]. The induction of apoptosis in atherosclerotic lesions may be a self-defense mechanism that is initiated in response to an increased rate of SMC proliferation. However, apoptosis may promote rupture of the atherosclerotic plaque by reducing the cellularity and thereby the stability of the plaque, leading to the formation of emboli [37]. Furthermore apoptosis may promote thrombosis on the plaque directly. Apoptotic SMCs as well as apoptotic ECs can act as a substrate for the generation of thrombin [107]. This

is due to the fact that apoptotic cells expose phosphatidyl serine (PS) on the surface early in the process. In the presence of factor V and VII, exposed PS can then act as a substrate for thrombin generation [108].

Besides the role of (disturbed) tissue homeostasis in the development of vascular diseases, the balance between proliferation and apoptosis indicates the viability of a TE construct. Accordingly the simultaneous measurement of proliferation and apoptosis of cells present in TE constructs offers the possibility to follow the growth behaviour of these vascular grafts. By analysing the balance between proliferation and apoptosis of cultured vascular cells, cell seeding protocols can be standardised and the efficiency of cell seeding and the success of cell culturing in three-dimensional porous scaffolds can be evaluated in detail.

2.8 Cell proliferation

In an organism, cell division is a tightly regulated process. Generally, cells do not undergo division unless they receive signals that instruct them to enter the active segments of the cell cycle. Resting cells are in the G0 phase of the cell cycle (quiescence). The signals that induce cells to divide are diverse and trigger a large number of signal transduction cascades. Once the cell is instructed to divide, it enters the active phase of the cell cycle, which consists of 4 successive phases as presented in figure 4. During the interphase, which is divided into the G1, S and G2 phase, the cell grows continuously. During the M phase cell growth stops, the nucleus divides first, and then the cell divides. DNA is replicated during the S phase. The G1 phase is a gap between mitosis and DNA synthesis (the M and S phase) and the G2 phase is a gap between the S and M phase [22].

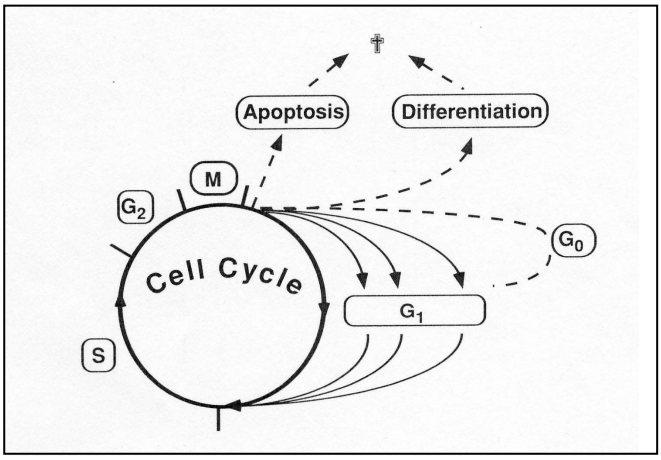

Figure 4: The concept of the standard cell division cycle (see text for a detailed description).

Entering the S phase and entering the M phase are two key events in the process of cell division and are triggered by a cell cycle control system. This system consists mainly of a set of protein complexes each composed of a regulatory sub-unit (a cyclin) and a catalytic unit (a cyclin-dependent protein kinase, Cdk). The Cdks are cyclically activated by both cyclin binding and phosphorylation [22].

Cells in the G0 phase are temporarily non-proliferating cells and can re-enter the cell cycle after adequate stimulation by growth factors or release of inhibitory factors. In contrast, cells in the terminally differentiated phase are non-proliferating cells and cannot re-enter the cell cycle. Differentiation and apoptosis ultimately lead to cell death and are important for the balance between cell growth and cell death.

2.9 Apoptotic cell death

Apoptosis versus necrosis

Cell death can occur by either of two distinct mechanisms, necrosis or apoptosis. These mechanisms are morphologically, biochemically and molecularly distinct from each other (as schematically represented in figure 5 [109]).

Necrosis or accidental cell death is the pathological process, which occurs when cells are exposed to a serious physical, chemical or osmotic injury. Necrosis begins with an impairment of the ability of the cell to maintain homeostasis. The cell membrane loses its selective permeability and ion-pumping capacity. This leads immediately to an influx of water and extracellular ions which causes swelling of the cell and its intracellular organelles (most notably the mitochondria). Eventually cell lysis occurs. Due to the ultimate breakdown of the plasma membrane and other cellular membranes, the cytoplasmic contents including lysosomal enzymes are released into the extracellular fluid inducing an inflammatory response in the adjacent viable tissues [36].

Apoptosis or programmed cell death defines a genetically encoded mechanism by which aged, unwanted or sub-lethally damaged cells are eliminated during development and other biological processes. During this process a specific pattern of abolition takes place under normal physiological conditions. The earliest changes include the loss of cell junctions and cell shrinkage by a loss of intracellular fluid and ions. The integrity of the cell membrane remains initially intact. Activation of caspases (cysteine dependent aspartic acid cleaving proteases) leads to a change of the mitochondrial membrane potential, accompanied by intracellular shifts in calcium and pH. Other characteristic features of apoptosis are chromatin aggregation, nuclear condensation and DNA fragmentation. The endoplasmic reticulum

transforms into vesicles that fuse with the cytoplasmic membrane. Cell blebbing occurs and membrane-bound vesicles or apoptotic bodies are formed. These bodies contain ribosomes, morphologically intact mitochondria and nuclear material. *In vivo*, the apoptotic bodies end up in the extracellular space, where they are phagocytosed by adjacent cells and macrophages. Due to this active and efficient mechanism for the removal of apoptotic cells *in vivo* no inflammatory response is induced. *In vitro*, the apoptotic bodies as well as the remaining cell fragments ultimately swell and finally lyse. This terminal phase of *in vitro* cell death has been termed secondary necrosis [36, 109].

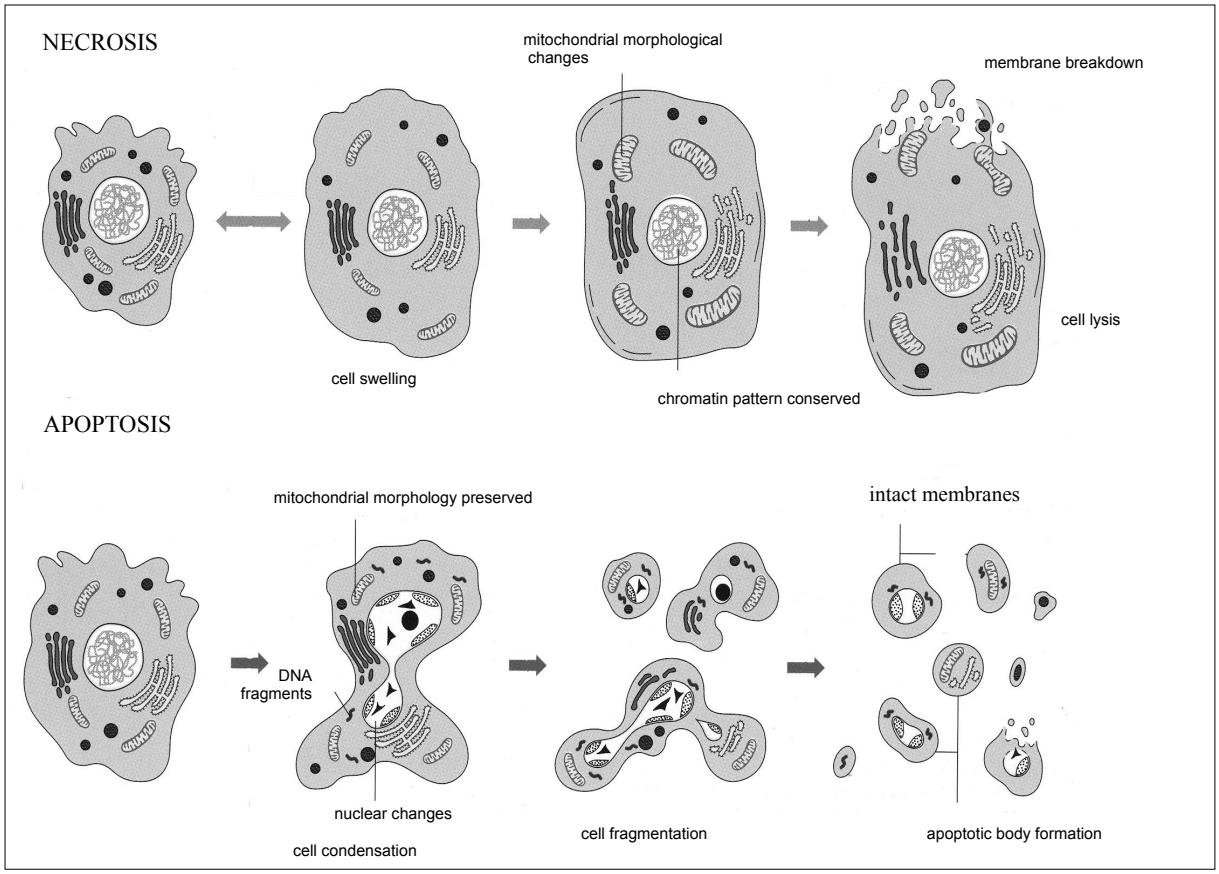

Figure 5: Illustration of the most prominent morphological features of necrosis and apoptosis [109].

The apoptotic cascade

Apoptosis is a kinetic event [110]. The entire duration of the process, from onset to total disintegration of the cells is relatively short and of variable length compared to the duration of the cell cycle [111]. The apoptotic response is mediated through either the intrinsic or the extrinsic pathway, depending on the origin of the death stimuli. The extrinsic pathway is initiated by low oxygen, nutrient or growth factor levels [112-114], damage to the cell membrane or activation of death receptors like tumor necrosis factor receptor (TNFR) and Fas receptor

(FasR). Binding of death receptor ligands such as TNF-α and FasL to their receptors causes the cytosolic domain of the receptors to recruit pro-caspase-8 and –10 [36]. Caspases belong to a family of intracellular proteases and their activation is considered to be the key event of apoptosis. The intrinsic pathway is triggered in response to a wide range of death stimuli that are generated from within the cell, such as oncogene activation, DNA damage and cell aging. Whether detachment of adherent cells from the ECM, a process designated as anoikis, is also a trigger of the intrinsic apoptotic cascade or a result of intrinsic or extrinsic triggering is unclear [115-119] [120]. Intrinsic signalling involves the permeabilisation of the mitochondrial membrane releasing cytochrome c and apoptosis-inducing factor (AIF) from the mitochondria. Cytochrome c binds to apoptotic protease activating factor (Apaf-1), present in the cytosol and this complex triggers activation of pro-caspase-9 and subsequently the apoptotic machinery. AIF is a protease which may be responsible for nuclear changes typical for apoptosis. The activated initiator caspases of the intrinsic pathway (caspase-9) and the extrinsic pathway (caspase-8 and -10) catalyse the activation of the effector caspases (caspase-3 and –7). A number of proteins have been identified that control these pathways of caspase activation, including caspase-associated recruitment domains (CARDs), death domains (DDs), death effector domains (DEDs), members of the bcl-2 family and inhibitor of apoptosis proteins (IAP) [36]. During progression of these pathways, the environment of the apoptotic cell is informed about the cell death decision. The environment responds with removal of the dying cell by phagocytosis. The structure of the plasma membrane changes in such a way that phagocytes can identify the cell as suicidal resulting in rapid degradation. Among these signals on the cell membrane of apoptotic cells are sugars, thrombospondin binding sites and PS. The most investigated signal used for the detection of apoptosis, is the exposure of PS on the cell surface [121]. A living cell keeps PS stringently located in the inner membrane leaflet of the plasma membrane that faces the cytosol. During apoptosis a phospholipid translocase is inhibited and a scramblase becomes activated initiating externalisation of PS from the inner to the outer leaflet of the plasma membrane.

2.10 Detection of proliferation and apoptosis

Detection of proliferation

A variety of methods is used to measure cell proliferation *in vitro* and *in vivo* [122]. The most straightforward method to determine cell proliferation is direct counting of the cells after several time periods with a hemacytometer. However, for this procedure cells have to be intact and present in suspension. Adherent cells present in porous TE scaffolds cannot be

isolated without cell damage [123]. Therefore, the method of cell counting is not suitable for determining the amount of adherent cells present in porous TE scaffolds. The development of fluorescent indicators of cellular DNA content has made the quantification of cell numbers more rapid and convenient. Several dyes exhibit fluorescence enhancement upon nucleic acid binding, including Hoechst 33258, propidium iodide (PI) and cyanine dyes [122, 124]. These dyes can be used after permeabilisation of the plasma membrane to quantify the amount of macroscopically intact cells in suspension by means of flow cytometry. In addition, the dyes can be used to quantify the amount of adherent cells present in porous TE scaffolds after total digestion of the cells and the ECM of the cell-seeded constructs, because the total DNA content is correlated to the number of cells present [124].

Other approaches to investigate cell proliferation are analysis of DNA synthesis or indirect parameters. To measure DNA synthesis, labelled DNA precursors (for example ^{3}H-thymidine) are added to the cells and their incorporation into DNA is subsequently quantified [122]. Indirect parameters include molecules that regulate the cell cycle. These molecules are analysed either by their activity or by quantifying their amounts by means of western blotting, ELISA or immuno histochemistry [122].

Finally, gene expression of markers of proliferation can be used to study cell proliferation by reversed transcriptase polymerase chain reaction (RT-PCR). An example of a marker of proliferation is cyclin E [125, 126 127]. Cyclin E is a member of the cyclin family and regulates the transition from the G1 to the S phase of the cell cycle which is a key event of this process [125]. A high level of the cyclin E protein facilitates this transition indicating enhanced proliferation [128, 129].

Detection of apoptosis: microscopy

Discriminating apoptosis from necrosis is necessary in order to learn how to modulate apoptosis in view of its potential therapeutic use and in view of the success of tissue engineering. A number of the various morphological and biochemical changes which occur during the apoptotic cascade as described above, can be exploited to discriminate vital and dying cells and to analyse the extent and the type of cell death. However, several problems have to be faced in studying apoptosis. Besides difficulties of cell preservation of morphological and biochemical integrity during the measurement, the nature of the apoptotic process itself gives rise to difficulties of its detection. For example, apoptosis is an elimination mechanism affecting individual cells, no inflammation is involved and within a few h from the onset, the cell is totally removed by phagocytosis. The consequence of rapid uptake and

elimination of apoptotic debris is that measuring apoptosis *in vivo* can underestimate this phenomenon occurring in the tissue [130].

The morphological appearance of cells undergoing apoptosis is both distinct and specific. Therefore assessment of these features by microscopy is a golden standard to identify apoptosis and should always accompany any biochemical method. Light microscopy is the most commonly used technique. The analysis of cells on cytospin preparations by light microscopy is distinct, fast and simple. During apoptosis, cell membrane blebbing, nuclear and cytoplasmic shrinkage, a reduced total cell volume and formation of apoptotic bodies can be identified. During necrosis, however, membrane dissolution or lysis, nuclear and cytoplasmic swelling and an increased total cell volume ('ghost cell') can be identified. In this way both cell death mechanisms can be distinguished. Light microscopy identifies features that generally occur after major biochemical events have taken place [130]. These biochemical changes can be studied by various techniques [110, 111, 130].

Detection of apoptosis: flow cytometry

The most common technique to study biochemical changes during the apoptotic process in cell populations is based on flow cytometry [110, 111]. With this technique, cell shrinkage is expressed by changes in cellular light-scatter signals. The forward-angle light scatter (FCS) relates to the cell diameter, the side-angle light scatter (SSC) reflects the conformation of intra cellular structures. During the initial stages of apoptosis the cell shrinks, while the membrane remains intact. As a consequence of these cellular changes the FSC decreases, while the SSC increases or remains unchanged. During necrosis, cell swelling occurs resulting in an increased FSC and decreased SSC signal. The advantage of flow cytometry is the possibility of combining the scatter signals to distinguish necrosis from apoptosis with analyses of fluorescent cell markers to identify biochemical features of the apoptotic cell as illustrated by the following examples. A change of the mitochondrial transmembrane potential in apoptotic cells can be measured by 3,3'-dihexyloxacarbocyanine iodide (DiOC6). DiOC6 accumulates in the mitochondria of viable cells and the efflux of the fluorochrome can be measured by an increase of the cellular fluorescence [110]. Cleavage of DNA in apoptotic cells can be detected by the presence of 3'hydroxyl-termini of the broken strands. The terminal deoxynucleotidyl transferase (TdT) mediated dUTP-biotin nick end labelling (TUNEL) assay uses a modified nucleotide (dUTP) in a reaction catalysed by an exogenous enzyme (TdT) to detect the strand breaks. The TUNEL method has become a standard technique for recognition of apoptosis in tissue sections [102]. Antibodies against caspases as well as annexin V, both fluorescently

labelled, are extensively used to detect apoptotic cells [123, 131]. Anti-caspase-3 is often used for this purpose because caspase-3 is a key effector in the apoptotic program [110, 132]. Annexin-V has a high (calcium-dependent) affinity to PS, which is translocated from the inner to the outer leaflet of the plasma membrane during apoptosis.

PI can be used in two distinct ways. A common procedure to measure apoptosis in cell cultures is the DNA fragmentation assay according to Nicoletti [133]. In this assay DNA is stained with PI after permeabilisation of the plasma membrane. Histograms of PI fluorescence show three distinct peaks of three separate cell populations. A G0/G1 region of normal diploid cells, a G2/M region of dividing cells with a double amount of DNA and an A0 region of hypo diploid cells [110, 111]. This sub-population of A0 cells shows reduced DNA stainability, indicating apoptotic cells in which DNA fragments appear and cell fragmentation has occurred. Alternatively, a combination of a fluorescent early-apoptotic label and PI can discriminate between early apoptosis, late apoptosis and necrosis because late apoptotic and necrotic cells stain with PI as a consequence of their compromised plasma membrane whereas early apoptotic cells do not [110]. Methods based on flow cytometry are suitable for cells present in suspension [110, 111]. Flow cytometry can also be performed using adherent cells after detachment of the cells from the support. However, cell detachment induces apoptosis by itself [134]. Therefore, flow cytometry is not an optimal quantitative technique to measure apoptosis of adherent cells [123].

Detection of apoptosis: other methods

Several other techniques have been developed for analysing apoptosis in cell cultures or tissues including agarose gel electrophoresis for detection of DNA fragmentation, enzyme-linked immuno sorbent assays (ELISAs) for detection of oligonucleosomes [135], caspase-3 activity or other apoptosis-related proteins and analyses of gene expression of apoptotic markers by RT-PCR. Tissue transglutaminase (tTG) mRNA expression levels can be used for the latter purpose [136]. tTG is a key protein mediating the process of apoptotic body formation. tTG is a multi-functional transamidating acyltransferase which becomes activated during the later phase of apoptosis. Activated tTG induces irreversible crosslinks in and between cytoplasmic proteins to produce a large, stable, insoluble protein scaffold [137]. This crosslinking of proteins stabilises cell and membrane structures of disintegrated cells and apoptotic bodies [136-138]. There are several advantages of the RT-PCR technique. One advantage is that it is possible to measure both events of apoptosis and proliferation in one single assay by analysing both tTG and cyclin E gene expression [139]. Another advantage is

that cells don't have to be detached from the support because RNA can directly be isolated from adherent cells.

Finally, another approach to analyse the mechanism of apoptosis is the use of inhibitors of caspases. By means of a fluorochrome-labelled inhibitor of caspases FAM-VAD-FMK (FLICA), cells can be labelled after caspase activation. Exposure of cells to FLICA results in the uptake of this inhibitor followed by covalent binding to activated caspases within the cells undergoing apoptosis. By binding to activated caspases FLICA irreversibly inactivates them, which causes the arrest of the apoptotic cascade. In combination with exposure of the cells to PI, the rate of cell entrance into apoptosis during a time interval can be estimated using flow cytometry [140]. By evaluating cell death kinetics instead of the amount of cells at a given time point, a more accurate assessment of the incidence of apoptosis is possible [140-143].

References

1. Martini, F. H. and Timmons, M. J., The cardiovascular system: vessels and circulation in: Human Anatomy, 2nd, Upper Saddle River, New Jersey, USA, Prentice Hall, 1997; 543-548.
2. Stevens, A. and Lowe, J., Support Cells and Extracellular Matrix in: Human Histology, second edition, 1999; 36-56.
3. Wang, H., Day, N., Valcic, M., Hsieh, K., Serels, S., Brink, P.R., and Christ, G.J. Intercellular communication in cultured human vascular smooth muscle cells`. Am.J.Physiol.Cell Physiol. 2001; 281: C75-C88.
4. Chamley-Campbell, J., Campbell, G.R., and Ross, R. The smooth muscle cell in culture. Physiol.Rev. 1979; 59: 1-61.
5. Mofett, D., Mofett, S., and Schauf, C., Muscle Physiology in: Human Physiology, second edition, Mosy-Year Book, Inc., 1993; 270-280.
6. Hayward, I.P., Bridle, K.R., Campbell, G.R., Underwood, P.A., and Campbell, J.H. Effect of extracellular matrix proteins on vascular smooth muscle cell phenotype. Cell Biol.Int. 1995; 19: 839-846.
7. Jacob, M.P., Badier-Commander, C., Fontaine, V., Benazzoug, Y., Feldman, L., and Michel, J.B. Extracellular matrix remodeling in the vascular wall. Pathol.Biol. 2001; 49: 326-332.
8. Hirai, J. and Matsuda, T. Self-organized, tubular hybrid vascular tissue composed of vascular cells and collagen for low-pressure-loaded venous system. Cell Transplant. 1995; 4: 597-608.
9. O'Callaghan, C.J. and Williams, B. Mechanical strain-induced extracellular matrix production by human vascular smooth muscle cells. Role of TGF-beta1. Hypertension 2000; 36: 319-324.
10. Ross, R. The smooth muscle cell. II. Growth of smooth muscle in culture and formation of elastic fibers. J.Cell Biol. 1971; 50: 172-186.
11. Davidson, J.M., P.A.LuValle, O.Zoia, D.Quaglino Jr., and M.G.Giro. Ascorbate differentially regulates elastin and collagen biosynthesis in vascular smooth muscle cells and skin fibroblasts by pretranslational mechanisms. J.Biol.Chem. 1997; 272: 345-352.

12. Lo, C.S., Tamaroglio, T., and Zhang, J. Regulation of fibronectin by platelet-derived growth factors in cultured rat thoracic aortic smooth muscle cells. J.Biomed.Sci. 1995; 2: 63-69.
13. Hayashi, A., Suzuki, T., and Tajima, S. Modulations of elastin expression and cell proliferation by retinoids in cultured vascular smooth muscle cells. J.Biochem. 1995; 117: 132-136.
14. Kleinman, H.K., R.J.Klebe, and G.R.Martin. Role of collagenous matrices in the adhesion and growth of cells. J.Cell Biol. 1981; 88: 473-485.
15. Ruoslahti, E., E.G.Hayman, and M.D.Pierschbacher. Extracellular matrices and cell adhesion. Arteriosclerosis 1985; 5: 581-594.
16. Armentano, R.L., Levenson, J., Barra, J.G., Fischer, E.I., Breitbart, G.J., Pichel, R.H., and Simon, A. Assessment of elastin and collagen contribution to aortic elasticity in conscious dogs. Am.J.Physiol. 1991; 260: H1870-H1877.
17. Li, D.Y., Brooke, B., Davis, E.C., Mecham, R.P., Sorensen, L.K., Boak, B.B., Eichwald, E., and Keating, M.T. Elastin is an essential determinant of arterial morphogenesis. Nature 1998; 393: 276-280.
18. Skinner, M.P., Raines, E.W., and Ross, R. Dynamic expression of $\alpha 1\beta 1$ and $\alpha 2\beta 1$ integrin receptors by human vascular smooth muscle cells. Am.J.Pathol. 1994; 145: 1071-1081.
19. Labat-Robert, J. Cell-matrix interactions in aging: role of receptors and matricryptins. Ageing Res.Rev. 2004; 3: 233-247.
20. Nikolovski, J. and Mooney, D.J. Smooth muscle cell adhesion to tissue engineering scaffolds. Biomaterials 2000; 21: 2025-2032.
21. Clymann, R.I. and Kramer, R.H. b1 and b3 integrins have different roles in the adhesion and migration of vascular smooth muscle cells on extracellular matrix. Exp.Cell Res. 1992; 200: 272-284.
22. Alberts, B., Bray, D., Johnson, A., Lewis, J., Raff, M., Roberts, K., and Walter, P., Tissues in: Essential Cell Biology: An Introduction to the Molecular Biology of the Cell, New York & London, Garland Publishing, Inc., 1998.
23. Roy, J., Tran, P.K., Religa, P., Kazi, M., Henderson, B., Lundmark, K., and Hedin, U. Fibronectin promotes cell cycle entry in smooth muscle cells in primary culture. Exp.Cell Res. 2002; 273: 169-177.
24. Braun, M., Pietsch, P., Schror, K., Baumann, G., and Felix, S.B. Cellular adhesion molecules on vascular smooth muscle cells. Cardiovasc.Res. 1999; 41: 395-401.
25. Rolfe, B.E., Muddiman, J.D., Smith, N.J., Campbell, G.R., and Campbell, J.H. ICAM-1 expression by vascular smooth muscle cells is phenotype-dependent. Atherosclerosis 2000; 149: 99-110.
26. Clymann, R.I., Goetzman, B.W., Chen, Y.QI., Mauray, F., Kramer, R.H., Pytela, R., and Schnapp, L.M. Changes in endothelial cell and smooth muscle cell integrin expression during closure of the ductus arteriosus: an immunohistochemical comparison of the fetal, preterm newborn, and full-term newborn rhesus monkey ductus. Ped.Res. 1996; 40: 198-208.
27. Ross, R. Atherosclerosis--an inflammatory disease. N.Engl.J.Med. 1999; 340: 115-126.
28. Ratcliff, A. Tissue engineering of vascular grafts. Matrix Biology 2000; 19: 353-357.
29. Jankowski, R.J. and Wagner, W.R. Directions in cardiovascular tissue engineering. Clin.Plast.Surg. 1999; 26: 605-16, ix.
30. Campbell, J.H., Efendy, J.L., and Campbell, G.R. Novel vascular graft grown within recipient's own peritoneal cavity. Circ.Res. 1999; 85: 1173-1178.

31. Shimizu, K. and *et al*. Host bone marrow cells are a source of donor intimal smooth muscle-like cells in murine aortic transplant arteriopathy. Nature Med 2001; 7: 738-741.
32. Cines, D.B., Pollak, E.S., Buck, C.A., Loscalzo, J., Zimmerman, G.A., McEver, R.P., Pober, J.S., Wick, T.M., Konkle, B.A., Schwartz, B.S., Barnathan, E.S., McCrae, K.R., Hug, B.A., Schmidt, A.M., and Stern, D.M. Endothelial cells in physiology and in the pathophysiology of vascular disorders. Blood 1998; 91: 3527-3561.
33. Libby, P. Inflammation in atherosclerosis. Nature 2002; 420: 868-874.
34. Ross, R. The pathogenesis of atherosclerosis: a perspective for the 1990s. Nature 1993; 362: 801-809.
35. Bennett, M.R. Apoptosis of vascular smooth muscle cells in vascular remodelling and atherosclerotic plaque rupture. Cardiovasc.Res. 1999; 41: 361-368.
36. Mayr, M. and Xu, Q. Smooth muscle cell apoptosis in arteriosclerosis. Exp.Gerontology 2001; 36: 969-987.
37. Liu, S.Q. Biomechanical basis of vascular tissue engineering. Crit.Rev.Biomed.Eng 1999; 27: 75-148.
38. Seifalian, A.M., Salacinski, H.J., Tiwari, J., Edwards, A., Bowald, S., and Hamilton, G. *In vivo* biostability of a poly(carbonate-urea)urethane graft. Biomaterials 2003; 24: 2549-2557.
39. Faries, P.L., LoGerfo, F.W., Arora, S., Hook, S., Pulling, M.C., Akbari, C.M., Campbell, D.M., and Pomposelli, Jr.R.G. A comparative study of alternative conduits for lower extremity revascularization: all-autologous conduit versus prosthetic grafts. J.Vasc.Surg 2000; 32: 1080-1090.
40. Fattori, R. and Piva, T. Drug-eluting stents in vascular intervention. Lancet 2003; 361: 247-249.
41. Ardissino, D., Cavallini, C., Bramucci, E., Indolfi, C., Marzocchi, A., Manari, A., Angeloni, G., Carosio, G., Bonizzoni, E., Colusso, S., Repetto, M., and Merlini, P.A. Sirolimus-eluting vs uncoated stents for prevention of restenosis in small coronary arteries: a randomized trial. JAMA 2004; 292: 2727-2734.
42. Waugh, J. and Wagstaff, A.J. The paclitaxel (TAXUS)-eluting stent: a review of its use in the management of de novo coronary artery lesions. AM.J.Cardiovasc.Drugs 2004; 4: 257-268.
43. Bos, G.W., Poot, A.A., Beugeling, T., van Aken, W.G., and Feijen, J. Small-diameter vascular graft prostheses: current status. Arch.Physiol Biochem. 1998; 106: 100-115.
44. Zilla, P. Endothelialisation of vascular grafts. Curr.Opin.Cardiol. 1991; 6: 877-868.
45. Salacinsky, H.J., Tiwari, A., Hamilton, G., and Seifalian, A.M. Cellular engineering of vascular bypass grafts: role of chemical coatings for enhancing endothelial cell attachment. Med.Biol.Eng.Comput. 2001; 39: 609-618.
46. Meinhart, J.G., Deutsch, M., Fischlein, T., Howanietz, N., Froschl, A., and Zilla, P. Clinical autologous *in vitro* endothelialization of 153 infrainguinal ePTFE grafts. Ann.Thorac.Surg. 2001; 71: S327-S331.
47. Zdrahala, R.J. Small caliber vascular grafts. Part I: state of the art. J.Biomater.Appl 1996; 10: 309-329.
48. Deutsch, M., Meinhart, J., and Zilla, P. Graft endothelialization by *in vitro* lining. Atherosclerosis 2000; 151: 93-
49. Bos, G.W., Scharenborg, N.M., Poot, A.A., Engbers, G.H., Beugeling, T., van Aken, W.G., and Feijen, J. Endothelialization of crosslinked albumin-heparin gels. Thromb. Haemost. 1999; 82: 1757-1763.
50. Wissink, M.J., Beernink, R., Poot, A.A., Engbers, G.H., Beugeling, T., van Aken, W.G., and Feijen, J. Improved endothelialisation of vascular grafts by local release of growth factor from heparinized collagen matrices. J.Control.Release 2000; 64: 114-

51. Wissink, M.J., Beernink, R., Scharenborg, N.M., Poot, A.A., Engbers, G.H., Beugeling, T., van Aken, W.G., and Feijen, J. Endothelial cell seeding of (heparinized) collagen matrices: effects of bFGF pre-loading on proliferation (after low density seeding) and procoagulant factors. J.Control.Release 2000; 67: 141-155.
52. Langer, R. and Vacanti, J.P. Tissue Engineering. Science 1993; 260: 920-926.
53. Weinberg, C.B. and Bell, E. A blood vessel model constructed from collagen and cultured vascular cells. Science 1986; 231: 397-400.
54. Hirai, J. and Matsuda, T. Venous reconstruction using hybrid vascular tissue composed of vascular cells and collagen: tissue regeneration process. Cell Transplant. 1996; 5: 93-105.
55. L'Heureux, N., Paquet, S., Labbe, R., Germain, L., and Auger, F.A. A completely biological tissue-engineered human blood vessel. FASEB J. 1998; 12: 47-56.
56. Scherberich, A. and Beretz, A. Culture of vascular cells in tridimensional (3-D) collagen: a methodological review. Therapie 2000; 55: 35-41.
57. Niklason, L.E., Gao, J., Abbott, W.M., Hirschi, K.K., Houser, S., Marini, R., and Langer, R. Functional arteries grown *in vitro*. Science 1999; 284: 489-493.
58. Mooney, D.J., Mazzoni, C.L., Breuer, C., McNamara, K., Hern, D., Vacanti, J.P., and Langer, R. Stabilized polyglycolic acid fibre-based tubes for tissue engineering. Biomaterials 1996; 17: 115-124.
59. Kim, B.S., Putnam, A.J., Kulik, T.J., and Mooney, D.J. Optimizing seeding and culture methods to engineer smooth muscle tissue on biodegradable polymer matrices. Biotechnol.Bioeng. 1998; 57: 46-54.
60. Shum-Tim, D., Stock, U., Hrkach, J., Shinoka, T., Lien, J., Moses, M.A., Stamp, A., Taylor, G., Moran, A.M., Landis, W., Langer, R., Vacanti, J.P., and Mayer, J.E., Jr. Tissue engineering of autologous aorta using a new biodegradable polymer. Ann.Thorac.Surg. 1999; 68: 2298-2304.
61. Tiwari, A., Salacinski, H.J., Punshon, G., Hamilton, G., and Seifalian, A.M. Development of a hybrid cardiovascular graft using a tissue engineering approach. FASEB J 2002; 16: 791-796.
62. Ozaki, H. and Karaki, H. Organ culture as a useful method for studying the biology of blood vessels and other smooth muscle tissues. Jpn.J.Pharmacol. 2002; 89: 93-100.
63. Schmedlen, R.H., Elbjeirami, W.M., Gobin, A.S., and West, J.L. Tissue engineered small-diameter vascular grafts. Clin.Plas.Surg. 2003; 30: 507-517.
64. Davies, M.G. and Hagen, P. Pathophysiology of vein graft failure: a review. Eur.J.Vas.Endovasc.Surg. 1995; 9: 7-18.
65. Greenwald, S.E. and Berry, C.L. Improving vascular grafts: the importance of mechanical and haemodynamic properties. J.Pathol. 2000; 190: 292-299.
66. Mitchell, S.L. and Niklason, L.E. Requirements for growing tissue-engineered vascular grafts. Cardiovasc.Pathol. 2003; 12: 59-64.
67. Heimli, H., Kahler, H., Endresen, M.J., Henriksen, T., and Lyberg, T. A new method for isolation of smooth muscle cells from human umbilical cord arteries. Scand.J.Clin.Lab Invest 1997; 57: 21-29.
68. Negre-Aminou, P., van Vliet, A.K., van Erck, M., van Thiel, G.C., van Leeuwen, R.E., and Cohen, L.H. Inhibition of proliferation of human smooth muscle cells by various HMG-CoA reductase inhibitors; comparison with other human cell types. Biochim.Biophys.Acta 1996; 1345: 259-268.
69. Li, Y., Ma, T., Kniss, D.A., Lasky, L.C., and Yang, S. Effects of filtration seeding on cell density, spatial distribution, and proliferation in nonwoven fibrous matrices. Biotechnol.Prog. 2001; 17: 935-944.

70. Wendt, D., Marsano, A., Jakob, M., Heberer, M., and Martin, I. Oscillating perfusion of cell suspensions through three-dimensional scaffolds enhances cell seeding efficiency and uniformity. Biotechnol.Bioeng. 2003; 84: 205-214.
71. Campbell, J.H. and Campbell, G.R. Culture techniques and their applications to studies of vascular smooth muscle. Clin.Sci. 1993; 85: 501-513.
72. Jaffe, E.A., Nachman, R.L., Bedker, C.G., and Minick, C.R. Culture of human endothelial cells derived from umbilical veins. J.Clin.Invest. 1973; 52: 2756-
73. Kallmes, D.F., Lin, H.B., Fujiwara, N.H., Short, J.G., Hagspiel, K.D., Li, S.T., Matsumoto, A.H., and Gary, J. Becker young investigator award: comparison of small-diameter type 1 collagen stent-grafts and PTFE sten-grafts in a canine model--work in progress. J.Vasc.Intervent.Radiol. 2001; 12: 1127-1133.
74. Campbell, J.H., Walker, P., Chue, W., Daly, C., Cong, H., Xiang, L., and Campbell, G.R. Body cavities as bioreactors to grow arteries. Int.Congress.Series 2004; 1262: 118-121.
75. Chesler, N.C., Conklin, B.S., Han, H.C., and Ku, D.N. Simplified ex vivo artery culture techniques for porcine arteries. J.Vasc.Invest. 1998; 4: 123-127.
76. Chue, W.L., Campbell, G.R., Caplice, N., Muhammed, A., Berry, C.L., Thomas, A.C., Bennett, M.B., and Campbell, J.H. Dog peritoneal and pleural cavities as bioreactors to grow autologous vascular grafts. J.Vasc.Surg. 2004; 39: 859-867.
77. Stegeman, J.P. and Nerem, R.M. Altered response of vascular smooth muscle cells to exogenous biochemical stimulation in two-and three-dimensional culture. Exp.Cell Res. 2003; 283: 146-155.
78. Stegemann, J.P. and Nerem, R.M. Phenotype modulation in vascular tissue engineering using biochemical and mechanical stimulation. Ann.Biomed.Eng 2002; 31: 391-402.
79. Lee, A.A., Graham, D.A., Dela, C.S., Ratcliffe, A., and Karlon, W.J. Fluid shear stress-induced alignment of cultured vascular smooth muscle cells. J.Biomech.Eng. 2002; 124: 37-43.
80. Conklin, B.S., Surowiec, S.M., Lin, P.H., and Chen, C. A simple physiologic pulsatile perfusion system for the study of intact vascular tissue. Med.Eng.Phys. 2000; 22: 441-449.
81. Martin, I., Wendt, D., and Heberer, M. The role of bioreactors in tissue engineering. Trends Biotechnol. 2004; 22: 80-86.
82. Nasseri, B.A., Pomerantseva, I., Kaazempur-Mofrad, M.R., Sutherland, F.W.H., Perry, T., Ochoa, E., Thompson, C.A., Mayer, J.E., Oesterle, S.N., and Vacanti, J.P. Dynamic rotational seeding and cell culture system for vascular tube formation. Tissue Eng. 2003; 9: 291-299.
83. Surowiec, S.M., Conklin, B.S., Jin S.Li, Peter H.Lin, Victor J.Weiss, Alan B.Lumsden, and Changyi Chen. A new perfusion culture system used to study human vein. J.Surg.Res. 2000; 88: 34-41.
84. Papadaki, M. and Eskin, S.G. Effects of fluid shear stress on gene regulation of vascular cells. Biotechnol.Prog. 1997; 13: 209-221.
85. Seliktar, D., Nerem, R.M., and Galis, Z.S. Mechanical strain-stimulated remodeling of tissue-engineered blood vessel constructs. Tissue Eng. 2003; 9: 657-666.
86. Kanda, K. and Matsuda, T. Mechanical stress-induced orientation and ultrastructural change of smooth muscle cells cultured in three-dimensional collagen lattices. Cell Transplant. 1994; 3: 481-492.

87. Bader, A., Steinhoff, G., Strobl, K., Schilling, T., Brandes, G., Mertsching, H., Tsikas, D., Froelich, J., and Haverich, A. Engineering of human vascular aortic tissue based on a xenogeneic starter matrix. Transplantation 2000; 70: 7-14.
88. Hoerstrup, S.P., Zund, G., Sodian, R., Schnell, A.M., Grunenfelder, J., and Turina, M.I. Tissue engineering of small caliber vascular grafts. Eur.J.Cardiothorac.Surg. 2001; 20: 164-169.
89. Liu, S.Q. and Goldman, J. Role of blood shear stress in the regulation of vascular smooth muscle cell migration. Trans.Biomed.Eng. 2001; 48: 474-483.
90. Williams, B. Mechanical influences on vascular smooth muscle cell function. J.Hypertension 1998; 16: 1921-1929.
91. Seliktar, D., Black, R.A., Vito, R.P., and Nerem, R.M. Dynamic mechanical conditioning of collagen-gel blood vessel constructs induces remodeling *in vitro*. Ann.Biomed.Eng 2000; 28: 351-362.
92. Solan, A., Mitchell, S., Moses, M., and Niklason, L. Effect of pulse rate on collagen deposition in the tissue-engineered blood vessel. Tissue Eng. 2003; 9: 579-586.
93. Watase, M., Awolesi, M.A., Ricotta, J., and Sumpio, B.E. Effect of pressure on cultured smooth muscle cells. Life Sci. 1997; 61: 987-996.
94. Redmond, E.M., Cahill, P.A., Hirsch, M., Wang, Y.N., Sitzmann, J.V., and Okada, S.S. Effect of pulse pressure on vascular smooth muscle cell migration: the role of urokinase and matrix metalloproteinase. Thromb.Haemost. 1999; 81: 293-300.
95. Zandonella, C. Tissue engineering: the beat goes on. Nature 2003; 421: 884-886.
96. Watanabe, M., Shin'oka, T., Tohyama, S., Hibino, N., Konuma, T., Matsumura, G., Kosaka, Y., Ishida, T., Imai, Y., Yamakawa, M., Ikada, Y., and Morita, S. Tissue-engineered vascular autograft: inferior vena cava replacement in a dog model. Tissue Eng. 2001; 7: 429-439.
97. Shino'ka, T., Imai, Y., and Ikada, Y. Transplantation of a tissue-engineered pulmonary artery. N.Engl.J.Med. 2001; 344: 532-533.
98. Matsumura, G., Hibino, N., Ikada, Y., Kurosawa, H., and Shino'ka, T. Successful application of tissue engineered vascular autografts: clinical experience. Biomaterials 2003; 24: 2303-2308.
99. Matsumura, G., Miyagawa-Tomita, S., Shinoka, T., Ikada, Y., and Kurosawa, H. First evidence that bone marrow cells contribute to the construction of tissue-engineered vascular autografts *in vivo*. Circulation 2003; 108: 1729-1734.
100. Evan, G.I. and Vousden, K.H. Proliferation, cell cycle and apoptosis in cancer. Nature 2001; 411: 342-348.
101. Mallat, Z. and Tedgui, A. Current perspective on the role of apoptosis in atherothrombotic disease. Circ.Res. 2001; 88: 998-1003.
102. Kolodgie, F.D., Narula, J., Guillo, P., and Virmani, R. Apoptosis in human atherosclerotic plaques. Apoptosis 1999; 4: 5-10.
103. Dimmeler, S., Haendeler, J., and Zeihe, A.M. Regulation of endothelial cell apoptosis in atherothrombosis. Curr.Opin.Lipidol. 2002; 13: 531-536.
104. Kaiser, D., Freyberg, M.A., and Friedl, P. Lack of hemodynamic forces triggers apoptosis in vascular endothelial cells. Biochem.Biophys.Res.Commun. 1997; 231: 586-590.
105. Rossig, L., Dimmeler, S., and Zeiher, A.M. Apoptosis in the vascular wall and atherosclerosis. Basic Res.Cardiol. 2001; 96: 11-22.

106. Bornfeldt, K.E. Intracellular signaling in arterial smooth muscle migration versus proliferation. Trends Cardiovasc.Med. 1996; 6: 143-151.

107. Flynn, P.D., Byrne, C.D., Baglin, T.P., Weissberg, P.L., and Bennett, M.R. Thrombin generation by apoptotic vascular smooth muscle cells. Blood 1997; 89: 4378-4384.

108. Bennett, M.R., Gibson, D., Schwartz, S.M., and Tait, J.F. Binding and phagocytosis of apoptotic rat vascular smooth muscle cells is mediated in part by exposure to phosphatidylserine. Circ.Res. 1995; 77: 1136-1142.

109. Vermes, I. and Haanen, C. Apoptosis and programmed cell death in health and disease. Adv.Clin.Chem. 1994; 31: 177-246.

110. Vermes, I., Haanen, C., and Reutelingsperger, C. Flow cytometry of apoptotic cell death. J.Immunol.Methods 2000; 243: 167-190.

111. Darzynkiewicz, Z., Bedner, E., and Smolewski, P. Flow cytometry in analysis of cell cycle and apoptosis. Semin.Hematol. 2001; 38: 179-193.

112. Orlov, S.N., Dam, T.V., Tremblay, J., and Hamet, P. Apoptosis in vascular smooth muscle cells: role of cell shrinkage. Biochem.Biophys.Res.Commun. 1996; 221: 708-715.

113. Orlov, S.N., Pchejetski, D., Taurin, S., Thorin-Trescases, N., Maximov, G.V., Psezhtetsky, A.V., Rubin, A.B., and Hamet, P. Apoptosis in serum-deprived vascular smooth muscle cells: Evidence for cell volume-independent mechanism. Apoptosis 2004; 9: 55-66.

114. Pelisek, J., Armeanu, S., and Nikol, S. Quiscence, cell viability, apoptosis and necrosis of smooth muscle cells using different growth inhibitors. Cell Prolif. 2001; 34: 305-320.

115. Frisch, S.M. and Francis, H. Disruption of epithalial cell-matrix interactions induces apoptosis. J.Cell Biol. 1994; 124: 619-626.

116. Frisch, S.M. and Screaton, R.A. Anoikis mechanisms. Cell Biol. 2001; 13: 555-562.

117. Grossman, J., Walther, K., Artinger, M., Kiesslinkg, S., and Scholmerich, J. Apoptotic signaling during initiation of detachment-induced apoptosis ("anoikis") of primary human intestinal epithelial cells. Cell Growth Diff. 2001; 12: 147-155.

118. Grossman, J. Molecular mechanisms of "detachment-induced apoptosis - Anoikis". Apoptosis 2002; 7: 247-260.

119. Zhan, M., Zhao, H., and Han, Z.C. Signalling mechanisms of anoikis. Histol.Histopathol. 2004; 19: 973-983.

120. Lance, A. and Kohn, E. Cancer and the homeless cell. Nature 2004; 430: 973-974.

121. Vermes, I., Haanen, C., and Steffens-Nakken, H. A novel assay for apoptosis. Flow cytometric detection of phosphatidylserine expression on early apoptotic cells using fluorescein labelled Annexin V. J.Immunol Methods 1995; 184: 39-51.

122. Pechhold, K., Craighead, N., Wesch, D., and Kabelitz, D. Measurement of Cellular Proliferation. Methods Microbiol. 2000; 32: 77-97.

123. van Engeland, M., Ramakers, F.C.S., Schutte, B., and Reutelingsperger, C.P.M. A novel assay to measure loss of plasma membrane asymmetry during apoptosis of adherent cells in culture. Cytometry 1996; 24: 131-139.

124. Jones, L.J., Gray, M., Yue, S.T., Haugland, R.P., and Singer, V.L. Sensitive Determination of Cell Number using the CyQuant Cell Proliferation Assay. J.Immunol.Methods 2001; 254: 85-98.

125. Ohtsubo, M., Theodoras, A.M., Schumacher, J., Roberts, J.M., and Pagano, M. Human cyclin E, a nuclear protein essential for the G1-to-S phase transition. Mol.Cell Biol. 1995; 15: 2612-2624.

126. Ikezawa, K., Ohtsubo, M., Norwood, T.H., and Narayanan, A.S. Role of Cyclin E and Cyclin E-dependent kinase in mitogenic stimulation by cementum-derived growth factor in human fibroblasts. FASEB J 1998; 12: 1233-1239.

127. Keyomarsi, K., Tucker, S.L., Buchholz, T.A., Callister, M., Ding, Y., Horogagyi, G.N., Bedrosian, I., Knickerbocker, C., Toyofuku, W., Lowe, M., Herliczek, T.W., and Bacus, S.S. Cyclin E and survival in patients with breast cancer. N.Engl.J.Med. 2002; 347: 1566-1575.

128. Muller-Tidow, C., Metzger, R., Kugler, K., Diederichs, S., Idos, G., Thomas, M., Dockhorn-Dworniczak, B., Schneider, P.M., Koeffler, H.P., Berdel, W.E., and Serve, H. Cyclin E is the only cyclin-dependent kinase 2-associated cyclin that predicts metastasis and survival in early stage non-small cell lung cancer. Canc.Res. 2001; 61: 647-653.

129. Sutherland, R.L. and Musgrove, E.A. Cyclin E and prognosis in patients with breast cancer. N.Engl.J.Med. 2002; 347: 1546-1547.

130. Allen, R.T., Hunter, W.J., and Agrawal, D.K. Morphological and biochemical characterization and analysis of apoptosis. J.Pharmacol.Toxicol.Methods 1997; 37: 215-228.

131. Michie, J., Akudugu, J., Binder, A., Van Rensburg, C.E.J., and Bohm, L. Flow cytometric evaluation of apoptosis and cell viability as a criterion of anti-tumour drug toxicity. Anticanc.Res. 2003; 23: 2675-2680.

132. King, M.A. and Radicchi-Mastroianni, M.A. Effects of caspase inhibition on camptothecin-induced Apoptosis of HL-60 cells. Apoptosis 2002; 49: 28-35.

133. Nicoletti, I., Migliorati, G., Pagliacci, M.C., Grinani, F., and Riccardi, C. A rapid and simple method for measuring thymocyte apoptosis by propidium iodide staining and flow cytometry. J.Immunol.Methods 1991; 139: 271-273.

134. Micoud, F., Mandrand, B., and Malcus-Vocanson, C. Comparison of several techniques for the detection of apoptotic astrocytes *in vitro*. Cell Prolif. 2001; 34: 99-113.

135. Salgame, P., Varadhachary, A.S., Primiano, L.L., Fincke, J.E., Muller, S., and Monestier, M. An ELISA for detection of apoptosis. Nucleic Acids Res. 1997; 25: 680-681.

136. Volokhina, E.B., Hulshof, R., Haanen, C., and Vermes, I. Tissue transglutaminase mRNA expression in apoptotic cell death. Apoptosis 2003; 8: 679-

137. Fesus, L. and Piacentini, M. Transglutaminas 2: An enigmatic enzyme with diverse fundctions. Trends Biochem.Sci. 2002; 27: 534-539.

138. Melino, G., Candi, E., and Steiner, P.M. Assays for transglutaminases in cell death. Methods Enzymol. 2000; 322: 433-472.

139. Heid, C.A., Stevens, J., Livak, K.J., and Williams, P.M. Real time quantitative PCR. Genome Res. 1996; 6: 986-994.

140. Smolewski, P., Bedner, E., Du, L., Hsieh, T.C., Wu, J.M., Phelps, D.J., and Darzynkiewicz, Z. Detection of caspases activation by fluorochrome-labeled inhibitors: Multiparameter analysis by laser scanning cytometry. Cytometry 2001; 44: 73-82.

141. Smolewski, P., Grabarek, J., Lee, B.W., Johnson, G.L., and Darzynkiewicz, Z. Kinetics of HL-60 cell entry to apoptosis during treatment with TNF-alpha or camptothecin assayed by the stathmo-apoptosis method. Cytometry 2002; 47: 143-149.

142. Wolbers, F., Buijtenhuijs, P., Haanen, C., and Vermes, I. Apoptotic cell death kinetics *in vitro* depend on the cell types and the inducers used. Apoptosis 2004; 9: 385-392.

143. Piotr Smolewski, Jerzy Grabarek, H.Dorota Halicka, and Zbigniew Darzynkiewicz. Assay of caspase activation in situ combined with probing plasma membrane integrity to detect three distinct stages of apoptosis. Apoptosis 2002; 265: 111-121.

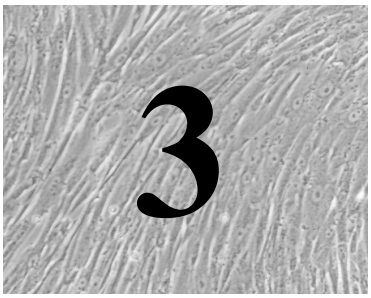

3

Tissue Engineering of Blood Vessels: Characterisation of Smooth Muscle Cells for Culturing on Collagen-and-Elastin-Based Scaffolds*

* P. Buijtenhuijs[1, 2], L. Buttafoco[1], A.A. Poot [1], W.F. Daamen[3], T.H. van Kuppevelt[3], P.J. Dijkstra[1], R.A.I. de Vos[4], L.M.T. Sterk[4], R.H. Geelkerken[2], J. Feijen[1], I. Vermes[1, 2]

Biotechnol. Appl. Biochem. 2004; 39: 141-149

[1] University of Twente, Faculty of Science & Technology, Department of Polymer Chemistry and Biomaterials, and Institute of Biomedical Technology (BMTI), P.O. Box 217, 7500 AE Enschede, The Netherlands

[2] Medisch Spectrum Twente, Hospital Group, Departments of Clinical Chemistry and Vascular Surgery, P.O. Box 50.000, 7500 KA Enschede, The Netherlands

[3]University Medical Centre Nijmegen, Department of Biochemistry 194, NCMLS, P.O. Box 9101, 6500 HB Nijmegen, The Netherlands

[4]Laboratory of Pathology Oost-Nederland, P.O. Box 377, 7500 AJ Enschede, The Netherlands

Abstract

Tissue engineering offers the opportunity to develop vascular scaffolds that mimic the morphology of natural arteries. We have developed a porous three-dimensional scaffold consisting of fibres of collagen and elastin interspersed together. Scaffolds were obtained by freeze-drying a suspension of insoluble type I collagen and insoluble elastin. In order to improve the stability of the obtained matrices, they were crosslinked by two different methods. A water-soluble carbodiimide, alone or in combination with a diamine, was used for this purpose: zero- or non-zero-length crosslinks were obtained. The occurrence of crosslinking was verified by monitoring the thermal behaviour and the free-amino-group contents of the scaffolds before and after crosslinking. Smooth muscle cells (SMCs) were cultured for different periods of time and their ability to grow and proliferate was investigated. SMCs were isolated from human umbilical and saphenous veins and the purity of the cultures obtained was verified by staining with a specific monoclonal antibody (mAb). Cultured cells were also identified by mAb against muscle actin and vimentin. After 14 d, a confluent layer of SMCs was obtained on non-crosslinked scaffolds. As for the crosslinked samples, no differences in cell attachment and proliferation were observed between scaffolds crosslinked using the two different methods. Cells cultured on the scaffolds were identified with an anti (α-smooth muscle actin) mAb. The orientation of SMCs resembled that of the fibres of collagen and elastin. In this way, it may be possible to develop tubular porous scaffolds resembling the morphological characteristics of native blood vessels.

Introduction

Atherosclerosis and related vascular diseases are the major causes of morbidity and mortality in the industrial world [1-4]. Atherosclerotic lesions are the result of an inflammatory response and damage of the arterial wall complicated by excessive lipid deposition [5]. Acute ischemic syndromes (i.e. unstable angina, myocardial infarction and stroke), aortic aneurysm and gangrene of the extremities are severe clinical manifestations of atherosclerosis. A method to overcome these clinical symptoms is the insertion of a bypass graft around an artery blocked or impeded by plaques.

The most common vascular graft for this application is an autologous saphenous vein or a mammary artery [4]. Both are flexible, viable, non-thrombogenic and biocompatible. Patency rates of these grafts are quite high, depending on the site of implantation [6, 7]. However, in around 30% of patients who undergo vascular reconstructions, a saphenous vein is

unavailable [8]; moreover, a mammary artery may not always have the proper size or length [4]. The scarcity of non-affected autologous grafts in patients with vascular diseases have led in the last decades to the use of synthetic vascular prosthesis, such as Dacron® fabric grafts [poly (ethylene terephthalate)] and Teflon® grafts [expanded poly(tetrafluoro ethylene)] [9, 10].

However, owing to early thrombotic occlusion of the smaller vessels, these synthetic materials represent a suitable alternative only for high-flow low-resistance conditions, which means large-diameter arteries (> 6 mm). In general, endothelialization of vascular grafts with autologous endothelial cells (ECs) prior to implantation would significantly improve graft patency [11]. Nowadays, inadequate EC adhesion and/or growth and cell detachment after restoration of the blood circulation form major obstacles in the development of functional small-diameter vascular prostheses [12]. On the other hand, results obtained by Zilla and co-workers [13] have shown that endothelialized expanded poly(tetrafluoroethylene) grafts perform equally to vein grafts in large-diameter blood vessels.

Tissue engineering is a new branch of science that combines the principles of engineering and life science, and has as an ultimate aim the creation of 'off-the-shelf' new organs [14-18]. As viable structures, tissue-engineered (TE) blood vessels should represent a responsive and self-renewing tissue with the inherent potential of healing and remodelling according to the requirements of their specific environment. Generally, most tissue engineering approaches rely on biodegradable synthetic or natural materials as a scaffold to provide a temporary biomechanical structure until autologous cells produce their own extra-cellular matrix [17]. For TE small-diameter blood vessels, several types of synthetic biodegradable polymers have been used including poly(glycolic acid) [17, 19-22], poly(lactic acid-glycolic acid), poly(*L*-lactic acid) and poly(carbonate-urea)urethane. In particular, a successful clinical implantation of a TE poly(carbonate-urea)urethane graft has been performed by Seifalian *et al.* [8]. Their study showed that the compliance properties of the vascular graft are retained post-implantation. Another implantation study of TE blood vessel is that of Shin'oka *et al.* [23]. They used a polyhexanolactone-poly(lactic acid) copolymer reinforced with woven poly(glycolic acid) and showed that the transplanted vessel was completely patent. Type-I-collagen structures [24-26] have also been studied extensively as a natural scaffold for the development of TE small-diameter blood vessels [20, 21, 24, 25]. However, no long-term successful application for such small-diameter vascular grafts has so far been described.

Our approach consists of preparing a TE blood vessel characterised by the same three-layered structure that is present in a native artery [27]. Until now, we have focused on the culture of smooth muscle cells (SMCs) from human umbilical and saphenous veins on biodegradable

flat scaffolds composed of insoluble collagen and insoluble elastin. Attempts to engineer blood vessels from collagen/elastin matrices have already been made in the past, but either decellularized matrices [28] or soluble proteins [29, 30] have been used. Despite the fact that (non-) autologous decellularized matrices may be an ideal solution in terms of composition, donor-site morbidity has to be taken into account. Moreover, when non-autologous or xenogeneic grafts are used, foreign-body responses have to be taken into consideration as well [31].
In the present paper the preparation and crosslinking of scaffolds obtained from collagen and elastin are described. Culturing of SMCs and their ability to grow and proliferate on such scaffolds has been investigated.

Materials

Insoluble collagen (type I from bovine Achilles tendons) and insoluble elastin (from equine ligamentum nuchae, purification as described in [32]) were kindly donated by Dr. T.H. van Kuppevelt, Department of Biochemistry, University Medical Centre Nijmegen, The Netherlands. Dulbecco's Modified Eagle's Medium (DMEM) was purchased from Gibco BRL (Breda, The Netherlands). Penicillin, streptomycin, fetal bovine serum and trypsin were purchased from Biowhittaker (Verviers, Belgium). Collagenase type 2 was purchased from Worthington Biochemical Corporation (Lakewood, NJ, USA). Paraformaldehyde, triton X-100 and glycine were from Merck Eurolab (Poole, Dorset, UK). Mouse monoclonal antibodies (mAbs) against human α-smooth muscle actin (α-SMA), human muscle actin (clone HHF35) and human vimentin, fluorescein isothiocyanate-labelled rabbit anti-mouse immunoglobulins (RAM-FITC) and fluorescent mounting media used for immuno fluorescence were purchased from DAKO (Glostrup, Denmark). Pooled human serum was acquired by overnight incubation of whole blood (from 16 healthy donors given with their informed consent) at 21^0C. Serum was obtained by centrifugation and subsequently pooled and stored at -80^0C. Morpholino ethane sulphonic acid (MES), N-(3-dimethylaminopropyl)-N'-ethylcarbodiimide hydrochloride (EDC), N-hydroxysuccinimide (NHS), poly(propylene glycol)-bis-(2-aminopropyl ether) (Jeffamine 230, J230) and all other chemicals were obtained from Sigma and Aldrich (St Louis, Missouri, USA).

Methods

Preparation of porous structures

A 2% (w/v) suspension of type I insoluble collagen derived from bovine Achilles tendon and insoluble elastin derived from equine ligamentum nuchae was swollen overnight at 6^0C in

0.05 M acetic acid. The suspension was homogenised first with a Philips Blender for 4 min and then for 15 min at 4^0C with an Ultra-Turrax T25 instrument (IKA Labortechnik, Staufen, Germany). The resulting suspension was frozen at -18^0C and subsequently freeze-dried.

Crosslinking

Collagen/elastin samples were crosslinked by two different methods. In both cases, N-(3-dimethylaminopropyl)-N'-ethylcarbodiimide hydrochloride (EDC) was used in combination with N-hydroxysuccinimide (NHS) (Scheme 1a). In the second method poly(propylene glycol)-bis-(2-aminopropyl ether) (J230) was added in combination with EDC and NHS [33] (Scheme 1b).

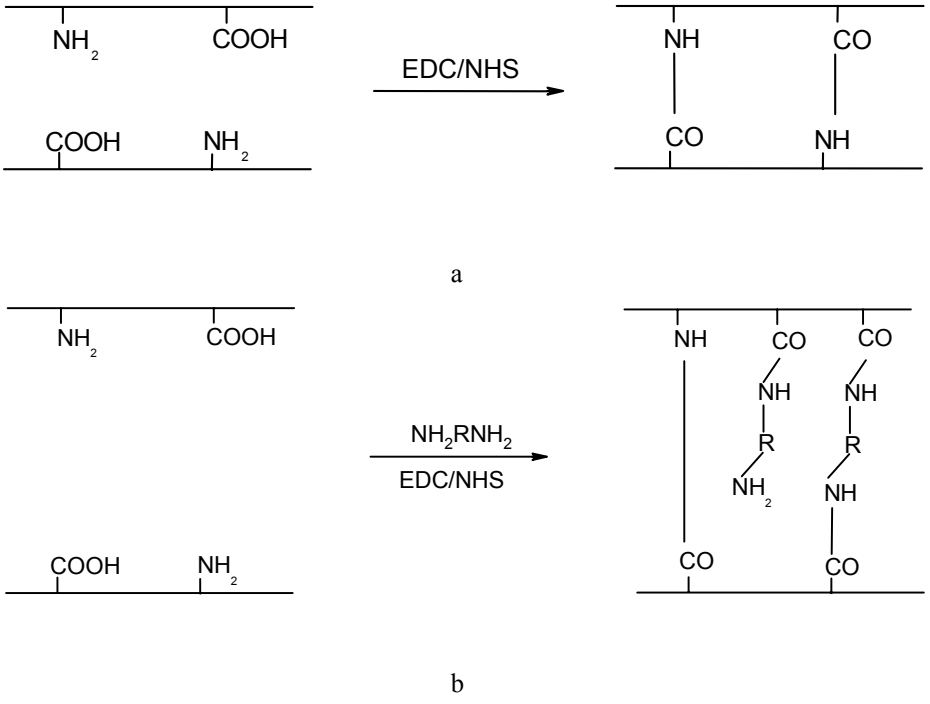

Scheme 1: Scheme of the crosslinking reactions of collagen/elastin scaffolds with EDC/NHS (a) and with J230/EDC/NHS (b).

Method 1: Crosslinking was carried out using 0.05 M MES buffer in 40% (v/v) ethanol (215 mL/g of sample) at pH 5.5 and 2.3 g of EDC and 0.56 g of NHS/g of collagen/elastin (EDC/NHS molar ratio: 0.4:1). The reaction was allowed to proceed for 2 h at room temperature. Samples were then washed for 2 h in 0.1 M Na_2HPO_4 to eliminate any EDC that had not reacted. A further washing step was performed with MilliQ water for another 2 h; water was changed every 30 min The obtained matrices were frozen at a temperature of -18^0C and then freeze-dried.

Method 2: The reaction was performed by adding the scaffolds to a buffered (0.05 M MES, pH 5.5 in 40% (v/v) ethanol) 0.062 M J230 solution (215 mL/g of sample). After 30 min, 5.75 g of EDC and 1.38 g of NHS were added/g of sample and crosslinking was performed overnight (molar ratio of J230: EDC: NHS: 2.1: 1: 0.4). The samples were then rinsed in Na_2HPO_4 and MilliQ water and subsequently freeze-dried as described above.

Determination of free-primary-amine-group content

The number of free primary amine groups present in a (crosslinked) collagen/elastin sample was determined using 2,4,6-trinitrobenzenesulfonic acid (TNBS) according to the following procedure.

Samples (3-5 mg) were incubated for 30 min in 1 mL of 4% (w/v) $NaHCO_3$. Then, 1 mL of TNBS (0.5% (w/v) in $NaHCO_3$) solution was added and the mixture was incubated at 40^0C for 2 h. In order to hydrolyse the samples, 3 mL of 6 M HCl was then added. This was performed at 60^0C for 90 min After dilution with 5 mL of MilliQ water and cooling to room temperature, the absorbance at 345 nm and/or at 420 nm was measured using a Varian Cary 300 Bio spectrophotometer. A reference solution was made by exactly the same procedure, except that HCl was added prior to adding TNBS.

The intensity of the absorbance was correlated with the concentration of free amino groups using a calibration curve obtained by measuring the absorbance of various glycine solutions having different concentrations (stock solution: 10 mg of glycine in 100 mL of 4% (w/v) $NaHCO_3$).

Shrinkage temperature

The shrinkage temperature of (crosslinked) collagen/elastin samples was measured using differential scanning calorimetry (DSC 7 instrument; Perkin Elmer, Norwalk, CT, USA). Samples (approximately 5 mg) were swollen overnight in 50 μL of PBS in high-pressure capsules. Samples were heated from 20 °C to 90 °C at a heating rate of 10^0C/min PBS was used as a reference. The onset of the endothermic peak, which indicates denaturation of the collagen triple helix, was recorded as the shrinkage temperature.

Structure and morphology of porous scaffolds

The structure and morphology of the samples were studied by means of histology and scanning electron microscopy respectively.

Different samples were embedded in paraffin and parallel and transverse sections were stained with the Masson Trichrome technique. Because of their different reactivities with the stains used, it was possible, in this way, to distinguish between collagen and elastin portions of the sample. In particular, Methyl Blue and Acid Fuchsine were used (Masson Trichrome technique) to stain respectively collagen (blue) and elastin (pink) [34]. The surface morphology of the scaffolds was examined using scanning electron microscopy. Samples were freeze-dried before analysis and then sputter-coated with gold in a Polaron E5600 sputter coater. Images were recorded with a scanning electron microscope (Leo Gemini 1550 FEG-SEM) working at different acceleration voltages.

Isolation and culturing of SMCs

SMCs were isolated from human umbilical and saphenous veins. Umbilical cords were obtained from women terminating normal pregnancies. Samples of saphenous veins were obtained from patients undergoing coronary artery bypass surgery. The procedures followed are in accordance with the policies of the Institutional ethical review board of the Hospital Group and all patients gave their informed consent. A segment of an umbilical vein or saphenous vein was cannulated at both ends, and cannules were kept in position with surgical sutures. The lumen of the blood vessel was carefully flushed several times with PBS to remove blood. The vein was then filled with 0.05% (w/v) trypsin/0.02% (w/v) EDTA and a moderate pressure was obtained by clamping the ends with haemostats. After incubation at 37^0C for 20 min, detached ECs were removed by flushing thoroughly with PBS. Subsequently a 0.075% (w/v) collagenase solution was introduced into the lumen of the blood vessel. After 45 min of digestion, SMCs were harvested by flushing thoroughly with culture medium. Cells were cultured to sub-confluence in 3-4 wks in a six-wells tissue culture polystyrene culture dish coated with gelatin (0.5% w/v) (g-TCPS), using DMEM containing 10% (v/v) filter-sterilised pooled human serum, 10% (v/v) filter-sterilised fetal bovine serum, 50 units/mL penicillin and 50 μg/mL streptomycin [35]. Culture medium was refreshed every 2 or 3 d. Cells were cultured in an incubator with humidified atmosphere at 37^0C and 5% CO_2 concentration [36]. When sub-confluent cultures were obtained, cells were detached with 0.125% (w/v) trypsin/0.05% (w/v) EDTA and subcultured for several passages up to 15 passages (with a split ratio of 1:3) [37].

Identification of SMCs by immuno fluorescent microscopy

Human umbilical-vein SMCs (passage 13) were cultured to 60% confluence on 0.5%-gelatin-coated glass slides. After washing with PBS, cells were fixed with 4% paraformaldehyde for 20 min, permeabilised with 0.2% triton X-100 for 5 min, quenched with 50 mM glycine for 5 min and washed again with PBS. Cell preparations were incubated with 2% BSA for 20 min and subsequently stained with a mAb against human α-SMA (1:50) for 30 min at 21^0C [35]. Preparations were further incubated for 30 min with RAM-FITC (1:100) in the dark at 21^0C and embedded in fluorescent mounting medium, before being examined with a Leitz Laborlux D microscope equipped with an Osram 100-W lamp for fluorescein excitation. Negative controls were obtained by omitting first antibodies and by staining human umbilical-vein ECs and human dermal fibroblasts with these antibodies.

Identification of SMCs by flow cytometry

Human umbilical vein SMCs (passage 13) were cultured in a six-wells TCPS culture dish to 80% confluence and removed from culture wells by trypsinisation. After centrifugation (300 g, 10 min, 21^0C), 70% (v/v) ethanol-fixed cells were incubated with 2% BSA in PBS for 20 min at 21^0C. Cell suspensions were then incubated for 30 min at 21^0C with mAbs against human α-SMA (1:50), human muscle actin (clone HHF35, 1:50) or human vimentin (1:25) followed by an incubation with RAM-FITC for a further 30 min in the dark at 21^0C. Cells were resuspended in PBS, filtered and measured on a Coulter flow cytometer [38]. Negative controls were obtained by omitting first antibodies and by staining human umbilical-vein ECs and human dermal fibroblasts with these antibodies.

Culturing SMCs on scaffolds of collagen and elastin

Flat porous matrices based on collagen and elastin with a defined pore size were used to examine the interaction of SMCs with these scaffolds. Scaffolds were sized to a diameter of 16 mm with a punching tool and were placed in 24-wells TCPS culture dishes with Viton O-rings (Eriks, Alkmaar, The Netherlands). Scaffolds were sterilised with 70% ethanol and washed three times with PBS. Sub-confluent cultures of human umbilical-vein SMCs were harvested by trypsinisation, centrifuged at 300 g for 10 min at 21^0C and resuspended in fresh culture medium. Cells were counted with a hemacytometer (Bürker, Marienfeld, Germany), seeded at a density of 200.000 cells/cm^2 [39] on the scaffolds and subsequently cultured under static conditions for up to 14 d in culture medium. Culture medium was refreshed every 2 or 3 d. After culturing, samples were fixed with formalin, impregnated with paraffin, cut into

transverse sections and stained using the standard elastic Van Gieson method at the Laboratory of Pathology Oost Nederland according to standard procedures. To identify SMCs, samples were also stained for α-SMA.

Results

Morphology of the porous collagen/elastin scaffolds

The morphology of the obtained porous scaffolds is highly dependent on the freezing temperature. The formation of water crystals in the structure during the freezing step determines the size of the pores obtained after freeze-drying [40]. In the present study, a temperature of -18^0C was used since under these conditions, scaffolds having a porosity of 98% and a pore size around 200 μm are obtained (figure 1). A very high porosity and a suitable pore size are in fact necessary requirements for SMCs to grow and proliferate into the scaffolds.

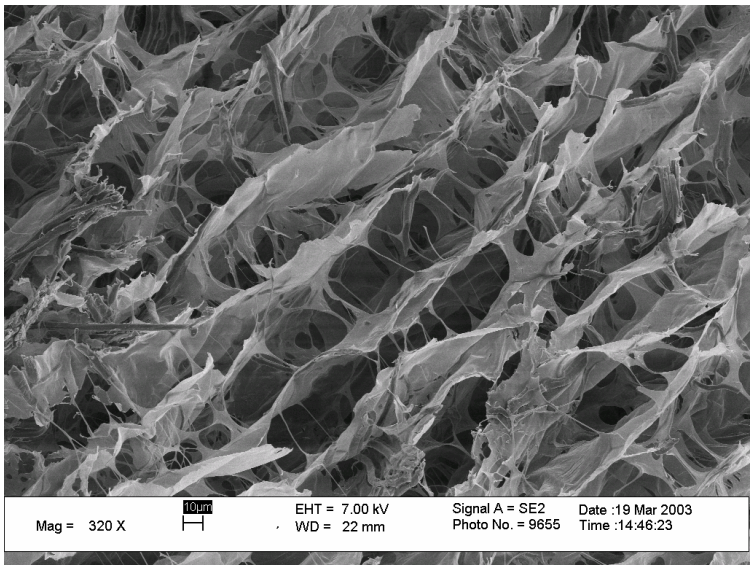

Figure 1: Scanning electron microscopy of a cross section of a collagen/elastin porous scaffold obtained by freeze-drying. (magnification 275X)

An interesting feature of the collagen/elastin samples is the ability of collagen to wrap elastin fibres and form a bridge between them. This was evident from both scanning electron microscope and histological pictures (figures 2a and 2b). Such an organized, open porous structure is retained also after crosslinking with either EDC/NHS or J230. After crosslinking, pores are > 80 μm in size, which is still big enough for SMCs to migrate into the scaffolds.

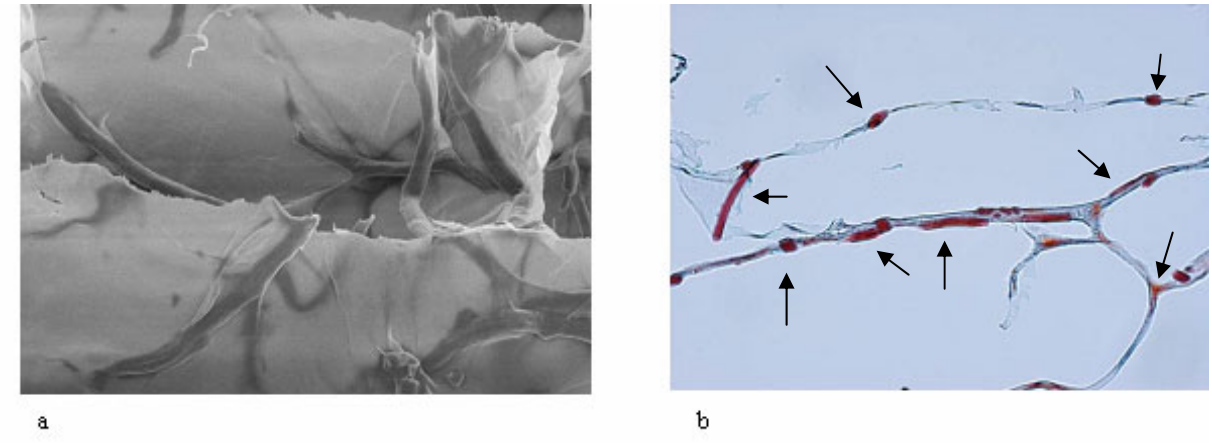

Figure 2: Scanning electron microscope and optical microscope pictures of the collagen/elastin matrix. Scanning electron microscope picture of a collagen/elastin matrix obtained by freeze-drying (a, magnification 1001X). The biggest fibres are elastin. Optical microscope picture of a histological transverse section of the collagen/elastin matrix stained with the Masson Trichrome technique (b, magnification 25X; elastin and collagen fibres are shown in black and grey respectively). Elastin fibres are indicated by an arrow.

Crosslinking

Crosslinking of collagen/elastin samples with a carbodiimide such as EDC involves the activation of carboxylic groups of glutamic and aspartic acid residues present on collagen/elastin scaffolds and the formation of zero-length bonds with the lysine and hydroxylysine residues. The behaviour of EDC has been well characterized in previous studies [33, 41]. An advantage of this crosslinking method is that, in this way, no foreign product is introduced and stable zero-length covalent linkages are produced between activated side groups. The presence of NHS is necessary in order to prevent secondary reactions [33, 42]. On the contrary, when the diamine is used, non-zero length crosslinks are also formed between two carboxylic acid groups of glutamic and/or aspartic residues. When compared with a zero-length crosslinked system, this structure permits more freedom of movement and consequently improved elasticity. The crosslinking efficiency was verified by measuring both the denaturation temperature and the content of free amino groups before and after crosslinking (Table 1). With the EDC/NHS system, a 76% decrease of free amino groups is observed, while the denaturation temperature increases to 80^0C.

Table 1: Free-amino-group content and denaturation temperature of (crosslinked) collagen/elastin samples.

Crosslinking method	*Free-amino-group content (nmol/mg)*	*Denaturation temperature (^{0}C)*
None	106.3	48.5 ± 0.5
EDC/NHS	25.4	80.0 ± 0.5
J230/EDC/NHS	68.9	74.5 ± 1.5

When J230 is used as a crosslinker, non-zero-length bonds between two carboxylic acid groups are also formed. Their activation is achieved by performing the reaction to take place in the presence of EDC/NHS. In this case an increase in denaturation temperature and a decrease in free amino groups can also be observed with respect to the non-crosslinked system (Table 1). When J230/EDC/NHS was used 68.9 nmol of amino groups/mg are present as compared to 106.3 nmol/mg in the non-crosslinked collagen/elastin matrix. During the reaction zero-length crosslinks can be formed as well as crosslinks via J230. Moreover there is also a possibility that J230 has only reacted at one side, leading to dangling groups containing amino end groups. The crosslinked scaffolds have a denaturation temperature of 74.5^{0}C, which is comparable with that of the EDC/NHS crosslinked scaffolds. Usually dangling groups destabilize helical structures and therefore it can be concluded that the crosslinking with the J230/EDC/NHS system was quite effective. The degree of crosslinking by zero-length coupling by J230/EDC/NHS and determination of the number of dangling groups is under investigation.

Identification of SMCs

Human SMCs have been successfully isolated and cultured from umbilical and saphenous veins using the collagenase-digestion method. Cultured cells are identified by the presence of the morphologically characteristic hill-and-valley pattern using phase-contrast microscopy and by immuno fluorescence staining techniques using specific mAbs against human α-SMA, human muscle actin (clone HHF35) and human vimentin. Immuno fluorescent microscopy, as well as flow cytometry, were performed as shown in figure 3. Filaments of α-SMA are clearly visible in human umbilical vein SMCs (figure 3a) as well as in saphenous vein SMCs. Fibroblasts isolated from human skin and ECs isolated from human umbilical veins, did not show fluorescence (results not shown). Fluorescence was also measured by flow cytometry. Histograms in figure 3 show the number of cells compared with fluorescence intensity. In this

way, 98% of the treated cells were shown to be positively stained with the mAb against human α-SMA as against 2% of the negative control cells in which the first antibody is omitted (figure 3b). The mAb against human muscle actin (clone HHF35) did not stain SMCs in a specific way; peaks of positively stained cells and negative control cells were overlapping so percentages of stained cells cannot be determined (figure 3c). With use of the mAb against human vimentin, 81% of the treated cells were positively stained as against 2% of the negative control cells (figure 3d).

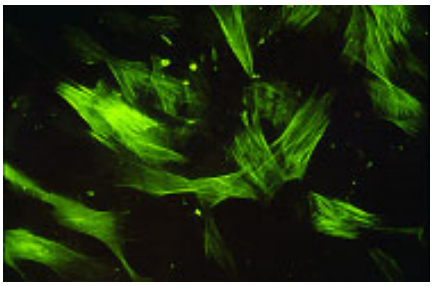

a

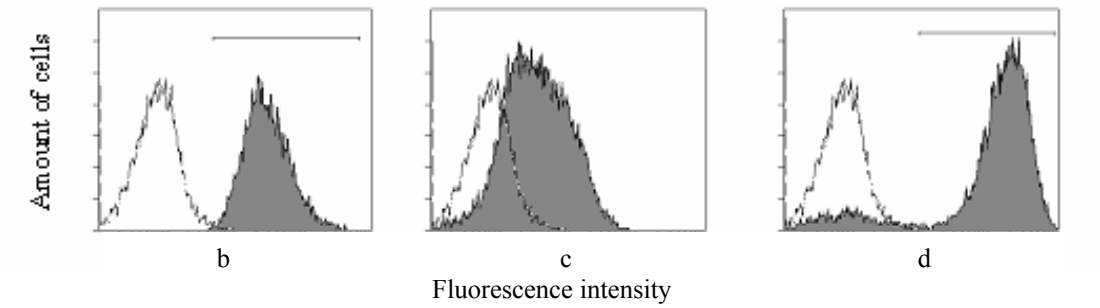

Figure 3: Immuno fluorescence staining (with FITC) of human α-SMA (a, b), human muscle actin (c) and human vimentin (d) in human vascular SMC cultures. Human umbilical-vein SMCs (passage 13) were cultured on glass slides to 60% confluence, and immuno fluorescent microscopy using the mAb against human α-SMA was performed (a, magnification 700X), or cells grown to 80% confluence and flow–cytometric analyses were performed using mAbs against human α-SMA (b), human muscle actin (clone HHF35, c) and human vimentin (d). Stained cells (dark-grey curves) were analysed and compared with negative control cells in which the first antibody was omitted (white curves). Horizontal bars (b and d): gate of stained cells to determine percentage of positively stained cells.

Culturing SMCs on scaffolds of collagen and elastin

SMCs adhere on flat scaffolds of collagen/elastin when cells are seeded with a density of 200.000 cells/cm^2. Differences in cell density were observed between non-crosslinked matrices on which cells were cultured for 7 and 14 d (figures 4a and 4b). A non-confluent cell

layer was obtained after 7 d of culturing, whereas after 14 d scaffolds were totally covered with SMCs. Cells grew in a multi layer on top of the matrix, and cells were also observed in between the fibres of collagen and elastin. Cells were oriented along the longitudinal axis of the collagen/elastin fibres.

No differences were observed in cell attachment and proliferation between collagen/elastin scaffolds crosslinked with either EDC/NHS or J230 in the presence of EDC/NHS (figures 4c and 4d). Immuno histochemical staining with the mAb against α-SMA gave a specific staining of the SMCs (results not shown).

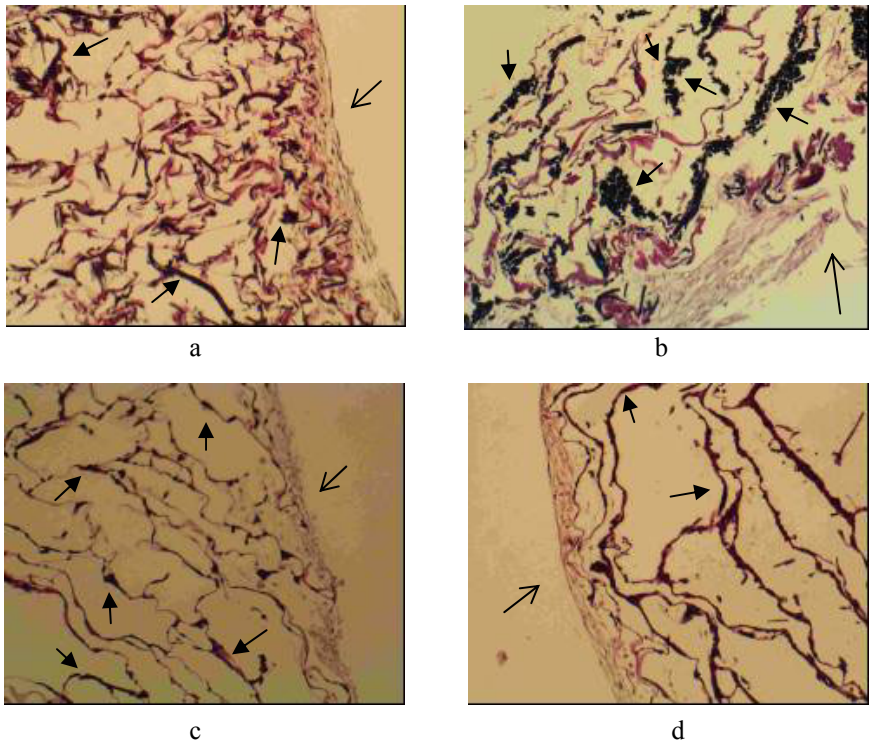

Figure 4: Histology of human umbilical-vein SMCs cultured on scaffolds of collagen and elastin. Transverse sections stained with the standard elastic Van Gieson method. Human umbilical-vein SMCs (passage 7) were seeded (200.000 cells/cm2) and cultured for 7 (a) and 14 (b) d on non-crosslinked collagen/elastin scaffolds (native) or cultured for 14 d on collagen/elastin scaffolds crosslinked with a carbodiimide (EDC/NHS, c) or crosslinked with a diamine (J230) in the presence of the carbodiimide (d). Magnification 100X. The SMC layer is indicated by a thin arrow (↑). Collagen and elastin are finely interspersed together, but the most evident elastin fibres are indicated by a filled arrow (↑).

Discussion

Collagen and elastin were chosen as the components of our scaffolds because these are the two most abundant proteins in native blood vessels. Scaffolds were prepared by freeze-drying a suspension of insoluble collagen and insoluble elastin. Porous three-dimensional scaffolds having a very high degree of porosity were obtained. From scanning electron microscopy and

histological analyses, it is possible to observe a certain interaction between the two proteins. In particular collagen is able to wrap elastic fibres. Moreover, the latter seem to follow the orientation of the collagenous part. This can be of extreme importance when the mechanical properties are taken into consideration. In fact, the strength of collagen can be coupled with the ability to elongate, which is typical of elastic fibres, thus contributing to the capacity to withstand the pulsations characterizing blood flow. Compliance and mechanical properties will be measured at a later stage when tubular scaffolds are prepared. In this way, it will be possible to compare the performance of such a scaffold with that of a native blood vessel. Considering the requirements needed for the intended application, scaffolds are crosslinked using either a carbodiimide or a diamine. It is known from the literature that crosslinking improves the thermal stability as well as the degradation resistance and the mechanical properties of the matrices[33]. Thermal stability is evaluated by recording the temperature at which the triple helix of collagen denatures, which can be assumed to be the denaturation temperature of the complete scaffold, since elastin is a very stable protein and no thermal transitions due to elastin are observed over the range of temperatures explored. Accordingly, the occurrence of crosslinking is also verified by the decrease of free amino groups in the scaffolds. The decrease is less evident for J230/EDC/NHS crosslinked scaffolds because, with this method, both zero-length crosslinking and crosslinking via J230 can take place. Moreover, dangling groups having an amino end-group can form as well.

SMCs were successfully isolated from both umbilical and saphenous veins. Cells can be cultured for several passages and can be identified by phase-contrast microscopy, immuno fluorescent microscopy and flow cytometry. Cultured SMCs grow in overlapping layers in a series of hills and valleys as described in literature [35, 36]. The appearance of this organisation at confluence distinguishes them *in vitro* from fibroblasts and myofibroblasts presenting a uniform monolayer aspect [37].

The phenotype of SMCs can be visualised using different mAbs. The mAb against α-SMA stains specifically the smooth muscle α-actin filaments that are present in SMCs and myofibroblasts [37, 43-45]. Of the cultured cells isolated from umbilical and saphenous veins, 98% were positively stained with this antibody, indicating that a pure culture of SMCs was obtained. Other mAbs are used to further specify the cells in culture. The mAb against muscle actin (clone HHF35) stained α- and γ-actin isotypes of skeletal and cardiac cells and SMCs and the mAb against vimentin stained this filament protein present in cells of mesenchymal origin, including ECs, SMCs and fibroblasts [36]. Both mAbs are less specific for SMCs than

the mAb against α-SMA. The former antibody stains cells in culture; however, this staining cannot be quantified, since the peak of positively stained cells overlapped with that of negative control cells. The latter mAb stained 81% of the cultured cells, indicating that the cultured cells are of mesenchymal origin.

In the present study we were able to demonstrate that SMCs adhere to, and proliferate on, three-dimensional porous scaffolds composed of collagen and elastin under optimised culture conditions for up to 14 d. Cells grow in multi layers on top of the matrix and grow in between fibres of collagen and elastin. Cells cultured on the scaffolds were again identified with the mAb against α-SMA. The influence of the crosslinking procedure used on SMC behaviour was evaluated. According to the histological results, neither the carbodiimide nor the diamine alter cell behaviour in a significant way. In all analysed samples, a multi layer of cells was observed. Moreover, the orientation of the cells resembles the orientation of the fibres of collagen and elastin, which can have great importance when tubular scaffolds having fibres oriented in a circumferential way are prepared. In the present study, cells were observed not only at the surface of, but also inside, the scaffolds. However, migration of cells has to be measured in a quantitative way in order to draw more definite conclusions. Migration can be further improved by adding platelet derived growth factor or matrix metalloproteinases [46] in the scaffolds and/or by culturing the cells under the influence of a pulsatile flow and a physiological pressure [47]. In such a dynamic environment, extracellular-matrix-protein production is enhanced. This production can be further improved by adding ascorbic acid, retinoids and/or transforming growth factor-β [48]. Once both the scaffold properties and the cell culturing conditions are optimised, ECs can be seeded. In this way, scaffolds resembling the morphological characteristics of native blood vessels could be obtained.

Conclusions

In the present study we have prepared collagen-and-elastin-based three-dimensional porous scaffolds suitable for tissue engineering of blood vessels. Crosslinking was successfully performed with either a carbodiimide or a diamine. Crosslinking did not alter the SMC culture on top of and inside the scaffolds under static conditions for up to 14 d. In the present study, static culturing of smooth muscle cells and their ability to grow and proliferate on such scaffolds have been investigated in order to characterise the behaviour of cells under these conditions. At a later stage, these results will be compared with those obtained by culturing the cells in a pulsatile flow system. It is known that, under the latter conditions, cell behaviour

shows greater similarity to that observed in a natural situation [49-51]. The results described are essential first steps towards the development of tubular scaffolds to be used as tissue-engineered vascular grafts.

Acknowledgement

We are grateful to M. Smithers (University of Twente, The Netherlands) for making scanning electron microscope pictures. R. Rieksen, medical photographer of the Laboratory of Pathology Oost Nederland (Enschede, The Netherlands) is kindly acknowledged for making immuno fluorescence microscope pictures. This project is financially supported by the IOP Senter (Den Haag, The Netherlands) (project IIE00003).

References

1. Ratcliff, A. Tissue Engineering of Vascular Grafts. Matrix Biology 2000; 19: 353-357.
2. Massia, S. P., Cell-extracellular matrix interactions relevant to vascular tissue engineering in: Tissue Engineering of Vascular Prosthetic Grafts, Austin, Texas, USA, RG Landes, 1999.
3. Jankowski, R.J. and Wagner, W.R. Directions in cardiovascular tissue engineering. Clin.Plast.Surg. 1999; 26: 605.
4. Campbell, J.H., Efendy, J.L., and Campbell, G.R. Novel vascular graft grown within recipient's own peritoneal cavity. Circ.Res. 1999; 85: 1173-1178.
5. Ross, R. Atherosclerosis--an inflammatory disease. N.Engl.J.Med. 1999; 340: 115-126.
6. Meinhart, J., Deutsch, M., and Zilla, P. Eight years of clinical endothelial cell transplantation. ASAIO J. 1997; 43: M515-M521.
7. Taylor, L., Edwards, J., and Porter, J. Present status of reversed saphenous vein bypass grafting: five year results of a modern series. J.Vasc.Surg. 1990; 11: 193-206.
8. Seifalian, A.M., Salacinski, H.J., Tiwari, J., Edwards, A., Bowald, S., and Hamilton, G. *In vivo* biostability of a poly(carbonate-urea)urethane graft. Biomaterials 2003; 24: 2549-2557.
9. Seifalian, A.M., Tiwari, A., and Salacinski, H.J. Improving the clinical patency of prosthetic vascular and coronary bypass grafts: the role of seeding and tissue engineering. Artif.Organs 2002; 26: 307-320.
10. Faries, P.L., LoGerfo, F.W., Arora, S., Hook, S., Pulling, M.C., Akbari, C.M., Campbell, D.M., and Pomposelli, Jr.R.G. A comparative study of alternative conduits for lower extremity revascularization: all-autologous conduit versus prosthetic grafts. J.Vasc.Surg 2000; 32: 1080-1090.
11. Zilla, P. Tissue engineering of vascular prostheses: Beyond the hype. Int.J.Artif.Organs 2002; 25: 629-632.
12. Zdrahala, R.J. Small caliber vascular grafts. Part I: state of the art. J.Biomater.Appl 1996; 10: 309-329.
13. Meinhart, J.G., Deutsch, M., Fischlein, T., Howanietz, N., Froschl, A., and Zilla, P. Clinical autologous *in vitro* endothelialization of 153 infrainguinal ePTFE grafts. Ann.Thorac.Surg. 2001; 71: S327-S331.
14. Berry, S. Honey I've shrunk biomedical technology! Trends Biotechnol. 2002; 20: 3-4.
15. Griffith, L.G. and Naughton, G. Tissue Engineering- Current Challenges and Expanding Opportunities. Science 2002; 295: 1009-1016.

16. Lavine, M., Roberts, L., and Smith, O. Bodybuilding: the bionic human. Science 2002; 295: 995-
17. Langer, R. and Vacanti, J.P. Tissue engineering. Science 1993; 260: 920-926.
18. Tabata, Y. Recent progress in tissue engineering. Drug Discovery Today 2001; 6: 483-487.
19. Niklason, L.E., Gao, J., Abbott, W.M., Hirschi, K.K., Houser, S., Marini, R., and Langer, R. Functional arteries grown *in vitro*. Science 1999; 284: 489-493.
20. Mooney, D.J., Mazzoni, C.L., Breuer, C., McNamara, K., Hern, D., Vacanti, J.P., and Langer, R. Stabilized polyglycolic acid fibre-based tubes for tissue engineering. Biomaterials 1996; 17: 115-124.
21. Kim, B.S., Putnam, A.J., Kulik, T.J., and Mooney, D.J. Optimizing seeding and culture methods to engineer smooth muscle tissue on biodegradable polymer matrices. Biotechnol.Bioeng. 1998; 57: 46-54.
22. Shum-Tim, D., Stock, U., Hrkach, J., Shinoka, T., Lien, J., Moses, M.A., Stamp, A., Taylor, G., Moran, A.M., Landis, W., Langer, R., Vacanti, J.P., and Mayer, J.E., Jr. Tissue engineering of autologous aorta using a new biodegradable polymer. Ann.Thorac.Surg. 1999; 68: 2298-2304.
23. Shino'ka, T., Imai, Y., and Ikada, Y. Transplantation of a tissue-engineered pulmonary artery. N.Engl.J.Med. 2001; 344: 532-533.
24. Weinberg, C.B. and Bell, E. A blood vessel model constructed from collagen and cultured vascular cells. Science 1986; 231: 397-400.
25. L'Heureux, N., Germain, L., Labbe, R., and Auger, F.A. *In vitro* construction of a human blood vessel from cultured vascular cells: a morphologic study. J.Vasc.Surg. 1993; 17: 499-509.
26. Hirai, J. and Matsuda, T. Venous reconstruction using hybrid vascular tissue composed of vascular cells and collagen: tissue regeneration process. Cell Transplant. 1996; 5: 93-105.
27. Fung, Y. C., Mechanical Properties of Living Tissues in: Biomechanics, 1, Springer, 1999.
28. Goissis, G., Suzigan, S., Parreira, D.R., Maniglia, J.V., Braile, D.M., and Raymundo. Preparation and characterization of collagen-elastin matrices from blood vessels intended as small diameter vascular grafts. Artif.Organs 2000; 24: 217-223.
29. Takahashi, K., Nakata, Y., Someya, K., and Hattori. Improvement of the physical properties of pepsin-solubilized elastin-collagen film by crosslinking. Biotechnol.Biochem. 1999; 63: 2144-2149.
30. Lefebvre, F., Gorecki, S., Bareille, R., Amedee, J., Bordenave, L., and Rabaud, M. New artificial connective matrix-like structure made of elastin solubilized peptides and collagens: elaboration, biochemical and structural properties. Biomaterials 1992; 13: 28-33.
31. Bader, A., Steinhoff, G., Strobl, K., Schilling, T., Brandes, G., Mertsching, H., Tsikas, D., Froelich, J., and Haverich, A. Engineering of human vascular aortic tissue based on a xenogeneic starter matrix. Transplantation 2000; 70: 7-14.
32. Daamen, W., Veerkamp, J.H., and van Kuppevelt, T.H. Purification of elastin and preparation of matrices for tissue engineering. Indust.Protein 2001; 9: 15-17.
33. Olde Damink, L.H.H., Dijkstra, P.J., van Luyn, M.J.A., van Wachem, P.B., Nieuwenhuis, P., and Feijen, J. Cross-linking of dermal sheep collagen using a water-soluble carbodiimide. Biomaterials 1996; 17: 765-773.
34. Brandbury, P. and Gordon, K. C., Theory and Practice of Histological Techniques, Chruchill Livingstone, Edingburgh, 1990; 119-142.
35. Heimli, H., Kahler, H., Endresen, M.J., Henriksen, T., and Lyberg, T. A new method for isolation of smooth muscle cells from human umbilical cord arteries. Scand.J.Clin.Lab Invest. 1997; 57: 21-29.

36. Chamley-Campbell, J., Campbell, G.R., and Ross, R. The smooth muscle cell in culture. Physiol.Rev. 1979; 59: 1-61.
37. Lefebvre, P., Nusgens, B.V., and Lapiere, C.M. Cultured myofibroblasts display a specific phenotype that differentiates them from fibroblasts and smooth muscle cells. Dermatology 1994; 189: 65-67.
38. Rolfe, B.E., Muddiman, J.D., Smith, N.J., Campbell, G.R., and Campbell, J.H. ICAM-1 expression by vascular smooth muscle cells is phenotype-dependent. Atherosclerosis 2000; 149: 99-110.
39. Rothenburger, M., Vischer, P., Volker, W., Glasmacher, B., Berendes, E., Scheld, H.H., and Deiwick, M. *In Vitro* Modelling of Tissue using Isolated Vascular Cells on a Synthetic Collagen Matrix as a Substitute for Heart Valves. Thorac.Cardiov.Surg. 2001; 49: 204-209.
40. Schoof, H., Apel, J., Heschel, I., and Rau, G.U. Control of pore structure ans size in freeze-dried collagen sponges. J.Biomed.Mat.Res. 2001; 58: 352-357.
41. Zeeman, R., Dijkstra, P.J., van Wachem, P.B., van Luyn, M.J.A., Hendriks, M., Cahalan, P.J., and Feijen, J. Successive epoxy and carbodiimide cross-linking of dermal sheep collagen. Biomaterials 1999; 20: 921-931.
42. Pieper, J.S., Oosterhof, A., Dijkstra, P.J., Veerkamp, J.H., and van Kuppevelt, T.H. Preparation and characterization of porous crosslinked collagenous matrices containing bioavailable chondroitin sulphate. Biomaterials 1999; 20: 847-858.
43. Eyden, B. The myofibroblast: an assessment of controversial issues and a definition useful in diagnosis and research. Ultrastruct.Pathol. 2001; 25: 39-50.
44. Negre-Aminou, P., van Vliet, A.K., van Erck, M., van Thiel, G.C., van Leeuwen, R.E., and Cohen, L.H. Inhibition of proliferation of human smooth muscle cells by various HMG-CoA reductase inhibitors; comparison with other human cell types. Biochim.Biophys.Acta 1996; 1345: 259-268.
45. Sartore, S., Chiavegato, A., Faggin, E., Franch, R., Puato, M., Ausoni, S., and Pauletto, P. Contribution of adventitial fibroblasts to neointima formation and vascular remodeling: from innocent bystander to active participant. Circ.Res. 2001; 89: 1111-1121.
46. Mason, D.P., Kenagy, R.D., Hasenstab, D., Bowen-Pope, D.F., Seifert, R.A., Coats, S., Hawkins, S.M., and Clowes, A.W. Matrix metalloproteinase-9 overexpression enhances vascular smooth muscle cell migration and alters remodeling in the injured rat carotid artery. Circ.Res. 1999; 85: 1179-1185.
47. Seliktar, D., Black, R.A., Vito, R.P., and Nerem, R.M. Dynamic mechanical conditioning of collagen-gel blood vessel constructs induces remodeling *in vitro*. Ann.Biomed.Eng. 2000; 28: 351-362.
48. Davidson, J.M., P.A.LuValle, O.Zoia, D.Quaglino Jr., and M.G.Giro. Ascorbate differentially regulates elastin and collagen biosynthesis in vascular smooth muscle cells and skin fibroblasts by pretranslational mechanisms. J.Biol.Chem. 1997; 272: 345-352.
49. Kim, B. and Mooney, D.J. Scaffolds for engineering smooth muscle under cyclic mechanical strain conditions. J.Biochem.Eng. 2000; 122: 210-215.
50. Lee, A.A., Graham, D.A., Dela, C.S., Ratcliffe, A., and Karlon, W.J. Fluid shear stress-induced alignment of cultured vascular smooth muscle cells. J.Biomech.Eng. 2002; 124: 37-43.
51. Stegeman, J.P. and Nerem, R.M. Altered response of vascular smooth muscle cells to exogenous biochemical stimulation in two-and three-dimensional culture. Exp.Cell Res. 2003; 283: 146-155.

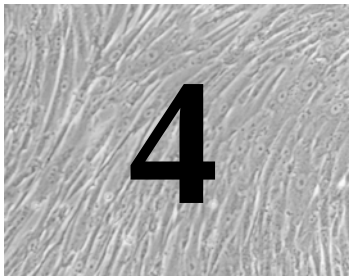

4

Spatial Cell Distribution after Filtration Seeding of Smooth Muscle Cells in Porous Scaffolds for Vascular Tissue Engineering*

* P. Engbers-Buijtenhuijs[1, 2], L. Buttafoco[1], A.A. Poot[1], R.H. Geelkerken[2], R.A.I. de Vos[3], L.M.T. Sterk[3], J. Feijen[1], and I. Vermes[1, 2]

[1] University of Twente, Faculty of Science & Technology, Department of Polymer Chemistry and Biomaterials, and Institute of Biomedical Technology (BMTI), P.O. Box 217, 7500 AE Enschede, The Netherlands

[2] Medisch Spectrum Twente, Hospital Group, Enschede, Department of Clinical Chemistry, P.O. Box 50.000, 7500 KA Enschede, The Netherlands

[3] Laboratory of Pathology Oost-Nederland, P.O. Box 377, 7500 AJ Enschede, The Netherlands

Abstract

After preparation of a porous biocompatible and biodegradable scaffold and isolation of the desired cell type, cell seeding is the next critical step in the process to produce an adequate tissue-engineered (TE) construct. Cell seeding plays an important role in determining the initial cell number and initial cell distribution in the TE scaffolds. A high number of initially seeded cells and a uniform cell distribution can improve the structural stability and biochemical composition of the engineered tissues. In this study, several cell seeding procedures were used to improve the spatial smooth muscle cell (SMC) distribution in scaffolds composed of collagen and elastin. Whereas with conventional static seeding, multiple static seeding or injection seeding a multi layer of SMCs on top of the scaffolds is obtained, the use of the described dynamic depth filtration seeding procedure results in the formation of a homogeneous structure of collagen and elastin fibres interspersed with SMCs. These porous constructs have elastic properties, appropriate mechanical strength, and a homogeneous distribution of cells, which makes them suitable for dynamic culturing mimicking *in vivo* conditions of human small- and medium-sized arteries.

Introduction

Tissue engineering is a discipline that applies the principles of engineering and life sciences to the development of biological substitutes that restore, maintain or improve tissue functions. Most vascular tissue engineering strategies aim at creating small-diameter blood vessel replacements closely mimicking the three-layered structure of a natural blood vessel. In this way the graft should have the potential to treat (cardio-) vascular diseases or to develop models to study vascular biology [1, 2]. As viable structures, tissue-engineered (TE) blood vessels should represent a responsive and self-renewing tissue with the inherent potential of healing and remodelling according to the requirements of their specific environment [3]. One strategy to create these biological substitutes employs seeding of autologous vascular cells in tubular scaffolds to provide a temporary biomechanical structure until the cells produce their own extra-cellular matrix [1]. Several approaches have been described in which different synthetic polymers [4-7] or natural polymers [8-10] were seeded and cultured with animal or human vascular cell types. All studies were aiming to produce a graft with sufficient mechanical and biological properties to function immediately after implantation [11].

After preparation of a porous biocompatible and biodegradable scaffold and isolation of the desired cell type, cell seeding is the next critical step in the process to produce a TE construct [12]. Cell seeding plays an important role in determining the initial cell number, initial cell

distribution, and subsequent cellular processes critical for tissue development, including proliferation, differentiation, and migration [13]. A high number of initially seeded cells can improve structural stability and biochemical composition of the engineered tissues. Furthermore, uniform cell distribution in the TE construct associated with intimate cell-cell interactions, is desirable for both normal functions and phenotypic expression of the vascular cells [12]. How to uniformly seed a high number of cells into porous scaffolds is thus a critical issue in tissue engineering. Static seeding of cells into a scaffold is the most commonly used seeding method for tissue culture. However, several studies reported low seeding efficiencies and non-uniform cell distributions within the scaffolds, which limits the use of static seeding in developing tissue equivalents [5, 12, 13]. Several new cell seeding methods, including dynamic mixing [5, 12, 14], agitation [5], rotational seeding [14, 15], perfusion flow-seeding [12] and vacuum seeding [16] have been developed to improve initial cell densities and distribution in the cell-polymer construct.

This paper describes the results of static culturing for up to 8 wks of smooth muscle cells (SMCs) seeded via different methods on biodegradable porous scaffolds composed of insoluble collagen or insoluble collagen and elastin. Elastin fibres in the collagenous scaffolds contribute to improved mechanical properties of the scaffolds which are able to withstand cyclic mechanical loading [11, 17]. Effects of several seeding procedures on cell growth and proliferation and on the spatial distribution of the cells in the porous scaffolds and the ability of cells to grow and proliferate were studied. In particular, the dynamic depth-filtration seeding method as described by Li *et al* [13], an injection procedure and a multiple seeding method were used to improve the initial cell seeding density and spatial cell distribution in the scaffolds. The results were compared with those obtained from the conventional static seeding procedure and will eventually be used for homogeneous seeding of SMCs in tubular scaffolds for tissue engineering of small-diameter blood vessels.

Materials

Dulbecco's Modified Eagle's Medium (DMEM) was purchased from Gibco BRL (Breda, The Netherlands). Penicillin, streptomycin, fetal bovine serum and trypsin/ethylene diamine tetra acetic acid (EDTA) were purchased from Biowhittaker (Verviers, Belgium). Gelatin type B from bovine skin, N-(3-dimetylaminopropyl)-N'-ethylcarbodiimide hydrochloride (EDC), N-hydroxysuccinimide (NHS), poly(propylene glycol)-bis-(2-aminopropyl ether) (J230), proteinase K and DNAse free RNAse were obtained from Sigma and Aldrich (St Louis, Missouri, USA). Mouse monoclonal antibodies (mAbs) against human α-smooth muscle actin

(α-SMA) and against human vimentin and fluorescein isothiocyanate-labelled rabbit anti mouse immunoglobulins (RAM-FITC) were purchased from DAKO (Glostrup, Denmark). Collagenase type 2 was purchased from Worthington Biochemical Corporation (Lakewood, N.J., USA). Human serum was acquired by overnight coagulation of blood (collected from healthy volunteers), subsequently pooled and stored at -80^{0}C. Insoluble collagen (type I from bovine achilles tendons) and insoluble elastin (from equine ligamentum nuchae), purified as described in [18] were kindly donated by dr. T.H. van Kuppevelt, Department of Biochemistry, University Medical Centre Nijmegen, The Netherlands.

Methods

Isolation of SMCs

SMCs were isolated from human umbilical veins by a collagenase digestion method according to the method of Heimli *et al*. [19] with some minor modifications as described previously [17]. Cells were cultured on gelatin-coated (0.5% w/v) tissue culture polystyrene (g-TCPS) culture dishes using DMEM containing 10% (v/v) heat-inactivated (30 min, 56^{0}C) pooled human serum, 10% (v/v) heat-inactivated (30 min, 56^{0}C) fetal bovine serum, 50 units/mL penicillin and 50 μg/mL streptomycin [19]. Culture medium was filtered (0.20 μm) before use. During culturing, medium was refreshed every 2-3 d. Cells were cultured in a humidified atmosphere containing 5% CO_2 inside an incubator at 37 ^{0}C (CleanAir Techniek bv, Woerden, The Netherlands) [20]. When sub-confluent cultures were obtained, cells were detached from the support with 0.125% (w/v) trypsin/0.05% (w/v) EDTA and subcultured for several passages (split ratio 1:3) [21]. Sub-confluent cultures of SMCs from passage 5 to 9 were used to seed scaffolds for vascular tissue engineering.

Identification of SMCs

SMCs were identified using mAbs against human α-SMA and human vimentin [19] [20]. Fluorescence of the used secondary antibody RAM-FITC was examined with immuno fluorescent microscopy and with flow cytometry as described earlier [17]. Negative controls were obtained by omitting first antibodies and by staining human umbilical vein endothelial cells (HUVECs) and human dermal fibroblasts with the used antibodies.

Scaffold properties

Porous scaffolds for tissue engineering applications were produced by freeze-drying (at –18^{0}C) a suspension of type I insoluble collagen or a suspension (1:1 w/w) of type I insoluble collagen and elastin. Crosslinking of the scaffolds was performed either with a water-soluble carbodiimide in combination with a succinimide (EDC/NHS) or with a diamine (J230) in the presence of EDC/NHS to improve the mechanical properties [22]. Scaffolds with a thickness of 1 mm (collagen) or 2 mm (collagen-elastin) were optimised in terms of pore size and cross-link density [17, 23]. Scaffolds had a porosity between 75 and 98 % and interconnective pores with sizes in the range of 9 to 340 μm as analysed by scanning electron microscopy [23]. Data are presented in table I.

Table I: Physical parameters of the scaffolds used [23]. Porosity and pore sizes of scaffolds either composed of insoluble collagen or insoluble collagen and elastin, non-crosslinked or crosslinked with EDC/NHS or J230/EDC/NHS, based on scanning electron microscopy analyses, are presented.

Composition	*Crosslinking method*	*Porosity (%)*	*Average pore size (μm)*
Collagen	none	98	340 ± 20
	EDC/NHS	75	180 ± 15
	J230/EDC/NHS	76	9 ± 3
Collagen/elastin	none	90	130 ± 30
	EDC/NHS	90	60 ± 40
	J230/EDC/NHS	90	30 ± 20

Static seeding of SMCs on porous scaffolds

Scaffolds composed of insoluble collagen were sized to a diameter of 16 mm with a punching tool, placed in 24-wells TCPS culture dishes and secured with Viton O-rings (Eriks, Alkmaar, The Netherlands). Non-crosslinked scaffolds or scaffolds either crosslinked with EDC/NHS or with J230 in the presence of EDC/NHS were used. After disinfection of the scaffolds with 70% ethanol (v/v) and subsequently rinsing (three times) with PBS, scaffolds were incubated overnight with culture medium. Sub-confluent cultures of human umbilical vein SMCs were harvested by trypsinisation (2 min, 0.125% trypsin/ 0.05% EDTA), centrifuged at 300 g for 10 min at 21^0 C and resuspended in fresh DMEM culture medium. Cells were counted with a hemacytometer (Bürker) and seeded on the scaffolds with a density of 400.000 cells/scaffold once at day 0 or three times at day 0, 2, and 4 (multiple seeding). Cells were subsequently cultured for up to 56 d under static conditions.

Dynamic seeding of SMCs in porous scaffolds

Seeding was done in porous scaffolds composed of insoluble collagen and elastin, non-crosslinked or either crosslinked with EDC/NHS or with J230 in the presence of EDC/NHS. After disinfection of the scaffolds with 70% ethanol (v/v) and subsequently rinsing (three times) with PBS, scaffolds were incubated overnight with culture medium. Two SMC seeding procedures, 1) filtration seeding or 2) injection seeding were used and compared with static seeding (as described above). In the first procedure, scaffolds were placed on the 0.20 μm filter of a filter flask and aliquots of 40 μL of a cell suspension containing 800.000 cells/mL, were placed on top of the scaffolds. Filtration seeding was carried out by applying a small pressure difference between the two sides of the filter (figure 1). The filtration cycle was repeated 12 times till 400.000 cells were filtrated per scaffold. In the second procedure, aliquots of 25 μL of a cell suspension containing 800.000 cells/mL, were injected with a sterile needle (Terumo Europe N.V., Leuven, Belgium) at 20 different sites till 400.000 cells were injected per scaffold. Both filtration and injection seeded scaffolds were transferred to 24-wells TCPS culture dishes and secured with Viton O-rings (Eriks, Alkmaar, The Netherlands). Cells were subsequently cultured for 14 d under static conditions.

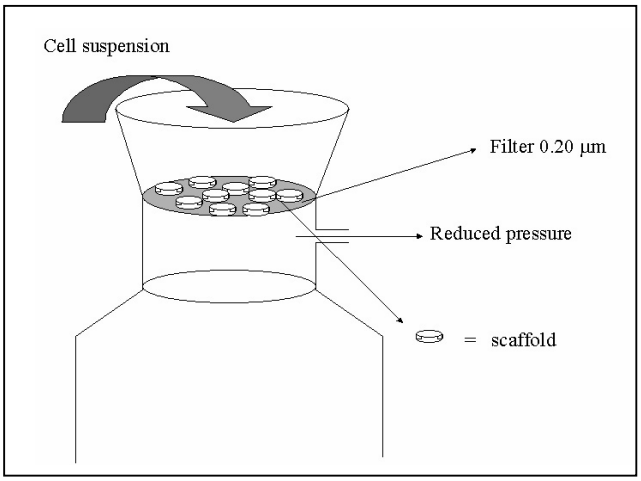

Figure 1: Schematic representation of the filtration seeding procedure. Porous scaffolds composed of insoluble collagen and elastin (with a diameter of 16 mm and a thickness of 2 mm) were placed on top of a 0.20 μm filter of a filter flask and aliquots of 40 μL of a cell suspension containing 800.000 cells/mL, were placed on top of the scaffolds. Filtration seeding was carried out by applying a small pressure difference between the two sides of the filter. The filtration cycle was repeated 12 times till 400.000 cells were filtrated per scaffold.

Histology

After culturing, cell-seeded scaffolds were rinsed with PBS and fixed with formalin (4% v/v) for at least 24 h. Samples were then impregnated with paraffin, cut into transverse sections and stained by the hematoxylin and eosin (HE), the elastic van Gieson (EG) procedure or by immuno staining of α-SMA according to standard procedures.

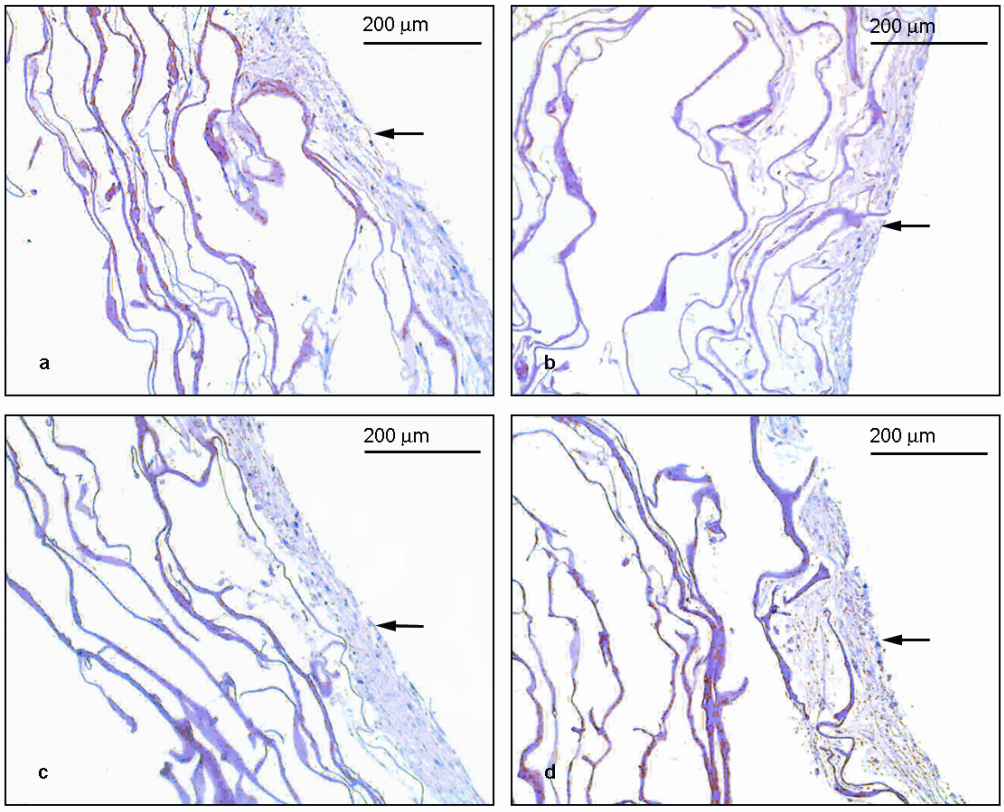

Figure 2: Histology of SMCs seeded on porous scaffolds composed of insoluble collagen and crosslinked with EDC/NHS. Cells were seeded in a static way on the scaffolds with a density of 400.000 cells/scaffold and subsequently cultured for 14 (a), 28 (b), 42 (c), and 56 (d) d. Transverse sections of the cell containing constructs showing the top and inside of the scaffolds were stained by the standard HE procedure. Scale bars are inserted in the pictures and the SMC multi layers are indicated by arrows.

Cell numbers

Numbers of SMCs present in the cell-seeded scaffolds after culturing were quantified by the CyQuant Cell Proliferation assay according to the manufacturer's instructions (Molecular Probes, Leiden, The Netherlands). Scaffolds were rinsed with PBS and digested with 500 µL proteinase K solution (1 mg/mL in PBS) for a minimum of 16 h at 56^0C. Samples were stored at -80^0C until analyses were performed. Various dilutions were prepared with cell-lysis buffer (Molecular Probes, Leiden, The Netherlands) supplemented with 180mM NaCl, 1 mM EDTA

and 1.35 Kunitz units/mL DNAse-free RNAse. Samples were then incubated for 1 h at RT to remove RNA and single stranded DNA. Finally, samples were mixed with CyQUANT® dye and after 2 min, fluorescence of the dye was measured in each well of 96 well plates using a Victor fluorescence analyser (PerkinElmer Life Sciences, Turku, Finland). Excitation and emission wavelengths were 480 and 520 nm respectively. The measured fluorescence intensities were correlated to the amount of SMCs using a calibration curve made by means of SMC dilutions with known concentrations, prepared from a sub-confluent SMC culture on g-TCPS. Cells were detached from the support with 0.125% (w/v) trypsin/0.05% (w/v) EDTA, counted with a hemacytometer (Bürker) and then analysed in the same way as described above to obtain a calibration curve.

Statistical analysis

Data represent mean ± standard error of the mean (SEM) of 4 to 6 experiments performed in duplicate. Statistical analyses were performed using an unpaired two-tailed t-test. Results were considered significantly different at p values < 0.05.

Results

SMCs isolated from human umbilical vein were successfully cultured and expanded on g-TCPS culture dishes. No microscopic abnormalities or changes in α-SMA or vimentin expression were observed during the SMC growth expansion time [17].

SMCs seeded in a static way on EDC/NHS-crosslinked porous scaffolds composed of insoluble collagen form a multi layer on top of the scaffolds after 14 d of culturing. This layer was stable for up to 8 wks (figure 2, see previous page). Cells were only observed on top of the scaffolds and in between the first collagen fibres from the top. No cell growth was observed inside the porous scaffolds for the duration of the experiment. Triple cell seeding at day 0, 2 and 4 resulted in a thicker SMC layer after 7 d of culturing compared to cell seeding once at day 0 (data not shown). After 14 d of culturing no differences in thickness of the SMC multi layers were observed.

Quantitative analyses of the amount of SMCs present on the porous scaffolds after 14 d of culturing resulted in 1.6 ($\pm$ 0.05)*10^6 cells per non-crosslinked scaffold and a comparable amount of 1.5 ($\pm$ 0.05)*10^6 cells per EDC/NHS crosslinked scaffold. A significantly lower amount of cells (1.3 $\pm$ 0.07*10^6) was found on J230/EDC/NHS crosslinked scaffolds compared to non-crosslinked scaffolds (figure 3). These data were confirmed in a qualitative way by histology.

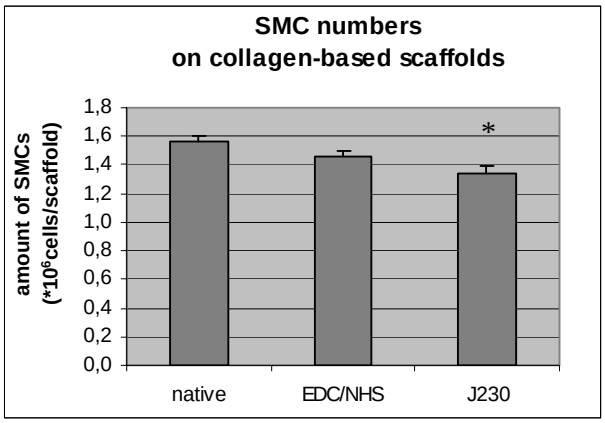

Figure 3: Amount of SMCs present on porous scaffolds composed of collagen, non-crosslinked (native), or either crosslinked with EDC/NHS or J230/EDC/NHS after static seeding and 14 d of culturing. Cell numbers were quantified by the CyQuant Cell Proliferation assay and the measured fluorescence intensities were correlated with the amount of SMCs using a calibration curve made with known numbers of SMCs. Cell numbers of six experiments performed in duplicate (± SEM) are presented. * indicates a significant difference compared to non-crosslinked scaffolds ($p < 0.05$).

Figure 4 shows the results of histology of SMCs seeded in 3 different ways on and in non-crosslinked porous scaffolds composed of insoluble collagen and elastin. Cells were observed on top of the scaffolds and in between the first collagen and/or elastin fibres from the top of the scaffolds using the control seeding procedure (figure 4a and b) as well as the injection seeding procedure (figure 4e and f). No cells were observed inside the scaffolds. In contrast, cells were also seen inside the scaffolds in between fibres of collagen and/or elastin using the filtration seeding procedure (figure 4 c and d). Comparable results were obtained using porous scaffolds either crosslinked with EDC/NHS (figure 5a) or J230/EDC/NHS (figure 5b), although in the latter case less cells were visible. Immuno histochemistry of the construct sections showed that cells present in and on the scaffolds were positively stained for the presence of α-SMA (data not shown).

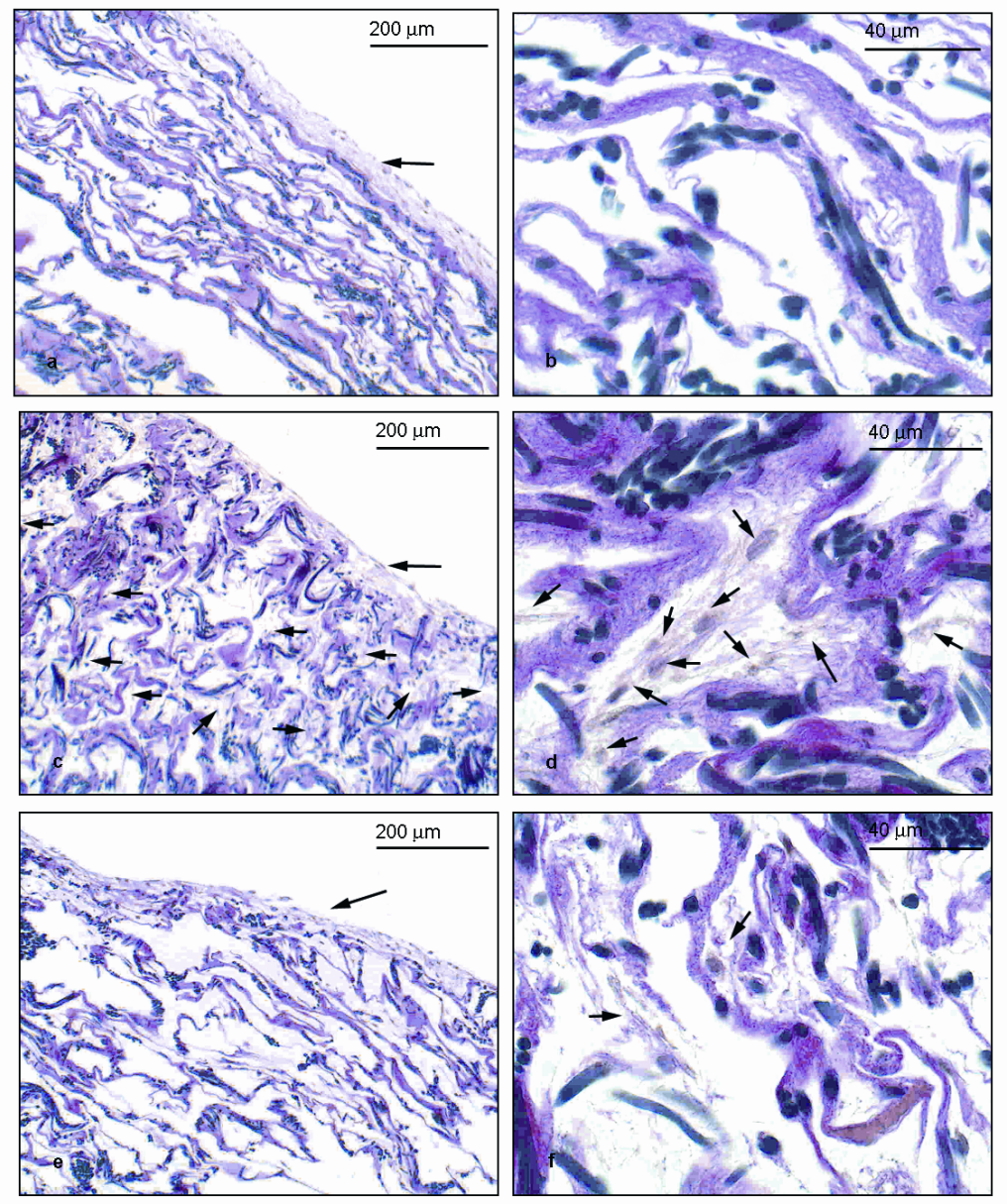

Figure 4: Histology of SMCs seeded in and on porous scaffolds composed of insoluble collagen and elastin (non-crosslinked) by static seeding (a, b), by the filtration procedure (c, d) or by the injection procedure (e, f) and subsequently cultured for 14 d. Transverse sections of the cell containing constructs showing the top and inside (a, c, e) or only the inside at higher magnification (b, d, f) were stained by the standard EG procedure. Scale bars are inserted in the pictures, the SMC multi layers are indicated by long arrows and individual cells inside the scaffold by small arrows.

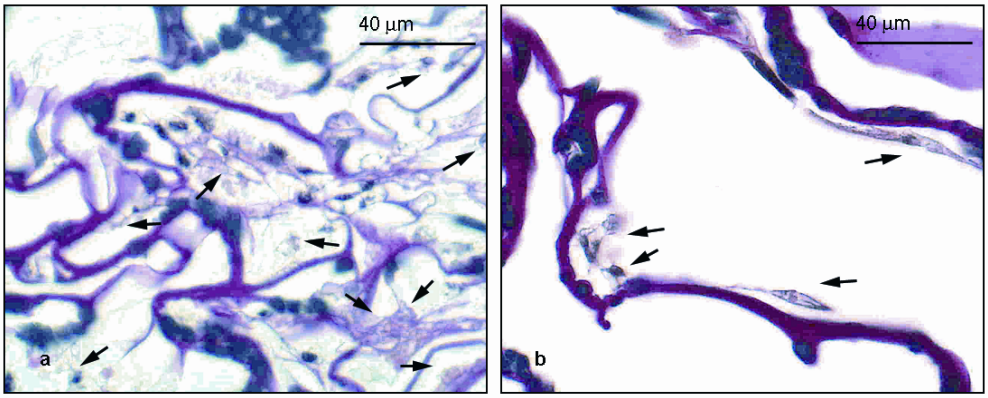

Figure 5: Histology of SMCs seeded by filtration in EDC/NHS (a) or J230/EDC/NHS (b) crosslinked scaffolds composed of insoluble collagen and elastin and subsequently cultured for 14 d. Transverse sections of the cell containing constructs showing the inside of the scaffolds were stained by the standard EG procedure. Scale bars are inserted in the pictures.

Crosslinking of the porous scaffolds with a water-soluble carbodiimide (EDC/NHS) did not significantly influence the cell number present in the scaffolds after 14 d of culturing (figure 6). 1.5 (± 0.08)*10^6 cells per non-crosslinked scaffold and 1.4 (± 0.2)*10^6 cells per EDC/NHS crosslinked scaffold were found. A significantly lower amount of cells per scaffold (0.9 ± 0.2*10^6) was found in the case of J230/EDC/NHS crosslinking (figure 6).

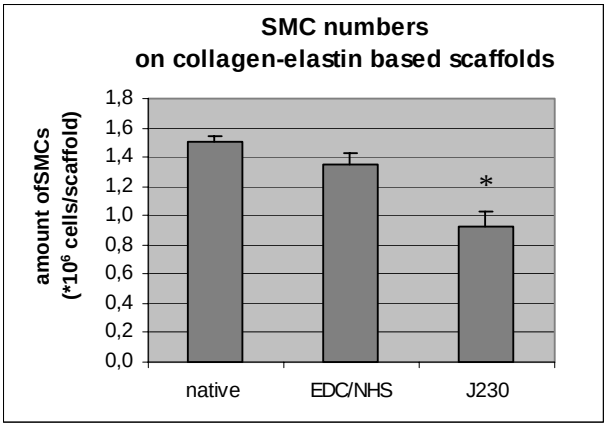

Figure 6: Amount of SMCs present in porous scaffolds composed of collagen and elastin, non-crosslinked (native), or either crosslinked with EDC/NHS or J230/EDC/NHS after filtration seeding and 14 d of culturing. Cell numbers were quantified by the CyQuant Cell Proliferation assay and the measured fluorescence intensities were correlated with the amount of SMCs using a calibration curve made with known numbers of SMCs. Cell numbers of four experiments performed in duplicate (± SEM) are presented. * indicates a significant difference compared to non-crosslinked scaffolds and EDC/NHS crosslinked scaffolds ($p < 0.05$).

Discussion

Pure SMC cultures of mesenchymal origin [17, 20] were used in this study. When cells were cultured on porous scaffolds composed of insoluble collagen, a stable and viable multi layer of SMCs was obtained on top of the scaffolds for at least 8 wks. Within 14 d, cells had proliferated on the scaffolds and formed a multi layer. No increase of thickness of this multi layer was subsequently observed for at least 8 wks. Also multiple (static) seeding did not enlarge this cell layer after 14 d of culturing indicating that a maximum amount of cells per scaffold was reached (~$1.5*10^6$ cells/scaffold). This may be explained by external mass transport limitations [24]. Scaffolds had to be secured in 24-wells TCPS culture dishes with Viton O-rings for effective cell seeding and to ensure that the scaffolds were kept in place. However, in this way, the bottom parts of the multi layer of SMCs on the scaffolds were refrained from nutrients and oxygen present in the culture medium as well as metabolic waste product exchange. One can speculate that high cell densities on top of the scaffolds and mass transport limitations could have resulted in decreased cell proliferation [13].

Our final aim is creating a small-diameter vascular graft closely mimicking the three-layered structure of a natural blood vessel. To deal with the requirements of a functional vascular graft (sufficient mechanical strength, elastic properties, compliance to the host vessel), scaffolds were optimised by preparing porous structures composed of insoluble collagen and elastin. In this way the mechanical properties of the scaffolds were improved [11, 17]. Elastin fibres interspersed with collagen fibres in the scaffolds did not affect cell attachment and proliferation. After static cell seeding and subsequent culturing, a stable multi layer of SMCs was formed on top of the scaffolds. No cell adherence nor cell growth or migration was observed inside the scaffolds composed of collagen and elastin seeded with SMCs in a static way and cultured for a maximum period of 8 wks.

To improve the cellular distribution in the scaffolds, several alternative seeding procedures were tested using porous scaffolds composed of collagen and elastin. In contrast to a multiple seeding procedure and an injection seeding procedure, cell attachment and growth within our porous scaffolds were observed using a dynamic depth-filtration seeding procedure, a process described by Li *et al* [13] and modified according to our specifications (figure 1). By means of filtration seeding, a structure of collagen and elastin fibres interspersed with SMCs instead of a multi layer of SMCs on top of the scaffolds (indicating two separate layers) was obtained. A homogeneous structure is essential for tissue engineering applications [13]. Because neither culturing SMCs for at least 8 wks after static seeding nor a multiple seeding process resulted in migration of cells into the porous scaffolds, it can be concluded that a dynamic depth-

filtration seeding procedure is needed to obtain a structure with a homogeneous distribution of cells inside. Depth filtration has been widely employed in waste-water treatment and several biomedical applications, including separation of leukocytes from blood [25] and homogeneous cell seeding in open porous scaffolds [13]. Depth filtration can be explained by distinguishing a sieving mechanism (mechanical entrapment) and an adhesion mechanism. The porosity, pore size and interconnectivity of the pores determine whether sieving will occur [25]. Several elementary mechanisms of cell sieving are known to play a role in the retention of cells during depth filtration including blocking of one or more cells in pores (pore plugging), interception of cells in dead ends of the porous structure and sedimentation of cells in the porous structure [13, 25, 26]. In our experiments, cell adhesion also plays a significant role in the retention of cells during depth filtration because collagen and elastin fibres possess cell adhesion ligands to which cells can adhere [13, 27-31]. Adhesion between SMCs and collagen/elastin fibres is mediated by specific cell surface receptors, including members of the integrin family [27-29, 31]. In the open porous scaffolds used in this study, the retention of cells (having sizes between 20 and 400 μm [20]) can occur at any place inside the structures via both mechanisms of sieving and adhesion because pore sizes are in the range of 30 to 130 μm (table I). This may explain the homogeneous distribution of cells over the scaffolds obtained after seeding by a depth filtration process. The fact that all pores at the top of the scaffolds are entries for the cells during the filtration process whereas only around 20 places are used as cell entries during the injection procedure, might explain the difference in cell distribution between these two seeding processes. Another possible explanation could be that the force applied to the cells by injection is too high for processes of interception, sedimentation and adhesion of the cells to occur. We did neither investigate these forces nor these processes of the retention of cells independently to verify these speculations.

A comparable amount of cells was found on statically seeded scaffolds compared to scaffolds seeded by filtration after 14 d of culturing. According to the presence of α-SMA fibres in the cells cultured on and in the porous scaffolds, no fundamental differentiation or dedifferentiation processes took place during culturing [32 20].

Crosslinking of the scaffolds either with a carbodiimide in combination with a succinimide (EDC/NHS) or with a diamine (J230) in the presence of EDC/NHS improved the mechanical properties of the TE scaffolds [23]. Crosslinking of the scaffolds composed of insoluble collagen or insoluble collagen and elastin with EDC/NHS, had no effect on cell attachment and proliferation inside the scaffolds for at least 14 d of culturing whereas crosslinking with J230 resulted in significantly lower cell numbers. This may be an indication that the density of cells

present in our porous scaffolds is dependent on the size of the pores (table I). Scaffolds composed of collagen and elastin crosslinked in the presence of a diamine spacer (J230) have smaller pore sizes (30 ± 20 μm) compared to non-crosslinked (130 ± 30 μm) or EDC/NHS crosslinked (60 ± 40 μm) scaffolds. However, also the chemical nature of J230 or the presence of dangling amine groups as a consequence of crosslinking with J230/EDC/NHS may have altered the ability of SMCs to adhere to and proliferate in these scaffolds [23]. The presence of J230 may contribute to an increased hydrophilic character of the scaffolds, which decreases protein adsorption and cell adhesion and increases levels of apoptosis of adherent cells [33].

The preparation of cell-seeded tubular constructs in an analogous way is the next step for tissue engineering of small-diameter blood vessels. These tubular TE scaffolds will be cultured in a pulsatile flow bioreactor to stimulate tissue formation. The optimisation of the processes to make tubular biodegradable scaffolds composed of collagen and elastin, to culture vascular cells inside these structures and to develop a suitable bioreactor to mimic the *in vivo* conditions of human small- and medium-sized arteries are now under investigation in our laboratories.

Conclusion

Filtration seeding of SMCs in porous scaffolds has a significant effect on the spatial cell distribution in the scaffolds, but has no effect on cell numbers after culturing. In contrast to a multiple seeding procedure and an injection seeding procedure, a structure of collagen and elastin fibres interspersed with SMCs was obtained by means of a dynamic depth filtration seeding procedure. Scaffolds composed of insoluble collagen and elastin were crosslinked using either EDC/NHS or J230/EDC/NHS. Crosslinking of the scaffolds with EDC/NHS did not influence culturing efficiency for at least 14 d of culturing. In contrast, crosslinking with J230/EDC/NHS had a detrimental effect on the amount of cells present on and in the porous scaffolds after static and filtration seeding.

Porous scaffolds composed of insoluble collagen and elastin crosslinked with EDC/NHS and seeded with human vascular SMCs by filtration are suitable to obtain biodegradable TE constructs with elastic properties, appropriate mechanical strength [23], and a homogeneous distribution of cells. These properties of the obtained TE constructs makes them suitable for dynamic culturing mimicking *in vivo* conditions of human small- and medium-sized arteries.

Acknowledgements

R. Rieksen, medical photographer of the Laboratory of Pathology Oost Nederland (Enschede, The Netherlands) is kindly acknowledged for making histology pictures.

References

1. Langer, R. and Vacanti, J.P. Tissue Engineering. Science 1993; 260: 920-926.
2. Nerem, R.M. Critical issues in vascular tissue engineering. Int.Congress Series 2004; 1262: 122-125.
3. Hoerstrup, S.P., Zund, G., Sodian, R., Schnell, A.M., Grunenfelder, J., and Turina, M.I. Tissue engineering of small caliber vascular grafts. Eur.J.Cardiothorac.Surg. 2001; 20: 164-169.
4. Mooney, D.J., Mazzoni, C.L., Breuer, C., McNamara, K., Hern, D., Vacanti, J.P., and Langer, R. Stabilized polyglycolic acid fibre-based tubes for tissue engineering. Biomaterials 1996; 17: 115-124.
5. Kim, B.S., Putnam, A.J., Kulik, T.J., and Mooney, D.J. Optimizing seeding and culture methods to engineer smooth muscle tissue on biodegradable polymer matrices. Biotechnol.Bioeng. 1998; 57: 46-54.
6. Shum-Tim, D., Stock, U., Hrkach, J., Shinoka, T., Lien, J., Moses, M.A., Stamp, A., Taylor, G., Moran, A.M., Landis, W., Langer, R., Vacanti, J.P., and Mayer, J.E., Jr. Tissue engineering of autologous aorta using a new biodegradable polymer. Ann.Thorac.Surg. 1999; 68: 2298-2304.
7. Niklason, L.E., Gao, J., Abbott, W.M., Hirschi, K.K., Houser, S., Marini, R., and Langer, R. Functional arteries grown *in vitro*. Science 1999; 284: 489-493.
8. Weinberg, C.B. and Bell, E. A blood vessel model constructed from collagen and cultured vascular cells. Science 1986; 231: 397-400.
9. Hirai, J. and Matsuda, T. Venous reconstruction using hybrid vascular tissue composed of vascular cells and collagen: tissue regeneration process. Cell Transplant. 1996; 5: 93-105.
10. L'Heureux, N., Paquet, S., Labbe, R., Germain, L., and Auger, F.A. A completely biological tissue-engineered human blood vessel. FASEB J. 1998; 12: 47-56.
11. Ratcliff, A. Tissue engineering of vascular grafts. Matrix Biol. 2000; 19: 353-357.
12. Wendt, D., Marsano, A., Jakob, M., Heberer, M., and Martin, I. Oscillating perfusion of cell suspensions through three-dimensional scaffolds enhances cell seeding efficiency and uniformity. Biotechnol.Bioeng. 2003; 84: 205-214.
13. Li, Y., Ma, T., Kniss, D.A., Lasky, L.C., and Yang, S. Effects of filtration seeding on cell density, spatial distribution, and proliferation in nonwoven fibrous matrices. Biotechnol.Prog. 2001; 17: 935-944.
14. Carrier, R.L., Papadaki, M., Rupnick, M., Schoen, F.J., Bursac, N., Langer, R., Freed, L.E., and Vunjak-Novakovic, G. Cardiac tissue engineering: cell seeding, cultivation parameters, and tissue construct characterization. Biotech.Bioeng. 1999; 64: 580-589.
15. Nasseri, B.A., Pomerantseva, I., Kaazempur-Mofrad, M.R., Sutherland, F.W.H., Perry, T., Ochoa, E., Thompson, C.A., Mayer, J.E., Oesterle, S.N., and Vacanti, J.P. Dynamic rotational seeding and cell culture system for vascular tube formation. Tissue Eng. 2003; 9: 291-299.
16. van Wachem, P.B., Stronck, J.W.S., Koers-Zuideveld, R., Dijk, F., and Wildevuur, C.R.H. Vacuum cell seeding: a new method for the fast application of an evenly distributed cell layer on porous vascular grafts. Biomaterials 1990; 11: 6021-606.
17. Buijtenhuijs, P., Buttafoco, L., Poot, A.A., Daamen, W.F., van Kuppevelt, T.H., Dijkstra, P.J., de Vos,

R.A.I., Sterk, L.M.Th., Geelkerken, R.H., Feijen, J., and Vermes, I. Tissue engineering of blood vessels: Characterisation of smooth muscle cells for culturing on collagen and elastin based scaffolds. Biotechnol.Appl.Biochem. 2003; 39: 141-149.

18. Daamen, W., Veerkamp, J.H., and van Kuppevelt, T.H. Purification of elastin and preparation of matrices for tissue engineering. Indust.Protein 2001; 9: 15-17.
19. Heimli, H., Kahler, H., Endresen, M.J., Henriksen, T., and Lyberg, T. A new method for isolation of smooth muscle cells from human umbilical cord arteries. Scand.J.Clin.Lab Invest. 1997; 57: 21-29.
20. Chamley-Campbell, J., Campbell, G.R., and Ross, R. The smooth muscle cell in culture. Physiol.Rev. 1979; 59: 1-61.
21. Lefebvre, P., Nusgens, B.V., and Lapiere, C.M. Cultured myofibroblasts display a specific phenotype that differentiates them from fibroblasts and smooth muscle cells. Dermatology 1994; 189: 65-67.
22. Olde Damink, L.H.H., Dijkstra, P.J., van Luyn, M.J.A., van Wachem, P.B., Nieuwenhuis, P., and Feijen, J. Cross-linking of dermal sheep collagen using a water-soluble carbodiimide. Biomaterials 1996; 17: 765-773.
23. Buttafoco, L., Engbers-Buijtenhuijs, P., Poot, A.A., Dijkstra, P.J., Daamen, W.F., van Kuppevelt, T.H., Vermes, I., and Feijen, J. First steps towards tissue engineering of small-diameter blood vessels: preparation of flat scaffolds of collagen and elastin by means of freeze-drying. J.Biomed.Mater.Res. 2004; submitted:
24. Martin, I., Wendt, D., and Heberer, M. The role of bioreactors in tissue engineering. Trends Biotechnol. 2004; 22: 80-86.
25. Bruil, A., van Aken, W.G., Beugling, T., Feijen, J., Steneker, I., Huisman, J.G., and Prins, H.K. Asymmetric membrane filters for the removal of leukocytes from blood. J.Biomed.Mater.Res. 1991; 25: 1459-1480.
26. Ives, K.J. Depth filtration of liquids. Filtr.Separ. 1970; 7: 700-704.
27. Kleinman, H.K., R.J.Klebe, and G.R.Martin. Role of collagenous matrices in the adhesion and growth of cells. J.Cell Biol. 1981; 88: 473-485.
28. Skinner, M.P., Raines, E.W., and Ross, R. Dynamic expression of a1b1 and a2b1 integrin receptors by human vascular smooth muscle cells. Am.J.Pathol. 1994; 145: 1071-1081.
29. Nikolovski, J. and Mooney, D.J. Smooth muscle cell adhesion to tissue engineering scaffolds. Biomaterials 2000; 21: 2025-2032.
30. Labat-Robert, J. Cell-matrix interactions in aging: role of receptors and matricryptins. Ageing Res.Rev. 2004; 3: 233-247.
31. Spofford, C.M. and Chillian, W.M. Mechanotransduction via the elastin-laminin receptor (ELR) in resistance arteries. J.Biomech. 2003; 36: 645-652.
32. Sartore, S., Chiavegato, A., Faggin, E., Franch, R., Puato, M., Ausoni, S., and Pauletto, P. Contribution of adventitial fibroblasts to neointima formation and vascular remodeling: from innocent bystander to active participant. Circ.Res. 2001; 89: 1111-1121.
33. Brodbeck, W.G., Shive, M.S., Colton, E., Nakayama, Y., Matsuda, T., and Anderson, J.M. Influence of biomaterial surface chemistry on the apoptosis of adherent cells. J.Biomed.Mater.Res. 2001; 55: 661-668.

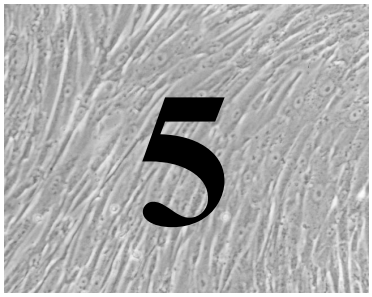

5

Analysis of the Balance Between Proliferation and Apoptosis of Cultured Vascular Smooth Muscle Cells for Tissue Engineering Applications*

* P. Engbers-Buijtenhuijs[1, 2], L. Buttafoco[1], A.A. Poot[1], R. H. Geelkerken[2], J. Feijen[1], and I.Vermes[1, 2]

Submitted for publication to Tissue Eng. 2005

[1] University of Twente, Faculty of Science & Technology, Department of Polymer Chemistry and Biomaterials, and Institute of Biomedical Technology (BMTI), P.O. Box 217, 7500 AE Enschede, The Netherlands

[2] Medisch Spectrum Twente, Hospital Group, Department of Clinical Chemistry, P.O. Box 50.000, 7500 KA Enschede, The Netherlands

Abstract

Tissue homeostasis, the balance between cell proliferation and apoptosis, is an important factor in tissue engineering. We describe a new method to analyse markers of both proliferation and apoptosis in one single assay to follow growth behaviour of cell cultures. A pure culture of human vascular smooth muscle cells (SMCs) was used in this study. SMCs were either cultured on gelatin coated tissue culture polystyrene (g-TCPS) or in three-dimensional porous scaffolds composed of collagen and elastin. mRNA concentrations of cyclin E and tissue transglutaminase (tTG), quantified by a real-time reversed transcriptase polymerase chain reaction and normalised to porphobilinogen deaminase mRNA concentrations, were analysed. tTG mRNA expression levels were increased when cells were cultured in serum-free culture medium compared to standard (serum-containing) culture medium on g-TCPS. Cyclin E mRNA expression levels are not significantly altered in these cell cultures. From these results we concluded that our assay could be used to characterise cell growth behaviour of SMCs *in vitro*. In addition we showed that this test is suitable to measure the balance between proliferation and apoptosis of SMCs present in tissue-engineered constructs. Crosslinking procedures of three-dimensional porous scaffolds composed of collagen and elastin employing carbodiimide and/or diamine reagents did not influence growth behaviour of SMCs inside the scaffolds.

Introduction

Cells for tissue engineering applications are isolated from (human) tissue and cultured *in vitro*. There is a significant variety between different batches of these cultures, which makes it difficult to perform experiments in a standardised way. In addition it is difficult to evaluate the success of cell seeding and culturing in three-dimensional porous scaffolds without quantitative growth behaviour techniques of these cells. The balance between proliferation and apoptosis of vascular cells is responsible for mediating profound changes in vascular architecture in normal development and disease [1] and therefore very important for the success of tissue engineering . Events of both proliferation and apoptosis can be measured *in vitro* by several qualitative as well as quantitative techniques. Most of the quantitative methods to study apoptosis in cell populations are based on flow cytometry of cells in suspension [2-4]. Flow cytometry can also be performed using adherent cells after detachment of the cells from the support. However, cell detachment induces apoptosis by itself [5]. Therefore, flow cytometry is not an optimal quantitative technique to measure apoptosis in adherent cells [6].

A new approach is to analyse mRNA expression levels of an apoptotic marker. Tissue transglutaminase (tTG) is a multi functional transamidating acyltransferase which becomes activated during the latter phase of apoptosis and which plays a role in the formation of apoptotic bodies. Activated tTG induces irreversible cross-links in and between cytoplasmatic proteins to produce a large, stable, insoluble protein scaffold [7]. This crosslinking of proteins stabilises cell and membrane structures of disintegrated cells and apoptotic bodies [8]. Volokhina *et al*. [9] showed that tTG mRNA expression could be used as a trace marker for detection and quantification of apoptosis of both circulating and adherent cells. mRNA expression levels were measured by a semi-quantitative real-time reversed transcriptase polymerase chain reaction (RT-PCR) [10]. In the present study, we describe the optimisation of this RT-PCR technique measuring tTG mRNA expression levels for analysis of apoptosis in SMC cultures. A DNA fragmentation assay measuring the incorporation of propidium iodide (PI) using flow cytometry was used as a reference test to measure apoptosis [5, 11].

Since markers of both apoptosis and proliferation have to be taken into account when considering growth behaviour [1], we measured mRNA expression levels of cyclin E as a marker of proliferation. Cyclin E regulates the transition from the G1 to the S phase of the cell cycle. A high level of the cyclin E protein facilitates this transition indicating enhanced proliferation [12, 13]. In this way, events of both proliferation and apoptosis can be analysed in one single assay. An additional advantage of this method is that cells don't have to be detached from the support because RNA can directly be isolated from adherent cells. Therefore, this method can ideally be performed for tissue engineering applications since RNA can be isolated from cells cultured inside porous scaffolds. Effects of different types of porous structures on growth behaviour of cells cultured inside the scaffolds could be analysed in a quantitative way.

In the present paper culturing of SMCs on gelatin-coated tissue culture polystyrene (g-TCPS) was used as a model to develop the methodology to analyse the balance between proliferation and apoptosis *in vitro*. To verify whether this method could be used for tissue engineering purposes, SMCs were seeded and cultured in three-dimensional porous scaffolds composed of collagen and elastin for tissue engineering of small-diameter blood vessels, as previously described [14]. By analysing tTG and cyclin E mRNA expression levels of these cells, the influence of two procedures to cross-link the scaffolds on SMC growth behaviour was investigated.

Materials

Dulbecco's Modified Eagle's Medium (DMEM) was purchased from Gibco BRL (Breda, The Netherlands). Penicillin, streptomycin, fetal bovine serum and trypsin/ethylene diamine tetra acetic acid (EDTA) were purchased from Biowhittaker (Verviers, Belgium). Gelatin type B from bovine skin, camptothecin (CPT), bovine serum albumin (BSA), propidium iodide (PI), N-(3-dimetylaminopropyl)-N'-ethylcarbodiimide hydrochloride (EDC), N-hydroxy-succinimide (NHS) and poly(propylene glycol)-bis-(2-aminopropyl ether) (J230) were obtained from Sigma and Aldrich (St Louis, Missouri, USA). Mouse monoclonal antibodies (mAbs) against human α-smooth muscle actin (α-SMA) and human vimentin and fluorescein isothiocyanate-labelled rabbit anti mouse immunoglobulins (RAM-FITC) were purchased from DAKO (Glostrup, Denmark). Human serum was acquired by overnight coagulation of blood (collected from healthy volunteers), subsequently pooled and stored at -80^{0}C. QIAmp RNA Blood Mini Kit was from QIAgen (Hilden, Germany). Primers, dithiotheitrol (DTT), and Moloney Murine Leukemia Virus (M-MLV) reverse transcriptase enzyme were obtained from Invitrogen (Paisley, UK). dNTPs were from Amersham Pharmacia Biotech (Cambridge, UK). RNAse inhibitor was from Roche (Basel, Switzerland). Insoluble collagen (type I from bovine achilles tendons) and insoluble elastin (from equine ligamentum nuchae, purification as in [15] were kindly donated by dr. T.H. van Kuppevelt, Department of Biochemistry, Katholieke Universiteit Nijmegen, The Netherlands.

Methods

Isolation and culturing of SMCs on g-TCPS

SMCs were isolated from human umbilical veins according to the method of Heimli *et al*. [16] with some minor modifications as previously described [14]. Cells were cultured on gelatin-coated (0.5% w/v) tissue culture polystyrene (g-TCPS) using DMEM containing 10% (v/v) heat-inactivated (30 min, 56^{0}C) pooled human serum, 10% (v/v) heat-inactivated (30 min, 56^{0}C) fetal bovine serum, 50 units/ml penicillin and 50 μg/ml streptomycin (standard culture medium) [16]. Culture medium was refreshed every 2-3 d. Cells were cultured in an incubator at 37^{0}C in a humidified atmosphere containing 5% CO_2. When sub-confluent cultures were obtained, cells were detached from the support with 0.125% (w/v) trypsin/0.05% (w/v) EDTA and subcultured for several passages with a maximum of 15 (split ratio 1:3) [17]. To analyse apoptosis and/or proliferation, SMCs were cultured to 80% of confluence (time point 0) and subsequently cultured in standard culture medium (control cells) or in serum-free culture

medium to induce apoptosis in a natural (mild) way [18]. To chemically induce apoptosis, cells were treated with CPT [19] (0.20 μM in standard culture medium).

Identification of SMCs

SMCs were identified using mAbs against human α-SMA and human vimentin [16, 20]. Fluorescence of the used secondary antibody RAM-FITC was examined with immuno fluorescent microscopy and with flow cytometry as described earlier [14]. Negative controls were obtained by omitting first antibodies and by staining human umbilical vein endothelial cells (HUVECs) and human dermal fibroblasts with the used antibodies.

DNA fragmentation assay

DNA fragmentation in cell cultures on g-TCPS was determined with flow cytometry using PI according to Nicoletti *et al.* [11]. After several culture time intervals, medium of the cell cultures was collected and adherent cells were detached from the support using a 0.125% trypsin/0.05% EDTA solution. Detached cells and cells present in the culture medium were washed and fixed in 70% ethanol. After another wash, cells were stained with 15 μM PI during 30 min at 37^0C [2] and PI fluorescence of individual cells was measured with a Coulter Epics XL flow cytometer, using System II TM software with the XL-2 or DOS configuration. Excitation was elicited at 488 nm with the Argon laser and measured using the long pass (>570 nm) filters. In each sample 10,000 events were measured and data were analysed with Coulter program Expo II.

RNA isolation and real-time RT-PCR method

RNA isolation was performed using QIAamp RNA Blood Mini Kit according to the manufacturer's instructions. A standard cDNA synthesis was performed as described by Volokhina *et al.* [9] and mRNA expression levels of tTG-mRNA and cyclin E-mRNA were determined using a TaqMan based, real-time RT-PCR technique according to Heid *et al.* [10]. Fragments of the tTG sequence were amplified using the primer (900 nM) and probe (200 nM) set as described by Volokhina *et al.* [9]. Fragments of the cyclin E sequence were amplified using the primer (300 nM) and probe (200 nM) set as described by Müller-Tidow *et al.* [13]. Probes were labelled at the 5' end with reporter fluorophore FAM and at the 3' end with TAMRA, which served as a quencher. Primer and probe concentrations were optimised following the guidelines of the provider. mRNA expression levels of the two proteins were normalised to mRNA expression levels of porphobilinogen deaminase (PBGD) as described

by Volokhina *et al.* [9]. To investigate if mRNA expression levels of PBGD could be used to normalise cyclin E and tTG mRNA expression levels of SMCs, the influence of serum starvation and CPT-treatment on the PBGD mRNA expression of SMCs was checked. After total RNA was isolated from SMCs cultured in standard culture medium, in serum-free culture medium or in CPT containing standard culture medium, the amount of RNA was determined by measuring the absorbance at 260 nm (A260) on a spectrophotometer. The purity of the isolated RNA was analysed by measuring the ratio of A260/A280 on a spectrophotometer. PBGD mRNA expression levels of 1 μg of RNA were then analysed. The number of cycles that it takes for the amplification plot to reach the threshold limit is called the threshold cycle (Ct-value) and is used for quantification. mRNA expression levels of tTG and cyclin E of cells cultured on g-TCPS were compared to levels at time point 0. mRNA expression levels of cells cultured on crosslinked scaffolds were compared to levels of cells cultured on non-crosslinked (native) scaffolds.

Culturing SMCs in three-dimensional porous scaffolds composed of collagen and elastin

Three-dimensional (circular) porous scaffolds for tissue engineering applications (diameter of 16 mm, thickness of 2 mm, porosity of 98% and a pore size of around 200 μm [14]) were used to examine the interaction of SMCs with the scaffolds. Scaffolds were composed of type I insoluble collagen (derived from bovine achilles tendons) and insoluble elastin (from equine ligamentum nuchae), prepared by freeze-drying and optimised in terms of pore size and cross-link density [14]. Crosslinking of the scaffolds was performed either with a water-soluble carbodiimide (EDC/NHS) or with a diamine (J230) in the presence of the carbodiimide, to improve the physical and mechanical properties [21]. Scaffolds were sterilised with 70% ethanol and washed three times with PBS before SMC seeding. SMCs were seeded at a density of 200.000 cells/cm^2 in the scaffolds using filtration seeding as described by Li *et al* [22] and subsequently cultured in 24 wells plates under static conditions for 14 d in DMEM culture medium. Culture medium was refreshed every 2-3 d. Cell attachment and growth were analysed by histology using a standard Elastic Von Gieson staining procedure on transverse sections of the tissue-engineered (TE) scaffolds at the Laboratory of Pathology Oost Nederland.

Statistical analysis

Data of the DNA fragmentation assay represent mean ± standard error of the mean (SEM) of 2 experiments performed in duplicate. Data of mRNA expression levels represent mean ± SEM of 5 experiments performed in duplicate. Statistical analyses of the influences of serum-free medium and CPT compared to control medium on SMC cultures were performed by using the Wilcoxon Rank sum test with correction for multiple testing (Holms' testing). Statistical analyses of DNA fragmentation and tTG mRNA expression levels for up to 240 h were performed using the ANOVA test and a post hoc Tukey's Honesthy Significant Difference test (HSD). In both cases p values < 0.05 were considered as statistical significant.

Results

Identification of SMCs

SMCs cultured on g-TCPS isolated from human umbilical veins, showed a characteristic morphology consisting of a hill and valley pattern 5 d after reaching confluence. Filaments of α-SMA (of 60% confluent cultures) were visualised using immuno fluorescent microscopy. Human skin fibroblasts and HUVECs were neither showing this characteristic hill and valley pattern nor this pattern of fluorescence (data not shown). Quantitative analyses of the presence of α-SMA filaments and vimentin were done with flow cytometry. Histograms in figure 1 show the number of cells versus fluorescence intensity. Using the mAb against human α-SMA, 98 % of the treated cells were positively stained, against 2 % of the negative control in which the first antibody was omitted (figure 1a). With the mAb against human vimentin, 81 % of the treated cells were positively stained, against 2% of the negative control cells (figure 1b), indicating that cultured cells are of mesenchymal origin [20]. Human skin fibroblasts and HUVECs were not positively stained with the mAb against α-SMA (data not shown).

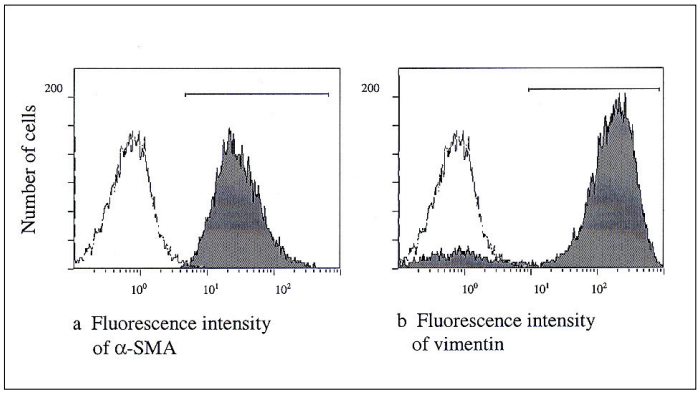

Figure 1: Flow cytometric analyses of immuno fluorescent staining of human α-SMA (a) and human vimentin (b) in SMCs cultured on g-TCPS. Cells were stained with primary mAbs against human α-SMA and human vimentin and a secondary antibody RAM-FITC (grey) or only with the secondary antibody as a negative control (white). Fluorescence was analysed with flow cytometry and numbers of cells were plotted against fluorescence intensity. Horizontal bars indicate gate of stained cells to determine percentage of positively stained cells.

DNA fragmentation assay

By means of flow cytometry of SMCs cultured on g-TCPS, diagrams of forward scatter (FSC) against side scatter (SSC) were obtained as shown in figure 2a, c and e. A change in scatter diagram in the lower scatter regions could be observed when cells were cultured in serum-free culture medium (figure 2c) or when cells were incubated with CPT (figure 2e) compared to control cells (figure 2a). Histograms of PI fluorescence of human SMCs showed three distinct peaks of three separate cell populations. A G0/G1 region of normal diploid cells, a G2/M region of dividing cells with a double amount of DNA and an A0 region of hypo diploid cells [2], as can be seen in figure 2b, d, and f. The sub population of A0 cells showed reduced DNA stainability, indicating apoptotic cells in which DNA fragments appear and cell fragmentation has occurred [2, 3].

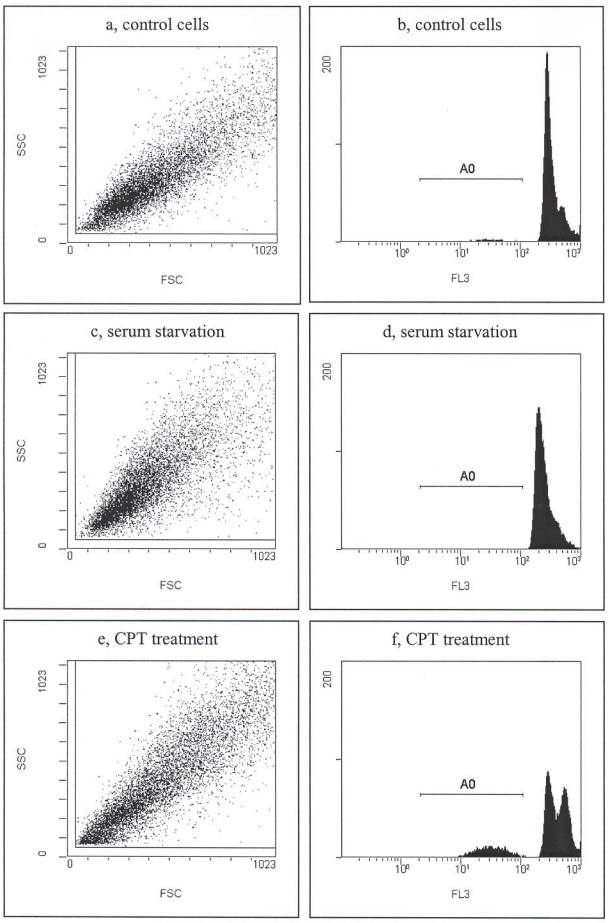

Figure 2: Apoptosis of SMCs cultured on g-TCPS measured by a DNA fragmentation assay. Cells were cultured for 48 h in serum-containing culture medium (control cells, a, b) or in serum-free culture medium (c, d) or treated with 0.20 µM CPT in serum-containing culture medium (e, f). DNA was stained with PI and scatter diagrams and PI fluorescence were analysed with flow cytometry. In scatter diagrams (a, c, e) SSC are plotted against FSC and in histograms (b, d, f) numbers of SMCs are plotted against PI fluorescence intensity (FL3). Horizontal bars (b, d, and f) indicate gate of apoptotic cells (A0) to determine percentage of apoptotic cells compared to the total amount of cells.

Percentages of apoptotic cells compared to the total amount of cells and compared to percentages of apoptotic cells at time point zero, were calculated. Percentages of apoptotic cells were increasing in time for CPT-treated cell cultures, whereas a slight increase in time of percentages of apoptotic cells was observed for SMCs cultured in standard culture medium. No apoptotic cells were observed in serum-free cultures for up to 48 h as can be seen in figure 3.

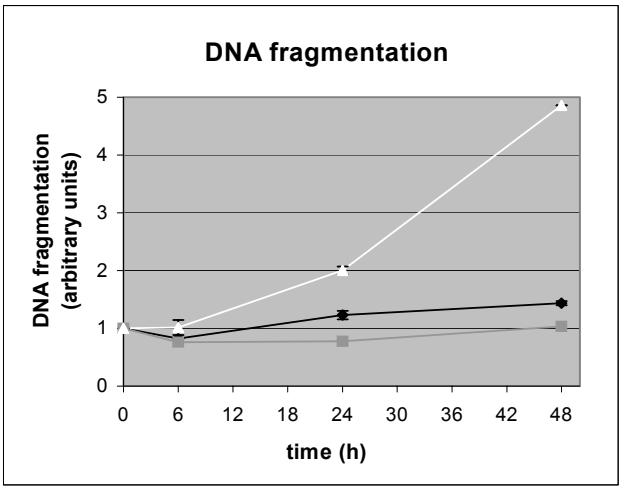

Figure 3: Apoptotic cell death of SMCs cultured on g-TCPS measured by a DNA fragmentation assay as a function of time. Cells were cultured in serum-containing culture medium (control cells, black) or in serum-free culture medium (grey) or treated with 0.20 μM CPT in serum-containing culture medium (white) for several culture time intervals. DNA was stained with PI and fluorescence was analysed with flow cytometry. Percentages of apoptotic cells compared to the total amount of cells and compared to percentages of apoptotic cells at time point zero, were calculated and plotted against time.

When analysing the G2/M region of the histograms of figure 2; CPT-treated cells showed a large peak of dividing cells whereas cells cultured in serum-free culture medium hardly showed a peak of dividing cells. Because it was not possible to distinguish the G0/G1 and G2/M peaks, calculations of the relative contributions were not made. Analysis of apoptosis in control cell cultures for up to 240 h showed an increase of A0 cells employing the DNA fragmentation assay (figure 4a).

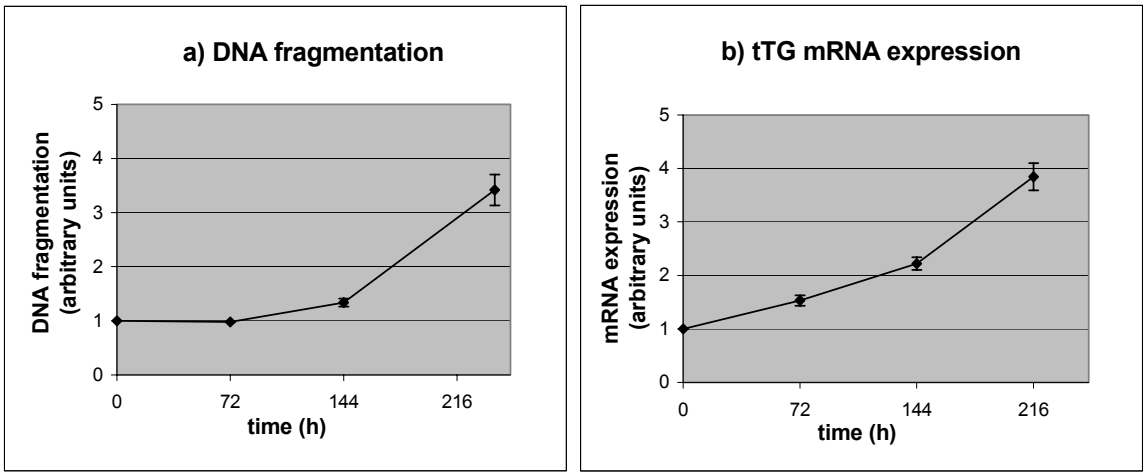

Figure 4: Apoptosis of SMCs cultured on g-TCPS measured by a DNA fragmentation assay and by analysing tTG mRNA expression levels as a function of time. Cells were cultured in serum-containing culture medium for several culture time intervals. DNA was stained with PI and fluorescence was analysed with flow cytometry. Percentages of apoptotic cells, compared to the total amount of cells measured and compared to percentages of apoptotic cells at time point zero were calculated and plotted against time (a). tTG mRNA expression levels were determined using a semi-quantitative real-time RT-PCR method. tTG mRNA expression levels, compared to levels at time point zero and normalised to mRNA expression levels of PBGD, were calculated and plotted against time (b).

tTG mRNA expression of SMCs cultured on g-TCPS

At least 25 µg total RNA was isolated from the cell cultures as determined by spectrophotometry. The ratio of A260/A280 was in between 1.7 and 1.9 indicating pure RNA. mRNA expression levels of PBGD in cultured SMCs were not influenced by serum starvation or CPT-treatment. This allowed us to use PBGD mRNA expression levels to normalise tTG and cyclin E mRNA expression levels for quantification. Analysis of tTG mRNA expression levels of control cell cultures on g-TCPS for up to 240 h showed an increase in tTG mRNA expression using the semi-quantitative real-time RT-PCR method (figure 4b). This increase resembles the increase of A0 cells measured with the DNA fragmentation assay (figure 4a). Results of the analyses of tTG mRNA expression levels in time of SMCs cultured on g-TCPS in culture medium with or without serum or treated with CPT in standard culture medium are shown in figure 5. After 24 h, an increase of tTG mRNA expression levels was observed for cells cultured in culture medium without serum whereas no increase was observed for cells cultured in standard culture medium with or without CPT. These results were not corresponding with results of the DNA fragmentation assay as shown in figure 3.

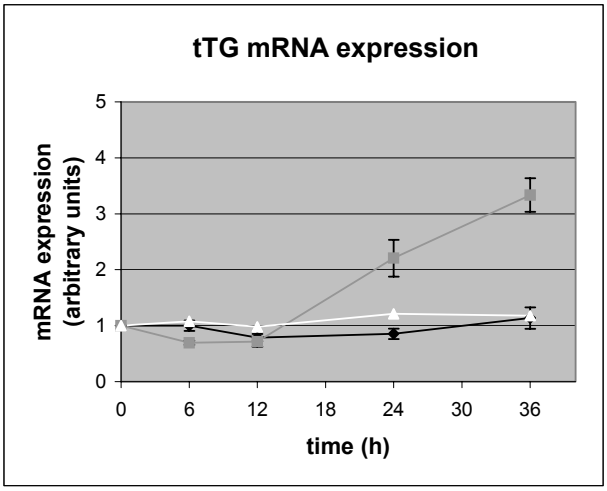

Figure 5: Apoptosis of SMCs cultured on g-TCPS measured by analysing tTG mRNA expression levels as a function of time. Cells were cultured in serum-containing culture medium (control cells, black) or in serum-free culture medium (grey) or treated with 0.20 μM CPT in serum-containing culture medium (white) for several culture time intervals and tTG mRNA expression levels were determined using a semi-quantitative RT-PCR method. tTG mRNA expression levels compared to levels at time point zero were calculated and plotted against time.

Cyclin E mRNA expression of SMCs cultured on g-TCPS

Cyclin E mRNA expression levels as a function of time in SMCs cultured on g-TCPS in culture medium with or without serum are shown in figure 6. After 6 and 12 h cyclin E mRNA expression levels in cells cultured in serum-free culture medium were reduced compared to cells cultured in standard culture medium. After more than 24 h, no differences were observed. Because CPT induced apoptosis cannot be detected by analysing tTG mRNA expression levels, cyclin E mRNA expression levels, required to be able to compare markers of proliferation and apoptosis, were not analysed in SMC cultures treated with CPT.

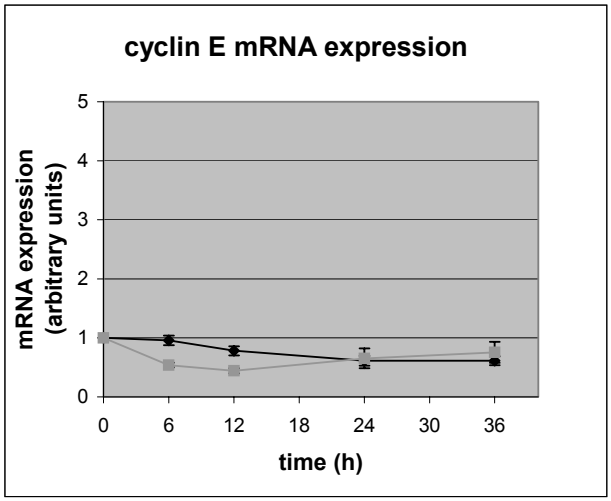

Figure 6:Proliferation ***of SMCs cultured on g-TCPS measured by analysing cyclin E mRNA expression levels as a function of time.*** Cells were cultured in serum-containing culture medium (control cells, black) or in serum-free culture medium (grey) for several culture time intervals and cyclin E mRNA expression levels were determined using a semi-quantitative real-time RT-PCR method. Cyclin E mRNA expression levels compared to levels at time point zero were calculated and plotted against time.

Tissue engineering application

SMC adhered and grew in multi layers on top of and inside the three-dimensional porous structures composed of collagen and elastin as observed by histology [14]. mRNA could be isolated from the TE scaffolds. The expression levels of PBGD in these cultured SMCs were not influenced by scaffold properties. This allowed us to use PBGD mRNA expression levels to normalise tTG and cyclin E mRNA expression levels for quantification. No significant changes were found in both cyclin E and tTG mRNA expression levels of SMCs cultured in the porous scaffolds, crosslinked either with EDC/NHS or with J230 in the presence of EDC/NHS compared to native scaffolds as can be seen in figure 7.

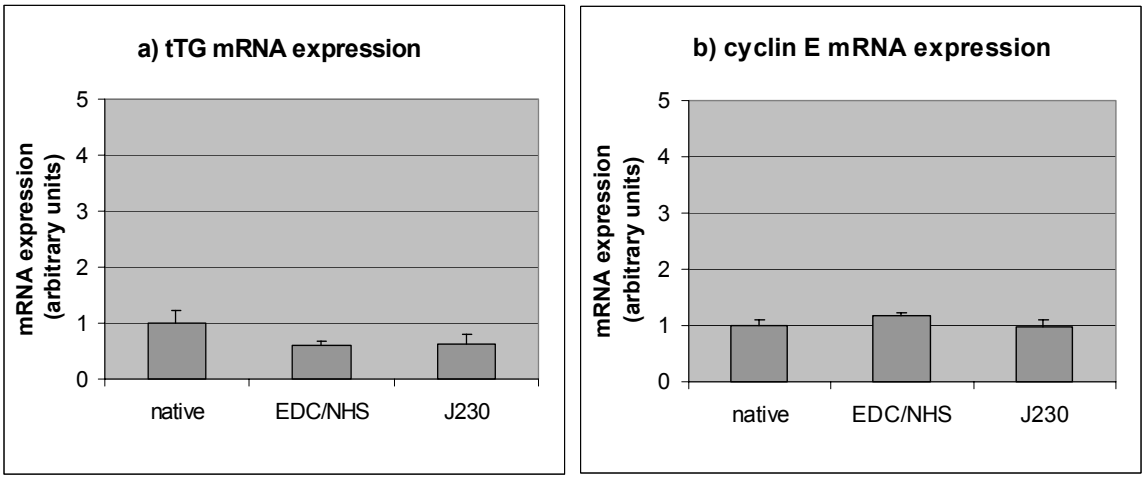

Figure 7: Apoptosis (a) and proliferation (b) of SMCs cultured for 14 d on TE scaffolds by analysing tTG and cyclin E mRNA expression levels. Scaffolds were composed of collagen and elastin and crosslinked with either a carbodiimide (EDC/NHS) or with a diamine (J230) in the presence of the carbodiimide. mRNA expression levels of tTG and cyclin E were determined using a semi-quantitative real-time RT-PCR method and mRNA expression levels of cells cultured on crosslinked scaffolds were compared to mRNA expression levels of cells cultured on native scaffolds.

Discussion

A pure SMC culture of mesenchymal origin [20] was used in this study to analyse the balance between proliferation and apoptosis. Cultured SMCs on g-TCPS grew in overlapping layers in a series of hills and valleys as described in literature [16]. The appearance of this organisation at confluence and the presence of α-smooth muscle actin filaments distinguish these cultured cells from endothelial cells, fibroblasts and myofibroblasts [17, 20]. From the results of our reference DNA fragmentation assay to measure apoptosis with flow cytometry, it can be concluded that CPT incubation induces apoptosis in SMCs cultured on g-TCPS in a time depending manner [19, 23]. DNA fragmentation was not observed when SMCs were cultured in serum-free culture medium. This result is in contrast with other research that shows an apoptosis-inducing effect of culturing SMCs in serum-free culture medium [18, 24] and is in contrast with the enhanced tTG mRNA expression level measured by our RT-PCR method. We suggest that due to the elevated tTG protein level, stable apoptotic bodies are formed by stabilisation of cell and membrane structures and that these apoptotic bodies are washed away during the procedure for flow cytometric analyses. In contrast, apoptosis induced by CPT incubation can be detected using the DNA fragmentation assay but can not be detected by analysing tTG mRNA expression levels. The latter can be explained by the fact that CPT

blocks DNA topoisomerase I complex that is necessary for replication and transcription [23]. Therefore, tTG transcription is inhibited in SMCs treated with CPT but DNA fragmentation is observed. These results clearly show that the optimal technique to analyse apoptosis depends on the inducer used. When SMCs cultured on g-TCPS in standard culture medium reach confluence (after 3-4 d), both enhanced DNA fragmentation and enhanced tTG mRNA expression are observed indicating that apoptosis is induced. From these results we conclude that in this case both methods are correlating.

When analysing the G2/M region of the flow cytometric histograms of cells cultured on g-TCPS, CPT-treated cells show a large peak of dividing cells compared to control cells. This can be explained by the fact that CPT binds irreversibly to the DNA topoisomerase I complex and in this way blocks the cell cycle in the S-phase. DNA duplication has occurred but mitosis have been blocked [19, 23]. On the contrary, cells cultured in serum-free culture medium hardly show a peak of dividing cells compared to control cells. This can be explained by the fact that no growth factors and other essential proteins are available in the culture medium.

When growth behaviour is taken into consideration, neither apoptosis nor proliferation alone will give satisfactory information, so markers of both biological events should be measured. With the described semi-quantitative real-time RT-PCR method it is possible to measure both events in one single assay by analysing cyclin E and tTG mRNA expression levels in SMCs [9, 12, 13, 25, 26]. mRNA expression levels of PBGD can be used for this purpose to normalise mRNA expression levels of both tTG and cyclin E to correct for differences in total RNA content. Cyclin E mRNA expression levels were not significantly altered in SMCs cultured on g-TCPS in standard culture medium for up to 36 h. SMCs cultured in serum-free culture medium showed reduced cyclin E mRNA expression levels after 6 and12 h compared to cells cultured in serum-containing medium, maybe due to the lack of growth factors present in normal serum. But after 24 h and 36 h we did not find significant differences in cyclin E mRNA expression levels between the two cultures suggesting an adaptation of the cell cycle [27]. Analysing both events of proliferation and apoptosis of SMCs within one single test is now possible in an accurate and reproducible way using the described new semi-quantitative real-time RT-PCR method.

We showed that the method is suitable for tissue engineering applications, by analysing the cyclin E and tTG mRNA expression levels of SMCs cultured in three-dimensional porous structures composed of collagen and elastin. These scaffolds are under investigation for tissue engineering of small-diameter blood vessels [14]. Cross-linking of the scaffolds either with a carbodiimide (EDC/NHS) or with a diamine (J230) in the presence of the carbodiimide does

not influence SMC growth behaviour as characterised by analysing the balance between apoptosis and proliferation using the new RT-PCR method described in this paper. These quantitative findings confirm our qualitative observations using histology as previously described [14]. We suggest that this method can be used to characterise and compare cell growth behaviour of different batches of cells. In addition, other mRNA expression levels of the same samples can easily be analysed in a similar way like the mRNA expression of extra-cellular matrix proteins of SMCs as described by Seliktar *et al* [28]. With this approach it will be possible to culture cells in a standardised way not only for obtaining a TE blood vessel but also for other kinds of tissue engineering purposes using a variety of cell types.

Acknowledgement

W. Daamen and A. van Kuppevelt (University Medical Centre Nijmegen, Department of Biochemistry 194, NCMLS, Nijmegen, The Netherlands) are kindly acknowledged for the donation of collagen and elastin. R.A.I. de Vos and L.M.T. Sterk (Laboratory of Pathology Oost-Nederland, Enschede, The Netherlands) are kindly acknowledged for performing histology.

Reference list

1. Vermeulen, K., Berneman, Z.N., and Van Bockstaele, D.R. Cell cycle and apoptosis. Cell Prolif. 2003; 36: 165-175.
2. Vermes, I., Haanen, C., and Reutelingsperger, C. Flow cytometry of apoptotic cell death. J.Immunol.Methods 2000; 243: 167-190.
3. Darzynkiewicz, Z., Bedner, E., and Smolewski, P. Flow cytometry in analysis of cell cycle and apoptosis. Semin.Hematol. 2001; 38: 179-193.
4. Michie, J., Akudugu, J., Binder, A., Van Rensburg, C.E.J., and Bohm, L. Flow cytometric evaluation of apoptosis and cell viability as a criterion of anti-tumour drug toxicity. Anticanc.Res. 2003; 23: 2675-2680.
5. Micoud, F., Mandrand, B., and Malcus-Vocanson, C. Comparison of several techniques for the detection of apoptotic astrocytes in vitro. Cell Prolif. 2001; 34 : 99-113.
6. van Engeland, M., Ramakers, F.C.S., Schutte, B., and Reutelingsperger, C.P.M. A novel assay to measure loss of plasma membrane asymmetry during apoptosis of adherent cells in culture. Cytometry 1996; 24: 131-139.
7. Fesus, L. and Piacentini, M. Transglutaminas 2: An enigmatic enzyme with diverse fundctions. Trends.Biochem.Sci. 2002; 27: 534-539.
8. Melino, G., Candi, E., and Steiner, P.M. Assays for transglutaminases in cell death. Methods Enzymol. 2000; 322: 433-472.
9. Volokhina, E.B., Hulshof, R., Haanen, C., and Vermes, I. Tissue transglutaminase mRNA expression in apoptotic cell death. Apoptosis 2003; 8: 679-

10. Heid, C.A., Stevens, J., Livak, K.J., and Williams, P.M. Real time quantitative PCR. Genome Res. 1996; 6: 986-994.
11. Nicoletti, I., Migliorati, G., Pagliacci, M.C., Grinani, F., and Riccardi, C. A rapid and simple method for measuring thymocyte apoptosis by propidium iodide staining and flow cytometry. J.Immunol.Methods 1991; 139: 271-273.
12. Ohtsubo, M., Theodoras, A.M., Schumacher, J., Roberts, J.M., and Pagano, M. Human cyclin E, a nuclear protein essential for the G1-to-S phase transition. Mol.Cell Biol. 1995; 15: 2612-2624.
13. Muller-Tidow, C., Metzger, R., Kugler, K., Diederichs, S., Idos, G., Thomas, M., Dockhorn-Dworniczak, B., Schneider, P.M., Koeffler, H.P., Berdel, W.E., and Serve, H. Cyclin E is the only cyclin-dependent kinase 2-associated cyclin that predicts metastasis and survival in early stage non-small cell lung cancer. Canc. Res. 2001; 61: 647 -653.
14. Buijtenhuijs, P., Buttafoco, L., Poot, A.A., Daamen, W.F., van Kuppevelt, T.H., Dijkstra, P.J., de Vos, R.A.I., Sterk, L.M.Th., Geelkerken, R.H., Feijen, J., and Vermes, I. Tissue engineering of blood vessels: Characterisation of smooth muscle cells for culturing on collagen and elastin based scaffolds. Biotechnol.Appl.Biochem. 2003; 39: 141-149.
15. Daamen, W., Veerkamp, J.H., and van Kuppevelt, T.H. Purification of elastin and preparation of matrices for tissue engineering . Indust.Protein 2001; 9: 15-17.
16. Heimli, H., Kahler, H., Endresen, M.J., Henriksen, T., and Lyberg, T. A new method for isolation of smooth muscle cells from human umbilical cord arteries. Scand.J.Clin.Lab.Invest 1997; 57 : 21-29.
17. Lefebvre, P., Nusgens, B.V., and Lapiere, C.M. Cultured myofibroblasts display a specific phenotype that differentiates them from fibroblasts and smooth muscle cells. Dermatology 1994; 189: 65-67.
18. Salgame, P., Varadhachary, A.S., Primiano, L.L., Fincke, J.E., Muller, S., and Monestier, M. An ELISA for detection of apoptosis. Nucleic Acids Res. 1997; 25: 680-681.
19. Orlov, S.N., Dan, T.V., Tremblay, J., and Hamet, P. Apoptosis in vascular smooth muscle cells: role of cell shrinkage. Biochem.Biophys.Res.Com. 1996; 221: 708-715.
20. Chamley-Campbell, J., Campbell, G.R., and Ross, R. The smooth muscle cell in culture. Physiol.Rev. 1979; 59: 1-61.
21. Pieper, J.S., Oosterhof, A., Dijkstra, P.J., Veerkamp, J.H., and van Kuppevelt, T.H. Preparation and characterization of porous crosslinked collagenous matrices containing bioavailable chondroitin sulphate. Biomaterials 1999; 20: 847- 858.
22. Li, Y., Ma, T. , Kniss, D.A., Lasky, L.C., and Yang, S. Effects of filtration seeding on cell density, spatial distribution, and proliferation in nonwoven fibrous matrices. Biotechnol.Prog. 2001; 17: 935-944.
23. King, M.A. and Radicchi-Mastroianni, M.A. Effects of caspase inhibition on camptothecin-induced Apoptosis of HL-60 cells. Apoptosis 2002; 49: 28-35.
24. Pelisek, J., Armeanu, S., and Nikol, S. Quiscence, cell viability, apoptosis and necrosis of smooth muscle cells using different growth inhibitors. Cell Prolif. 2001; 34: 305-320.
25. Keyomarsi, K., Tucker, S.L., Buchholz, T.A., Callister, M., Ding, Y., Horogagyi, G.N., Bedrosian, I., Knickerbocker, C., Toyofuku, W., Lowe, M., Herliczek, T.W., and Bacus, S.S. Cyclin E and survival in patients with breast cancer. N.Eng.J.Med. 2002; 347: 1566-1575.

26. Sutherland, R.L. and Musgrove, E.A. Cyclin E and prognosis in patients with breast cancer. N.Eng.J.Med. 2002; 347: 1546-1547.
27. Evan, G.I. and Vousden, K.H. Proliferation, cell cycle and apoptosis in cancer. Nature 2001; 411: 342-348.
28. Seliktar, D., Nerem, R.M., and Galis, Z.S. Mechanical strain-stimulated remodeling of tissue-engineered blood vessel constructs. Tissue Eng. 2003; 9: 657-666.

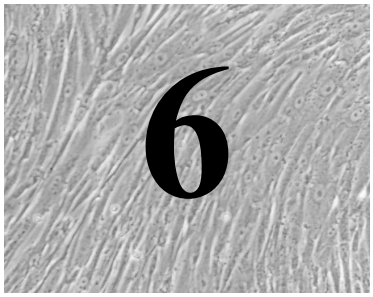

Apoptotic Cell Death Kinetics *in vitro* Depend on the Cell Types and the Inducers Used*

* F. Wolbers, P. Buijtenhuijs, C. Haanen, and I. Vermes

Apoptosis 2004; 9: 385-392

Medisch Spectrum Twente, Hospital Group, Department of Clinical Chemistry, P.O. Box 50.000, 7500 KA Enschede, The Netherlands

Abstract

In vitro exposure of cells to a fluorochrome-labelled inhibitor of caspases (FLICA) labels cells after caspase activation and arrests further progress of apoptotic cell death. The labelled apoptotic cells can be quantified in relation to time of apoptosis induction with flow cytometry. Loss of membrane integrity (late apoptosis and cell death) was measured with exposure to propidium iodide (PI). From the labelling patterns with FLICA and PI the apoptotic cell death kinetics were calculated. HL60 cells and human umbilical vein endothelial cells (HUVECs) were incubated in the presence of the fluorescent inhibitor of caspases, FAM-VAD-FMK (20 mM, FLICA) for up to 48 h. Apoptosis was induced by camptothecin (CPT, 0.15 μM) or by a mixture of tumour necrosis factor alpha (TNF-α, 3 nM) and cycloheximide (CHX, 50 μM). Samples were counter-stained with PI. Incubation of HL60 cells with CPT induced apoptosis in 92% of cells within the first 18 h at a rate of 5% per h while incubation TNF-α/CHX resulted in apoptosis in 76% of the cells within the first 6 h at a rate of 12% per our. Incubation of HUVECs with TNF-α/CHX induced apoptosis in 65% of the cells within the first 18 h at a rate of 3.7% per h during the first 6 h of the incubation. During incubation with TNF-α/CHX the remaining viable HL60 cells and HUVECs entered apoptosis within 48 h at an approximate rate of 0.2% per h. However, on the road of the cell death, HL60 cells showed a transit from the viable ($FLICA^-$/ PI^-) to early ($FLICA^+$/ PI^-) and further to late apoptotic populations ($FLICA^+$/ PI^+), while HUVECs entered directly from the viable to the late apoptotic stage. Apoptotic turnover rate depends on the stimulus used to induce apoptosis, while the type of the cell determines the way of the transition within the apoptotic cascade.

Introduction

Apoptosis is a kinetic event [1]. The entire duration of apoptosis, from onset to total disintegration of the cell is relatively short and of variable length in comparison to the duration of cell cycle [2]. The various inducers of apoptosis start the process by activation of intracellular cysteine-aspartic acid proteases (caspases) [3, 4]. The process of their activation is considered to be the key event of apoptosis [5, 6]. Exposure of cells to a fluorescent inhibitor of caspases FAM-VAD-FMK (FLICA) stains viable cells supravitally [7, 8]. When these cells enter apoptosis, the intracellular FLICA blocks the activation of caspases and arrests further progress of the apoptotic cascade and prevents cellular disintegration [7, 8]. The arrested apoptotic cells, labelled with FLICA, can be followed through the apoptotic cascade and

identified by flow cytometry [7-10]. The fluorescent labelling of cells that enter into apoptosis and the labelling of dead cells with propidium iodide (PI) offers the possibility to estimate the rate of cell entrance into apoptosis, to measure the cumulative apoptotic turnover in time and to follow the occurrence of cell death in time [5-12]. Accordingly, this assay allows to measure the rate-constants between the different stages of the apoptotic cascade and the pattern of the apoptotic process [9]. We compared the cell death kinetics of HL60 cells and human umbilical vein endothelial cells (HUVECs) by using different inducers to initiate apoptotic cell death *in vitro*.

Materials

Human promyelocytic leukemic HL60 cells were obtained from the German Collection of Microorganisms (Braunschweig, Germany). Tissue culture equipment was supplied by Corning (Badhoevedorp, The Netherlands). RPMI-1640 medium, trypsin/ethylene diamine tetra acetic acid (EDTA) solution, penicillin, streptomycin, fetal calf serum, L-Glutamine, fungizone were obtained from BioWhittaker (Verviers, Belgium). Medium 199 (with Hanks salts, L Glutamine and 25 mM N-[2-hydroxyethyl] piperazide-N'-[2-ethanesulphonic acid, HEPES) was from Life Technologies (Grand Island, NY, USA). Camptothecin (CPT), tumour necrosis factor-α (TNF-α), cycloheximide (CHX), propidium iodide (PI) and gelatin were purchased from Sigma and Aldrich (St. Louis, Missouri, USA). FAM-VAD-FMK and z-VAD-FMK were from R&D Systems (Inc. Minneapolis, MN, USA). Lyophilised FAM-VAD-FMK was obtained from Intergen Co. (Purchase, NY, USA).

Methods

HL60 cells

HL60 cells were cultured in RPMI-1640 medium supplemented with 10% (v/v) heat-inactivated and filter-sterilised fetal calf serum, 100 units/mL penicillin, 100 μg/mL streptomycin, 2 mM L-Glutamine and 250 μg/mL fungizone ($RPMI^+$ medium). Cell cultures were maintained in a 5% CO_2 humidified atmosphere at 37^0C. The medium was refreshed every 3-4 d. Exponentially growing cells were used in the experiments.

HUVECs

HUVECs were isolated from umbilical vein, by the method of Jaffe *et al.* [13], using trypsin solution (0.05% (w/v) trypsin/0.02% (w/v) EDTA in PBS (trypsin solution). The obtained

endothelial cells were cultured on 0.5% (w/v) gelatin-coated tissue culture polystyrene flasks. Culture medium consisted of 50% Medium 199 (with Hanks salts, L-Glutamine and 25 mM HEPES) and 50% RPMI-1640 medium with L-glutamine, supplemented with 20% (v/v) heat-inactivated and filter-sterilised human pooled serum, 100 units/mL penicillin, 100 μg/mL streptomycin and 2 mM L-glutamine. Cell cultures were maintained in a fully humidified atmosphere at 37^0C and 5% CO_2. Medium was refreshed every 3-4 d. Confluent cultures were subcultured for up to 5 passages after detachment with use of trypsin solution.

Modulation of apoptosis

CPT or TNF-α and CHX were used in final concentrations of 0.15 μM, 3 nM and 50 μM, respectively. The solution of FAM-VAD-FMK was mixed with a solution of the unlabeled inhibitor z-VAD-FMK in a 1:4 molar ratio. The z-VAD-FMK/fluorescent FAM-VAD-FMK (FLICA) mixture was added to the cell cultures to yield a 20 mM final concentration of the inhibitor.

HL60 cell staining

HL60 cells (0.5 x 10^6 cells/mL) were treated with either CPT (0.15 μM) or TNF-α/CHX (3 nM/50 μM) in the continuous presence of FLICA (20 mM) for different time periods, as specified under results. After incubation, cells were washed twice, resuspended in 0.5 mL PBS and stained with 1 μg/mL PI for 30 s before measurement. Samples were kept on ice until flow cytometry.

HUVEC staining

HUVECs grown to 80% confluence, were treated with either CPT (0.15 μM) or TNF-α/CHX (3 nM/50 μM) in the continuous presence of FLICA (20 mM) for different time periods. During the final 30 min of incubation, 50 μg/mL PI was added to the culturing medium. After incubation supernatants were collected, and adherent cells were detached with trypsin solution. After centrifugation, supernatants and detached cells were pooled, washed twice and resuspended in PBS. Samples were kept on ice until flow cytometry.

Flow cytometry

Green FLICA fluorescence and red PI fluorescence of individual cells were measured with a Coulter Epics XL flow cytometer, using System II ™ software with the XL-2 or DOS

configuration. Excitation was elicited at 488 nm with the Argon laser and measured using the standard band pass (530 nm ± 20 nm) and long pass (>570 nm) filters. In each sample 10,000 events were measured. Flow cytometry data were analysed with the computer program Expo II and gates were set with several controls.

Statistical analysis

Results are shown as mean ± standard deviation of the mean of 1 to 4 separate experiments of each time point. The kinetics of HL60 cells and HUVECs revealed exponential curves. Two tangents were drawn and slopes were determined with linear regression.

Results

HL60 cells

Apoptosis was initiated in HL60 cells by incubation with 0.15 μM CPT or by incubation with a mixture of TNF-α and CHX in final concentrations of 3 nM and 50 μM, respectively. Figure 1a shows light microscopy of untreated cells and cells treated with CPT for 6 h with and without FAM-VAD-FMK (FLICA). Figure 1b shows the bivariate distributions of green and red fluorescence intensity levels from cells 'supravitally' stained with FLICA and PI. Four distinct sub-populations which differ in fluorochrome binding can be identified: Viable, or non-apoptotic cells, show neither FLICA nor PI fluorescence (figure 1b, t = 0 h, quadrant B). Because HL60 cells have the propensity to spontaneously differentiate, some cells in control cultures may represent dying cells that were terminally differentiated (figure 1b, t = 0 h, quadrant C-E). In the initial phase of apoptosis, the caspases become activated and FLICA binds to these activated caspases. In this early phase the plasma membrane is still able to exclude PI. In the initial phase of apoptosis, HL60 cells are $FLICA^+/ PI^-$, early apoptotic (figure 1b, t = 6-24 h, quadrant C). Subsequently, HL60 cells loose their plasma membrane integrity and their ability to exclude PI. These late apoptotic cells are $FLICA^+/ PI^+$ (figure 1b, t= 6-24 h, quadrant D). Finally, HL60 cells loose the ability to bind FLICA, because the caspases are either inhibited or degraded, and become $FLICA^-/ PI^+$. This phase is called the 'necrotic stage' of apoptosis (figure 1b, t = 6-24 h, quadrant E). In the continuous presence of FLICA during the entire culturing period, the transition from $FLICA^+/ PI^+$ (late apoptotic) to $FLICA^-/PI^+$ (necrotic) is prevented (figure 1b). The same transitions of HL60 cells were observed when apoptosis was induced by TNF-α/CHX treatment.

a

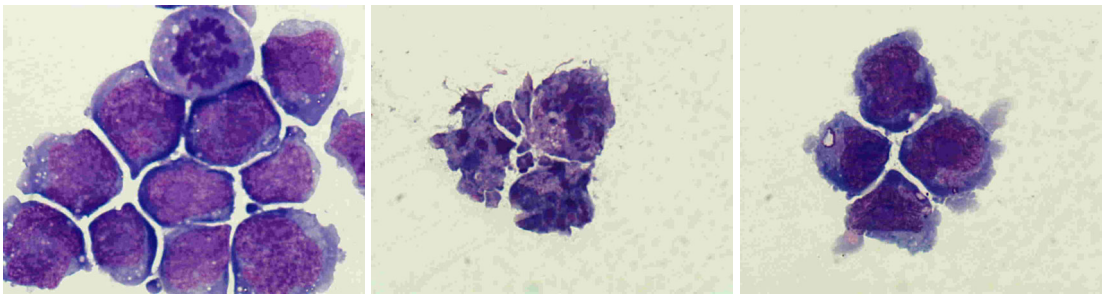

HL60 controle HL60 CPT HL60 CPT FLICA

b

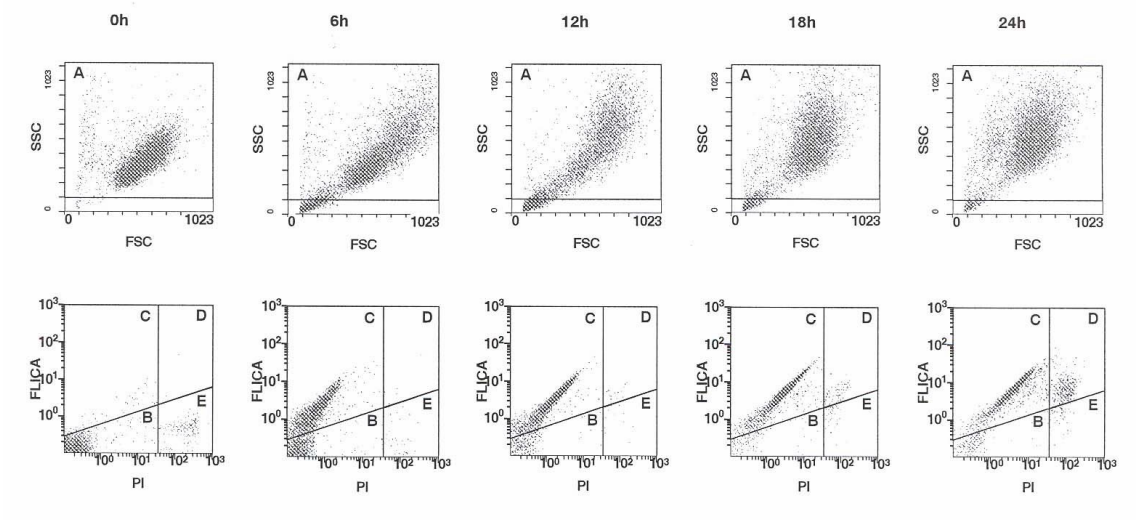

Figure 1: HL60 cells treated with camptothecin (CPT) in the presence of fluorochrome labelled inhibitor of caspases (FLICA). Light microscopy (LM) of untreated HL60 cells (HL60 Control), HL60 cells treated with 0.15 μM CPT (HL60 CPT) and treated with CPT in the presence of FLICA (HL60 CPT FLICA) for 6 h. HL60 cells were stained with May Grünwald Giemsa staining. Magnification of the LM-pictures is 100X (a). Dual fluorescence staining of HL60 cells. HL60 cells were incubated with CPT to initiate apoptosis in the continuous presence of 20 mM FAM-VAD-FMK (FLICA) for 0, 6h, 12h, 18h and 24h and were supravitally stained with propidium iodide (PI). The cells presented in gate A were used to plot FLICA fluorescence in relation to PI fluorescence. Four cell sub-populations (B-E) can be identified on these scatter diagrams, differing in their capability to bind FLICA and PI. Scatter diagrams show results from a representative experiment (b).

The results from the scatter diagrams obtained from 3 different experiments, with either one of the inducers of apoptosis, are plotted as a function of time (figure 2). The plots represent the averaged number of events (%) of each quadrant in relation to CPT incubation (figure 2a) and TNF-α/CHX treatment (figure 2b). The maximum number of early apoptotic cells was at 6 h during TNF-α/CHX and 18 h during CPT treatments, retrospectively.

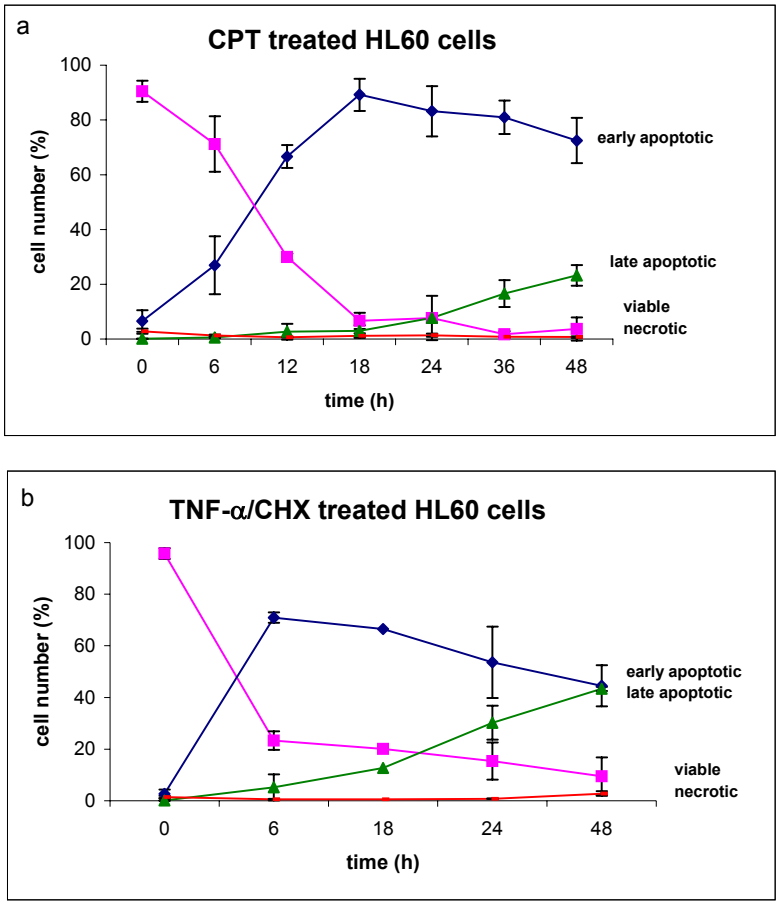

Figure 2: The relative amounts of viable, early apoptotic, late apoptotic and necrotic HL60 cells during apoptosis. The different cell populations of the quadrants shown in figure 1b were plotted as a function of time after CPT (a) or tumour necrosis factor-α/cycloheximide (TNF-α/CHX) treatments (b) in the continuous presence of FLICA. The plots represent the averaged cell numbers of 3 experiments for each time point.

Furthermore, figure 2 clearly shows that in both cases the transition of cells from $FLICA^+/ PI^+$ to $FLICA^-/ PI^+$ is prevented in the continuous presence of FLICA. The apoptotic cascade is thus halted at the late apoptotic stage ($FLICA^+/ PI^+$).

The kinetics of cell accumulation during treatment with CPT or TNF-α/CHX were measured by plotting the accumulation of apoptotic cells (quadrant C and D, $FLICA^+$ cells) as a function of time. The slope of the plot provides an estimation of the cell transition into apoptosis, as shown in figure 3. This figure reveals two different slopes, representing different rates of cell

transition into apoptosis. During the first 18 h of incubation with CPT, 92% of HL60 cells undergo apoptosis at an approximate rate of 5% per h. The remaining cells undergo apoptosis between 18 and 48 h at an approximate rate of 0.2% per h (figure 3a).

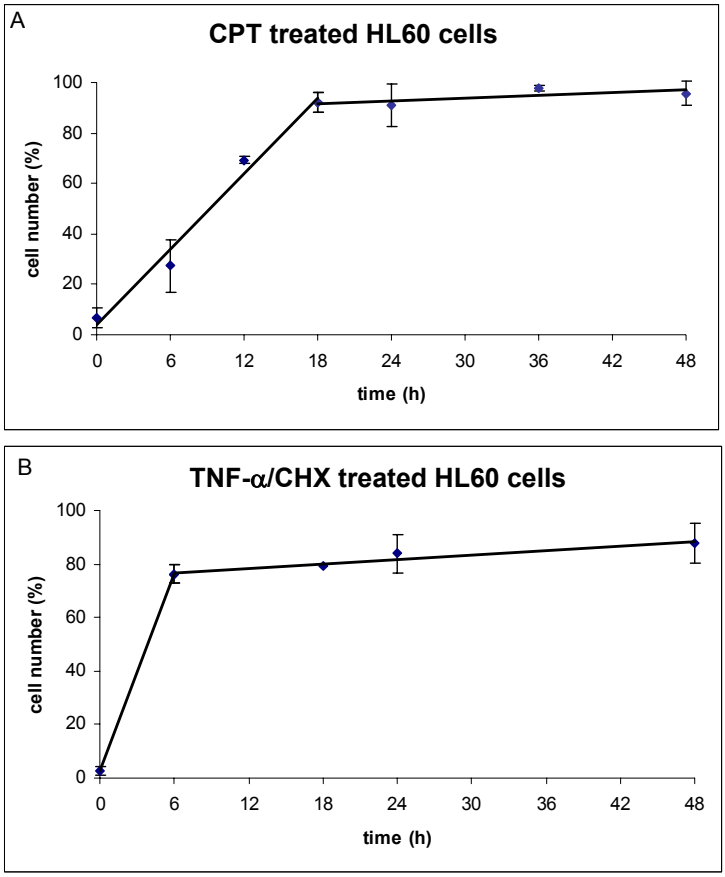

Figure 3: Kinetics of FLICA labelled cell accumulation in HL60 cultures treated with CPT (A) or TNF-α/CHX (B) in the continuous presence of FLICA. The percentages of FLICA positive cells (quadrant C and D) are plotted as a function of time and represent the averaged cell numbers of 3 experiments for each time point.

When HL60 cells were treated with a mixture of TNF-α/CHX to initiate apoptosis (figure 3b), it appeared that 76% of the cells undergo apoptosis at an approximate rate of 12% of cells per h during the first 6 h of incubation. The remaining cells undergo apoptosis between 6 and 48 h at an approximate rate of 0.3% of cells per h.

a

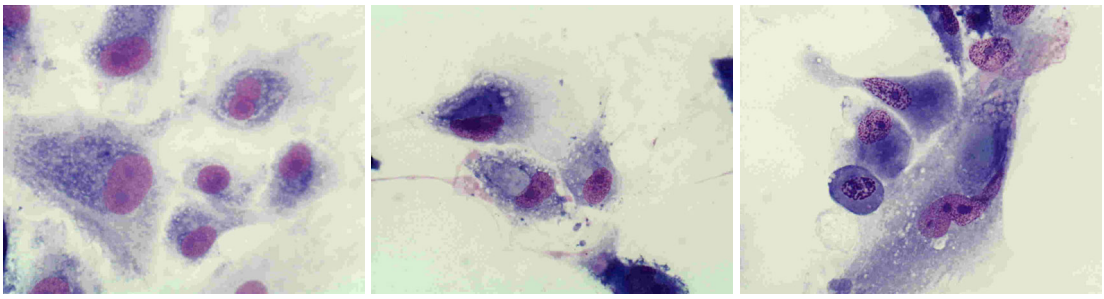

HUVEC controle HUVEC TNFα/CHX HUVEC TNFα/CHX

b

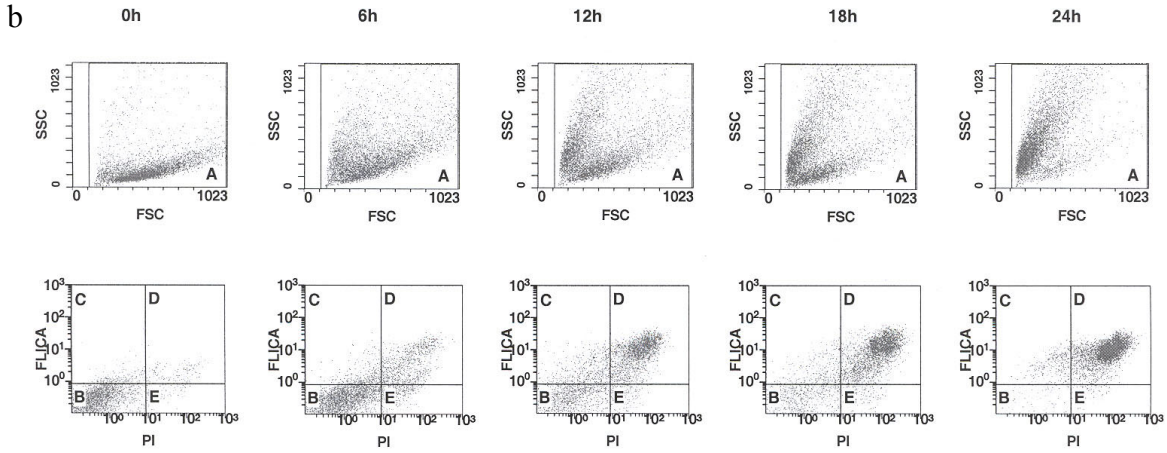

Figure 4: HUVECs treated with TNF-α/CHX in the presence of FLICA. Light microscopy of untreated HUVECs and HUVECs treated with 3 nM TNF-α and 50 μM CHX for 6 h. HUVECs were stained with May Grünwald Giemsa staining. Magnification of the pictures is 50X (a). Dual fluorescence staining of HUVECs. HUVECs were incubated with TNF-α/CHX in the continuous presence of 20 mM FLICA for 0, 6h, 12h, 18h and 24h, and were stained with PI. The cells presented in gate A were used to plot FLICA fluorescence in relation to PI fluorescence. Four cell sub-populations (B-E) can be identified, differing in their capability to bind FLICA and PI. Scatter-diagrams show results from a representative experiment (b).

HUVECs

Incubation with a mixture of TNF-α/CHX, initiates apoptosis also in HUVECs (figure 4a). In the continuous presence of FLICA, TNF-α/CHX induces in HUVECs a direct transition from $FLICA^-/ PI^-$ (viable quadrant) to the $FLICA^+/ PI^+$ (late apoptotic) quadrant (figure 4b, t = 6-24 h, quadrant D).

Figure 5 shows the results of each time point, plotted as function of time in the scatter diagrams obtained in different experiments. The kinetics of cell accumulation during treatment with TNF-α/CHX can be measured by plotting the accumulation of apoptotic cells (quadrant C and D, $FLICA^+$ cells) as a function of time. The slope of the plot provides an estimate of the cell transition into apoptosis.

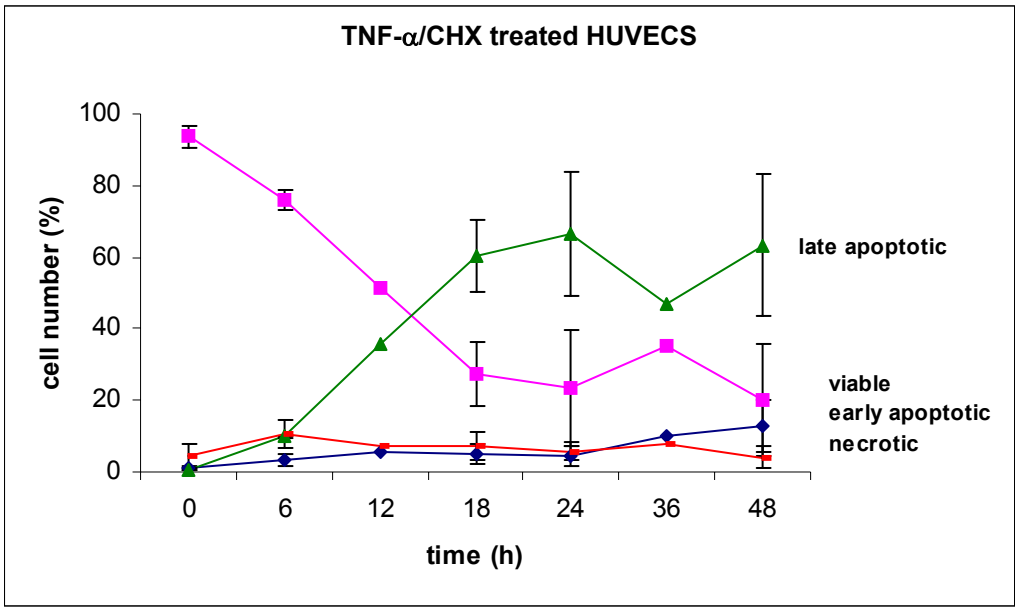

Figure 5: The relative amounts of viable, early apoptotic, late apoptotic and necrotic HUVECs during TNF-α/CHX induced apoptosis. The different cell populations of the quadrants as shown in figure 4b were plotted as a function of time in the continuous presence of FLICA. The plots represent the averaged cell numbers of 1-4 experiments of each time point.

Figure 6 shows two different slopes, revealing different rates of cell transition into apoptosis. During the first 18 h of incubation 65% of the HUVECs undergo apoptosis, at an approximate rate of 3.7% of cells per h. The remaining cells undergo apoptosis between 18 and 48 h at an approximate rate of 0.2% of cells per h.

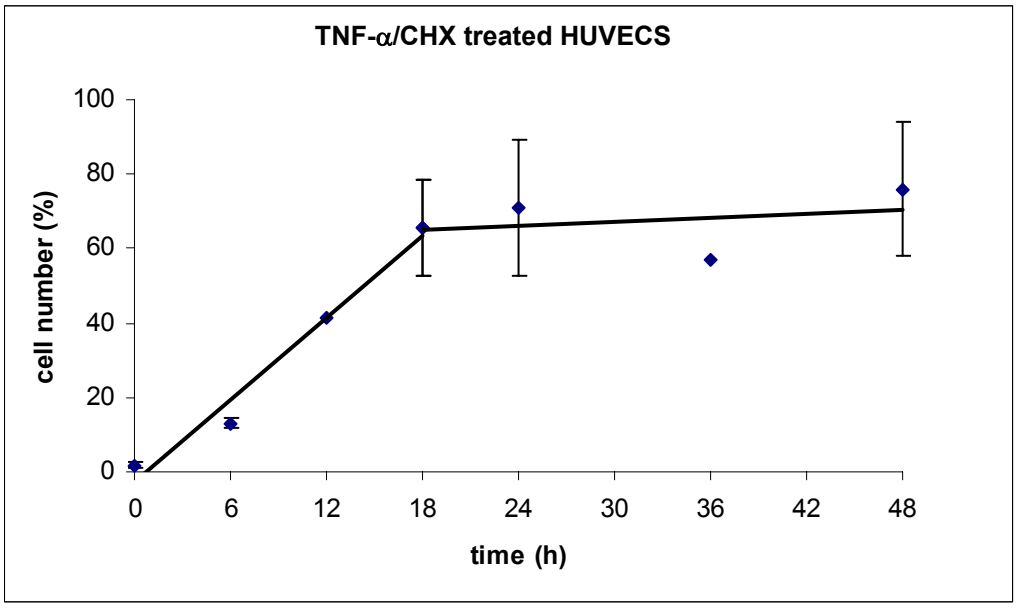

Figure 6: Kinetics of FLICA labelled cell accumulation in HUVECs cultures treated with TNF-α/CHX in the continuous presence FLICA. The percentages of FLICA positive cells (quadrant C and D) are plotted as a function of time and represents the averaged cell number of 1-4 experiments of each time point.

Discussion

In this study, the cell death kinetics of HL60 cells were compared with HUVECs by using different inducers to initiate apoptosis. When cells were incubated with CPT, 92% of HL60 cells undergo apoptosis during the first 18 h of incubation at an approximate rate of 5% of cells per h. Incubation with TNF-α/CHX proved to be a stronger inducer of apoptosis, because 76% of the cells undergo apoptosis during the first 6 h of incubation at an approximate rate of 12% of cells per h. The remaining cells undergo apoptosis between 6 and 48 h at an approximate rate of 0.2-0.3% of cells per h (figure 3). These results are comparable with the results obtained by Darzynkiewicz and colleagues [2, 8, 9]. These authors found during the initial 8 h of incubation with CPT that HL60 cells undergo apoptosis at an approximate rate of 7% per h. The remaining cells entering apoptosis for up to 48 h at a rate of 1% of cells per h. When HL60 cells were incubated with TNF-α/CHX, 50% of the cells underwent apoptosis during the initial 6 h at an approximate rate of 8% of cells per h. The remaining cells underwent apoptosis between 6 and 24 h at a rate approximating 2.5% of cells per h. In our study 65% of the HUVECs underwent apoptosis at an approximate rate of 3.7% of cells per h during the first 18 h of incubation with TNFα/CHX. The remaining HUVECs underwent apoptosis for up to 48 h at a rate of 0.2 % of cells per h (figure 6). Accordingly, the rate of the apoptotic cell death in HL60 cells does not differ essentially from that in HUVECs. However, HL60 cells and HUVECs show a different pattern of transition during the course of the cell death cascade. CPT-treated and TNF-α/CHX-treated HL60 cells, in the continuous presence of FLICA, transit from the viable quadrant to the early apoptotic quadrant and then to the late apoptotic quadrant (figure 1b), while the transition from the viable quadrant to the early apoptotic quadrant is skipped when HUVECs, in the continuous presence of FLICA are incubated with TNF-α/CHX (figure 4b). We speculate that at the time the caspases are activated in HUVECs, the plasma membrane has lost already a part of its integrity and therefore behaves as a population in the late apoptotic quadrant. A possible explanation for the difference between HL60 and HUVECs seen in the scatter diagrams might be the phenomenon of anoikis [14-17]. Anoikis induces apoptosis due to inadequate cell-matrix interactions. One of the questions in anoikis research is how the caspase cascade is initially activated by simple detachment of cells. It has been reported that anoikis in HUVECs requires interactions between the death receptor Fas and Fas ligand [15]. Adherent endothelial cells are resistant to Fas-mediated apoptosis, because Fas-L and Fas do not interact. However, in response to specific stimuli (TNF-α) or injury, which causes cell detachment, endothelial cells

become sensitised to Fas-mediated apoptosis, via an increase in Fas expression and Fas receptor surface levels [15]. However, enhanced Fas expression alone is not sufficient to sensitise adherent HUVECs for Fas-mediated killing. One additional step in Fas-signalling seems necessary in the regulation of anoikis. The down-modulation of the endogenous caspase-8 inhibitor (c-Flip) during cell detachment may be a causal event in detachment-induced caspase-8 activation and HUVECs anoikis. In our study, HUVECs were treated with TNF-α/CHX in the continuous presence of FLICA, which prevents anoikis, because caspase activation is inhibited. Anoikis may explain the difference seen in the transition-scatter diagrams between HL60 cells and HUVECs, but further study is needed in order to reveal the exact mechanism.

Conclusion

FLICA induces an arrest of cells in apoptosis (stathmo-apoptosis) and makes it possible to measure the amount of cells present in different stages of the apoptotic cascade and to calculate cell death kinetics. This technique allows to measure apoptotic cell death rate not only in cultured cells in suspension but in adherent cells as well. The rate of apoptotic cell death depends on the stimulus used to induce apoptosis. TNF-α/CHX showed to be a stronger inducer of apoptosis then CPT in HL60 cells. However, the cell death rate is similar when the same stimulus is applied in different cell types. The rate of the apoptotic cell death in TNF-α/CHX-treated HL60 cells does not differ much from that in TNF-α/CHX- treated HUVECs, but different transitions during the course of the cell death cascade is seen when the same inducer (TNF-α/CHX) is used. TNF-α/CHX-treated HL60 cells, in the continuous presence of FLICA, transit from the viable quadrant to first the early apoptotic quadrant and then to the late apoptotic quadrant. When HUVECs are treated with TNF-α/CHX, in the continuous presence of FLICA, a direct transition from the viable quadrant to the late apoptotic quadrant is seen. Accordingly, cell death kinetics depend on the type of the cell in a qualitative manner and on the stimulus used to induce apoptosis in a quantitative manner.

References

1. Vermes, I., Haanen, C., and Reutelingsperger, C. Flow cytometry of apoptotic cell death. J.Immunol.Methods 2000; 243: 167-190.
2. Darzynkiewicz, Z., Bedner, E., and Smolewski, P. Flow cytometry in analysis of cell cycle and apoptosis. Semin.Hematol. 2001; 38: 179-193.
3. Thornberry, N.A. and Lazebnik, Y. Caspases: Enemies within. Science 1998; 281: 1312-1316.

4. Hengartner, M.O. The biochemistry of apoptosis. Nature 2000; 407: 770-776.
5. Grabarek, J. and Amstad, P. Use of fluorescently labelled caspase inhibitors as affinity labels to detect activated caspases. Hum.Cell 2002; 15: 1-12.
6. Grabarek, J. and Darzynkiewicz, Z. In situ activation of caspases and serine proteases during apoptosis detected by affinity labelling their enzyme active centers with fluorochrome-tagged inhibitors. Exp Hematol. 2002; 30: 982- 989.
7. Smolewski, P., Grabarek, J., Phelps, D.J., and Darzynkiewicz, Z. Arresting apoptosis by fluorochrome-labelled inhibitor of caspases. Int.J.Oncol. 2001; 19: 657-663.
8. Smolewski, P., Bedner, E., Du, L., Hsieh, T.C., Wu, J.M., Phelps, D.J., and Darzynkiewicz, Z. Detection of caspases activation by fluorochrome-labeled inhibitors: Multiparameter analysis by laser scanning cytometry. Cytometry 2001; 44: 73-82.
9. Smolewski, P., Grabarek, J., Lee, B.W., Johnson, G.L., and Darzynkiewicz, Z. Kinetics of HL-60 cell entry to apoptosis during treatment with TNF-alpha or camptothecin assayed by the stathmo-apoptosis method. Cytometry 2002; 47: 143- 149.
10. Smolewski, P., Grabarek, J., Halicka, H.D., and Darzynkiewicz, Z. Assay of caspase activation in situ combined with probing plasma membrane integrity to detect three distinct stages of apoptosis. J.Immunol.Meth. 2002; 265: 111-121.
11. Bedner, E., Smolewski, P., Amstad, P., and Darzynkiewicz, Z. Activation of caspases measured in situ by binding of fluorochrome labelled inhibitors of caspases (FLICA): Correlation with DNA fragmentation. Exp.Cell Res. 2000; 259: 308-313.
12. Teodori, L., Grabarek, J., Smolewski, P., Ghibelli, L., Bergamaschi, A., De Nicola, M., and Darzynkiewicz, Z. Exposure of cells to static magnetic field accelerates loss of integrity of plasma membrane during apoptosis. Cytometry 2002; 49: 113-118.
13. Jaffe, E.A., Nachman, R.L., Bedker, C.G., and Minick, C.R. Culture of human endothelial cells derived from umbilical veins. J.Clin.Invest. 1973; 52: 2756-
14. Ruoslahti, E. and Reed, J.C. Anchorage dependence, integrins, and apoptosis. Cell 1994; 77: 477-478.
15. Aoudjit, F. and Vuori, K. Matrix attachment regulates Fas-induced apoptosis in endothelial cells: A role for c-Flip and implications for anoikis. J.Cell Biol. 2001; 152: 633-644.
16. Frisch, S.M. and Screaton, R.A. Anoikis mechanisms. Cell Biol. 2001; 13: 555-562.
17. Grossman, J. Molecular mechanisms of "detachment-induced apoptosis - Anoikis". Apoptosis 2002; 7: 247-260.

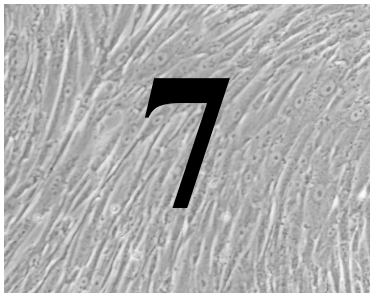

A Novel Time Resolved Fluorometric Assay of Anoikis Using Europium-labelled Annexin V in Cultured Adherent Cells*

* P. Engbers-Buijtenhuijs[1,2], M. Kamphuis[1], G. van der Sluijs Veer[1], C. Haanen[1], A. A. Poot[2], J. Feijen[2], I. Vermes[1,2]

Apoptosis 2005; 10: 429-437

[1] Medisch Spectrum Twente, Hospital Group, Department of Clinical Chemistry, Enschede, P.O. Box 50.000, 7500 KA, The Netherlands.

[2] University of Twente, Faculty of Science & Technology, Department of Polymer Chemistry and Biomaterials and Institute of Biomedical Technology (BMTI), Enschede, P.O. Box 217, 7500 AE, The Netherlands.

Abstract

Adherent cells undergo apoptosis when detached from their home ground, a process called anoikis (homelessness). We developed a new and sensitive method to analyse apoptosis and anoikis of adherent cell types using a time resolved fluorometric assay with Europium-labelled Annexin V. Anoikis was induced with tumor necrosis factor-α/cycloheximide (TNF-α/CHX) and three cell fractions of the cell cultures were prepared and analysed. Fraction 1 consisted of adherent cells, analysed while growing on their support (without detachment by trypsinisation). Fraction 2 contained detached cells due to anoikis (floating cells) and fraction 3 contained apoptotic bodies. Both fractions 2 and 3 were present in the culture medium and were isolated by differential centrifugation. TNF-α/CHX treatment of three different types of adherent cell cultures induced a significant increase of the amount of floating cells (anoikis) and apoptotic bodies compared to control cell cultures. Also in the adherent cell fractions a small amount of apoptosis was observed.

The novel time resolved assay provides the ability to analyse the cell death cascade in adherent cell cultures of the same sample at the same time in a sensitive and reproducible way.

Introduction

Adherent cells are dependent for survival on continuous engagement of cellular integrins to the extra-cellular matrix [1, 2]. Detachment of adherent cells from the extra-cellular matrix induces almost immediately apoptosis, a phenomenon designated 'anoikis' or homelessness [3, 4]. Anoikis is of relevance in the physiological development of tissues [5, 6]. Without anoikis, detached cells could possibly reattach to distantly localised matrices, resume growth and contribute to the metastatic growth of cancers [5, 7, 8]. Apoptosis occurring in detached cells would abrogate this mechanism and in this way provide a stringent control of appropriate cell number and tissue organisation. Therefore anoikis is a form of apoptosis with pertinent relevance to tissue homeostasis. On the other hand activation of death receptors in adherent cells will cause detachment of those cells from their support inducing anoikis [5]. To measure anoikis in adherent cells, it is therefore of utmost importance that the viable cells are not disrupted from their location and cells detached from their support should be taken into consideration [9, 10]. Several techniques can be used to identify different stages of the apoptotic pathway of cells *in vitro* [9, 11]. At present analyses of a wide choice of parameters are used ranging from simple cell sizing to measuring of cell membrane properties, cytoplasmic

constituents, cell organelles, DNA content and nuclear chromatin [11]. Most of the techniques for reliable quantitative measurement of apoptosis are excellent for the analysis of apoptosis of cells in suspension but are not suitable for adherent cells because of the occurrence of anoikis due to detachment of the cells [12]. Annexin V binding is extensively used to analyse apoptosis [13]. This is based on the high, Ca^{2+}-dependent affinity of Annexin V to phosphatidylserine (PS). Cells under viable conditions maintain phospholipid asymmetry over the two leaflets of the plasma membrane with PS mainly located at the inner leaflet. During apoptosis (or necrosis) PS is translocated to the outer leaflet of the plasma membrane and can then be recognised by Annexin V binding. Fluorescently labelled Annexin V has been used to analyse apoptosis by means of flow cytometry or microscopy[11]. For performing flow cytometry on adherent cells, cells should first be detached from the support. This procedure of detaching the cells induces apoptosis itself [10]. Therefore, flow cytometry can never be an optimal quantitative technique to measure apoptosis in adherent cells [9, 10].

We developed a new very sensitive method to analyse anoikis in adherent cell cultures using the principles of the Dissociation Enhanced Lanthanide Fluoro Immuno Assay (DELFIA® [14], Wallac Oy, Turku, Finland). DELFIA® assays utilise a lanthanide metal (Europium) chelate label which is practically non-fluorescent. However, after binding of Europium-labelled Annexin V to PS, Europium is efficiently dissociated from the labelled compound by the low pH of the commercial available enhancement solution (Wallac Oy, Turku, Finland). The free Europium ion then rapidly forms a new, highly fluorescent and stable chelate with the components of this enhancement solution. The principles of the DELFIA® method are represented schematically in figure 1b [15-17]. By using this novel time resolved fluorometric assay using Europium-labelled Annexin V, the occurrence of apoptosis was measured in three different cell fractions derived from adherent cell cultures as represented schematically in figure 1a. The occurrence of apoptosis was analysed in cells which were still attached to the culture surface, anoikis was measured in detached cells (floating cells) and the final stage of the apoptotic pathway was investigated by analysing apoptotic bodies[18]. Because by differential centrifugation we are able to separate detached cells and apoptotic bodies from the cell debris which is present in the culture medium due to necrotic cell death, necrosis is excluded from the analyses.

Results of our new test were compared with results of the standard DNA fragmentation assay according to Nicoletti[19] and with results of flow cytometric measurements of apoptotic bodies

[20]. With the very sensitive time resolved fluorometric Annexin V assay we could analyse the processes of apoptosis and anoikis in more detail compared to existing assays.

Materials

Dulbecco's Vogt Modified Eagle's minimal essential Medium (DMEM) was purchased from Gibco BRL (Breda, The Netherlands). Penicillin, streptomycin, fetal bovine serum, trypsin/ethylene diamine tetra-acetic acid (EDTA) and RPMI-1640 medium were purchased from Biowhittaker (Verviers, Belgium). Camptothecin (CPT), tumour necrosis factor-α (TNF-α), gelatin type B from bovine skin, cycloheximide (CHX), and propidium iodide (PI) were from Sigma (St. Louis, Missouri, USA). N-[2-hydroxyethyl] piperazine-N'-[2-ethane sulfonic acid] (HEPES) was from Brunschwig (Amsterdam, The Netherlands). Medium 199 (M199) (with 20 mM HEPES) and L-Glutamine were from Life Technologies (Grand Island, New York, USA). Fetal bovine serum was heat-inactivated (30min, 56^0C) before use. Human serum was acquired by overnight incubation of whole blood (collected from 16 healthy volunteers) at 4 ^{0}C. Serum was obtained by centrifugation and subsequently pooled and stored at –80 ^{0}C. Before use, serum was heat inactivated (30min, 56^0C) and filter-sterilised. Europium-label-reagent and enhancement solution were from Amersham Pharmacia Biotech (Woerden, The Netherlands). Flow-Count^{TM} Fluorospheres were from Beckman-Coulter (Mijdrecht, The Netherlands). Other buffer components and salts (NaCl, KCl, $MgCl_2$, $CaCl_2 \cdot 2H_2O$, $NaHCO_3$) and solutions of May-Grünwald and Giemsa were obtained from Merck (Darmstadt, Germany). Annexin V and fluorescein isothiocyanate-(FITC)-labelled Annexin V were provided by Dr. Reutelingsperger (University of Maastricht, The Netherlands). HMEC cultures were donated by Dr. P. Koolwijk of the Netherlands Organisation for Applied Scientific Research (TNO-PG, Leiden, The Netherlands) in co-operation with E. W. Ades of Centers for Disease Control and Prevention (CDC, Atlanta, USA) and T. J. Lawley of Emory University (Atlanta, USA).

Methods

Culturing of human micro-vascular endothelial cells (HMECs)

HMECs) were cultured in 1% (w/v) gelatin-coated culture flasks at a seeding density of 40,000 cells/cm^2. Culture medium consisted of M199 medium supplemented with 10% (v/v) pooled human serum, 10% (v/v) fetal bovine serum, 100 units/mL penicillin, 100 μg/mL streptomycin and 2 mM L-glutamine. Medium was refreshed every 2-3 d. Confluent cultures

were subcultured after detachment using a trypsin solution (0.05% trypsin/0.02% EDTA in PBS).

Culturing of human umbilical vein endothelial cells (HUVECs)

HUVECs were isolated from human umbilical veins, according to the method of Jaffe *et al*. [21]. Umbilical cords were obtained from women terminating normal pregnancies. The procedure followed was in accordance with the policies of the institutional ethical review board of the Hospital Group (ECOM). Cells were cultured in 1% (w/v) gelatin-coated culture flasks at a seeding density of 40,000 cells/cm^2. Culture medium consisted of 50% M199 medium and 50% RPMI-1640 medium, supplemented with 20% (v/v) pooled human serum, 100 units/mL penicillin, 100 μg/mL streptomycin and 2 mM L-glutamine. Medium was refreshed every 2-3 d. Confluent cultures were subcultured (to a maximum of 5 passages) after detachment using a trypsin solution (0.05% trypsin/0.02% EDTA in PBS).

Culturing of human umbilical vein smooth muscle cells (SMCs)

SMCs were isolated from human umbilical veins according to the method of Heimli *et al*. [22] with some minor modifications as described previously [23]. Cells were cultured in 1% (w/v) gelatin-coated culture flasks at a seeding density of 40,000 cells/cm^2. Culture medium consisted of DMEM supplemented with 10% (v/v) pooled human serum, 10% (v/v) fetal bovine serum, 100 units/mL penicillin and 100 μg/mL streptomycin [22]. Medium was refreshed every 2-3 d. Confluent cultures were subcultured (to a maximum of 12 passages) after detachment using a trypsin solution (0.125% trypsin/0.05% EDTA in PBS) [24, 25].

Modulation of apoptosis/anoikis

All cell cultures were maintained in a humidified atmosphere at 37°C and 5% CO_2. Cells were grown to 80% confluence and subsequently either cultured in their standard culture medium (control cells) or treated for 16 h with 3 nM TNF-α and 50 μM CHX in standard culture medium (TNF-α/CHX) to induce apoptosis/anoikis [26].

Labelling Annexin V with Europium

Annexin V was first transferred in carbonate buffer (50 mM $NaHCO_3$/ 150 mM NaCl, pH 8.5) by gel filtration using a Sephadex ® G-25 m PD-10 Column (Amersham Pharmacia Biotech, Woerden, The Netherlands). Europium-label-reagens (2 mg/mL) was used to label Annexin V

with Europium during 20 h at RT. The obtained Eu^{3+}-labelled Annexin V was purified by gel filtration using a Sephadex ® G-25 m PD-10 Column in carbonate buffer (50 mM $NaHCO_3$/ 150 mM NaCl, pH 8.5). The final fraction was diluted with glycerol (1:1) to a final concentration of 0.4 g/L Europium-labelled Annexin V.

Europium-labelled Annexin V time resolved fluorometric assay to measure apoptosis

For this time resolved fluorometric assay, three fractions of the adherent cell cultures grown in 96 wells plates (Corning, Badhoevedorp, The Netherlands) were prepared and analysed as represented schematically in figure 1. Fraction 1 consisted of viable adherent cells and these cells were analysed while growing on their support (without detachment by trypsinisation). Supernatants of the adherent cell cultures were collected and two other fractions were isolated: floating cells and apoptotic bodies. After centrifugation of the supernatants (low speed, 1,000 g, 3 min, room temperature (RT)), apoptotic cells detached from their support were obtained from the pellets (fraction 2, floating cells). Supernatants of these centrifuged samples were collected and centrifuged (high speed, 3,500 g, 15 min, RT). Apoptotic bodies derived from the apoptotic cells as a result of a final stage of apoptosis were then obtained from the pellets (fraction 3). To analyse apoptosis, the three fractions of the cell cultures (adherent cells, floating cells and apoptotic bodies) were separately washed with a solution of 10 mM HEPES, supplemented with 137 mM NaCl, 2.68 mM KCl, 1.7 mM $MgCl_2$, 25 mM glucose and 2.5 mM $CaCl_2.2H_2O$ and pH 7.4 (HEPES buffer). Adherent cells (fraction 1) were then incubated with Europium-labelled Annexin V (final concentration of 0.4 mg/l in HEPES buffer for 30 min at RT). Pellets of floating cells (fraction 2) and apoptotic bodies (fraction 3) were resuspended in Europium-labelled Annexin V (final concentration of 0.4 mg/l) in HEPES buffer for 30 min at RT. After washing with HEPES buffer, the three fractions were incubated with (commercial available) enhancement solution [15] for 5 min at RT to convert the Europium label into the highly fluorescent chelate. Time resolved fluorescence was measured in each sample on a Victor fluorescence analyser (PerkinElmer Life Sciences, Turku, Finland). Excitation and emission wavelengths were 340 and 615 nm respectively. Fluorescence was normalised against control cell cultures.

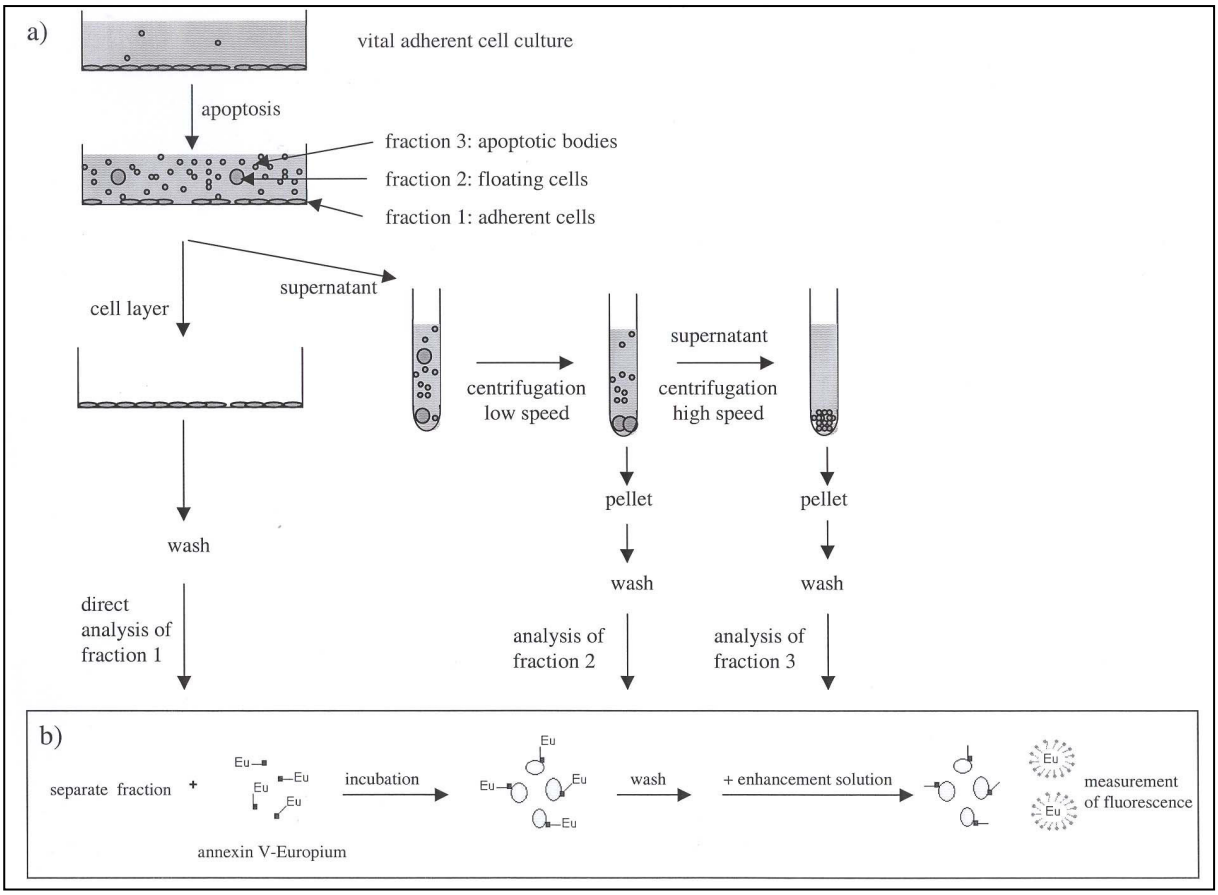

Figure 1: Work flow diagram of the different steps involved in the Europium-labelled Annexin V time resolved fluorometric assay to analyse the cell death cascade. (a) Three fractions of the adherent cell cultures were prepared. Fraction 1 consisted of adherent cells, analysed while growing on their support (without detachment by trypsinisation). Fraction 2 contained detached cells due to anoikis (floating cells) and fraction 3 contained apoptotic bodies. Both fractions 2 and 3 were present in the culture medium and were isolated by differential centrifugation. (b) Apoptosis was then analysed in the three separate fractions by using the DELFIA® principle (Wallac Oy, Turku, Finland). DELFIA® assays utilise a lanthanide (Europium) chelate label which becomes highly fluorescent after forming a new lanthanide chelate within a protective micelle in specially developed enhancement solution (Wallac Oy, Turku, Finland).

DNA fragmentation assay to measure apoptosis

The occurrence of apoptosis in the adherent and floating cell fractions together was measured by flow cytometry using PI according to Nicoletti *et al.* [19]. After culturing, cells already present in the culture medium (floating cells) were collected and subsequently adherent cells were detached from the support using a 0.125% trypsin/0.05% EDTA solution. The two fractions were combined, washed with PBS, fixed in 70% ethanol and after another wash stained with 15 µM PI for 30 min at 37^0C [11]. PI fluorescence of individual cells was measured with a Coulter Epics XL flow cytometer, using System II TM software with the XL-2 or DOS

configuration. Excitation was elicited at 488 nm with the Argon laser and emission was measured using the long pass (>570 nm) filters. In each sample 10,000 events were measured and data were analysed with Coulter program Expo II. Percentages of PI positive cells were compared to the total amount of cells and normalised against control cells which reflects the amount of apoptosis in the two cell fractions (adherent and floating cell fraction) together.

Flow cytometric measurements of apoptotic bodies

After culturing, 200 μL aliquots of culture medium/supernatant were centrifuged (1,000 g, 3 min, RT). 100 μL aliquots of supernatants were stained for 30 min (in the dark) with FITC-labelled Annexin V (final concentration of 12.8 μg/mL) in HEPES buffer. 40,000 Flow-Count™ Fluorospheres (with a nominal diameter of 10 μm) were then added as internal standard and the amount of apoptotic bodies were analysed on a Coulter Epics XL flow cytometer, using System II TM software with the XL-2 or DOS configuration. Excitation was elicited at 488 nm with the Argon laser and emission was measured using the standard band pass (530 ± 20 nm) filters. In each sample a fixed number of 2,000 Flow-Count™ Fluorospheres were measured and the ratio of the amount of Annexin V positive apoptotic bodies was calculated based on the number of added Flow-Count™ Fluorospheres [20]. Analyses were done with Coulter program Expo II. Ratios were normalised against control cells.

Morphology

After cells were cultured to 80% of confluence, anoikis was induced by TNF-α/CHX. Adherent cells still present on their culturing support and apoptotic cells detached from their support (floating cells) were analysed. An aliquot of the culture medium containing floating cells was centrifuged on glass slides at 700 rpm for 10 min with low acceleration using a Shandron cyto centrifuge (Shandron, Pittsburg, USA). Adherent cells still present on their culturing support and floating cells collected on the glass slides were fixed with methanol, stained with May-Grünwald-Giemsa and examined for their morphology. Confluency was quantified by counting cells based on light microscopy.

Statistical analyses

All data represent mean ± standard error of the mean (SEM) of several experiments performed in duplicate. Data were analysed using Student's T-test and considered significantly different at p-values < 0.05.

Results

Optimisation and validation of the technique

The variables of the technique as described under Methods were first optimised. Optimal parameters for time of centrifugation, time of labelling with Europium-labelled Annexin V and concentration of the Europium-labelled Annexin V were 15 min, 30 min, and 0.4 mg/L respectively. To evaluate the reproducibility of the technique, coefficients of variation (CVs) for intra- and inter-assay precisions were determined for viable and apoptotic HMEC-cultures ($n = 10$). The CVs for intra- as well as inter-assay precisions for both viable and apoptotic cell-cultures were less than 10%. Linearity and sensitivity of the technique were evaluated by measuring PS exposure in serial dilutions of floating cells derived from control HMEC cultures. The sensitivity limit of the method was ten thousand cells per measurement and the method showed a linear response between 10,000 and at least 75,000 cells per measurement with a coefficient of correlation of 0.95.

Apoptosis of HMEC cultures determined by three different techniques

HMECs were cultured in control medium or cultured in medium supplemented with TNF-α/CHX to induce apoptosis/anoikis. Two standard methods to analyse apoptosis were used as reference tests. The traditional DNA fragmentation assay for measurement of apoptosis (figure 2a) does not allow separately testing of apoptosis in floating cells present in the supernatant and in cells detached by trypsinisation. With use of the here described Europium-labelled Annexin V fluorometric assay it is possible to analyse these fractions separately (fraction 1 and 2). However, to be able to compare the DNA fragmentation test with the time resolved fluorometric assay, floating cells in the supernatant of the cell cultures and cells still attached to the support were analysed together in this experiment (figure 2c). With use of flow cytometry based on FITC-labelled Annexin V binding as well as particle size the amount of apoptotic bodies derived from the cell cultures was analysed (figure 2b) and results of the Europium-labelled Annexin V fluorometric assay analysing apoptotic bodies (figure 2d) are compared with results of this assay. As can be seen from figure 2, results of the three different methods show all that TNF-α/CHX induces apoptosis in HMEC cultures compared to control.

An advantage of our new time resolved fluorometric assay is the possibility to analyse adherent and floating cells as well as apoptotic bodies in one single assay.

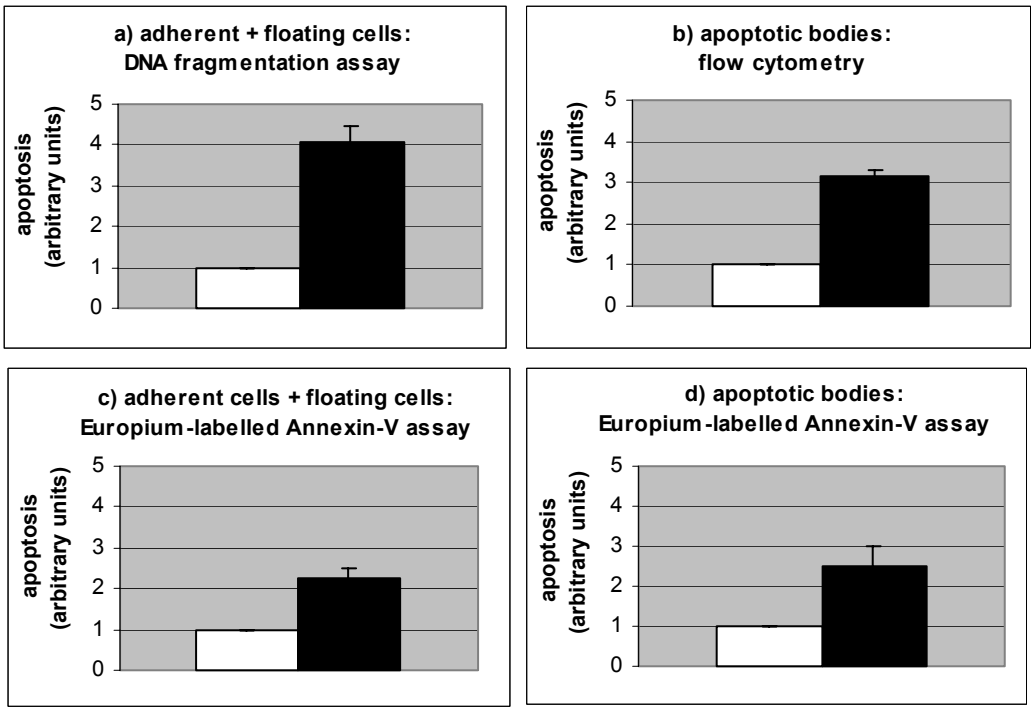

Figure 2: Apoptosis/anoikis of adherent HMEC cultures determined by three different techniques. HMECs were cultured and treated with TNF-α/CHX in culture medium. Apoptosis was then analysed by three different techniques as described in Methods. Apoptosis induced by TNF-α/CHX (closed bars) was normalised against apoptosis found in control cell cultures (open bars). (a) Apoptosis in HMEC cultures determined by a DNA fragmentation assay. Floating cells in the supernatant of the cell cultures and cells detached from the support by trypsinisation were analysed together. (b) Amount of apoptotic bodies present in culture medium of HMEC cultures analysed by FITC-fluorescence with use of flow cytometry. (c) Time- resolved fluorescence of Europium-labelled Annexin V of the adherent cell fraction of HMEC cultures (fraction 1) + floating cells derived from the HMEC cultures (fraction 2) determined by the time resolved fluorometric assay. Floating cells in the supernatant of the cell cultures and cells still attached to the support were analysed together to compare the results with the DNA fragmentation assay. (d) Time- resolved fluorescence of Europium-labelled Annexin V of apoptotic bodies derived from the HMEC cultures (fraction 3) determined by the time resolved fluorometric assay. SEM values are indicated by bars.

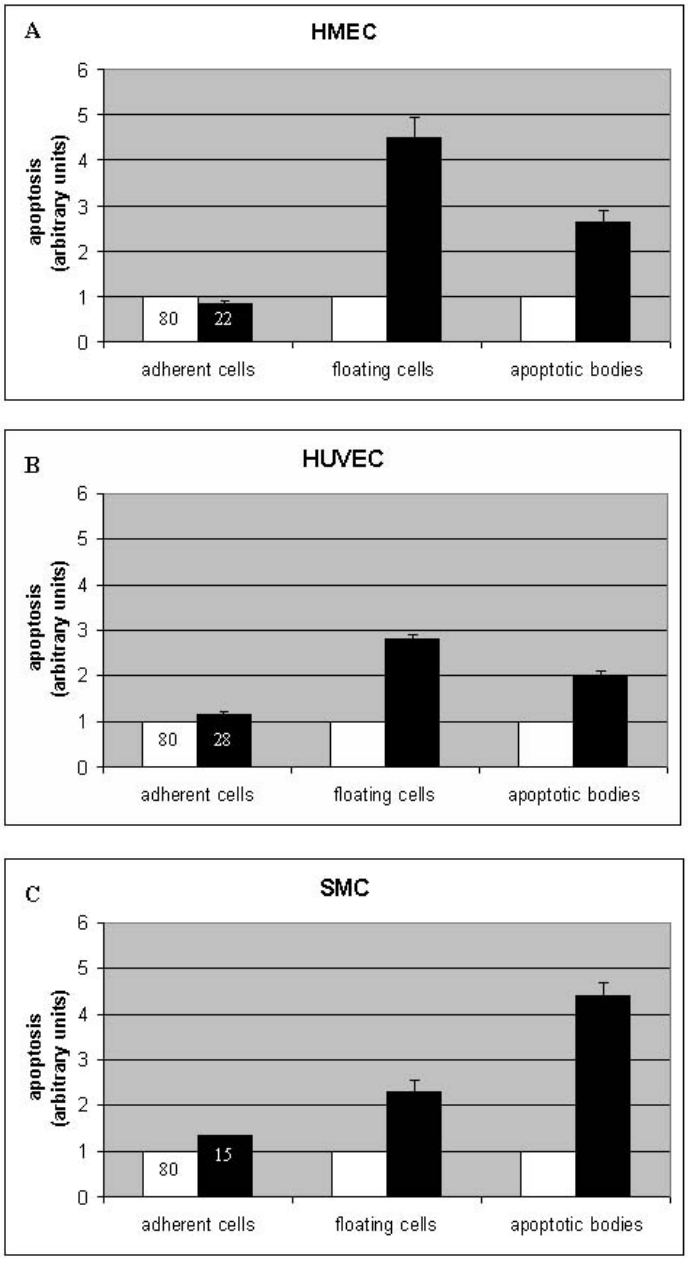

Figure 3: Cell death measured in three different adherent cell cultures by the Europium-labelled Annexin V time resolved fluorometric assay. Cells were cultured and treated with TNF-α/CHX in culture medium. Apoptosis was then analysed by analysing the phosphatidyl serine exposure at the outer plasma membrane with Europium-labelled Annexin V as described in the methods. Apoptosis induced by TNF-α/CHX (closed bars) was normalised against apoptosis found in control cell cultures (open bars). Three fractions of the cell cultures were analysed (adherent cells, floating cells and apoptotic bodies). Fluorescence of Europium-labelled Annexin V of these three fractions of (a) HMEC cultures (b) HUVEC cultures and (c) SMC cultures were separately analysed. Numbers in the diagrams show the percentages of confluency of the adherent cell fractions determined by microscopy and SEM values are indicated by bars.

Apoptosis of three different adherent cell cultures determined by the Europium-labelled Annexin V time resolved fluorometric assay

In control cell cultures of HMEC, HUVEC and SMC, without apoptotic inducers, high fluorescence intensity was found in the adherent cell fractions and no (significant) increase was found after treatment with TNF-α/CHX of the three cell cultures (figure 3a, b and c respectively). However, in this figure, the fluorescence intensity was not correlated to the amount of cells measured. When the fluorescence intensity was correlated to the number of cells measured, TNF-α/CHX induced a significant increase of apoptotic cells in the adherent cell fraction of all cell types analysed (figure 4). TNF-α/CHX treatment of these three different adherent cell cultures induced a significant increase of the amount of floating cells and apoptotic bodies compared to control cultures (figure 3). The same responses were observed when 0.15 μM camptothecin supplemented to the culture medium or culture medium without serum (serum starvation) were used to induce anoikis (results are not shown).

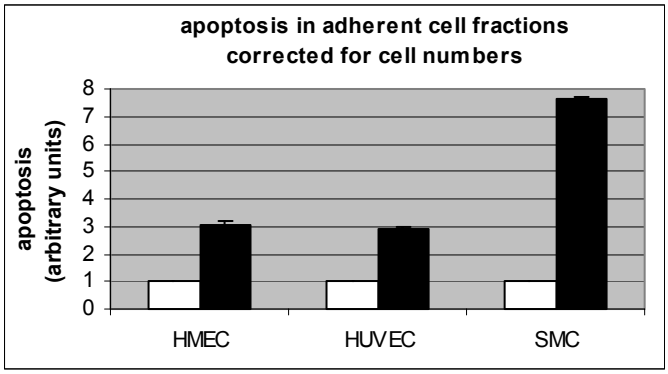

Figure 4: Fluorescence intensity of Europium-labelled Annexin V of the adherent cell fractions of HMECs, HUVECs and SMCs corrected for the cell numbers measured. Cells were cultured and treated with TNF-α/CHX in culture medium. Apoptosis was then analysed by analysing the phosphatidyl serine exposure at the outer plasma membrane with Europium-labelled Annexin V as described in the methods. Apoptosis induced by TNF-α/CHX (closed bars) was normalised against apoptosis found in control cell cultures (open bars). Fluorescence of Europium-labelled Annexin V of the adherent cell fractions of HMEC cultures, HUVEC cultures and SMC cultures was corrected for the cell numbers measured. SEM values are indicated by bars.

Morphology

From morphological analyses it can be seen that TNF-α/CHX induces anoikis of HMECs, HUVECs and SMCs. Control cell cultures were approximately 80% confluent (for the HMEC culture see figure 5a) whereas after treatment with TNF-α/CHX, confluencies of approximately 22% of HMECs (figure 5b), 28% of HUVECs, and 15% of SMCs were observed. No morphological abnormalities were observed in the attached cells of both the control cell cultures and the TNF-α/CHX treated cell cultures (figure 5c). When floating cells present in the culture medium were analysed, apoptotic cells were observed (figure 5d). These apoptotic cells showed apoptotic body formation. Free apoptotic bodies could not be detected by light microscopy.

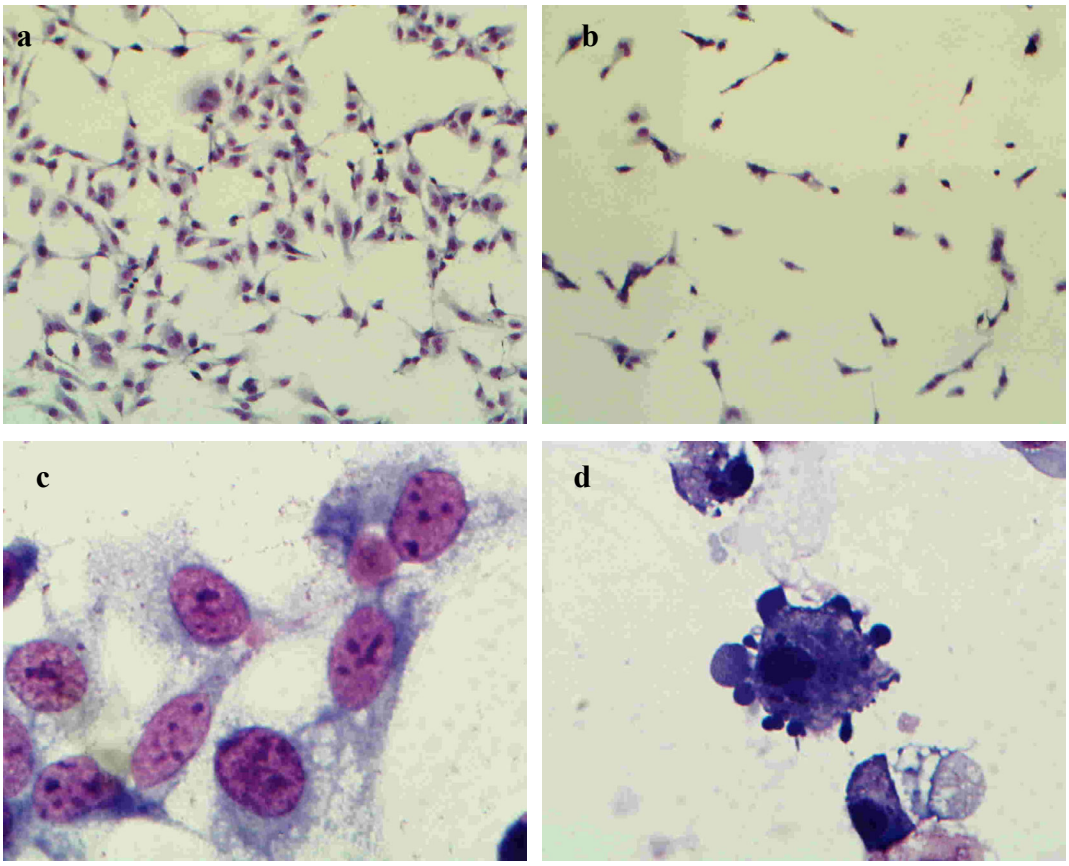

Figure 5: Morphology of HMEC cultures. Cells were cultured to 80% of confluence and treated with TNF-α/CHX in culture medium. May-Grünwald-Giemsa staining of the cells was performed to analyse morphology of the isolated three fractions of the cell cultures (adherent cells, floating cells and apoptotic bodies). (a) Control HMECs cultured in standard culture medium on gelatin-coated culture flasks (magnification: 100X). (b) HMECs of a culture treated with TNF-α/CHX, still present on the surface of gelatin-coated culture flasks (magnification: 100X). (c) HMECs of a culture treated with TNF-α/CHX, still present on the surface of gelatin-coated culture flasks (magnification: 1000X). (d) Apoptotic HMECs which were detached from their support as a result of an early stage of apoptosis (fraction 2) and centrifuged on glass slides (magnification: 1000X).

Discussion

DELFIA® assays have been employed in routine laboratory techniques [14] but have never been used to measure apoptosis or anoikis. This technique conveys three major benefits: 1st) the Stokes shift is large (almost 300 nm), 2nd) the emission peak is very sharp and 3rd) the Europium chelate fluorescence has a very long decay time compared to that of conventional fluorochromes. This significantly reduces the background signal and gives greater resolution and sensitivity. We described here a new method to analyse apoptosis/anoikis in adherent cell cultures using Europium-labelled Annexin V in a DELFIA® system. By analysing apoptosis in three different cell fractions, adherent cells, floating cells and apoptotic bodies, the occurrence of apoptosis/anoikis could be measured directly without manipulation of the cell cultures like trypsinisation. Based on the CVs for intra- and inter assay precisions this assay proved to be reproducible and sensitive to study apoptotic cell death in different adherent cell types. The assay showed a linear response between 10,000 and at least 75,000 cells per measurement. The assay can easily be performed, even in 96 wells culture dishes, in one run eliminating the inter assay variation. The most important advantage is that different stages of the apoptotic cascade can be analysed in one single assay. This is in contrast with standard flow cytometry analysing DNA fragmentation and measuring the amount of apoptotic bodies. The DNA fragmentation assay is not sensitive enough to distinguish between adherent cells and floating cells. On the other hand when the amount of apoptotic bodies is analysed by flow cytometry one cannot distinguish floating cells and apoptotic bodies. Results of both methods are comparable to results of our new Europium-labelled Annexin V time resolved fluorometric assay (figure 2). However apoptosis-induced increments in both fractions are different due to the fact that different parameters are analysed with use of different techniques. DNA fragmentation and forming of apoptotic bodies are both late events in the apoptotic cascade compared to membrane changes measured by Annexin V binding [11]. With use of this novel time resolved fluorometric assay, double labelling using propidium iodide [11] to exclude necrosis from the analyses, cannot be performed. This may be considered as a disadvantage. However, by analysing the three different cell fractions derived from adherent cell cultures as described in this paper, necrosis is excluded from the analyses.

Our study demonstrates that apoptotic stimuli significantly increase the number of floating cells and apoptotic bodies present in the culture medium, which is a direct proof for the anoikis principle of adherent cells [2] (figure 3). We did not find an increase of Europium fluorescence of the adherent cell fraction, which not necessarily implies that apoptosis is not induced in this fraction by TNF-α/CHX. We found a remarkable decrease of confluency in all

three cell types induced by TNF-α/CHX (a decrease of 58% for HMECs, 52% for HUVECs and 65% for SMCs). Accordingly, the fluorescence intensity of Europium-labelled Annexin V of TNF-α/CHX treated cells compared to control cells was increased with a factor of 3 for HMECs and HUVECs and with a factor of 7.5 for SMCs when correlated to the number of cells analysed. Based on this observation we can speculate that we also showed TNF-α/CHX induced apoptosis in the adherent cell fractions (figure 4 and 5). The fact that the adherent cell fraction can be studied directly in the culture dish without detachment using e.g. trypsin eliminates the possibility of inducing apoptosis by artefacts [9, 10]. The relative increases of the amount of apoptotic adherent cells, floating cells and apoptotic bodies induced by TNF-α/CHX (figures 3 and 4), indicating anoikis, were not the same in the three different adherent cell types used. These findings confirm our previous observations that cell death kinetics depend on the type of the cell [27]. Further study is needed in order to describe these differences into detail and to reveal the exact mechanism.

Conclusions

According to our knowledge this is the first direct quantitative technique to measure anoikis in adherent cell cultures. Our assay provides the ability to analyse anoikis and further steps of the apoptotic cascade of the same sample at the same time. Apoptotic stimuli increase the number of apoptotic floating cells and apoptotic bodies which is a direct proof for the anoikis principle of adherent cells [2].

Acknowledgement

Dr. P. Koolwijk of the Netherlands Organisation for Applied Scientific Research (TNO-PG, Leiden, The Netherlands), E. W. Ades of the Centers for Disease Control and Prevention (CDC, Atlanta, USA) and T. J. Lawley of Emory University (Atlanta, USA) are kindly acknowledged for the donation of HMEC cultures. Dr. C. Reutelingsperger (University of Maastricht, The Netherlands) is kindly acknowledged for the donation of Annexin V and FITC-labelled Annexin V.

References

1. Meredith, J.E., Fazeli, B., and Schwartz, M.A. The extracellular matrix as a cell survival factor. Mol. Biol. Cell 1993; 4: 953-961.
2. Ruoslahti, E. and Reed, J.C. Anchorage dependence, integrins, and apoptosis. Cell 1994; 77: 477-478.

3. Grossman, J., Walther, K., Artinger, M., Kiesslinkg, S., and Scholmerich, J. Apoptotic signaling during initiation of detachment-induced apoptosis ("anoikis") of primary human intestinal epithelial cells. Cell Growth & Diff. 2001; 12: 147-155.
4. Frisch, S.M. and Francis, H. Disruption of epithelial cell-matrix interactions induces apoptosis. J.Cell Biol. 1994; 124: 619-626.
5. Frisch, S.M. and Screaton, R.A. Anoikis mechanisms. Cell Biol. 2001; 13: 555-562.
6. Danial, N.N. and Korsmeyer, S.J. Cell death: Critical control points. Cell 2004; 116: 205-219.
7. Lance, A. and Kohn, E. Cancer and the homeless cell. Nature 2004; 430: 973-974.
8. Douma, S., van Laar, T., Zevenhoven, J., Meeuwissen, R., van Garderen, E., and Peeper, D.S. Suppression of anoikis and induction of metastasis by the neurotrophic receptor TrkB. Nature 2004; 430: 1034-1039.
9. Darzynkiewicz, Z., Bedner, E., and Smolewski, P. Flow cytometry in analysis of cell cycle and apoptosis. Semin.Hematol. 2001; 38: 179-193.
10. Micoud, F., Mandrand, B., and Malcus-Vocanson, C. Comparison of several techniques for the detection of apoptotic astrocytes *in vitro*. Cell Prolif. 2001; 34: 99-113.
11. Vermes, I., Haanen, C., and Reutelingsperger, C. Flow cytometry of apoptotic cell death. J.Immunol.Methods 2000; 243: 167-190.
12. van England, M., Ramakers, F.C.S., Schutte, B., and Reutelingsperger, C.P.M. A novel assay to measure loss of plasma membrane asymmetry during apoptosis of adherent cells in culture. Cytometry 1996; 24: 131-139.
13. Vermes, I., Haanen, C., and Steffens-Nakken, H. A novel assay for apoptosis. Flow cytometric detection of phosphatidylserine expression on early apoptotic cells using fluorescein labelled Annexin V. J.Immunol Methods 1995; 184: 39-51.
14. Hemmilä, I. Fluoroimmunoassays and immunofluorometric assays. Clin.Chem. 1985; 31: 359-370.
15. Hemmilä, I., Dakabu, S., and Mukkala, e.al. Europium as a label in time-resolved immunofluorometric assays. Anal.Biochem. 1984; 137: 335-343.
16. Diamandis, E.P. Immunoassays with Time-Resolved Fluorescence Spectroscopy: Principles and Applications. Clin.Biochem. 1988; 21: 139-150.
17. Gudgin, E.F., Pollak, A., and Diamandis, E.P. Ultrasensitive bioanalytical assays using time-resolved fluorescence detection. Pharmac.Ther. 1995; 66: 207-235.
18. Simak, J., Holada, K., and Vostal, J.G. Release of annexin V-binding membrane microparticles from cultured human umbilical vein endothelial cells after treatment with camptothecin. BMC Cell Biology 2002; 3: 1-10.
19. Nicoletti, I., Migliorati, G., Pagliacci, M.C., Grinani, F., and Riccardi, C. A rapid and simple method for measuring thymocyte apoptosis by propidium iodide staining and flow cytometry. J.Immunol.Methods 1991; 139: 271-273.
20. Nieuwland, R., Berckmans, R.J., Rotteveel-Eijkman, R.C., Maquelin, K.N., Roozendaal, K.J., Jansen, P.G.M.t.H.K., Eijsman, L., Hack, C.E., and Sturk, A. Cell-derived microparticles generated in patients during cardiopulmonary bypass are highly procoagulant. Circulation 1997; 96: 3534-3541.
21. Jaffe, E.A., Nachman, R.L., Bedker, C.G., and Minick, C.R. Culture of human endothelial cells derived from umbilical veins. J.Clin.Invest. 1973; 52: 2756-

22. Heimli, H., Kahler, H., Endresen, M.J., Henriksen, T., and Lyberg, T. A new method for isolation of smooth muscle cells from human umbilical cord arteries. Scand.J.Clin.Lab.Invest 1997; 57: 21-29.
23. Buijtenhuijs, P., Buttafoco, L., Poot, A.A., Daamen, W.F., van Kuppevelt, T.H., Dijkstra, P.J., de Vos, R.A.I., Sterk, L.M.Th., Geelkerken, R.H., Feijen, J., and Vermes, I. Tissue engineering of blood vessels: Characterisation of smooth muscle cells for culturing on collagen and elastin based scaffolds. Biotechnol.Appl.Biochem. 2003; 39: 141-149.
24. Chamley-Campbell, J., Campbell, G.R., and Ross, R. The smooth muscle cell in culture. Physiol.Rev. 1979; 59: 1-61.
25. Lefebvre, P., Nusgens, B.V., and Lapiere, C.M. Cultured myofibroblasts display a specific phenotype that differentiates them from fibroblasts and smooth muscle cells. Dermatology 1994; 189: 65-67.
26. Smolewski, P., Grabarek, J., Lee, B.W., Johnson, G.L., and Darzynkiewicz, Z. Kinetics of HL-60 cell entry to apoptosis during treatment with TNF-alpha or camptothecin assayed by the stathmo-apoptosis method. Cytometry 2002; 47: 143-149.
27. Wolbers, F., Buijtenhuijs, P., Haanen, C., and Vermes, I. Apoptotic cell death kinetics *in vitro* depend on the cell types and the inducers used. Apoptosis 2004; 9: 385-392.

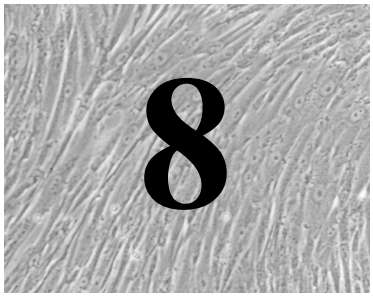

8

Development of a Bioreactor for Tissue Engineering of Small-Diameter Blood Vessels: Design of a Pulsatile Flow System*

* L. Buttafoco1, P. Engbers-Buijtenhuijs[1,2], A.A. Poot[1], P. J. Dijkstra[1], I. Vermes[1,2], J.Feijen[1]

Submitted for publication to Biotech. Bioeng., 2005

[1] University of Twente, Faculty of Science & Technology, Department of Polymer Chemistry and Biomaterials, and Institute of Biomedical Technology (BMTI), P.O. Box 217, 7500 AE Enschede, The Netherlands

[2] Medisch Spectrum Twente, Hospital Group, Department of Clinical Chemistry, P.O. Box 50.000, 7500 KA Enschede, The Netherlands

Abstract

A pulsatile flow bioreactor for tissue engineering of small-diameter blood vessels was developed. The bioreactor consists of four vessels mounted in four parallel chambers. Culture medium can be perfused through the vessels inside the chambers using a peristaltic pump. The closed-circuit system was pressurised to 100 mmHg. This set up allows pulsatile flow (120 beats/min) and fluctuation of pressure inside the vessels between approximately 80 and 120 mmHg, simulating physiological conditions. Two types of vessels were used to further characterise the system. Vessels were either made of non-porous silicone rubber or of porous collagen/elastin crosslinked with N-(3-dimethylaminopropyl)-N'-ethylcarbodiimide (EDC) and N-hydroxysuccinimide (NHS). The latter scaffolds were seeded with smooth muscle cells (SMCs) and cultured in the bioreactor up to 14 d.

The flow rate in the vessels increased linearly with the number of beats/min. At an average flow rate of 9.6 mL/min, an average wall shear rate of 61 s^{-1} was reached, comparable to the lower wall shear rates in the human carotid artery (60-775 s^{-1}). Increasing the flow rate from 3 to 9.6 mL/min leads to an increase of Reynolds numbers from 29 to 96, which is also in the same range as found for the carotid artery. Pressures were monitored proximal and distal to the vessels and outside the vessels in the chambers. After 1 d of culture of SMCs on crosslinked collagen/elastin scaffolds in the bioreactor, no significant differences were measured between the average pressures over the wall and along the length of the tube. After 14 d of culture, the average pressure inside the vessel was 14 mmHg higher than the average pressure outside the vessel, which is caused by decreased permeability of the tube after longer culture times. A versatile bioreactor for vascular tissue engineering, able to accommodate a broad range of vessel sizes, easy to handle, clean and maintain was thus developed. Moreover, this system can be used as a valuable *in vitro* model to study the effects of physical forces on (developing) tissues and to predict the response of tissue-engineered constructs once implanted *in vivo*.

Introduction

Tissue engineering is a discipline that applies the principles of engineering and life sciences for the development of biological substitutes that can restore, maintain or improve tissue functions. For this reason, polymeric scaffolds, which function as temporary templates with adequate mechanical properties to prevent failure of the constructs during dynamic culture, have been developed. The ideal engineered scaffold should degrade and resorb at a controlled rate, to match cell proliferation, extra-cellular matrix (ECM) production and tissue ingrowth

in vitro and/or *in vivo*. Finally, the resulting tissue should mimic the biomechanical characteristics of the natural tissue [1]. Vascular tissue engineering deals with creating functional blood vessels *in vitro,* either to treat (cardio-)vascular diseases or to develop models to study vascular biology [2]. Most vascular tissue engineering strategies aim at creating grafts mimicking the three-layered structure of a natural blood vessel. One strategy to create these biological substitutes is to use cells seeded in porous scaffolds. Various tissue engineering approaches have been proposed, using either natural [3-6] or synthetic [7-9] materials, but many challenges still have to be overcome before a suitable vascular replacement is available [10]. In the past, either vascular cell culture models [11, 12] or animal models [13, 14] have been used to evaluate the effects of chemical and mechanical stimuli on cell proliferation, phenotype, alignment, migration and ECM production. However, the proper phenotype of cells and mechanical stimuli for cell organisation and development of the desired ECM structure are often lacking in cell culture models [15]. These characteristics are more easily accomplished in animal models, but, in this case, it is not possible to study the effect of distinct factors (*e.g.* growth factors) or to vary the hemodynamics.

With the development of bioreactors, advantages of both cell culture and animal models were combined. Bioreactors are generally defined as devices in which biological and/or biochemical processes develop under closely monitored and tightly controlled environmental and operating conditions [16]. For tissue engineering of blood vessels, numerous research groups have designed their own bioreactors. In particular, spinner flasks and rotating bioreactors have been developed to enhance mass transfer of nutrients, oxygen and waste products [17]. In the spinner flask bioreactor, culture medium is flowing continuously around immobile scaffolds. During seeding, cells are transported to and into the scaffold by convection. The flow of the medium enhances mass transfer but may also generate turbulent eddies. These could be detrimental for the development of the new tissue, since a turbulent flow generally prevents a homogeneous distribution of oxygen and nutrients over the construct [18].

Rotating bioreactors provide the constructs with a dynamic culture environment, laminar flow and high mass transfer rates. However, these systems are often complex, expensive or not capable of reproducing physiological hemodynamics [16, 17]. Other bioreactors [9, 19-22] have been manufactured to mimic the physiological conditions of the human vasculature and to investigate the role of single factors. The most detailed analysis of such a bioreactor is reported by Conklin *et al.* [15], who described a system able to generate a pulsatile flow by means of a cam-driven syringe, a peristaltic pump and a compliance chamber. Physiological

haemodynamics could thus be simulated and the effect of different factors, like shear stress or pressure, was evaluated on intact vascular tissue for up to 48 h. All these studies demonstrated that an environment resembling *in vivo* conditions may promote both the development of constructs with sufficient mechanical strength to be implanted and the modulation of appropriate cellular functions. However, the optimal bioreactor set up and culture conditions for the development of a functional arterial graft remain to be elucidated and the biggest challenge remains how to grow three-dimensional structures that contain more than a few layers of SMCs [23].

The objective of this study is to develop a bioreactor for tissue engineering of small-diameter blood vessels. Such a bioreactor should be suitable to develop functional tissue-engineered (TE) vascular grafts from constructs incorporating living human vascular smooth muscle cells (SMCs) embedded in scaffolds composed of natural proteins and/or synthetic polymers. These constructs should be ultimately lined with endothelial cells (ECs) to provide a living, responsive and non-thrombogenic blood conduit. In order to reach this aim, a compact and relatively inexpensive bioreactor, adapted from the system devised by Bardy *et al.* [24] and Perrée *et al.* [25], was developed in our laboratories. In this bioreactor, physiologic-like flow and pressure were mimicked. The flow dynamics of the system were characterized using either a silicone tube or a porous tubular scaffold of insoluble collagen and insoluble elastin as vessel. The flow conditions in the bioreactor were compared to those experienced *in vivo.* Moreover, the system was set up to culture SMC-seeded porous tubular scaffolds and thus to investigate the response of these constructs to dynamic loading.

Materials and Methods

Bioreactor system

A pulsatile flow system was designed for tissue engineering of small-diameter vascular grafts (figure 1). A peristaltic roller-pump (Watson Marlow Sci-Q-323, Brussels, Belgium) was used to pump fluid from a custom-made three-port glass fluid reservoir via highly distensible silicone tubing (Watson Marlow, Brussels, Belgium, inner diameter (ID): 3.2 mm x outer diameter (OD): 6.4 mm) to four custom-made glass chambers and back to the fluid reservoir. Approximately three-quarters of the fluid reservoir (60 mL) were filled with culture medium, while air filled the remaining volume. The air acts as a source of oxygen for the cells during culturing and is used to achieve the desired pressure. A pressure of 100 mmHg was applied to the fluid reservoir and regulated by means of an electronically controlled Venturi valve (T5200-50, Fairchild Company, Winston-Salem, NC, USA). The applied pressure was

monitored proximal and distal to the vessels as well as outside the vessels in the glass chambers by pressure sensors (Edwards Lifesciences LLC, Unterschleissheim, GmbH, Instrumentation Department, Academic Medical Centre of Amsterdam, The Netherlands), and a scope meter (Fluke 199BM scopemeter, Adquipment Medical B.V., Hellevoetsluis, The Netherlands) throughout the duration of the experiment.

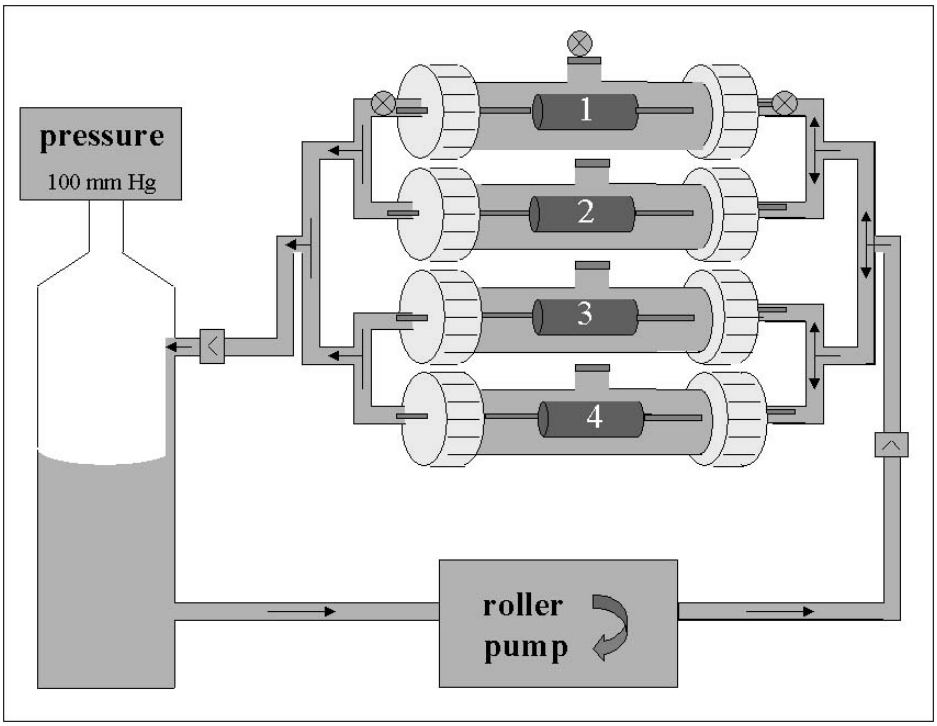

Figure 1: Schematic representation of the bioreactor used in this study. The vessels were mounted in four parallel chambers filled with fluid. The chambers were connected through silicone tubing to the peristaltic pump and the fluid reservoir, respectively. Fluid was perfused through the vessels inside the flow chambers. A pressure of 100 mmHg was applied to the fluid reservoir (⊗ represents a pressure sensor, ⌒ represents a valve).

The pressure sensors were calibrated at atmospheric pressure (0 mmHg) and 100 mmHg above atmospheric pressure before every experiment by a pneumatic transducer tester (DALE20, DALE technology, Carson city, NV, USA). Alternatively, pressure signals were displayed by an oscilloscope (DATEX cardiocap II, Helsinki, Finland). Two valves (DATEX, Helsinki, Finland) preventing a back flow of the culture medium, were inserted at the proximal and distal position of the chambers, in order to obtain a more accurate reproduction of the pressure wave-forms experienced by blood vessels *in vivo* during ventricular systole and diastole. In this particular design, four chambers could be placed in a single incubator in parallel with respect to each other, all driven by a single pump. Silicone tubing (Watson

Marlow, Brussels, Belgium, 3.2 mm ID x 6.4 mm OD) was cannulated and tied on both ends with sutures (Ethicon Mersilene, Johnsson & Johnsson Intl., St. Stevens-Woluwe, Belgium) to thin-walled stainless–steel tubes having an outside diameter of 3 mm, which matches the inside diameter of the used vessels at physiological pressure. Alternatively, porous tubular scaffolds of insoluble collagen type I from bovine Achilles tendon and insoluble elastin from equine ligamentum nuchae (porosity 94%, average pore size 131 μm, ID 3 mm, OD 6 ± 1 mm) were used as vessel. Prior to use, these scaffolds were crosslinked with a carbodiimide N-(3-dimethylaminopropyl)-N'-ethylcarbodiimide (EDC) in combination with N-hydroxysuccinimide (NHS), as previously described [26]. SMCs isolated from human umbilical vein [27], were seeded on the crosslinked collagen/elastin scaffolds (10^7 cells/scaffold) by means of a filtration seeding procedure. The cells were dynamically cultured in the bioreactor for 1 up to 14 d.

During analyses, the vessels were mounted inside the chambers and these were connected to the silicone tubing by Discofix connectors (Discofix-3 and Discofix-5, B. Braun, Melsungen, AG, Germany). The outside of the vessels was in contact with culture medium in the chambers (ca. 20 mL). The fluid reservoir, the chambers containing the vascular grafts and the pressure sensors were placed in humidified atmosphere inside an incubator at 37 ^{0}Cand 5% CO_2 (CleanAir Techniek bv, Woerden, The Netherlands). A peristaltic roller pump (Watson Marlow, Brussels, Belgium) inserted between the proximal side of the flow chambers and the fluid reservoir, generated pressure pulses in the system (30-120 beats/min). Vessels of various lengths and diameters could be accommodated in this system and cultured for extended periods of time. Vessels with a length of approximately 4 cm were used for the experiments described in this paper.

Flow dynamics

Simplified model of an artery

In order to make an estimation of the flow characteristics in the vessels, several major simplifications have been made. It is assumed that:

- the vessels are straight, non-porous, rigid tubes, with a smooth luminal surface;
- entrance effects are neglected;
- the flow inside the vessels is steady.

The flow dynamics of the system were studied using PBS instead of culture medium as a solvent. However, the reported results are also valid if culture medium is used, since the two fluids have a relative viscosity of 1.05.

Flow rate

The flow rate (φ) inside the vessels was determined experimentally, by measuring the volume of fluid collected from the silicone tubing mounted in each chamber during 1 min The measurements were repeated 3 times.

Nature of the flow

The nature of the flow (laminar or turbulent) inside the vessels was evaluated by calculating the Reynolds number (Re) [28]:

$$\mathrm{Re} = \frac{d * \overline{V} * \rho}{\mu} \qquad (1)$$

where d is the internal diameter of the vessel (0.3 cm), ρ the density (1 g/cm^3) and μ the viscosity of PBS (0.719 centipoise at 37 ^{0}C). The mean velocity ($\overline{V}$) was calculated from the flow rate ($\varphi = (\overline{V} * \pi * d^2)/ 4$).

Shear rate

The wall shear rate ( ) was calculated from the following equation [28]:

$$\dot{\gamma} = \frac{4 * \varphi}{\pi * r^3} \qquad (2)$$

where r is the radius of the vessel.

Shear stress

The wall shear stress (τ) was calculated from [29]:

$$\tau = \frac{4 * \mu * \varphi}{\pi * r^3} \qquad (3)$$

Wall stress

The wall stress was calculated from [28]:

$$\text{Wall stress} = \frac{\overline{\Delta P} * r}{Thickness_{wall}} \qquad (4)$$

where $\overline{\Delta P}$ is the average trans-wall pressure difference. This was calculated by subtracting the value of the mean pressure measured outside the vessel in the chamber from the mean pressure at the entrance of the vessel. The mean pressure was calculated by adding one third of the pulse pressure to the diastolic pressure (see below). The pulse pressure is the difference between systolic and diastolic pressure. No attenuation of the pressure wave because of the dissipative mechanisms associated with the viscoelastic materials comprising the vessel wall was considered [30].

Results and Discussion

Bioreactors can be defined as devices in which biological and/or biochemical processes can be performed under controlled environmental conditions [16]. *In vivo* the blood vessel wall is continuously exposed to two types of haemodynamic forces: a tensile stress, which has a perpendicular, a circumferential and a longitudinal component relative to the vessel wall and a tractive force, caused by blood flow, parallel to the longitudinal axis of the vessel and determined by vessel geometry and fluid viscosity [31]. Mechanical stimuli contribute to induce orientation of both smooth muscle cells (SMCs) [22, 32] and ECs [33] and enhance ECM production and tissue formation thus yielding a more functional construct [34, 35].

In the current study, a sophisticated but simple bioreactor, adapted from the system devised by Bardy *et al.* [24] and Perrée *et al.* [25] was designed to improve the spatial distribution and organisation of the cells in porous tubular scaffolds for tissue engineering of small-diameter blood vessels. In this system, the vessels were cannulated inside glass chambers and connected through highly distensible silicone tubing to a peristaltic roller pump and to a fluid reservoir. In contrast to the flow system of Bardy *et al.* and Perrée *et al.*, four chambers placed in parallel were used in this study (figure 1). The peristaltic roller pump generated a continuous pulsatile flow through the lumen of the vessels. Moreover, in contrast to the former flow system, the glass chambers had no open connection to the air during perfusion.

In order to verify whether the haemodynamic forces present in the vessels are similar to those in arteries *in vivo* and thus to prove the applicability of this system for tissue engineering of blood vessels, the flow dynamic properties were estimated using the simplifications mentioned above. Blood vessels normally consist of a number of different materials and cells, arranged in a complex manner. About 70% of the walls of the arteries consists of water, whereas the rest is constituted by a mesh of fibres (*e.g.* collagen and elastin) with (visco)elastic properties. However, in order to describe the system developed in our laboratories with the equations available in literature, the vessels were assumed to be long, straight, rigid tubes, with a smooth and non-porous inner surface. Although the equations describing such tubes cannot account for the complexity of the cardiovascular system, they provide a good starting point [36].

Experimentally, it was found that increasing the rotational speed of the pump from 30 to 120 beats/min resulted in a linear increase of the average flow rate from 3.0 to 9.6 mL/min per vessel (figure 2). No differences were observed in the flow recorded for each of the four parallel vessels. The measured flow rates are much lower than in the human carotid artery (5-35 mL/s) [37, 38]. However, it has been documented that mechanical stimulation in the form of a periodic stretch is the main factor influencing the orientation of SMCs and the synthesis of ECM components [22, 39]. Therefore it was considered to be more important to mimic the pressure pulses in a native artery rather than the flow rate. In the developed set up, flow rate and pulsations cannot be controlled independently. However, use of two separate pumps to control the flow and the pressure pulses can easily solve this problem.

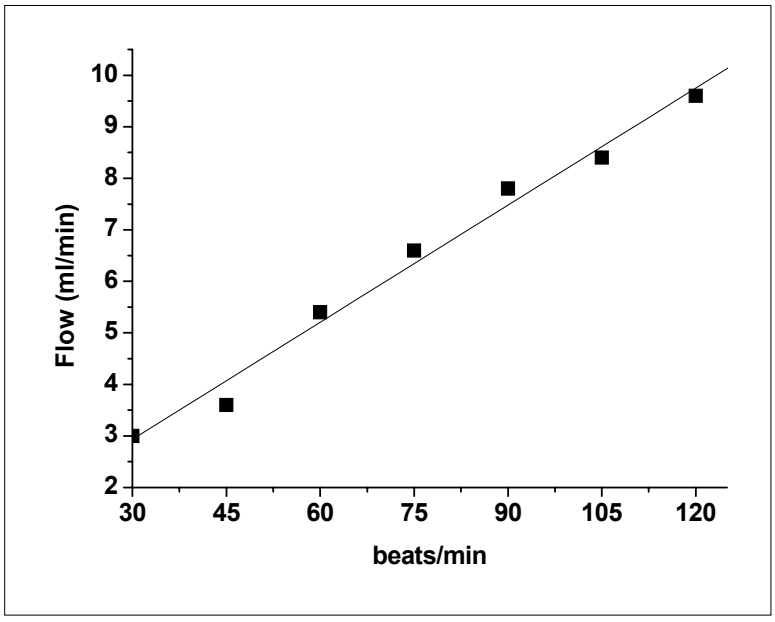

Figure 2: Dependence of the flow rate inside the vessels on the number of beats/min.

In the carotid artery, a waveform analogous to that shown in figure 3a is present. The systolic (120 mmHg) and diastolic (80 mmHg) pressure are the maximum and minimum pressure, respectively. The mean pressure (93 mmHg) is the average pressure throughout the cardiac cycle. It can be calculated by adding one third of the pulse pressure to the diastolic pressure. The pulse pressure is the difference between systolic and diastolic pressure. The possibility to reproduce these natural conditions in the vessels of the bioreactor is advantageous since it is known that dynamic mechanical conditioning induces SMC orientation in TE constructs [40, 41]. When a silicone tube is used as vessel in our system and the rotational speed of the pump is set at 120 beats/min, the pressure in a position proximal to the vessel oscillates between 46 and 144 mmHg ($\overline{P}$ = 78 mmHg) (figure 3b). No significant pressure drop is observed along the length of the vessel ($\overline{\Delta P}$ = 4 mmHg), since a pressure of 48-127 mmHg ($\overline{P}$ = 74 mmHg) is found at the distal position. Though the measured values are different from those in a natural artery of a healthy subject (80-120 mmHg) [42], it is possible to reproduce a pressure waveform in the flow system similar to the natural one. Since the bioreactor described in this paper is a closed system, the pressure in the vessels mounted in the four separate chambers was the same.

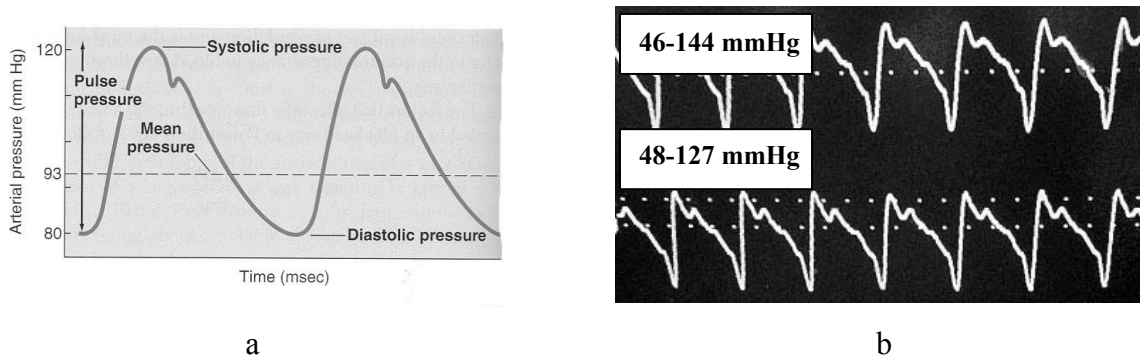

a b

Figure 3: Pressure waveform characteristic of the blood flow in the carotid artery (a) and pressure waveform obtained in the pulsatile flow bioreactor, at an average pressure of 100 mmHg and 120 beats/min, with a silicone tube as vessel (b).. The mean pressure is the average pressure throughout the cardiac cycle; it equals diastolic pressure + 1/3 pulse pressure. Pulse pressure is the difference between systolic and diastolic pressure. Top and bottom curves in figure 3b present the pressure waveforms at the proximal and distal position to the vessel, respectively.

In a human carotid artery, Reynolds numbers vary from 2 up to 560, depending on whether the values are calculated at the diastole or at the systole or whether the vessels have some atherosclerotic plaques [43]. In vessels with a diameter of 6 mm, a length of 20 cm and a mean

blood velocity blood of 3.6 cm/s the Reynolds number is 72 [30]. Under the conditions described, Reynolds numbers vary between 29 (30 beats/min) and 96 (120 beats/min).

These values indicate that the flow is laminar (Re < 2100 [28]), a condition necessary to have efficient and homogeneous transfer of oxygen and nutrients to the three-dimensional construct. This transfer can be limited under static culture conditions, where the transport of nutrients and oxygen can only take place through diffusion [40]. Reduced nutrients and oxygen transfer to three-dimensional constructs is generally one of the main problems to be addressed in tissue engineering of blood vessels [16].

Under the conditions described above (120 beats/min, flow rate = 9.6 mL/min), the average wall shear rate is 61 s^{-1}, a value fitting the lower range of shear rates found in the human carotid artery (60-775 s^{-1}) [44]. Changes of the vessel diameter and flow rate as a consequence of the pulsatile blood flow will influence this value causing its continuous variation.

Also the values of wall shear stress are important in tissue engineering of blood vessels, since wall shear stress is known to influence the biochemistry of ECs [45] and the permeability of the arterial wall to macromolecules. *In vivo,* the different vessels adapt their internal diameter to blood flow, thus achieving minimal expenditure of energy for transportation of blood [45]. Under physiological circumstances, the mean wall shear stress varies from 10 to 26 dyne/cm^2, from the aorta to the capillaries, respectively [46]. Mean wall shear stresses decrease with age due to the age-dependent increase in the diameter of blood vessels [47, 48]. In the system described in this study, the values of wall shear stress increase from 0.13 dyne/cm^2 at 30 beats/min to 0.43 dyne/cm^2 at 120 beats/min Values down to $5 \cdot 10^{-4}$ dyne/cm^2 are known to enhance cell viability and proliferation [49]. Moreover, low-shear-stress preconditioning of TE vascular grafts has been proven to be a successful method to enhance retention of seeded ECs *in vitro* [50].

Arterial wall stress is another significant parameter in determining the properties of a vessel during arterial development and is dependent on the transmural pressure and on the mechanical properties of the vessel wall [51]. In a carotid artery, an average wall stress of $93 \cdot 10^3$ dyne/cm^2 can be estimated considering a mean arterial pressure of 70 mmHg [52], an ID of 4 mm and an OD of 6 mm. As a consequence of the pulsatile blood flow, the vessel is continuously dilated and contracted. The transmural pressure, the ID and OD of the vessel and the wall thickness determine the stress exercised on the wall of the vessel. In a closed system as described here, a difference in pressure observed along the length or across the wall of a vessel can be related to its porosity as well as to its elasticity. When silicone tubing is used as a vessel, the values of pressure recorded at the entrance, at the exit of the vessel and in the

area surrounding it, in the flow chamber, are 46-144 mmHg, 48-127 mmHg and 63 mmHg, respectively (figure 3b). No significant pressure drop ($\overline{\Delta P}$ = 5 mmHg, $\overline{P}_{entrance}$ = 79 mmHg; $\overline{P}_{exit}$ = 74 mmHg) is present along the length of the vessel, whereas a maximum $\overline{\Delta P}$ of 16 mmHg is present across the wall of the silicone tube. The difference in pressure observed between the inner and outer side of the vessel is due to the lack of porosity of the silicone tube. The maximal trans-wall pressure of 16 mmHg resulted in an average wall stress of $21 \cdot 10^3$ dyne/cm^2, much lower than that estimated for a human carotid artery. This low wall stress might contribute to prevent bursting of a scaffold once cultured in the bioreactor.

The pressures were measured under the same conditions (flow rate = 9.6 mL/min per vessel, 120 beats/min) with EDC/NHS crosslinked porous tubular scaffolds of collagen/elastin. In previous work, we have shown that crosslinking of collagen/elastin structures with EDC/NHS results in relatively stiff materials [26]. Moreover, it has been reported that the physical properties of a scaffold change in time during SMC culture [53]. After 1 d of culture with SMCs under dynamic conditions, no significant differences in pressure were observed along the length or over the wall of the crosslinked collagen/elastin constructs ($P_{entrance}$ = 80-91 mmHg; P_{exit} = 81-91 mmHg; P_{ouside} = 84-93 mmHg). The high porosity of the vessels (94%) ensures equilibration of the pressure to an average value of 85 ± 2 mmHg, thus preventing attenuation of the pressure pulses. The absence of a trans-wall pressure difference in this particular case, most probably prevented the scaffolds from bursting. On the contrary, after 14 d of culture in such a dynamic environment, SMCs have migrated and grown throughout the porous construct. SMCs are responsible for the ability of a blood vessel to contract and to relax, thus enhancing the elasticity of the vessel [53]. Moreover, as a consequence of the presence of SMCs, the porosity of the constructs decreases. Both these effects were visible in the pressure values recorded. A pressure of 61-124 mmHg was found at the entrance of the construct (figure 4), but due to the acquired elasticity and the decreased porosity of the construct, a pressure of 49-105 mmHg was measured in the environment around the construct in the flow chamber ($\overline{\Delta P}_{wall}$ = 14 mmHg, $\overline{P}_{entrance}$ = 82 mmHg, $\overline{P}_{outside\ vessel}$ = 68 mmHg). This corresponds to an average wall stress of $19 \cdot 10^3$ dyne/cm^2, comparable to that observed with the silicone tube. Pressure values 51-102 mmHg, similar to those outside the vessel in the flow chamber, were found at the exit of the construct ($\overline{\Delta P}_{length}$ = 14 mmHg, $\overline{P}_{exit}$ = 68 mmHg). Evidently the attenuation of the pulse occurred partly through the wall and not along the length of the scaffold.

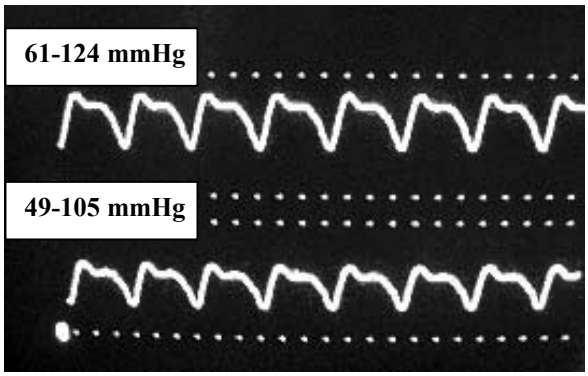

Figure 4: Pressure waveform obtained in the pulsatile flow bioreactor, at an average pressure of 100 mmHg and at 120 beats/min, with an EDC/NHS crosslinked porous tubular scaffold of collagen and elastin (weight ratio 1:1) cultured for 14 d with SMCs. Top curve proximal position, bottom curve outside the vessel in the chamber.

A suitable bioreactor for tissue engineering of small-diameter blood vessels has been developed. Further experiments are currently being performed to analyse the physical and biological properties of the collagen/elastin constructs and of SMC-seeded hybrid structures of poly(1,3-trimethylene carbonate)co(D,L-lactide) and insoluble collagen, cultured in the bioreactor.

Conclusions

The bioreactor described in the current study is versatile and functional, being able to accommodate a broad range of vessel sizes, easy to handle, clean and maintain. Moreover, the possibility to disconnect the chambers from the bioreactor permits to seed the scaffolds *in situ*, reducing the risks associated with handling and transferring the constructs between different systems. The scaffolds can be accessed singularly, thus permitting to correct eventual anomalies in one of the vessels without affecting other samples. Continuous observation of the vessels is possible through the glass chamber walls by direct vision, thus allowing immediate detection of any macroscopic evidence of bacterial or fungal contamination throughout the culture period.

The flow dynamic properties of this bioreactor have been roughly estimated using silicone tubing as a vessel at an average pressure of 100 mmHg and 120 beats/min. Under these conditions, a flow rate of 9.6 mL/min in each vessel results in an average wall shear rate of 61 s^{-1}, comparable to that in the carotid artery. Pressure waveforms are also similar to arterial waveforms. In contrast, values of average wall stress and wall shear stress are lower than *in vivo*. This may be advantageous in terms of structural stability of the cultured vessel as well

as cell viability and proliferation. Physical and biological characterisation of SMC-seeded porous tubular scaffolds cultured in the bioreactor is currently being performed.
Use of ultrasound equipment can permit accurate and continuous monitoring of the pulsatile flow inside the vessels and of their change in diameter. A system as the one described above could also serve as a valuable *in vitro* model to study the effects of physical forces on (developing) tissues and to predict the response of the TE constructs once implanted *in vivo.*

Acknowledgement

J. Perrée and T.G. van Leeuwen (Academic Medical Centre, University of Amsterdam, Laser Centre, Amsterdam, The Netherlands) and the department of Medical Technology (Medisch Spectrum Twente, Enschede, The Netherlands) are kindly acknowledged for their help in the design of this equipment. B.H.L. Betlem and C. Kruit (Process Dynamics and Control Group, Faculty of Science and Technology, University of Twente, Enschede, The Netherlands) are thanked for the useful discussions.

References

1. Langer, R. and Vacanti, J.P. Tissue Engineering. Science 1993; 260: 920-926.
2. Seifalian, A. M., Giudiceandrea, A., Schmidt-Rixen, T., and Hamilton, G., Non compliance: the silent acceptance of a villain in: Tissue engineering of vascular prosthetic grafts, 1999; 621.
3. L'Heureux, N., Paquet, S., Labbe, R., Germain, L., and Auger, F.A. A completely biological tissue-engineered human blood vessel. FASEB J. 1998; 12: 47-56.
4. Campbell, J.H., Efendy, J.L., and Campbell, G.R. Novel vascular graft grown within recipient's own peritoneal cavity. Circ.Res. 1999; 85: 1173-1178.
5. Bader, A., Steinhoff, G., Strobl, K., Schilling, T., Brandes, G., Mertsching, H., Tsikas, D., Froelich, J., and Haverich, A. Engineering of human vascular aortic tissue based on a xenogeneic starter matrix. Transplant. 2000; 70: 7-14.
6. Weinberg, C.B. and Bell, E. A blood vessel model constructed from collagen and cultured vascular cells. Science 1986; 231: 397-400.
7. Mooney, D.J., Mazzoni, C.L., Breuer, C., McNamara, K., Hern, D., Vacanti, J.P., and Langer, R. Stabilized polyglycolic acid fibre-based tubes for tissue engineering. Biomaterials 1996; 17: 115-124.
8. Hoerstrup, S.P., Zund, G., Sodian, R., Schnell, A.M., Grunenfelder, J., and Turina, M.I. Tissue engineering of small caliber vascular grafts. Eur.J.Cardiothorac.Surg. 2001; 20: 164-169.
9. Niklason, L.E., Gao, J., Abbott, W.M., Hirschi, K.K., Houser, S., Marini, R., and Langer, R. Functional arteries grown *in vitro*. Science 1999; 284: 489-493.
10. Mitchell, S.L. and Niklason, L.E. Requirements for growing tissue-engineered vascular grafts. Cardiovasc.Pathol. 2003; 12: 59-64.

11. Campbell, J.H. and Campbell, G.R. Culture techniques and their applications to studies of vascular smooth muscle. Clin.Sci. 1993; 85: 501-513.
12. Jaffe, E.A., Nachman, R.L., Bedker, C.G., and Minick, C.R. Culture of human endothelial cells derived from umbilical veins. J.Clin.Invest. 1973; 52: 2756.
13. Kallmes, D.F., Lin, H.B., Fujiwara, N.H., Short, J.G., Hagspiel, K.D., Li, S.T., Matsumoto, A.H., and Gary, J. Becker young investigator award: comparison of small-diameter type 1 collagen stent-grafts and PTFE sten-grafts in a canine model--work in progress. J.Vasc.Intervent.Radiol. 2001; 12: 1127-1133.
14. Campbell, J.H., Walker, P., Chue, W., Daly, C., Cong, H., Xiang, L., and Campbell, G.R. Body cavities as bioreactors to grow arteries. Int.Congress.Series 2004; 1262: 118-121.
15. Conklin, B.S., Surowiec, S.M., Lin, P.H., and Chen, C. A simple physiologic pulsatile perfusion system for the study of intact vascular tissue. Med.Eng.Phys. 2000; 22: 441-449.
16. Martin, I., Wendt, D., and Heberer, M. The role of bioreactors in tissue engineering. Trends Biotechnol. 2004; 22: 80-86.
17. Nasseri, B.A., Pomerantseva, I., Kaazempur-Mofrad, M.R., Sutherland, F.W.H., Perry, T., Ochoa, E., Thompson, C.A., Mayer, J.E., Oesterle, S.N., and Vacanti, J.P. Dynamic rotational seeding and cell culture system for vascular tube formation. Tissue Eng. 2003; 9: 291-299.
18. Wendt, D., Marsano, A., Jakob, M., Heberer, M., and Martin, I. Oscillating perfusion of cell suspensions through three-dimensional scaffolds enhances cell seeding efficiency and uniformity. Biotechnol.Bioeng. 2003; 84: 205-214.
19. Surowiec, S.M., Conklin, B.S., Jin S.Li, Peter H.Lin, Victor J.Weiss, Alan B.Lumsden, and Changyi Chen. A new perfusion culture system used to study human vein. J.Surg.Res. 2000; 88: 34-41.
20. Papadaki, M. and Eskin, S.G. Effects of fluid shear stress on gene regulation of vascular cells. Biotechnol.Prog. 1997; 13: 209-221.
21. Seliktar, D., Nerem, R.M., and Galis, Z.S. Mechanical strain-stimulated remodeling of tissue-engineered blood vessel constructs. Tissue Eng. 2003; 9: 657-666.
22. Kanda, K. and Matsuda, T. Mechanical stress-induced orientation and ultrastructural change of smooth muscle cells cultured in three-dimensional collagen lattices. Cell Transplant. 1994; 3: 481-492.
23. Zandonella, C. Tissue engineering: the beat goes on. Nature 2003; 421: 884-886.
24. Bardy, N., Karillon, G.J., Merval, R., Samuel, J.L., and Tedgui, A. Differential effects of pressure and flow on DNA and protein synthesis and on fibronectin expression by arteries in a novel organ culture system. Circ.Res. 1995; 77: 684-694.
25. Perree, J., van Leeuwen, T.G., Kerindongo, R., Spaan, J.A.E., and Van Bavel, E. Function and structure of pressurized and perfused porcine carotid arteries. Am.J.Pathol. 2003; 163: 1743-1750.
26. Buttafoco, L., Engbers-Buijtenhuijs, P., Poot, A.A., Dijkstra, P.J., Daamen, W.F., van Kuppevelt, T.H., Vermes, I., and Feijen, J. First steps towards tissue engineering of small-diameter blood vessels: preparation of flat scaffolds of collagen and elastin by means of freeze-drying. J.Biomed.Mat.Res. 2004; submitted:
27. Buijtenhuijs, P., Buttafoco, L., Poot, A.A., Daamen, W.F., van Kuppevelt, T.H., Dijkstra, P.J., de Vos, R.A.I., Sterk, L.M.Th., Geelkerken, R.H., Feijen, J.., and Vermes, I. Tissue engineering of blood vessels: Characterisation of smooth muscle cells for culturing on collagen and elastin based scaffolds. Biotechnol Appl. Biochem. 2004; 39: 141-149.

28. Foust, A.S., Wenzel, L.A., Clump.C.W., Maus, L., and Andersen, L.B. Principles of unit operations. New York: Wiley 1980; 2nd ed. vol. 1:
29. Greenwald, S.E. and Berry, C.L. Improving vascular grafts: the importance of mechanical and haemodynamic properties. J.Pathol. 2000; 190: 292-299.
30. Caro, C. G., Pedley, T. J., Schroter, R. C., and Seed, W. A., The systemic arteries in: The mechanics of the circulation, Oxford, University press, 1978; 243-349.
31. Gan, L., Sjogren, L.S., Doroudi, R., and Jern, S. A new computerized biomechanical perfusion model for ex vivo study of fluid mechanical forces in intact conduit vessels. J.Vasc.Res. 1999; 36: 68-78.
32. Kanda, K. and Matsuda, T. Behavior of arterial wall cells cultured on periodically stretched substrates. Cell Transplant. 1993; 2: 475-484.
33. Davies, P. Haemodynamic influences on vascular remodelling. Transp.Immunol. 1997; 5: 245-
34. Seliktar, D., Black, R.A., Vito, R.P., and Nerem, R.M. Dynamic mechanical conditioning of collagen-gel blood vessel constructs induces remodeling *in vitro*. Ann.Biomed.Eng 2000; 28: 351-362.
35. Stegemann, J.P. and Nerem, R.M. Phenotype modulation in vascular tissue engineering using biochemical and mechanical stimulation. Ann.Biomed.Eng 2002; 31: 391-402.
36. Whitmore, R. L., The circulatin system in: Rheology of the circulation, Pergamon Press Ltd, 1968; 17-34.
37. Papathanasopoulou, P., Zhao, S., Koehler, U., Robertson, M.B., Long, Q., Hoskins, P., :Xu, Y., and Marshall, I. MRI measurements of time-resolved wall shear stress vectors in a carotid bifurcation model, and comparison with CFD predictions. J.Mag.Reson. 2003; 17: 153-162.
38. Kaazempur-Mofrad, M.R., Isasi, A.G., Younis, H.F., Chan, R.C., Hinton, D.P., Sukhova, G., LaMuraglia, G.M., Lee, R.T., and Kamm, R.D. Characterisation of the atherosclerotic carotid bifurcation using MRI, finite element modeling, and histology. Ann.Biomed.Eng. 2004; 32: 932-946.
39. Stegeman, J.P. and Nerem, R.M. Altered response of vascular smooth muscle cells to exogenous biochemical stimulation in two-and three-dimensional culture. Exp.Cell Res. 2003; 283: 146-155.
40. Carrier, R.L., Papadaki, M., Rupnick, M., Schoen, F.J., Bursac, N., Langer, R., Freed, L.E., and Vunjak-Novakovic, G. Cardiac tissue engineering: cell seeding, cultivation parameters, and tissue construct characterization. Biotech.Bioeng. 1999; 64: 580-589.
41. Lee, A.A., Graham, D.A., Dela, C.S., Ratcliffe, A., and Karlon, W.J. Fluid shear stress-induced alignment of cultured vascular smooth muscle cells. J.Biomech.Eng. 2002; 124: 37-43.
42. Stock, U.A. and Vacanti, J.P. Cardiovascular physiology during fetal development and implications for tissue engineering. Tissue Eng. 2001; 7: 1-7.
43. Bale-Glickman, J., Selby, K., Saloner, D., and Savas, O. Experimental flow studies in exact-replica phantoms of atherosclerotic carotid bifurcations under steady input conditions. J.Biomech.Eng.Trans. 2003; 125: 38-48.
44. Stokholm, R., Oyre, S., Ringgaard, S., Flaagoy, H., Paaske, W.P., and Pedersen, E.M. Determination of wall shear rate in the human carotid artery by magnetic resonance techniques. Eur.J.Vasc.Endovasc.Surg. 2000; 20: 427-433.
45. Samijo, S.K., Willigers, J.M., Barkhuysen, R., Kitslaar, P.J.E.H.M., Reneman, R.S., Brands, P.J., and Hoeks, A.P.G. Wall shear stress in the human common carotid artery as function of age and gender. Cardiovas.Res. 1998; 39: 515-522.

46. Labarbera, M. Principles of design of fluid transport-systems in zoology. Science 1990; 249: 992-1000.
47. Perktold, K., Thurner, E., and Kenner, T. Flow and stress characteristics in rigid walled and compliant carotid-artery bifurcation models. Med.Biol.Eng.Comput. 1994; 32: 19-26.
48. Duncan, D.D., Bargeron, C.B., Borchardt, S.E., Deters, O.J., Gearhart, S.A., Mark, F.F., and Friedman, M.H. The effect of compliance on wall shear in casts of a human aortic bifurcation. J.Biomech.Eng.Trans. 1990; 112: 183-188.
49. Porter, B., Zauel, R., Stockman, H., Guldberg, R., and Fyhrie, D. 3-D computational modeling of media flow through scaffolsd in a perfusion bioreactor. J.Biomech. 2004; in press.
50. Baguneid, M., Murray, D., Salacinski, H.J., Fullert, B., Hamilton, G., Walker, M., and Seifalian, A.M. Shear-stress preconditioning and tissue-engineering-based paradigms for generating substitutes. Biotechnol.Appl.Biochem. 2004; 39: 151-157.
51. Wentzel, J.J., Kloet, J., Andhyiswara, I., Oomen, J.A.F., Schuurbiers, J.C.H., de Smet, B., Post, M.J., de Kleijn, D., Pasterkamp, G., Borst, C., Slager, C.J., and Krams, R. Shear-stress and wall-stress regulation of vascular remodeling after balloon angioplasty - Effect of matrix metalloproteinase inhibition. Circulation 2001; 104: 91-96.
52. Fung, Y. C., Mechanical properties and active remodeling of blood vessels in: Biomechanis, mechanical properties of living tissues, Springer, 1999.
53. Bank, A.J. and Kaiser, D.R. Smooth muscle relaxation - Effects on arterial compliance, distensibility, elastic modulus, and pulse wave velocity. Hypertension 1998; 32: 356-359.

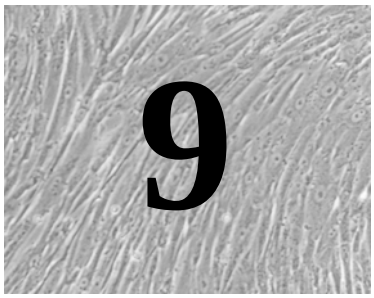

9

Biological Characterisation of Vascular Grafts Cultured in a Bioreactor*

* P. Engbers-Buijtenhuijs[1, 2], L. Buttafoco[1], A.A. Poot[1], R. H. Geelkerken[2], R.A.I. de Vos[3], L.M.T. Sterk[3], J. Feijen[1], and I.Vermes[1, 2]

Submitted for publication to Biomaterials, 2005

[1] University of Twente, Faculty of Science and Technology, Department of Polymer Chemistry and Biomaterials and Institute of Biomedical Technology (BMTI), P.O. Box 217, 7500 AE Enschede, The Netherlands

[2] Medisch Spectrum Twente, Hospital Group, Departments of Clinical Chemistry and Vascular Surgery, P.O. Box 50.000, 7500 KA Enschede, The Netherlands

[3]Laboratory of Pathology Oost-Nederland, P.O. Box 377, 7500 AJ Enschede, The Netherlands

Abstract

This study describes the development of a tissue-engineered construct mimicking the structure of a natural blood vessel. SMCs were cultured in porous tubular scaffolds composed of type I insoluble collagen and insoluble elastin under pulsatile flow conditions. Under these dynamic culture conditions an average wall shear rate, systolic and diastolic pressures and pressure wave forms comparable to conditions in the human carotid artery were obtained. It was shown that culturing of SMCs in tubular scaffolds crosslinked with N-(3-dimetylaminopropyl)-N'-ethylcarbodiimide hydrochloride (EDC) in combination with N-hydroxysuccinimide (NHS) under dynamic conditions results in enhanced tissue formation compared to static conditions. Higher SMC numbers, a more homogeneous distribution of SMCs over the scaffolds and a higher collagen mRNA expression level were found when cells were cultured under dynamic compared to static conditions. Higher cyclin E mRNA expression levels were measured after dynamic compared to static culturing, indicating that cell proliferation was enhanced. tTG mRNA expression levels were not influenced by the culture conditions, indicating that the higher cell numbers in the TE scaffolds cultured under dynamic conditions cannot be explained by decreased apoptosis but only by increased cell proliferation. The higher cell numbers obtained after dynamic compared to static culturing also resulted in higher total glucose consumption and lactate formation by the tissue-engineered constructs. However, the glucose consumption and lactate formation per cell present in the constructs were lower after dynamic compared to static culturing, indicating that cell metabolism under dynamic conditions was more aerobic. In addition, actual glucose and lactate concentrations and pH and pCO_2 values in the flow chambers used for dynamic culturing are indicative of improved mass transport under dynamic compared to static conditions.

Introduction of a luminal monolayer of endothelial cells in the cultured scaffolds might result in constructs suitable for *in vivo* applications. However, for clinical applications, optimisation of the cell culture conditions is required to improve the elastin production by the seeded SMCs and shorten the time to produce a vascular graft using this procedure.

Introduction

No functional small-diameter synthetic vascular prostheses have been developed yet, in contrast to large-diameter vascular grafts (inner diameter > 6 mm) which are extensively used in vascular surgery and remain patent for more than 10 yrs after implantation [1-4]. Today research on the development of artificial small-diameter blood vessels has been directed to the

field of tissue engineering. Tissue engineering is a discipline that applies the principles of engineering and life sciences to the development of biological substitutes that restore, maintain or improve tissue functions [5]. Most vascular tissue engineering strategies aim at creating small-diameter blood vessel replacements closely mimicking the three-layered structure of a natural blood vessel. In this way, several requirements for successful implantation should be met. The graft should have sufficient strength not to burst with changes in blood pressure, an elastic vessel wall able to withstand cyclic mechanical loading, compliance matching with the adjacent host vessel, and a luminal lining that is anti-thrombotic [6]. Besides these requirements, tissue-engineered (TE) blood vessels, as viable structures, should represent a responsive and self-renewing tissue with the inherent potential of healing and remodelling according to the requirements of their specific environment [7].

Approaches to prepare a TE small-diameter blood vessel include the use of synthetic [6-10] or natural materials [11, 12] as scaffolds for autologous cell seeding. These scaffolds provide a temporary biomechanical structure until cells produce their own extracellular matrix (ECM) [5]. Short-comings of these strategies include insufficient mechanical properties, a lack of elastin deposition and long culture time periods. The development of bioreactors in which biological and/or biochemical processes develop under monitored and controlled environmental and operating conditions could further improve the potential of tissue engineering [13]. Several studies on culturing of vascular cells in tubular scaffolds in specific bioreactors demonstrate that an environment resembling *in vivo* conditions may promote both the development of TE constructs with sufficient mechanical strength to be implanted [7, 8, 14] and the modulation of appropriate cellular functions [12, 15]. Continuous mechanical loading has at least three different effects on smooth muscle cells (SMCs), i: acceleration of the orientation of SMCs, ii: acceleration of the production of collagen fibre bundles and iii: induction of the phenotypic modulation of SMCs from a synthetic to a contractile state [15]. However, the optimal bioreactor design and culture conditions for the development of a functional arterial graft remain to be elucidated [13, 16].

This paper describes the biological properties of human vascular SMCs seeded in tubular scaffolds composed of type I insoluble collagen and insoluble elastin and cultured in a pulsatile flow bioreactor [17]. Under these dynamic culture conditions a pulsatile volumetric flow rate of 9,6 mL/min (with 120 beats/min) in each vessel results in an average wall shear rate of 61 s^{-1}, comparable to that in the human carotid artery. Pressure waveforms with a mean pressure of 82-mmHg are also similar to arterial waveforms. In contrast values of average wall stress and wall shear stress are lower than *in vivo*. The relatively low trans-wall pressure

difference in this particular bioreactor and the presence of elastin fibres in the scaffolds, most probably prevented the scaffolds from bursting under cyclic mechanical stress [13, 17, 18]. Other studies use a silicon support in the lumen of the vessel to regulate the degree of deformation under these conditions [8, 19 14]. The lack of any support inside the tubular scaffolds in our system enables us to simulate wall shear rate and arterial pressure comparable to the conditions in the human carotid artery simultaneously, in contrast to other systems where those parameters are investigated separately [19-25]. The effects of the dynamic compared to static culture conditions on final cell numbers, distribution, proliferation, apoptosis and ECM production of the seeded SMCs inside the TE constructs were evaluated in time. During culturing, changes of the culture medium composition due to active cell metabolism and processes mentioned above were followed.

Materials

Dulbecco's Modified Eagle's Medium (DMEM) was purchased from Gibco BRL (Breda, The Netherlands). Penicillin, streptomycin, fetal bovine serum and trypsin/ethylene diamine tetra acetic acid (EDTA) were purchased from Biowhittaker (Verviers, Belgium). Gelatin type B from bovine skin, N-(3-dimetylaminopropyl)-N'-ethylcarbodiimide hydrochloride (EDC), N-hydroxysuccinimide (NHS), poly(propylene glycol)-bis-(2-aminopropyl ether) (Jeffamine 230, J230), proteinase K and DNAse-free RNAse were obtained from Sigma and Aldrich (St Louis, Missouri, USA). Mouse monoclonal antibodies (mAbs) against human α-smooth muscle actin (α-SMA) and human vimentin and fluorescein isothiocyanate-labelled rabbit anti mouse immunoglobulins (RAM-FITC) were purchased from DAKO (Glostrup, Denmark). Collagenase type 2 was purchased from Worthington Biochemical Corporation (Lakewood, N.J., USA). Human serum was acquired by overnight coagulation of blood (collected from healthy volunteers), subsequently pooled and stored at -80^{0}C. QIAmp RNA Blood Mini Kit was from QIAgen (Hilden, Germany). Dithiothreitol (DTT) and Moloney Murine Leukaemia Virus (M-MLV) reverse transcriptase enzyme were obtained from Invitrogen (Paisley, UK). dNTPs were from Amersham Pharmacia Biotech (Cambridge, UK). RNAse inhibitor was from Roche (Basel, Switzerland). Primer and probe sequences of cyclin E, tissue transglutaminase (tTG) and type I collagen (COL1A1) and TaqMan® Gene Expression Assays for glyceraldehyde-3-phosphate dehydrogenase (GAPDH) and elastin (ELN) were from Applied Biosystems (Nieuwerkerk A/D IJssel, The Netherlands). Insoluble collagen (type I from bovine achilles tendons) and insoluble elastin (from equine ligamentum nuchae),

purified as described in [26] were kindly donated by dr. T.H. van Kuppevelt, Department of Biochemistry, University Medical Centre Nijmegen, The Netherlands.

Methods

Isolation of SMCs

SMCs were isolated from human umbilical veins by a collagenase digestion method according to the method of Heimli *et al.* [27] with some minor modifications as previously described [28]. Cells were cultured on gelatin-coated (0.5% w/v) tissue culture polystyrene (g-TCPS) using DMEM containing 10% (v/v) heat-inactivated (30 min, 56^0C) pooled human serum, 10% (v/v) heat-inactivated (30 min, 56^0C) fetal bovine serum, 50 units/mL penicillin and 50 μg/mL streptomycin [27]. Culture medium was filtered (0.20 μm) before use. During culturing, medium was refreshed every 2-3 d. Cells were cultured in a humidified atmosphere containing 5% CO_2 inside an incubator at 37 ^{0}C (CleanAir Techniek bv, Woerden, The Netherlands) [29]. When sub-confluent cultures were obtained, cells were detached from the support with 0.125% (w/v) trypsin/0.05% (w/v) EDTA and subcultured for several passages (split ratio 1:3) [30]. Sub-confluent cultures of SMCs from passage 5 to 9 were used to seed tubular scaffolds for tissue engineering applications.

Identification of SMCs

SMCs were identified using mAbs against human α-SMA and human vimentin [27, 29]. Fluorescence of the secondary antibody RAM-FITC was examined with immuno fluorescent microscopy and with flow cytometry as described earlier [28]. Negative controls were obtained by omitting first antibodies and by staining human umbilical vein endothelial cells (HUVECs) and human dermal fibroblasts using the above mentioned antibodies.

Scaffold properties

Porous tubular scaffolds with an inner diameter of 3 mm, an outer diameter of approximately 6 mm and a length of 4 cm, were produced by freeze drying a suspension of type I insoluble collagen and insoluble elastin (1:1 w/w) at -18^0C as described by Buttafoco *et al* [18]. Scaffolds were optimised in terms of pore size and cross-link density [28]. To improve the mechanical properties, crosslinking of the scaffolds was performed either with a water-soluble carbodiimide in combination with a succinimide (EDC/NHS) or with a diamine (J230) in the presence of EDC/NHS [31, 32]. Non-crosslinked scaffolds, EDC/NHS crosslinked scaffolds and J230/EDC/NHS crosslinked scaffolds had a porosity of 95%, 94%, and 93% respectively and

an average pore size of 143 μm, 131 μm, and 151 μm respectively as determined by Micro Computed Tomography (Micro-CT) [18]. Human aortic SMCs in suspension at 37^0C have a length of 54.5 ± 1.5 μm and a diameter of 7.5 ± 0.3 μm [33]. The pores of all our scaffolds were interconnected and after crosslinking more than 80% of the pore volume was accessible for SMCs [18].

Seeding SMCs in tubular scaffolds

Tubular scaffolds were cannulated and tied on both ends with sutures (Ethicon Mersilene, Johnsson & Johnsson Intl., St. Stevens-Woluwe, Belgium) to thin-walled stainless–steel tubes having an outside diameter of 3 mm, which matches the inside diameter of the vessels at physiological pressure. Scaffolds were then mounted in custom-made glass flow chambers in which the outside and the inside of the scaffolds were in contact with fluid (figure 1).

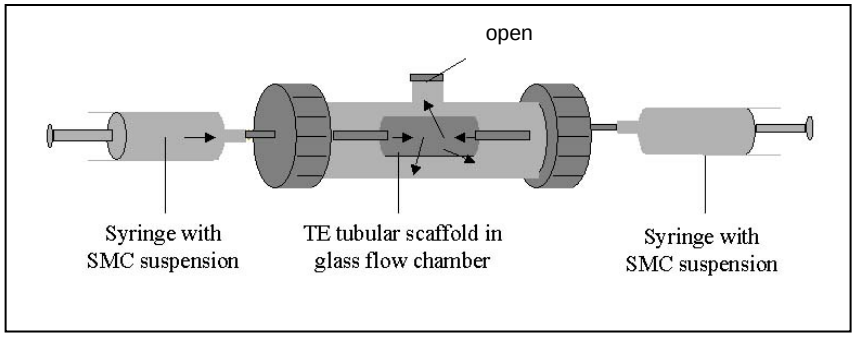

Figure 1: Schematic representation of the flow chamber and the procedure used for cell seeding. A TE tubular scaffold is mounted in a glass flow chamber. Two syringes were used to infuse an SMC suspension in the wall of the scaffold from both luminal sides as indicated by arrows.

After disinfection of the scaffolds with 70% ethanol for 10 min and rinsing (three times) with PBS, scaffolds were incubated overnight with (serum containing) culture medium to enhance cell attachment. SMCs from sub-confluent cultures were detached from their g-TCPS support with 0.125% (w/v) trypsin/0.05% (w/v) EDTA. Cell concentrations were determined with a hemacytometer (Bürker) and a suspension of 20-mL containing 10^7 SMCs were seeded into each scaffold by a filtration seeding procedure. The technique of filtration seeding promotes a more uniform cell distribution inside three-dimensional porous scaffolds compared to static seeding procedures [34-37]. Two syringes were used to infuse the cell suspension in the lumen from both ends of the scaffold simultaneously (figure 1). In this way cells were filtered through the porous wall of the scaffold. The flow chamber was totally filled with culture medium, the top opening was closed and the seeded scaffolds were placed in an incubator (37^0C and 5% CO_2) and rotated 90^0 along the longitudinal axis every 30-60 min for the first

2.5 h to promote homogeneous cell adhesion in the scaffolds. Subsequently, cells were allowed to adhere statically in the scaffolds for an additional period of 24 h.

Culturing SMCs under pulsatile flow conditions

After seeding, flow chambers containing cell-seeded scaffolds were mounted in a bioreactor in which pulsatile blood flow and arterial pressure can be varied (figure 2) [17]. In this system, a peristaltic roller-pump (Watson Marlow Sci-Q-323, Brussels, Belgium) was used to pump culture medium from a custom-made three-port glass fluid reservoir (60 mL) via highly distensible silicone rubber tubing (Watson Marlow, Brussels, Belgium, 3.2 mm ID x 6.4 mm OD) to four custom-made glass flow chambers in parallel position. In this way, a pulsatile flow of culture medium was obtained through the lumen of the cell-seeded tubular scaffolds. The scaffolds were surrounded by culture medium inside the flow chambers (figures 1 and 2). A pressure of 100-mm Hg was applied to the culture medium reservoir and regulated by means of an electronically controlled Venturi valve (T5200-50, Fairchild Company, Winston-Salem, NC, USA). The applied pressure was monitored by pressure sensors (Edwards Lifesciences LLC, Unterschleissheim, GmbH, Germany). Pressure signals were displayed by means of a pressure transducer (Instrumentation Department, Academic Medical Centre of Amsterdam, The Netherlands) and a scope meter (Fluke 199BM scopemeter, Adquipment Medical B.V., Hellevoetsluis, The Netherlands) throughout the duration of the experiment. Two valves (DATEX, Helsinki, Finland) preventing back flow of the culture medium, were inserted at the proximal and distal position of the chambers, in order to obtain a more accurate reproduction of the pressure wave-forms experienced by blood vessels *in vivo* during ventricular systole and diastole. The culture medium reservoir and the flow chambers containing the cell-seeded scaffolds were placed in humidified atmosphere inside an incubator (37^0C and 5% CO_2). By increasing the rotational speed of the roller pump, pressure pulses were gradually increased from 30 to 120 beats/min in 3 d of culturing. After 3 d, a volumetric flow rate of 10 mL/min in each vessel resulted in an average wall shear rate of 61 s^{-1} [17], which fits the lower range of shear rates found in the human carotid artery (60-775 s^{-1}) [38]. Pressure waveforms with a mean pressure of 82-mm Hg, a systolic pressure of 124-mm Hg and a diastolic pressure of 61 mm Hg, similar to the waveforms in the human carotid artery were established in the constructs. The average Reynolds number was 96 [17], which is indicative of laminar flow [39]. Laminar flow is necessary for efficient and homogeneous transfer of oxygen, nutrients and waste products to and from the three-dimensional construct [35, 40].

Cells seeded in tubular scaffolds were cultured under these dynamic conditions, or under

static conditions as control, for 1, 3, 7, or 14 d. In the static environment flow chambers containing cell-seeded scaffolds were placed inside an incubator (37^0C and 5% CO_2) but were not mounted in the bioreactor. Culture medium inside the flow chambers used for dynamic and static culturing as well as medium inside the culture medium reservoir in case of dynamic culturing were refreshed every 2 d. At the predetermined time periods, the TE constructs were disconnected from the bioreactor and characterised in terms of morphology and biological properties.

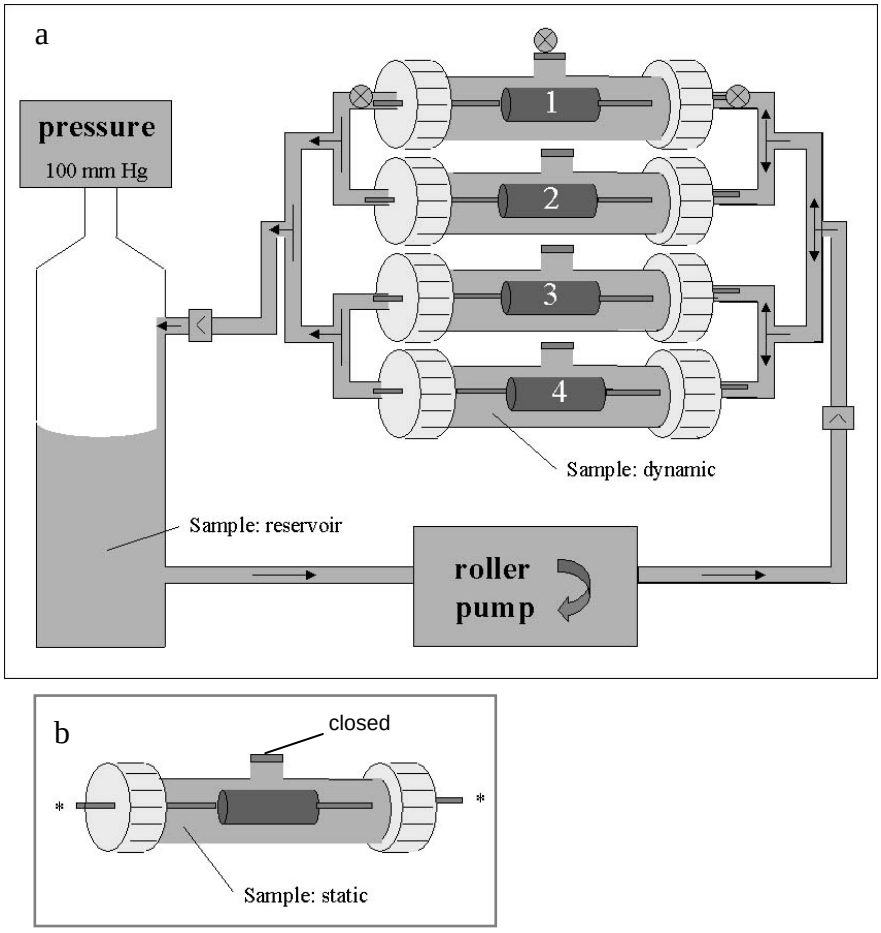

Figure 2: Schematic representation of dynamic culturing in the pulsatile flow bioreactor used in this study (a) compared to static culturing (b). For dynamic culturing, TE constructs were mounted in four parallel flow chambers filled with culture medium and mounted in the bioreactor (placed in a incubator, 37 ^{0}C and 5% CO_2). Culture medium was pumped with a roller pump from the reservoir through silicone rubber tubing and through the lumens of the constructs. A pressure of 100-mm Hg was applied to the culture medium reservoir. Arrows show the direction of the culture medium flow. Places of culture medium sampling for evaluation of the metabolic parameters are indicated and ⊗ represents a pressure sensor and ⌃ respresents a valve (a). For static culturing, TE constructs were mounted in flow chambers filled with culture medium and placed inside an incubator (37 ^{0}C and 5% CO_2) but were not mounted in the bioreactor. * indicates open mounting sides of the flow chambers during static culturing. Sampling point of culture medium for evaluation of metabolic parameters is presented (b).

Cell numbers

Numbers of SMCs present in the TE constructs were quantified by the CyQuant Cell Proliferation assay according to the manufacturer's instructions (Molecular Probes, Leiden, The Netherlands). Construct samples with a length of 7 mm were rinsed with PBS and digested with 200 μL proteinase K solution (1 mg/mL in PBS) for a minimum of 16 h at 56^0C. Samples were stored at -80^0C until analyses were performed. Various dilutions were prepared with cell-lysis buffer (Molecular Probes, Leiden, The Netherlands) supplemented with 180mM NaCl, 1 mM EDTA and 1.35 Kunitz units/mL DNAse-free RNAse. Samples were then incubated for 1 h at RT to remove the RNA and single stranded DNA. Finally, samples were mixed with CyQUANT® dye and after 2 min, fluorescence of the dye was measured in each well of 96 well plates using a Victor fluorescence analyser (PerkinElmer Life Sciences, Turku, Finland). Excitation and emission wavelengths were 480 and 520 nm respectively. The measured fluorescence intensities were correlated to the amount of SMCs using a calibration curve made by means of dilutions with known concentrations of SMCs from a sub-confluent culture on g-TCPS. Cells were detached from the support with 0.125% (w/v) trypsin/0.05% (w/v) EDTA, counted with a hemacytometer (Bürker) and then analysed in the same way as described above to obtain a calibration curve.

Histology

After culturing, 3-mm pieces of the TE constructs were rinsed with PBS and fixed with formalin (4% v/v) for at least 24h. Samples were then impregnated with paraffin, cut into transverse sections and stained by the hematoxylin and eosin procedure (HE) or by immuno staining of α-SMA according to standard procedures.

RNA isolation and cDNA synthesis

Messenger RNA (mRNA) gene transcripts of the SMCs present in the TE constructs after culturing were quantified by a semi-quantitative RT-PCR method on a real-time TaqMan analyser (7900 HT Sequence Detection System, Applied Biosystems, Nieuwerkerk A/D IJssel, The Netherlands) [41, 42]. Construct samples after 7 and 14 d of culturing with a length of 7 mm were rinsed with PBS and total RNA contents were harvested by disrupting the cell membranes with 600 μl of cell lysis buffer (Buffer RLT® of QIAgen, Hilden, Germany) containing 1% (v/v) β-mercaptoethanol using a mechanical homogeniser. Cell numbers in the scaffolds were first determined with the CyQuant Cell Proliferation assay after which RNA

was isolated from the same amount of cells either cultured under dynamic or static conditions. One volume of 70% ethanol was added to the lysates and total RNA was isolated from each sample using the QIAamp RNA Blood Mini columns and kit according to the manufacturer's instructions. A standard cDNA synthesis with Moloney Murine Leukaemia Virus (M-MLV) reverse transcriptase enzyme was performed as described by Volokhina *et al.* [43].

Real-time semi-quantitative PCR

mRNA expression levels were determined using the gene specific primer and probe sequences for cyclin E, tTG, type I collagen (COL1A1), and elastin (ELN). Fragments of the cyclin E sequence were amplified using the primer (300 nM) and probe (200 nM) set as described by Müller-Tidow *et al.* [44]. Fragments of the tTG sequence were amplified using the primer (900 nM) and probe (200 nM) set as described by Volokhina *et al.* [43]. Fragments of the COL1A1 sequence were amplified using the primer (300 nM) and probe (100 nM) set as described by Martin *et al.* [35, 45]. Fragments of the ELN sequence and GAPDH sequence were amplified using standard assays of Applied Biosystems (Nieuwerkerk A/D IJssel, The Netherlands). Primer and probe concentrations were optimised following the guidelines of the provider. mRNA expression levels of tTG, cyclin E, COL1A1 and ELN were normalised to mRNA expression levels of GAPDH [14, 45]. To investigate whether mRNA expression levels of GAPDH could be used to normalise mRNA expression levels of SMCs, the influence of culture conditions (static or dynamic) on the GAPDH mRNA expression of SMCs was analysed. After total RNA was isolated, the amount of RNA was determined by measuring the absorbance at 260 nm (A260) on a spectrophotometer. The purity of the isolated RNA was analysed by measuring the ratio of A260/A280 on a spectrophotometer. GAPDH mRNA expression levels of 1 μg of RNA were then analysed. mRNA expression levels of cells cultured under dynamic conditions for 7 and 14 d were compared to expression levels of cells cultured under static conditions for 7 d.

Metabolic parameters during culturing

To analyse the metabolic activity of the SMCs present in the TE constructs during culturing, several metabolic parameters of the culture medium were evaluated in time. Acidity (pH), partial oxygen (pO_2) and carbon dioxide pressures (pCO_2), and glucose and lactate concentrations of culture medium inside the flow chambers and inside the culture medium reservoir (figure 2) were measured every 48 h prior to culture medium refreshment. 3-mL samples of culture medium were measured within 15 min after sampling with a blood-gas

analyser (Radiometer, ABL 700 series, Copenhagen, Denmark). Measurements of freshly prepared culture medium were performed for determination of the baseline data at time point zero. Because culture medium was refreshed every 2 d, actual values of the glucose and lactate concentrations did not represent total glucose consumption and total lactate formation. Cumulative glucose consumption and lactate formation were calculated and plotted against time. In case of culturing under dynamic conditions, total glucose consumption and lactate formation per TE construct were calculated by taking the sum of the amount present in a flow chamber and a quarter of the amount present in the culture medium reservoir.

Statistical analyses

Data represent mean ± standard error of the mean (SEM) of two to four experiments performed in duplicate. Differences in cell numbers and relative mRNA expression levels between experimental groups were analysed using an unpaired two-tailed t-test. Differences within experimental groups at different culture time points were analysed using a paired two-tailed t-test. Results were considered significantly different at p values < 0.05.

Results

Culture conditions

SMCs isolated from human umbilical vein were successfully cultured and expanded on g-TCPS. No microscopic abnormalities or changes in α-SMA or vimentin expression were observed during the expansion time [28]. After 28 d of culturing, approximately $10*10^6$ cells were obtained, the amount required for seeding one scaffold of 4 cm length. About 36 d of cell culturing were necessary to obtain an appropriate amount of cells for the experiments described in this study. During dynamic culturing in the bioreactor, repeated observation of the cell-seeded scaffolds through the glass flow chamber walls showed a good stability of the scaffolds and no macroscopic evidence of a bacterial or fungal contamination during culture periods.

Influence of crosslinking and culture conditions on SMC growth

Compared with non-crosslinked collagen/elastin tubular scaffolds, crosslinking of the scaffolds with EDC/NHS did not significantly influence cell numbers present inside the scaffolds after 7 d of dynamic culturing. In contrast, crosslinking of the scaffolds with J230/EDC/NHS resulted in significantly lower cell numbers compared to non-crosslinked and EDC/NHS crosslinked scaffolds after 7 d of dynamic culturing (figure 3). In addition, in

EDC/NHS crosslinked scaffolds significantly higher cell numbers were found after 7 d of dynamic compared to static culturing. These data were confirmed by histology.

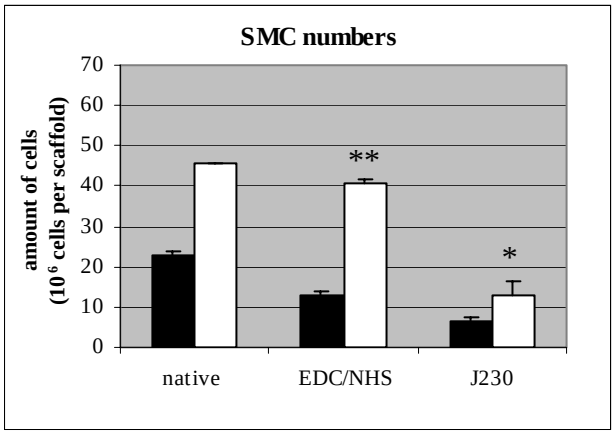

Figure 3: Amount of SMCs present in tubular scaffolds composed of collagen and elastin, not crosslinked (native) or either crosslinked with EDC/NHS or J230/EDC/NHS. Constructs were cultured for 7 d under static (closed bars) or dynamic conditions (open bars). Cell numbers were quantified by the CyQuant Cell Proliferation assay and the measured fluorescence intensities were correlated to the amount of SMCs using a calibration curve made of SMC dilutions of known concentration. Cell numbers of three experiments performed in duplicate (± SEM) are presented. * indicates a significant difference compared to native and EDC/NHS crosslinked scaffolds cultured under dynamic conditions ($p < 0.05$). ** indicates a significant difference compared to EDC/NHS crosslinked scaffolds cultured under static conditions ($p < 0.05$).

SMC proliferation and cell distribution

A significant increase of the amount of SMCs present in tubular EDC/NHS crosslinked scaffolds was found after 7 and 14 d of dynamic culturing, compared to day 1 and 3 (figure 4). In addition, significantly higher cell numbers were found after 7 and 14 d of dynamic compared to static culturing. The same trends were observed by histology (figure 5). A difference in cell distribution in the scaffolds was observed after 7 and 14 d of culturing under dynamic compared to static conditions. Under dynamic conditions, cells grew inside and on the "adventitial" side of the tubular scaffolds. In contrast, under static conditions, cell growth was observed predominantly on the "adventitial" side of the scaffolds. Immuno histochemistry of the construct sections showed that cells present in and on the scaffolds were positively stained for the presence of α-SMA after dynamic and static culturing (figure 6).

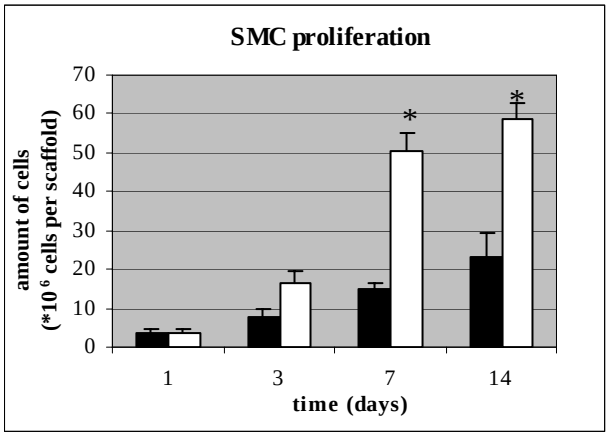

Figure 4: Amount of SMCs present in tubular scaffolds composed of collagen and elastin crosslinked with EDC/NHS after 1, 3, 7, and 14 d of culturing under static (closed bars) or dynamic conditions (open bars). Cell numbers were quantified by the CyQuant Cell Proliferation assay and the measured fluorescence intensities were correlated to the amount of SMCs using a calibration curve made with known numbers of SMCs. Cell numbers of three experiments performed in duplicate (± SEM) are presented. * indicates a significant difference compared to 1 and 3 d of culturing under dynamic conditions and compared to 7 or 14 d of culturing under static conditions ($p < 0.05$).

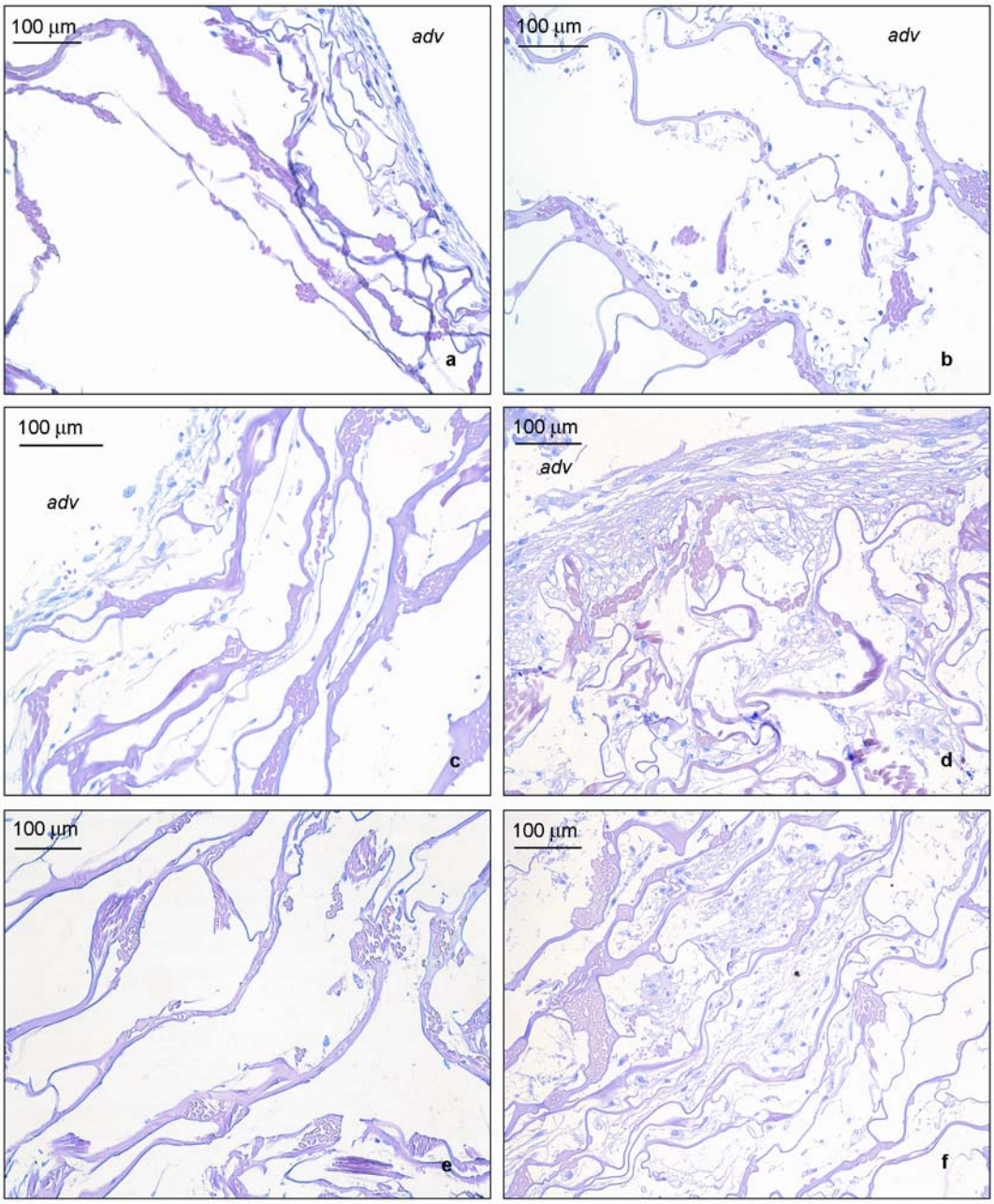

Figure 5: Histology of SMCs present in tubular scaffolds composed of collagen and elastin crosslinked with EDC/NHS after 7 d (a, b) or 14 d (c-f) of culturing under static (a, c, e) or dynamic conditions (b, d, f). Transverse sections of the cell containing constructs showing the inner and "adventitial" (adv) side (a-d) or only the inner side (e, f) were stained by the standard haematoxylin and eosin (HE) procedure. Scale bars are inserted in the pictures.

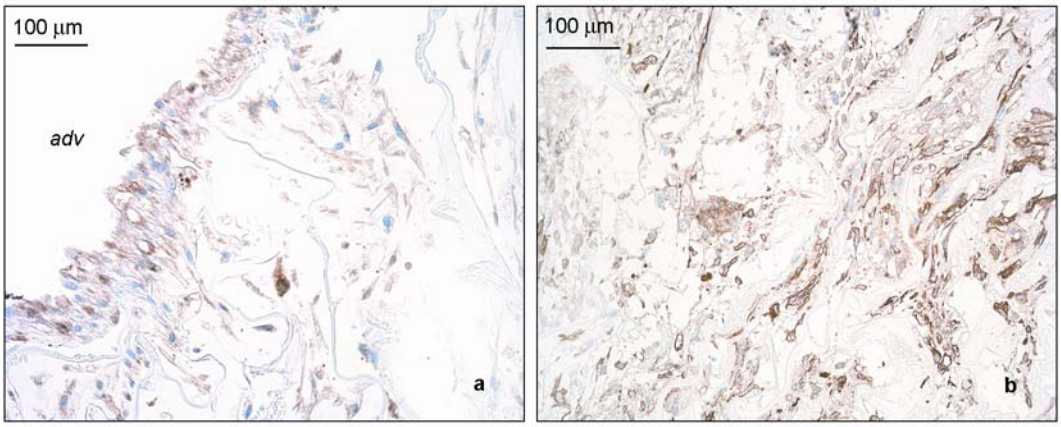

Figure 6: Immuno histochemistry of α-SMA of SMCs present in tubular scaffolds composed of collagen and elastin crosslinked with EDC/NHS after 14 d of culturing under static (a) or dynamic conditions (b). Transverse sections of the cell containing constructs showing the inner and "adventitial" (adv) side (a) or only the inner side (b) were stained for α-SMA. Scale bars are inserted in the pictures.

TaqMan based RT-PCR

As determined by spectrophotometry, at least 35 µg total RNA was isolated from each sample of the TE constructs after 7 and 14 d of culturing under static or dynamic conditions. After 1 and 3 d of culturing, not enough RNA could be isolated for reliable analyses of the mRNA expression levels. Ratios of A260/A280 were in between 1.7 and 1.9 indicating pure RNA. Compared to static culture conditions, GAPDH mRNA expression in SMCs was not influenced by culturing under dynamic conditions. This allowed us to use GAPDH mRNA expression levels for quantification of cyclin E, tTG, COL1A1 and ELN mRNA expression levels.

SMC proliferation and apoptosis

Significantly higher cyclin E mRNA expression levels of SMCs were measured after 7 d of culturing in tubular EDC/NHS crosslinked scaffolds under dynamic compared to static conditions (figure 7a). After 14 d of culturing no significant difference in cyclin E mRNA expression was measured under dynamic compared to static conditions. In addition, no increase of cyclin E mRNA expression in time was found during dynamic culturing. No significant differences of tTG mRNA expression levels after 7 and 14 d of culturing were found under dynamic compared to static conditions (figure 7b). Also no significant difference in time of tTG mRNA expression was found during dynamic or static culturing.

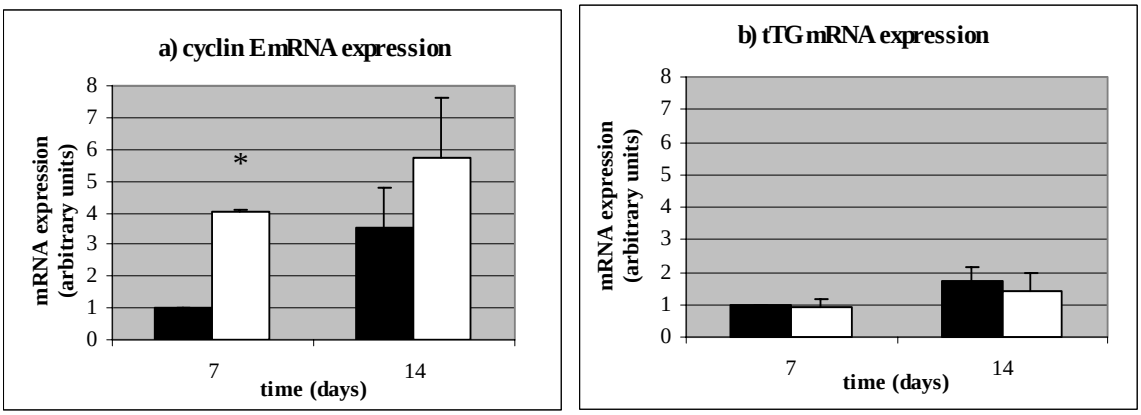

Figure 7: Proliferation (cyclin E mRNA expression, a) and apoptosis (tTG mRNA expression, b) of SMCs present in tubular scaffolds composed of collagen and elastin crosslinked with EDC/NHS after 7 and 14 d of culturing under static (closed bars) or dynamic conditions (open bars). mRNA expression levels of cyclin E and tTG were quantified by real-time RT-PCR analyses and normalised against GAPDH mRNA expression levels. mRNA expression levels of cells cultured for 7 d under static conditions were arbitrarily set at 1 unit. Relative mRNA expression levels were determined from three experiments performed in duplicate (± SEM).
* indicates a significant difference compared to 7 d of static culturing ($p < 0.05$).

ECM production

Collagen mRNA expression levels of SMCs in tubular EDC/NHS crosslinked scaffolds were significantly higher after 14 d of culturing under dynamic compared to static conditions. Moreover, expression levels were significantly higher after 14 d of dynamic culturing compared to 7 d of static and dynamic culturing (figure 8). Elastin mRNA expression levels of SMCs in tubular EDC/NHS crosslinked scaffolds were detected, however, levels were too low for quantitative analyses.

Metabolic parameters during culture

Figures 9 and 10 show the changes of the metabolic parameters of culture medium as function of culturing time in the flow chambers during dynamic and static culturing and in the culture medium reservoir in case of dynamic culturing (see figure 2 for sampling points of culture media). During the first 6 d of culturing, pH values of culture medium were significantly higher in the reservoir compared to the flow chambers used for dynamic and static culturing. In addition, during this time period, pH values of culture medium were significantly higher in the flow chambers used for dynamic compared to static culturing (figure 9a). pO_2 of culture medium in the flow chambers used for dynamic and static culturing as well as in the reservoir did not significantly change (figure 9b). During the first 6 d of culturing, pCO_2 of culture

medium was significantly higher in the flow chambers used for dynamic and static culturing compared to the reservoir. During this time period, pCO_2 of culture medium was significantly lower in the flow chambers used for dynamic compared to static culturing (figure 9c). The same trends of the changes of pH, pO_2 and pCO_2 as function of culturing time as described above were measured after 8 to 14 d of culturing, however no significant differences can be shown because data represent a single measurement.

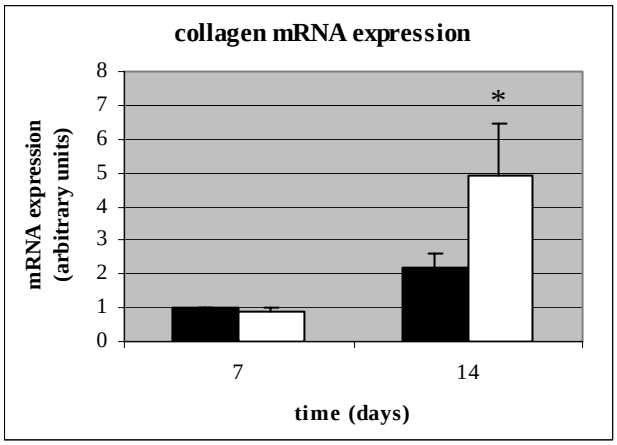

Figure 8: Collagen mRNA expression levels of SMCs present in tubular scaffolds composed of collagen and elastin crosslinked with EDC/NHS after 7 and 14 d of culturing under static (closed bars) or dynamic conditions (open bars). Type I collagen mRNA expression levels were quantified by real-time RT-PCR analyses and normalised against GAPDH mRNA expression levels. mRNA expression levels of cells cultured for 7 d under static conditions were arbitrarily set at 1 unit. Relative mRNA expression levels were determined from three experiments performed in duplicate (± SEM). * indicates a significant difference compared to 7 d of static and dynamic culturing and 14 d of static culturing ($p < 0.05$).

After 6 d of culturing, actual glucose concentrations in the culture medium were significantly lower in the flow chambers used for dynamic and static culturing compared to the reservoir. The same trends of the changes of the actual glucose concentrations as function of culturing time were measured after 8 to 14 d of culturing, however no significant differences can be shown because data represent a single measurement. In addition, after 4 and 6 d of culturing, the actual glucose concentrations in culture medium were significantly higher in the flow chambers used for dynamic compared to static culturing (figure 10a). After 2 and 4 d of culturing, actual lactate concentrations in culture medium were significantly higher in the flow chambers used for dynamic and static culturing compared to the reservoir. After 4 and 6 d of culturing, lactate concentrations in culture medium were significantly lower in the flow chambers used for dynamic compared to static culturing (figure 10b). The same trends of the changes of the actual lactate concentrations as function of culturing time as described above

were measured after 8 to 14 d of culturing, however no significant differences can be shown because data represent a single measurement.

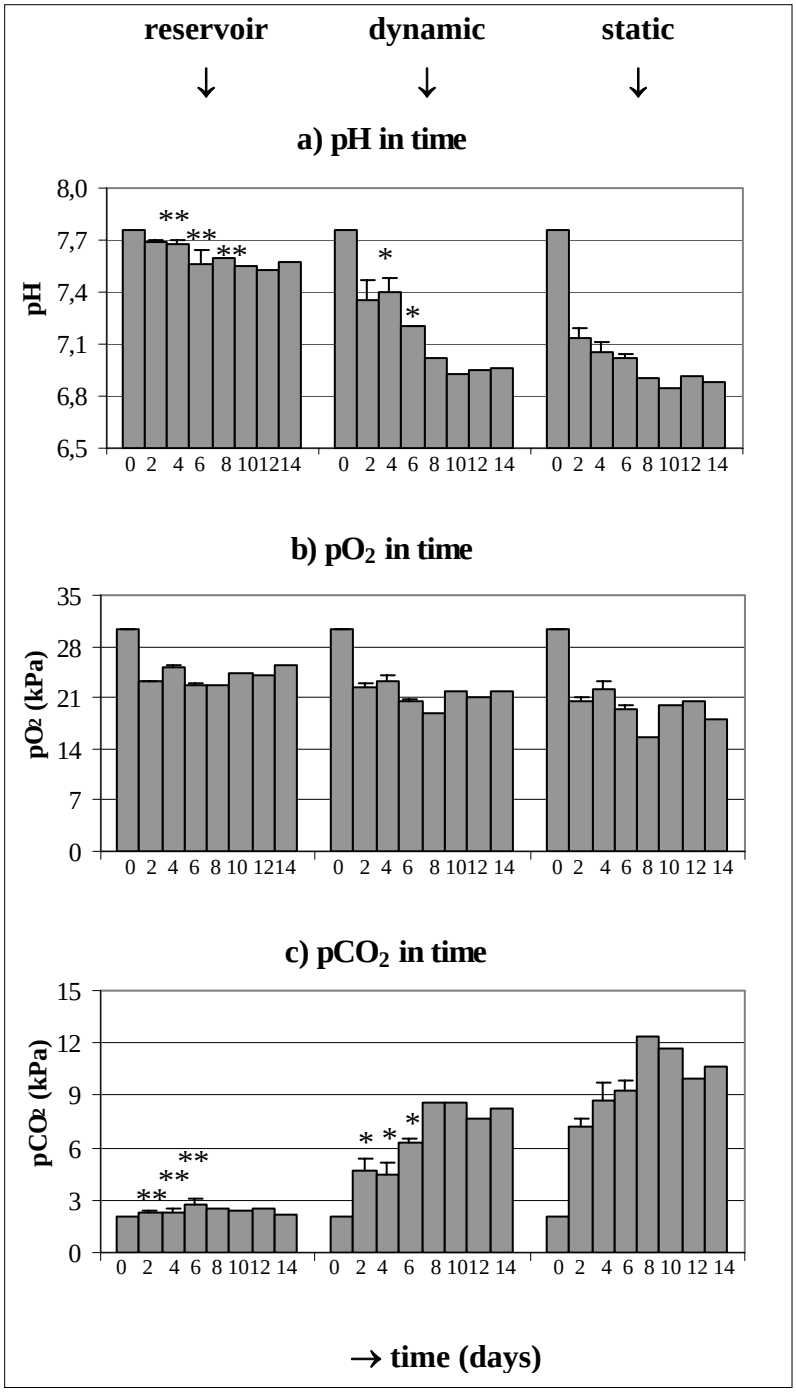

Figure 9: pH (a), pO_2 (b) and pCO_2 (c) of culture medium in the reservoir and the flow chambers used for dynamic and static culturing plotted against time. The parameters were measured every 48 h prior to culture medium refreshment. Measurements of freshly prepared culture medium were performed for evaluation of the baseline data at time point zero. Data represent four measurements (± SEM) during the first 6 d and a single measurement for days 8 to 14. * indicates a significant difference compared to flow chambers used for static culturing. ** indicates a significant difference compared to flow chambers used for dynamic and static culturing.

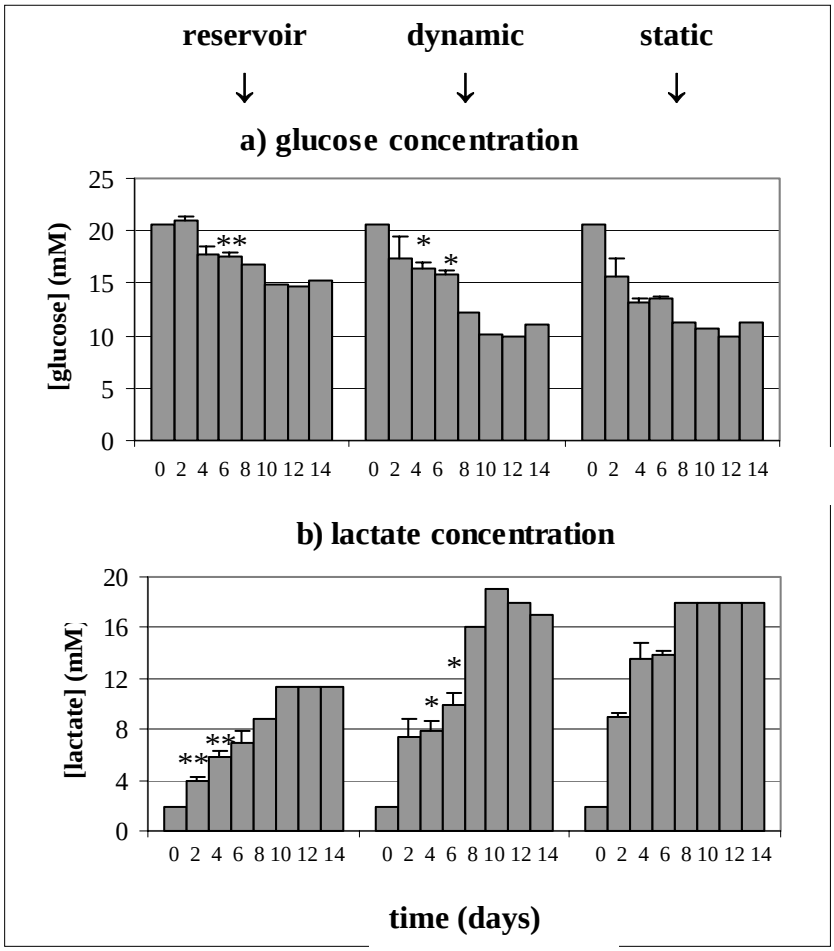

Figure 10: Actual glucose (a) and lactate (b) concentrations of culture medium in the reservoir and the flow chambers used for dynamic and static culturing plotted against time. The parameters were measured every 48 h prior to culture medium refreshment. Measurements of freshly prepared culture medium were performed for evaluation of the baseline data at time point zero. Data represent four measurements (± SEM) during the first 6 d and a single measurement for days 8 to 14. * indicates a significant difference compared to flow chambers used for static culturing. ** indicates a significant difference compared to flow chambers used for dynamic and static culturing.

Figure 11 shows the total cumulative glucose consumption and lactate formation by the cells during dynamic compared to static culturing. Till 6 d of culturing, total cumulative glucose consumption and lactate formation were not significantly different under dynamic compared to static conditions. In contrast, after 14 d, both total cumulative glucose consumption and lactate formation were higher in case of dynamic compared to static culturing.

Assuming that the amount of cells present in the TE constructs did not change between 12 and 14 d of dynamic and static culturing, the glucose consumption and lactate formation in this time interval expressed per cell can be calculated. In this way, 5 and 8 pmol/cell of glucose consumption and 8 and 14 pmol/cell of lactate formation under dynamic and static conditions

were found respectively. In contrast to the total cumulative glucose consumption and lactate formation, the glucose consumption and lactate formation per cell after 12 to 14 d of culturing were higher under static compared to dynamic conditions.

For O_2 and CO_2 no total cumulative consumption and formation can be determined because both O_2 and CO_2 can diffuse through the silicone rubber tubing of the bioreactor and both are delivered by input of compressed air to the reservoir during dynamic culturing. During static culturing, both O_2 and CO_2 can diffuse through the open mounting sides of the flow chambers.

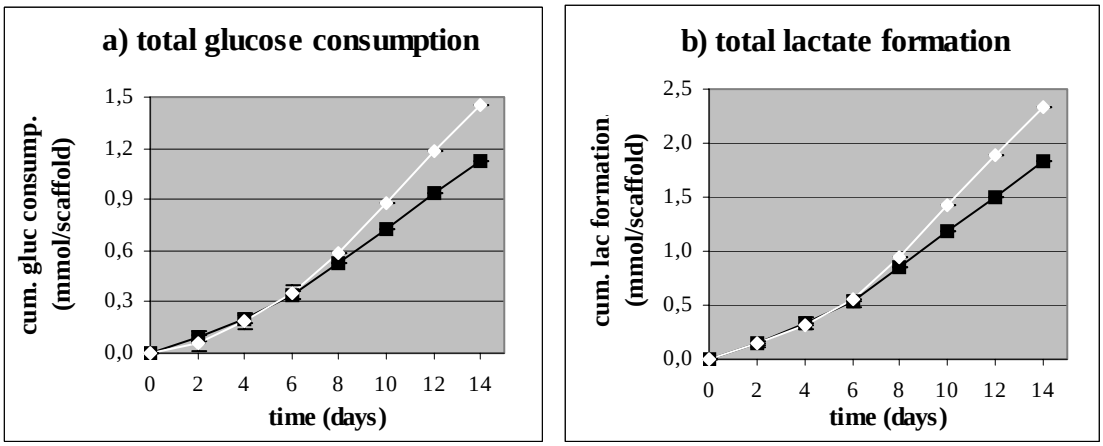

Figure 11: Cumulative (cum) glucose consumption (a) and lactate formation (b) in case of dynamic (white line) and static (black line) culturing plotted against time. Actual values of the parameters were measured every 48 h prior to culture medium refreshment. Measurements of freshly prepared culture medium were performed for evaluation of the baseline data at time point zero. To calculate the total glucose consumption and total lactate formation per TE construct in case of the dynamic conditions, the sum of the amounts present in a flow chamber and a quarter of the amounts present in the reservoir were taken. Data represent four measurements (± SEM) during the first 6 d and a single measurement for days 8 to 14.

Discussion

It was shown that culturing of SMCs in porous tubular scaffolds composed of insoluble type I collagen and insoluble elastin under dynamic conditions results in enhanced tissue formation compared to static conditions. A pure SMC culture of mesenchymal origin [28, 29] was used in this study. SMCs were seeded in the scaffolds by filtration (figure 1) and cultured in a bioreactor in which physiological conditions in terms of wall shear rate, pulsatile flow and arterial pressure were reproduced (figure 2) [17]. The composition of the scaffolds in which cells were seeded influenced the cell numbers present in the TE constructs after 7 d of culturing. Crosslinking of the tubular scaffolds with EDC/NHS did not influence the amount of cells whereas crosslinking of the scaffolds with J230/EDC/NHS had a detrimental effect on the

amount of cells present inside the scaffolds (figure 3). J230 functions as a spacer incorporated into the scaffolds. The chemical nature of J230 or the presence of dangling amine groups as a consequence of crosslinking with J230/EDC/NHS may have altered the ability of SMCs to adhere, proliferate and migrate in these scaffolds [46]. The presence of J230 may contribute to an increased hydrophilic character of the scaffolds, which decreases protein adsorption and cell adhesion and increases levels of apoptosis of adherent cells [47]. In addition to the evaluation of the biological properties of the TE constructs, their mechanical properties were evaluated in our laboratories [18]. From these results, it was concluded that crosslinked scaffolds have a better ability to withstand load compared to non-crosslinked scaffolds. Considering both the biological and mechanical properties of the TE constructs, EDC/NHS crosslinked scaffolds were selected for further studies.

Culturing of SMCs under dynamic conditions in the porous tubular scaffolds for at least 7 d resulted in a more homogeneous distribution of SMCs over the scaffolds compared to static culture conditions. After 14 d of dynamic culturing, porous tubular scaffolds entirely occupied with cells were obtained whereas after 14 d of static culturing, SMCs were predominantly present on the outer ("adventitial") side of the constructs (figure 5). According to the presence of α-SMA fibres in the cells cultured under both dynamic and static conditions (figure 6), no fundamental differentiation or dedifferentiation processes took place during culturing [29, 48]. By means of histology and scanning electron microscopy we were not able to show that SMCs orient in a circumferential way mimicking the *in vivo* situation. However, the question remains whether this orientation is strictly necessary to obtain a functional construct. One can speculate that after implantation, cells present in the graft will mature and orient according to the need of the specific tissue.

Cell proliferation in our TE constructs cultured under dynamic conditions was verified by showing a significant increase of cell numbers in time (figure 4), by histology (figure 5), and by an enhanced cyclin E mRNA expression level of the cells after 7 d of dynamic compared to static culturing (figure 7). After 14 d of culturing under dynamic conditions, both cyclin E mRNA expression levels and cell numbers were not significantly increased compared to 7 d of culturing. In contrast to mRNA expression levels of cyclin E, tTG mRNA expression levels were not influenced by the culture conditions, indicating that the higher cell numbers in the TE scaffolds cultured under dynamic conditions cannot be explained by decreased apoptosis but only by increased cell proliferation. The question remains whether apoptosis has occurred during the first 6 d of culturing because it was not possible to measure tTG mRNA expression during this time period due to low cell numbers. After 7 d of culturing, cell fragments or

apoptotic bodies possibly formed due to apoptosis during the first days could have been lost during RNA isolation.

A significant increase of the collagen mRNA expression level of SMCs cultured under dynamic compared to static conditions was measured and expression levels were significantly higher after 14 compared to 7 d of dynamic culturing (figure 8). In addition, after 14 d of dynamic and static culturing, TE constructs with increased high strain stiffness compared to values after 7 d of culturing were obtained, confirming the production of collagen [18]. We also measured elastin mRNA expression levels of the SMCs cultured under static or dynamic conditions. However levels were too low for quantitative analyses. One can speculate that the newly synthesised cellular matrix present in the constructs and the dynamic culture conditions provide appropriate signals to the vascular cells for stimulation of elastin production. Longer culture time periods, culture medium supplements or co-culturing various vascular cell types in the present model are approaches that can be tested to improve the elastin production [19, 49].

The consumption of O_2 and glucose and the formation of CO_2 and lactate in culture medium is an indication of active cell metabolism. Under aerobic conditions, CO_2 and water is formed out of glucose and O_2, whereas under anaerobic conditions, lactate is formed. Total glucose consumption and lactate formation were not significantly different between dynamic and static culture conditions during the first 8 d of culturing (figure 11). However, during this time period the actual pH and glucose concentrations were significantly higher whereas the actual pCO_2 and lactate concentrations were significantly lower inside the flow chambers used for dynamic compared to static culturing (figures 9 and 10). This is indicative of mass transport between the culture media in the reservoir and the flow chambers. After 14 d of dynamic culturing, total glucose consumption and lactate formation were higher than under static conditions. This was related to the higher cell numbers present under dynamic conditions. Again the actual glucose and lactate concentrations, pH and especially the lower pCO_2 values in the flow chambers used for dynamic culturing during day 10-14, are indicative of improved mass transport under dynamic compared to static conditions. This is in agreement with other studies showing that dynamic culture conditions may contribute to reduction of external mass-transfer limitations [35].

Under static conditions, significantly higher glucose consumption and lactate formation per cell present in the TE constructs were found compared to dynamic conditions. The lower lactate formation per cell under dynamic culture conditions suggests that cell metabolism was more aerobic compared to static conditions. In addition, the higher glucose consumption per

cell under static compared to dynamic culture conditions shows the lower efficiency of anaerobic compared to aerobic cell metabolism.

For clinical applications, the culture period needed for graft production should be as short as possible [19]. In our laboratory, 28 d of SMC expansion *in vitro* after isolation from a human umbilical vein were necessary to obtain enough cells to seed one scaffold of 4 cm length [10, 19]. Subsequently, 14 d of culturing were necessary to obtain vessels with a uniform distribution of SMCs and appropriate mechanical properties. Introduction of a luminal monolayer of endothelial cells might result in TE constructs suitable for *in vivo* applications. Appropriate endothelial cell adhesion and resistance to shear stress can be achieved in a cell-seeded tubular scaffold as described by Gulbins *et al*. [50]. This can be done within 7 d of culturing [8, 19, 50]. All together, we would need 49 d (7 wks) to produce a vascular graft of 4 cm length. This production time will even be longer when longer blood vessels are needed for specific vascular reconstructions (i.e. ~15 cm for coronary bypass and 15 cm to more than 30 cm for peripheral reconstructions) [19]. Cell sources, culture medium components, cell seeding efficiency, cell-culture conditions, and bioreactor design are all elements that should be optimised to decrease culture and maturation periods

Conclusion

Culturing of SMCs in porous tubular scaffolds of insoluble type I collagen and insoluble elastin under dynamic conditions simulating conditions of the human carotid artery in terms of wall shear rate, pulsatile flow and arterial pressure, stimulates tissue formation. Higher SMC numbers, a more homogeneous distribution of SMCs over the scaffolds and a higher collagen mRNA expression were found when cells were cultured under dynamic compared to static conditions. Dynamic culturing of SMCs in porous tubular scaffolds crosslinked with a carbodiimide in combination with a succinimide (EDC/NHS) resulted in TE constructs with appropriate mechanical strength [18] and a homogeneous distribution of SMCs. This was attributed to a higher collagen mRNA expression level and enhanced cell proliferation during dynamic compared to static culturing. Under dynamic culture conditions, mass transport of nutrients and waste products to and from the cells present in the TE constructs was improved and cell metabolism was more aerobic compared to static conditions. Introduction of a luminal monolayer of endothelial cells in the cultured scaffolds might result in constructs suitable for *in vivo* applications. However, for clinical applications, optimisation of the cell culture conditions is required to decrease the time to produce a vascular graft using this procedure.

Acknowledgements

H. Jahr and G.J.V.M.van Osch (Erasmus University, Medical Center, Department of Orthopaedics, Rotterdam, The Netherlands) are kindly acknowledged for providing collagen primer and probe sequences for real-time TaqMan® based RT-PCR. W. Daamen and Dr. A. van Kuppevelt (University Medical Center Nijmegen, The Netherlands) are kindly acknowledged for the donation of collagen and elastin. R. Rieksen, medical photographer of the Laboratory of Pathology Oost Nederland (Enschede, The Netherlands) is kindly acknowledged for making histology pictures.

References

1. Zdrahala, R.J. Small caliber vascular grafts. Part I: state of the art. J.Biomater.Appl. 1996; 10: 309-329.
2. Bos, G.W., Poot, A.A., Beugeling, T., van Aken, W.G., and Feijen, J. Small-diameter vascular graft prostheses: current status. Arch.Physiol Biochem. 1998; 106: 100-115.
3. Faries, P.L., LoGerfo, F.W., Arora, S., Hook, S., Pulling, M.C., Akbari, C.M., Campbell, D.M., and Pomposelli, Jr.R.G. A comparative study of alternative conduits for lower extremity revascularization: all-autologous conduit versus prosthetic grafts. J.Vasc.Surg 2000; 32: 1080-1090.
4. Seifalian, A.M., Salacinski, H.J., Tiwari, J., Edwards, A., Bowald, S., and Hamilton, G. *In vivo* biostability of a poly(carbonate-urea)urethane graft. Biomaterials 2003; 24: 2549-2557.
5. Langer, R. and Vacanti, J.P. Tissue Engineering. Science 1993; 260: 920-926.
6. Ratcliff, A. Tissue engineering of vascular grafts. Matrix Biol. 2000; 19: 353-357.
7. Hoerstrup, S.P., Zund, G., Sodian, R., Schnell, A.M., Grunenfelder, J., and Turina, M.I. Tissue engineering of small caliber vascular grafts. Eur.J.Cardiothorac.Surg. 2001; 20: 164-169.
8. Niklason, L.E., Gao, J., Abbott, W.M., Hirschi, K.K., Houser, S., Marini, R., and Langer, R. Functional arteries grown *in vitro*. Science 1999; 284: 489-493.
9. Shum-Tim, D., Stock, U., Hrkach, J., Shinoka, T., Lien, J., Moses, M.A., Stamp, A., Taylor, G., Moran, A.M., Landis, W., Langer, R., Vacanti, J.P., and Mayer, J.E., Jr. Tissue engineering of autologous aorta using a new biodegradable polymer. Ann.Thorac.Surg. 1999; 68: 2298-2304.
10. Shinoka, T., Imai, Y., and Ikada, Y. Transplantation of a tissue-engineered pulmonary artery. N.Engl.J.Med. 2001; 344: 532-533.
11. Weinberg, C.B. and Bell, E. A blood vessel model constructed from collagen and cultured vascular cells. Science 1986; 231: 397-400.
12. Seliktar, D., Black, R.A., Vito, R.P., and Nerem, R.M. Dynamic mechanical conditioning of collagen-gel blood vessel constructs induces remodeling *in vitro*. Ann.Biomed.Eng. 2000; 28: 351-362.
13. Mitchell, S.L. and Niklason, L.E. Requirements for growing tissue-engineered vascular grafts. Cardiovasc.Pathol. 2003; 12: 59-64.
14. Seliktar, D., Nerem, R.M., and Galis, Z.S. Mechanical strain-stimulated remodeling of tissue-engineered blood vessel constructs. Tissue Eng. 2003; 9: 657-666.
15. Hirai, J. and Matsuda, T. Self-organized, tubular hybrid vascular tissue composed of vascular cells and collagen for low-pressure-loaded venous system. Cell Transplant. 1995; 4: 597-608.
16. Zandonella, C. Tissue engineering: the beat goes on. Nature 2003; 421: 884-886.

17. Buttafoco, L., Engbers-Buijtenhuijs, P., Poot, A.A., Dijkstra, P.J., Vermes, I., and Feijen, J. Development of a bioreactor for tissue engineering of small-diameter blood vessels: Design of a pulsatile flow system. this thesis, University of Twente, chapter 8 2005;
18. Buttafoco, L., Engbers-Buijtenhuijs, P., Poot, A.A., Dijkstra, P.J., Vermes, I., and Feijen, J. Dynamic vs. static smooth muscle cell culture in tubular collagen/elastin matrices for vascular tissue engineering. thesis of L.Buttafoco, University of Twente, chapter 7 2005;
19. L'Heureux, N., Paquet, S., Labbe, R., Germain, L., and Auger, F.A. A completely biological tissue-engineered human blood vessel. FASEB J. 1998; 12: 47-56.
20. Kanda, K. and Matsuda, T. Mechanical stress-induced orientation and ultrastructural change of smooth muscle cells cultured in three-dimensional collagen latices. Cell Transplant. 1994; 3: 481-492.
21. Papadaki, M. and Eskin, S.G. Effects of fluid shear stress on gene regulation of vascular cells. Biotechnol.Prog. 1997; 13: 209-221.
22. Watase, M., Awolesi, M.A., Ricotta, J., and Sumpio, B.E. Effect of pressure on cultured smooth muscle cells. Life Sci. 1997; 61: 987-996.
23. Liu, S.Q. and Goldman, J. Role of blood shear stress in the regulation of vascular smooth muscle cell migration. Trans.Biomed.Eng. 2001; 48: 474-483.
24. Lee, A.A., Graham, D.A., Dela, C.S., Ratcliffe, A., and Karlon, W.J. Fluid shear stress-induced alignment of cultured vascular smooth muscle cells. J.Biomech.Eng. 2002; 124: 37-43.
25. Solan, A., Mitchell, S., Moses, M., and Niklason, L. Effect of pulse rate on collagen deposition in the tissue-engineered blood vessel. Tissue Eng. 2003; 9: 579-586.
26. Daamen, W., Veerkamp, J.H., and van Kuppevelt, T.H. Purification of elastin and preparation of matrices for tissue engineering. Indust.Protein 2001; 9: 15-17.
27. Heimli, H., Kahler, H., Endresen, M.J., Henriksen, T., and Lyberg, T. A new method for isolation of smooth muscle cells from human umbilical cord arteries. Scand.J.Clin.Lab Invest. 1997; 57: 21-29.
28. Buijtenhuijs, P., Buttafoco, L., Poot, A.A., Daamen, W.F., van Kuppevelt, T.H., Dijkstra, P.J., de Vos, R.A.I., Sterk, L.M.Th., Geelkerken, R.H., Feijen, J., and Vermes, I. Tissue engineering of blood vessels: Characterisation of smooth muscle cells for culturing on collagen and elastin based scaffolds. Biotechnol.Appl.Biochem. 2003; 39: 141-149.
29. Chamley-Campbell, J., Campbell, G.R., and Ross, R. The smooth muscle cell in culture. Physiol.Rev. 1979; 59: 1-61.
30. Lefebvre, P., Nusgens, B.V., and Lapiere, C.M. Cultured myofibroblasts display a specific phenotype that differentiates them from fibroblasts and smooth muscle cells. Dermatology 1994; 189: 65-67.
31. Pieper, J.S., Oosterhof, A., Dijkstra, P.J., Veerkamp, J.H., and van Kuppevelt, T.H. Preparation and characterization of porous crosslinked collagenous matrices containing bioavailable chondroitin sulphate. Biomaterials 1999; 20: 847-858.
32. Olde Damink, L.H.H., Dijkstra, P.J., van Luyn, M.J.A., van Wachem, P.B., Nieuwenhuis, P., and Feijen, J. Cross-linking of dermal sheep collagen using a water-soluble carbodiimide. Biomaterials 1996; 17: 765-773.
33. Yannas, I.V. Tissue regeneration templates based on collagen-glycosaminoglycan copolymers. Adv.Pol.Sci. 1995; 122: 219-244.
34. Li, Y., Ma, T., Kniss, D.A., Lasky, L.C., and Yang, S. Effects of filtration seeding on cell density, spatial distribution, and proliferation in nonwoven fibrous matrices. Biotechnol.Prog. 2001; 17: 935-944.
35. Martin, I., Wendt, D., and Heberer, M. The role of bioreactors in tissue engineering. Trends Biotechnol. 2004; 22: 80-86.

36. van Wachem, P.B., Stronck, J.W.S., Koers-Zuideveld, R., Dijk, F., and Wildevuur, C.R.H. Vacuum cell seeding: a new method for the fast application of an evenly distributed cell layer on porous vascular grafts. Biomaterials 1990; 11: 6021-606.
37. Engbers-Buijtenhuijs, P., Buttafoco, L., Poot, A.A., de Vos, R.A.I., Sterk, L.M.T., Geelkerken, R.H., Feijen, J., and Vermes, I. Effects of filtration seeding of smooth muscle cells in three-dimensional porous scaffolds on cell spatial distribution for tissue engineering of blood vessels. This thesis, University of Twente, chapter 4 2005;
38. Stokholm, R., Oyre, S., Ringgaard, S., Flaagoy, H., Paaske, W.P., and Pedersen, E.M. Determination of wall shear rate in the human carotid artery by magnetic resonance techniques. Eur.J.Vasc.Endovasc.Surg. 2000; 20: 427-433.
39. Foust, A.S., Wenzel, L.A., Clump.C.W., Maus, L., and Andersen, L.B. Principles of unit operations. New York: Wiley 1980; 2nd ed. vol. 1:
40. Carrier, R.L., Papadaki, M., Rupnick, M., Schoen, F.J., Bursac, N., Langer, R., Freed, L.E., and Vunjak-Novakovic, G. Cardiac tissue engineering: cell seeding, cultivation parameters, and tissue construct characterization. Biotech.Bioeng. 1999; 64: 580-589.
41. Heid, C.A., Stevens, J., Livak, K.J., and Williams, P.M. Real time quantitative PCR. Genome Res. 1996; 6: 986-994.
42. Engbers-Buijtenhuijs, P., Buttafoco, L., Poot, A.A., Geelkerken, R.H., Feijen, J., and Vermes, I. Analysis of the balance between proliferation and apoptosis of cultured vascular smooth muscle cells for tissue engineering applications. Tissue Eng. 2004; submitted:
43. Volokhina, E.B., Hulshof, R., Haanen, C., and Vermes, I. Tissue transglutaminase mRNA expression in apoptotic cell death. Apoptosis 2003; 8: 679-
44. Muller-Tidow, C., Metzger, R., Kugler, K., Diederichs, S., Idos, G., Thomas, M., Dockhorn-Dworniczak, B., Schneider, P.M., Koeffler, H.P., Berdel, W.E., and Serve, H. Cyclin E is the only cyclin-dependent kinase 2-associated cyclin that predicts metastasis and survival in early stage non-small cell lung cancer. Canc.Res. 2001; 61: 647-653.
45. Mandl, E.W., Jahr, H., Koevoet, J.L.M., van Leeuwen, J.P.T.M., Weinans, H., Verhaar, J.A.N., and van Osch, G.J.V.M. Fibroblast growht factor-2 in serum-free medium is a potent mitogen and reduces dedifferentiation of human ear chondrocytes in monolayer culture. Matrix Biol. 2004; 23: 231-241.
46. Buttafoco, L., Engbers-Buijtenhuijs, P., Poot, A.A., Dijkstra, P.J., Daamen, W.F., van Kuppevelt, T.H., Vermes, I., and Feijen, J. First steps towards tissue engineering of small-diameter blood vessels: preparation of flat scaffolds of collagen and elastin by means of freeze-drying. J.Biomed.Mater.Res. 2004; submitted:
47. Brodbeck, W.G., Shive, M.S., Colton, E., Nakayama, Y., Matsuda, T., and Anderson, J.M. Influence of biomaterial surface chemistry on the apoptosis of adherent cells. J.Biomed.Mater.Res. 2001; 55: 661-668.
48. Sartore, S., Chiavegato, A., Faggin, E., Franch, R., Puato, M., Ausoni, S., and Pauletto, P. Contribution of adventitial fibroblasts to neointima formation and vascular remodeling: from innocent bystander to active participant. Circ.Res. 2001; 89: 1111-1121.
49. Ross, R. The smooth muscle cell. II. Growth of smooth muscle in culture and formation of elastic fibers. J.Cell Biol. 1971; 50: 172-186.
50. Gulbins, H., Dauner, M., Petzold, R., Goldemund, A., Anderson, I., Doser, M., Meiser, B., and Reichart, B. Development of an artificial vessel lined with human vascular cells. J.Thor.Cardiovasc.Surg. 2004; 128: 372-377.

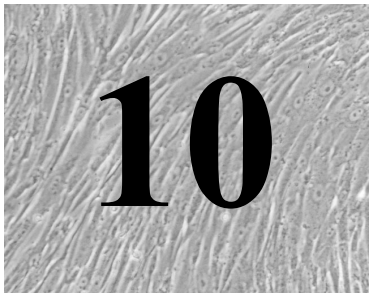

Summary and Future Perspectives

Summary

Tissue engineering is a discipline that applies the principles of engineering and life sciences to the development of biological substitutes that restore, maintain or improve tissue functions. Research to produce functional small-diameter blood vessel replacements (inner diameter < 6 mm) has been directed to this field of tissue engineering. The development of small-diameter vascular grafts is important for use in vascular surgery to replace a blood vessel which is affected by atherosclerosis or related vascular diseases. The artificial blood vessel may serve as an equivalent of an artery or as a model to study vascular biology. This thesis describes the development of tissue-engineered (TE) autologous vascular prostheses, exclusively composed of biological materials and vascular cells, especially for small-diameter applications. A TE construct mimicking the media (middle layer) of a natural blood vessel in terms of morphology, mechanical strength [1] and appropriate cellular functions was produced. In addition, several methods to evaluate tissue homeostasis in the TE constructs were investigated.

Chapter 2 gives a literature overview of SMC functions and the role of SMCs in the development of vascular diseases. The progress in the field of tissue engineering to produce functional small-diameter vascular grafts using autologous vascular cells cultured in synthetic or natural polymeric scaffolds and different methods to evaluate tissue homeostasis in the TE constructs are described.

In *Chapter 3* first steps towards tissue engineering of small-diameter blood vessels are described. Human vascular smooth muscle cells (SMCs), isolated from human umbilical and saphenous vein, were seeded on flat porous scaffolds composed of insoluble collagen and insoluble elastin. After 14 d of static culturing, a confluent layer of SMCs was obtained on the scaffolds. From these results we concluded that it might be possible to develop cell-seeded tubular constructs resembling the morphological characteristics of native blood vessels.

Cell seeding plays an important role in determining the initial cell distribution in the TE scaffolds. A uniform cell distribution can improve the structural stability and biochemical composition of the engineered tissues. Results of several cell seeding procedures to improve the spatial SMC distribution in scaffolds composed of insoluble collagen and insoluble elastin are described in *chapter 4*. Whereas with conventional static seeding, multiple static seeding or injection seeding a multi layer of SMCs on top of the scaffolds is obtained, the use of the described dynamic depth filtration seeding procedure results in the formation of a homogeneous structure of collagen and elastin fibres interspersed with SMCs. Crosslinking of the scaffolds with water-soluble N-(3-dimetylaminopropyl)-N'-ethylcarbodiimide

hydrochloride (EDC) in combination with N-hydroxysuccinimide (NHS) did not influence the amount of cells in the scaffolds after 14 d of culturing. In contrast, crosslinking with poly(propylene glycol)-bis-(2-aminopropyl ether) (Jeffamine 230, J230) in the presence of EDC/NHS had a detrimental effect on the amount of cells present in the scaffolds after 14 d of culturing. The porous constructs crosslinked with EDC/NHS, seeded with SMCs by filtration and statically cultured had elastic properties, appropriate mechanical strength [1], and a homogeneous distribution of cells, which makes them suitable dynamic culturing mimicking *in vivo* conditions of human small- and medium-sized arteries.

Tissue homeostasis is maintained by a precisely regulated balance between synthesis and degradation of cellular components. The balance between cell proliferation and apoptosis is responsible for mediating tissue homeostasis in natural viable tissues as well as functional TE constructs. Therefore, research was carried out to obtain a suitable method for evaluation of tissue homeostasis in TE constructs. From the results described in *Chapter 5* it was concluded that a RT-PCR method evaluating markers of proliferation and apoptosis could be used to characterise cell growth behaviour of SMCs *in vitro*. In addition, we showed that the test is suitable to evaluate tissue homeostasis of SMCs present in TE constructs.

Chapter 6 deals with differences in apoptotic cell death kinetics between cultured cells present in suspension and cultured adherent cells. For this purpose fluorochrome-labelled inhibitor of caspases (FLICA) and propidium iodide (PI) were used to measure the amount of cells present in different stages of the apoptotic cascade. It was found that cell death kinetics depend in a qualitative manner on the type of cell under investigation and depend in a quantitative manner on the stimulus used to induce apoptosis.

In *Chapter 7* the development of a new and sensitive method to analyse apoptosis and anoikis of adherent cell types using a time resolved fluorometric assay with Europium-labelled Annexin V is described. Anoikis (homelessness) is the process in which adherent cells undergo apoptosis when detached from their substrate. With the novel time resolved assay it is possible to analyse the cell death cascade in cultured adherent cells in a sensitive and reproducible way.

The development of a pulsatile flow bioreactor for tissue engineering of small-diameter blood vessels is described in *chapter 8*. In this system arterial pressures (80-120 mmHg) and pulses (120 beats/min) can be established. At an average flow rate of 10 mL/min, an average wall shear rate of 61 s^{-1} and average Reynolds numbers of 96 are obtained. The latter is indicative of laminar flow. Laminar flow is necessary for efficient and homogeneous transfer of oxygen, nutrients and waste products to and from the three-dimensional constructs. A versatile

bioreactor for vascular tissue engineering, able to accommodate a broad range of vessel sizes, easy to handle, clean and maintain was thus developed.

The development of a TE construct mimicking the structure of a natural blood vessel using the pulsatile flow bioreactor is described in *chapter 9*. SMCs were seeded and cultured in porous tubular scaffolds composed of insoluble collagen and insoluble elastin under dynamic culture conditions. It is shown that culturing of SMCs under dynamic conditions in tubular scaffolds crosslinked with EDC/NHS results in enhanced tissue formation compared to static culture conditions. Higher SMC numbers, a more homogeneous distribution of SMCs over the scaffolds and a higher collagen mRNA expression were found when cells were cultured under dynamic conditions. Higher cyclin E mRNA expression levels were measured after dynamic compared to static culturing, indicating that cell proliferation was enhanced. tTG mRNA expression levels were not influenced by the culture conditions, indicating that the higher cell numbers in the TE scaffolds cultured under dynamic conditions cannot be explained by decreased apoptosis but only by increased cell proliferation. The higher cell numbers obtained after dynamic compared to static culturing also resulted in higher total glucose consumption and lactate formation by the TE constructs. However, the glucose consumption and lactate formation per cell present in the constructs were lower after dynamic compared to static culturing, indicating that cell metabolism under dynamic conditions was more aerobic. In addition, actual glucose and lactate concentrations and pH and pCO_2 values in the flow chambers used for dynamic culturing are indicative of improved mass transport under dynamic compared to static conditions. The TE construct obtained has appropriate mechanical strength not to burst with changes in pressure and an elastic vessel wall able to withstand cyclic mechanical loading as exerted in our newly developed bioreactor [1]. In addition the TE construct represents a viable tissue with the inherent potential of healing and remodelling according to the requirements of the specific environment.

Future perspectives

Progress has been made in tissue engineering of small-diameter blood vessels. We have shown that it is possible to develop a TE construct mimicking the media (middle layer) of a natural blood vessel in terms of morphology, mechanical strength and appropriate cellular functions after 14 d of dynamic culturing. Introduction of a luminal monolayer of endothelial cells in the cultured scaffolds might result in constructs suitable for *in vivo* applications. However, several technical questions have to be solved to realise clinical application of a TE blood vessel. A first question is how to obtain viable autologous cells. The external jugular

vein [2] or saphenous vein [3] has already successfully been used to isolate vascular cells for clinical applications. In theory, these tissues could provide the three cell types needed for the preparation of the TE blood vessel. However, atherosclerosis is a systemic disease and patients suffering from a vascular disease do not always have appropriate blood vessels. A second question for the potential of clinical application of a TE blood vessel is how to standardise cell culturing since there is a significant variety between different batches of cell cultures. Expansion of cell numbers *in vitro* may lead to several phenotypic and functional cell changes [4]. A final important question is how to scale up the process to prepare a blood vessel with a size needed for specific vascular reconstructions (i.e. ~15 cm for coronary bypass and 15 cm to more than 30 cm for peripheral reconstructions). Up-scaling requires that a relatively large number of cells must be obtained from the initial biopsy, in a culture time period as short as possible. It is obvious that this type of engineered autologous tissue is not designed to be used for emergency surgery. Many factors can be optimised to reduce preparation time. For example, biopsy size, culture medium components, serum selection and bioreactor design are all elements that are currently under investigation to decrease culture and maturation periods [5-7].

Important new developments in tissue engineering involve the use of stem cells and gene therapy [8-11]. Stem cells are unique cells that have the capacity of self-renewal and of differentiation into a variety of distinct cell types [12, 13]. Many mature organs, including bone marrow [9, 14, 15], skin [9, 16, 17], brain [18, 19], peripheral blood [20, 21] and epithelial tissue [22] maintain a pool of undifferentiated stem cells [8]. Such stem cells allow replacement of damaged cells throughout life. Circulating progenitors of SMCs have been reported and may arise from the same circulating cells that give rise to ECs [23-28]. The vascular bi-potential of such adult progenitors may enable their use in the creation of autologous vessel grafts [6, 11, 29-31]. Host bone marrow is a source of these progenitor cells. The bone marrow is at centre stage for future technological developments in tissue engineering [26]. It contains a large pool of progenitor cells and offers the additional advantage of being easily harvested and cultured from an adult individual [9, 15, 32-35]. Endothelial progenitor cells have been used to improve the biocompatibility of vascular grafts. Artificial grafts first seeded with autologous cells from canine [36] and ovine [37] bone marrow and subsequently implanted were found to have increased surface endothelialization compared to controls. Matsumura *et al.* [38] were the first who reported the use of autologous bone marrow cells to seed porous scaffolds for human transplantation studies. Postoperative examinations revealed no dilation or rupture of the grafts, which were not calcified. There were no thrombotic complications, the grafts were

patent and the patients were doing well. Main advantages of using autologous bone marrow cells for tissue engineering are that patients do not need extra hospitalisation for vein harvesting, there are no considerations of cell culturing to obtain a sufficient amount of cells and there is a low risk of contamination.

Gene therapy of cells to be transplanted can be used to further improve the qualities of stem cells or mature cells in tissue engineering applications [8, 39]. A possible candidate for gene therapy concerning tissue engineering of vascular grafts is a retroviral vector encoding human tissue plasminogen activator (tPA), transduced in ECs to decrease graft thrombosis [40]. Another example is a retroviral vector encoding endothelial nitric oxide synthase (eNOS), transduced in ECs to decrease platelet aggregation and SMC proliferation [41].

References

1. Buttafoco, L., Engbers-Buijtenhuijs, P., Poot, A.A., Dijkstra, P.J., Vermes, I., and Feijen, J. Dynamic vs. static smooth muscle cell culture in tubular collagen/elastin matrices for vascular tissue engineering. To be submitted 2005.
2. Meinhart, J., Deutsch, M., and Zilla, P. Eight years of clinical endothelial cell transplantation. ASAIO J. 1997; 43: M515-M521.
3. Shino'ka, T., Imai, Y., and Ikada, Y. Transplantation of a tissue-engineered pulmonary artery. N.Engl.J.Med. 2001; 344: 532-533.
4. Chamley-Campbell, J., Campbell, G.R., and Ross, R. The smooth muscle cell in culture. Physiol.Rev. 1979; 59: 1-61.
5. L'Heureux, N., Paquet, S., Labbe, R., Germain, L., and Auger, F.A. A completely biological tissue-engineered human blood vessel. FASEB J. 1998; 12: 47-56.
6. Niklason, L.E., Gao, J., Abbott, W.M., Hirschi, K.K., Houser, S., Marini, R., and Langer, R. Functional arteries grown *in vitro*. Science 1999; 284: 489-493.
7. Martin, I., Wendt, D., and Heberer, M. The role of bioreactors in tissue engineering. Trends Biotechnol. 2004; 22: 80-86.
8. Kaji, E.H. and Leiden, J.M. Gene and stem cell therapies. JAMA 2001; 285: 545-550.
9. Bianco, P. and Robey, P.G. Stem cells in tissue engineering. Nature 2001; 414: 118-121.
10. Lovell-Badge, R. The future for stem cell research. Nature 2001; 414: 88-91.
11. Asahara, T. and Kawamoto, A. Endothelial progenitor cells for postnatal vasculogenesis. Am.J.Pysiol. 2004; 287: C572-C579.
12. Reya, T., Morrison, S.J., Clarke, M.F., and Weissman, I.L. Stem cells, cancer, and cancer stem cells. Nature 2001; 414: 105-111.
13. Surani, M.A. Reprogramming of genome function through epigenetic inheritance. Nature 2001; 414: 122-128.

14. Asahara, T., Masuda, H., Takahashi, T., Kalka, C., Pastore, C., Silver, M., Kearne, M., Magner, M., and Isner, J.M. Bone marrow origin of endothelial progenitor cells responsible for postnatal vasculogenesis in physiological and pathological neovascularization. Circ.Res. 1999; 85: 221-228.
15. Carmeliet, P. and Luttun, A. The emerging role of the bone marrow-derived stem cells in (therapeutic) angiogenesis. Thromb.Haemost. 2001; 86: 289-297.
16. Toma, J.G., Akhavan, M., Fernandes, K.J., Barnabe-Heider, F., Sadikot, A., Kaplan, D.R., and Miller, F.D. Isolation of multipotent adult stem cells from the dermis of mammalian skin. Nat.Cell Biol. 2001; 3: 778-784.
17. Wojakowski, W., Tendera, M., Michalowska, A.M.M., Kucia, M., Maslankiewicz, K., Wyderka, R., Ochala, A., and Ratajczak, M.Z. Mobilisation of CD34/CXCR4+, CD34/CD117, c-met+ stem cells, and mononuclear cells expressing early cardiac, muscle, and endothelial markers into peripheral blood in patients with acute myocardial infarction. Circulation 2004; 110: 3213-3220.
18. Rietze, R.L., Valcanis, H., Brooker, G.F., Thomas, T., Voss, A.K., and Bartlett, P.F. Purification of a pluripotent neural stem cell from the adult mouse brain. Nature 2001; 412: 736-739.
19. Cassidy, R. and Frisen, J. Stem cells on the brain. Nature 2001; 412: 690-691.
20. Asahara, T., Murohara, T., Sullivan, A., Silver, M., van der, Z.R., Li, T., Witzenbichler, B., Schatteman, G., and Isner, J.M. Isolation of putative progenitor endothelial cells for angiogenesis. Science 1997; 275: 964-967.
21. Yamamoto, K., Takahashi, T., Asahara, T., Ohura, N., Sokabe, T., Kamiya, A., and Ando, J. Proliferation, differentiation, and tube formation by endothelial progenitor cells in response to shear stress. J.Appl.Physiol. 2003; 95: 2081-2088.
22. Slack, J.M. Stem cells in epithelial tissues. Science 2000; 287: 1431-1433.
23. Nishikawa, S.I., Nishikawa, S., Hirashima, M., Matsuyoshi, N., and Kodama, H. Progressive lineage analysis by cell sorting and culture identifies FLK1+VE-cadherin+ cells at a diverging point of endothelial and hemopoietic lineages. Development 1998; 125: 1747-1757.
24. Yamashita, J., Itoh, H., Hirashima, M., Ogawa, M., Nishikawa, S., Yurugi, T., Naito, M., Nakao, K., and Nishikawa, S.-I. Flk1-positive cells derived from embryonic stem cells serve as vascular progenitors. Nature 2000; 408: 92-96.
25. Shimizu, K. and *et al*. Host bone marrow cells are a source of donor intimal smooth muscle-like cells in murine aortic transplant arteriopathy. Nature Med 2001; 7: 738-741.
26. Kadner, A., Hoerstrup, S.P., Zund, G., Eid, K.M.C., Melnitchouk, S., Grunenfelder, J., and Turina, M.I. A new source for cardiovascular tissue engineering: human bone marrow stromal cells. Eur.J.Cardiothorac Surg. 2002; 21: 1055-1060.
27. Sata, M. Circulating vascular progenitor cells contribute to vascular repair, remodeling, and lesion formation. Trends Cardiovasc.Med. 2003; 13: 249-253.
28. Urbich, C. and Dimmeler, S. Endothelial progenitor cells; characterisation and role in vascular biology. Cir.Res. 2004; 95: 343-353.
29. Kinner, B., Zaleskas, J.M., and Spector, M. Regulation of smooth muscle actin expression and contraction in adult human mesenchymal stem cells. Exp.Cell Res. 2002; 278: 72-83.

30. Hori, Y., Nakamura, T., Kimura, D., Kaino, K., Kurokawa, YU., Satomi, S., and Shimizu, Y. Experimental study on tissue engineering of the small intestine by mesenchymal stem cell seeding. J.Surg.Res. 2002; 102: 156-160.
31. Xaymardan, M., Zhen, J., Duignan, I., Chin, A., and Edelberg, J.M. Heterogeneity of adult bone marrow endothelial precursor cells. Cardiovas.Res. 2004; 13: S200.
32. Pittenger, M.F., Mackay, A.M., Beck, S.C., Jaiswal, R.K., Douglas, R., Mosca, J.D., Moorman, M.A., Simonetti, D.W., Craig, S., and Marshak, D.R. Multilineage potential of adult human mesenchymal stem cells. Science 1999; 284: 143-147.
33. Herzog, E.L., Chai, L., and Krause, D.S. Plasticity of marrow-derived stem cells. Blood 2003; 102: 3483-3493.
34. Vogel, G. Can old cells learn new tricks? Science 2000; 287: 1418-1419.
35. Koc, O.N. and Lazarus, H.M. Mesenchymal stem cells: heading into the clinic. Bone Marrow Transplant. 2001; 27: 235-239.
36. Bhattacharya, V., McSweeney, P.A., Shi, Q., Bruno, B., Ishida, A., Nash, R., Storb, R.F., Sauvage, L.R., Hammond, W.P., and Wu, M.H.D. Enhanced endothelialisation and microvessel formation in polyester graft seeded with CD34+ bone marrow cells. Blood 2000; 95: 581-585.
37. Kaushal, S., Amiel, G.E., Guleserian, K.J., Shapira, O.M., Perry, T., Sutherland, F.W., Rabkin, E., Moran, A.M., Schoen, F.J., Atala, A., Soker, S., Bischoff, J., and Mayer, J.E. Functional small-diameter neovessels created using endothelial progenitor cells expanded *in vivo*. Nat.Med. 2001; 7: 1035-1040.
38. Matsumura, G., Hibino, N., Ikada, Y., Kurosawa, H., and Shino'ka, T. Successful application of tissue engineered vascular autografts: clinical experience. Biomaterials 2003; 24: 2303-2308.
39. Bonadio, J. Tissue engineering via local gene delivery: update and future prospects for enhancing the technology. Adv.Drug Delivery Rev. 2000; 44: 185-194.
40. Dunn, P.F., Newman, K.D., Jones, M., Yamada, I., Shayani, V., Virmani, R., and Dichek, D.A. Seeding of vascular grafts with genetically modified endothelial cells. Circulation 1996; 93: 1439-1446.
41. Kader, K.N., Akella, R., Ziats, N.P., Lakey, L.A., Harasaki, H., Ranieri, J.P., and Bellamkonda, R.V. eNOS-overexpressing endothelial cells inhibit platelet aggregation and smooth muscle cell proliferation *in vitro*. Tissue Eng. 2000; 6: 241-251.

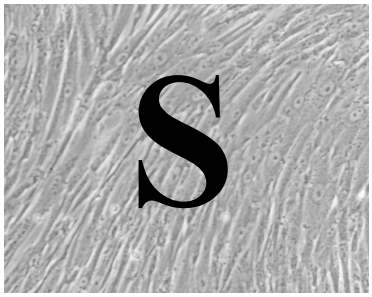

Nederlandse Samenvatting

Samenvatting

Atherosclerose ofwel aderverkalking vormt één van de belangrijkste doodsoorzaken in de westerse wereld. Deze ziekte kenmerkt zich door het geleidelijk vernauwen van slagaders die uiteindelijk dichtslibben. Bovendien kunnen stolsels die een slagader vernauwen loslaten en vervolgens kleine of middelgrote bloedvaten afsluiten. Verstopping van bloedvaten kan tot levensbedreigende situaties leiden zoals hart- of herseninfarcten. Voor de vervanging van aangetaste grote diameter bloedvaten zijn kunststof implantaten beschikbaar. Deze functioneren goed voor een periode van tenminste tien jaar. Door het optreden van trombose zijn deze vaatprothesen echter ongeschikt voor het vervangen van beschadigde kleine diameter (< 6 mm) bloedvaten zoals de kransslagaders en vaten in de ledematen. Tot op heden worden gezonde aders of slagaders van de patiënt zelf gebruikt voor de vervanging van deze kleine diameter bloedvaten. Het gebruik van deze autologe bloedvaten heeft een aantal beperkingen. Er is slechts een beperkt aantal bloedvaten geschikt voor gebruik in reconstructieve operaties en deze kunnen bovendien zelf aangetast en daardoor onbruikbaar zijn. Daarnaast kunnen complicaties optreden als aders (zoals de vene saphena) gebruikt worden in de arteriële bloedcirculatie waar verhoogde stroming en druk aanwezig zijn.

'Tissue engineering' (weefseltechnologie) is een interdisciplinair onderzoeksgebied met als doel het ontwikkelen van biologische structuren die beschadigde of slecht functionerende lichaamsdelen kunnen vervangen of de functie kunnen verbeteren. Een strategie voor het ontwikkelen van functionele bloedvatprothesen met een kleine diameter is hierop gebaseerd. Door het gebruik van biologisch afbreekbare materialen en gezonde lichaamseigen vaatwandcellen wordt geprobeerd de structuur van een natuurlijke bloedvatwand na te maken. Dit proefschrift beschrijft de ontwikkeling van een bloedvatprothese met kleine diameter gebaseerd op de principes van 'tissue engineering'.

Een natuurlijk bloedvat bestaat uit meerdere lagen. Aan de binnenzijde bevindt zich een endotheelcellaag (tunica intima). Deze laag is van belang voor een continue doorstroom van het bloed. De middelste laag (tunica media) bestaat voornamelijk uit gladde spiercellen. Deze cellen maken het bloedvat bestand tegen het pulseren van de bloedstroom. Tenslotte bevindt zich aan de buitenzijde een laag met fibroblasten en vezels van collageen en elastine die het bloedvat stevigheid en vorm geven (tunica adventitia). In dit proefschrift wordt beschreven hoe een buisje, vergelijkbaar met de middelste laag van een natuurlijk bloedvat op basis van morfologie en mechanische en celbiologische eigenschappen, is vervaardigd. Tevens zijn in

dit proefschrift verschillende nieuwe methoden beschreven die gebruikt kunnen worden voor het bestuderen van geprogrammeerde celdood (apoptose).

Hoofdstuk 2 van dit proefschrift geeft een literatuuroverzicht van de functies van gladde spiercellen en de rol van deze cellen in de ontwikkeling van vaatziekten. De voortgang in het vervaardigen van een kleine diameter bloedvat prothese door het toepassen van de principes van 'tissue engineering' zijn beschreven. Tevens zijn verschillende methodes om de balans tussen celdood en celgroei te bestuderen zijn beschreven.

In *hoofdstuk 3* worden de eerste stappen van het onderzoek beschreven. Menselijke gladde spiercellen, geïsoleerd uit een ader van een navelstreng of uit het onderbeen, werden gezaaid op vlakke poreuze dragers van onoplosbare collageen en elastine vezels. De cellen werden gekweekt onder statische kweekomstandigheden en na 14 dagen was er een laag van gladde spiercellen boven op de matrix ontstaan. Uit deze resultaten werd geconcludeerd dat het mogelijk zou moeten zijn om op dezelfde manier buisvormige structuren te maken. Door cellen te kweken in deze buisjes zou het mogelijk moeten zijn om een kunstbloedvat te maken die lijkt op een natuurlijk bloedvat.

Een hoge celdichtheid en een uniforme verdeling van de cellen over de poreuze dragers zijn van essentieel belang voor de stabiliteit van de matrix en de groeicondities van de cellen. De resultaten van verschillende zaai procedures om de celdichtheid en uniforme cel verdeling over de poreuze dragers te verbeteren zijn beschreven in *hoofdstuk 4*. Met de standaard statische zaaimethode waren na 14 dagen kweken meerdere lagen van gladde spiercellen gevormd boven op de poreuze drager van onoplosbaar collageen en elastine. Dezelfde resultaten werden verkregen wanneer meerdere keren gezaaid werd (op dag 2, 4 en 6) of wanneer een celsuspensie op verschillende plaatsen in de poreuze drager geïnjecteerd werd. Door dynamische diepte filtratie te gebruiken, werd een betere verdeling van de cellen over de dragers bereikt. Na 14 dagen kweken was een homogene verdeling van de gezaaide gladde spiercellen tussen de vezels van collageen en elastine gevormd.
De mechanische eigenschappen van de poreuze dragers van collageen en elastine vezels kunnen worden verbeterd door de vezels te 'crosslinken' (vernetten) met bepaalde chemische stoffen. Het 'crosslinken' van de matrices met water oplosbaar N-(3-dimetylaminopropyl)-N'-ethylcarbodiimide hydrochloride (EDC) in combinatie met N-hydroxysuccinimide (NHS) bleek geen invloed te hebben op de celgroei. Daarentegen bleken de cellen na het

'crosslinken' van de matrices met poly(propylene glycol)-bis-(2-aminopropyl ether) (Jeffamine 230, J230) in aanwezigheid van EDC/NHS minder goed te groeien in en op de dragers. De poreuze structuren verkregen na het 'crosslinken' van de collageen en elastine vezels met een homogene verdeling van gladde spiercellen bleken elastische eigenschappen en voldoende mechanische sterkte te hebben om de cellen te kweken onder dynamische kweekomstandigheden. Deze dynamische kweekomstandigheden bootsen de condities in slagaders (met kleine tot middelgrote diameter) van het menselijk lichaam na. Dit laatste wordt verder beschreven in *hoofdstuk 8 en 9*.

Homeostase is het vermogen van een organisme om invloeden van buitenaf binnen bepaalde grenzen te compenseren. Dit wordt in stand gehouden door een nauw gereguleerd evenwicht tussen aanmaak en afbraak van cellulaire componenten. Het evenwicht tussen celgroei en celdood (proliferatie en apoptose) reguleert tevens dit evenwicht in natuurlijke vitale lichaamsdelen maar ook in functionele structuren die gebruikt worden voor 'tissue engineering'. Om deze reden werd onderzoek gedaan om een geschikte methode te vinden om homeostase van de cellen gekweekt in de poreuze dragers te bestuderen. In *hoofdstuk 5* wordt een 'reversed transcriptase polymerase chain reaction (RT-PCR)' methode beschreven waarbij tegelijkertijd de mate van cel proliferatie en apoptose gemeten kan worden. Voor deze methode moet de totale hoeveelheid RNA van de gekweekte cellen geïsoleerd worden. Dit kan eenvoudig gedaan worden uit cellen die gekweekt zijn in driedimensionale poreuze dragers die gebruikt worden voor 'tissue engineering'. Op deze manier kan naar de mRNA expressie van verschillende markers (voor proliferatie en apoptose) gekeken worden.

Apoptose is een ingewikkeld proces waarbij oude, slecht functionerende of overbodige cellen worden opgeruimd door het lichaam. Tijdens dit proces vallen de cellen in kleine stukken uiteen en door middel van fagocytose worden de celresten opgeruimd door omliggende cellen. Hierdoor wordt een ontstekingsreactie voorkomen. Men kan zich voorstellen dat door het uiteindelijk verdwijnen van de celresten het moeilijk is om een goede methode op te zetten om nauwkeurig dit proces te volgen.

Hoofdstuk 6 beschrijft het gebruik van een fluorochrome gelabelde remmer van caspases (FLICA) en propidium jodide (PI) om de kinetiek van het apoptotische proces te bestuderen. De kinetiek bleek afhankelijk te zijn van het type van de cellen en van de stimulus van het apoptotische proces. Er werd met name een verschil gevonden tussen de kinetiek van het

apoptotische proces van cellen die op een oppervlak groeien (waaronder gladde spiercellen) en van cellen die in suspensie groeien (waaronder bijvoorbeeld bloedcellen).
Tijdens het apoptotisch proces verliezen cellen die op een oppervlak groeien het contact met dit oppervlak. Dit proces wordt anoikis genoemd.

Hoofdstuk 7 beschrijft een nieuwe methode om het fenomeen anoikis op een nauwkeurige manier te bestuderen. De methode is gebaseerd op de binding van annexine V met phosphatidylserine, wat zich aan de buitenkant van apoptotische cellen presenteert. Met deze methode worden verschillende fracties van de gekweekte cellen bestudeerd. Ten eerste worden cellen die nog op het oppervlak groeien geanalyseerd. Ten tweede worden cellen die los zijn gelaten en in het kweekmedium zweven geïsoleerd en geanalyseerd. En ten derde worden cellen die uiteen zijn gevallen in fragmenten geïsoleerd en geanalyseerd. Op deze manier kan men een goed beeld krijgen van het gehele apoptotische proces.

Het kweken van de gladde spiercellen onder dynamische omstandigheden die de condities in een slagader van het menselijk lichaam nabootsen, is belangrijk om de oriëntatie, de groei en de eiwitproductie van de cellen te stimuleren. In *hoofdstuk 8* wordt de ontwikkeling van een bioreactor beschreven. In het systeem kunnen cellen onder arteriële bloeddrukken (van 80-120 mmHg) en een pulserende vloeistofstroom gekweekt worden. De rheologische eigenschappen van het systeem werden gekarakteriseerd, gebruikmakend van siliconrubber buisjes of buisvormige EDC/NHS gecrosslinkte poreuze dragers van onoplosbaar collageen en elastine. Bij een gemiddelde flow snelheid van kweekmedium van 10 mL/min, werden een gemiddelde afschuifsnelheid aan de wand van 61 s^{-1} en een gemiddeld Reynolds getal van 96 berekend. Deze waarden zijn van dezelfde orde van grootte als die in een menselijke halsslagader. Het Reynolds getal duidt op laminaire stroming. Laminaire stroming is nodig voor een efficiënt en homogeen transport van zuurstof, voedingsstoffen en afvalproducten naar en van de driedimensionale structuren.

In *hoofdstuk 9* wordt de ontwikkeling van een buisje met een structuur die lijkt op de structuur van de middelste laag van een natuurlijk bloedvat beschreven. Gladde spiercellen werden gezaaid in buisvormige poreuze dragers van onoplosbaar collageen en elastine. De cellen werden gekweekt onder dynamische kweekcondities in de bioreactor. Aangetoond werd dat het kweken van gladde spiercellen in buisjes van collageen en elastine onder dynamische kweek omstandigheden resulteert in verbeterde weefsel opbouw vergeleken met statische

kweekomstandigheden. Meer gladde spiercellen, een betere verdeling van de cellen in de driedimensionale poreuze dragers en een hogere mRNA expressie van collageen werden gevonden wanneer cellen werden gekweekt onder dynamische omstandigheden. Een hogere mRNA expressie van cycline E werd gevonden wanneer cellen werden gekweekt onder dynamische omstandigheden wat duidt op een hogere mate van cel proliferatie vergeleken met statische kweekomstandigheden. Geen verschillen in mRNA expressie van 'tissue transglutaminase' (een maat voor apoptose) werden gevonden wanneer cellen werden gekweekt onder dynamische of statische kweekomstandigheden. Deze resultaten wijzen erop dat het grotere aantal cellen gevonden na het dynamisch kweken van de cellen in de buisjes niet toegeschreven kan worden aan een verlaagde mate van apoptose maar uitsluitend verklaard kan worden door toegenomen celgroei. Het grotere aantal cellen gevonden na het dynamisch kweken van de cellen in de buisjes heeft geresulteerd in een toegenomen totale glucose consumptie en lactaat productie door de cellen in de buisjes. Echter, de glucose consumptie en lactaat productie uitgedrukt per cel was lager na het dynamisch kweken. Dit houdt in dat het cel metabolisme onder dynamische kweekomstandigheden meer aëroob moet zijn vergeleken met het metabolisme van de cellen gekweekt onder statische omstandigheden. Tevens zijn de gemeten werkelijke waarden voor glucose en lactaat concentraties, pH en pCO_2 in de flow kamers die gebruikt zijn voor het dynamisch kweken een indicatie dat het massatransport van zuurstof, voedingsstoffen en afvalstoffen van en naar de cellen verbeterd is ten opzichte van statisch kweken.

De op deze manier vervaardigde buisvormige structuren zijn vitaal gebleken en hebben voldoende mechanische eigenschappen. De buisjes kunnen veranderingen in (bloed)druk en de pulserende (bloed) stroom opvangen. Na het introduceren en kweken van een binnenlaag van endotheelcellen in de buisvormige structuren zouden de buisjes gebruikt kunnen worden voor *in vivo* studies. Voor de klinische toepassing van de kunstbloedvaten die op deze manier vervaardigd zullen kunnen worden, zijn verbeteringen van de kweekcondities nodig. Deze verbeteringen zullen ervoor moeten zorgen dat de tijd die nodig is om een patiënteigen kunstbloedvat te maken zo kort mogelijk zal zijn zodat de kunstbloedvaten gebruikt kunnen worden in de vaatchirurgie ter vervanging van kleine diameter beschadigde bloedvaten.

Hoofdstuk 10 geeft een samenvatting van dit proefschrift en in dit hoofdstuk wordt nader ingegaan op mogelijke verbeteringen van het kweekproces.

Dankwoord

"De weg is het doel." Met dit doel voor ogen werkte de Noorse schaatser Johann Olav Koss naar de Olympische Spelen van 1994 in Lillehammer toe en won daar uiteindelijk 3 keer GOUD. Over de lange weg naar dit succes heeft hij het boek 'Effect' geschreven. Wanneer een experiment weer eens mislukte of de resultaten niet zo waren als ik had gehoopt, heb ik wel eens aan deze stelling gedacht. Het proefschrift wat voor u ligt is het resultaat van mijn eigen lange weg en daarmee is het doel bereikt: ik heb de weg bewandeld en ontzettend veel geleerd! Van tevoren wist ik dat deze weg niet gemakkelijk zou zijn: iedereen kon me dat zo mooi vertellen. Maar toen ik er zelf middenin stond moest ik toch zélf oplossingen verzinnen; niemand kon me dát mooi vertellen! Toch heb ik het niet alleen gedaan: velen hebben me geholpen en met dit dankwoord wil ik iedereen voor die hulp bedanken.

Allereerst wil ik mijn beide promotoren bedanken voor de mogelijkheid die zij mij hebben geboden dit promotie onderzoek uit te voeren. Prof. Vermes, beste Istvan, zonder uw uitzonderlijke kennis, onuitputtelijke enthousiasme en grote vertrouwen zou ik niet zoveel bereikt hebben. Bedankt voor alles. Ik vond het leuk om met u samen te werken en ik heb ontzettend veel van u geleerd en ik hoop nog veel van u te leren de komende jaren.
Prof. Feijen, bedankt voor de intensieve maar zeer nuttige werkbesprekingen en het kritisch lezen en verbeteren van mijn proefschrift. Ik was elke keer weer benieuwd vanuit welke hoek u naar mijn werk zou kijken en stond elke keer weer versteld van uw kritische opmerkingen. Ook van u heb ik ontzettend veel geleerd.
Verder ben ik veel dank verschuldigd aan mijn assistent promotor André Poot. Beste André, bedankt voor het delen van je kennis en ervaring en voor het verbeteren van mijn proefschrift. Ik heb veel aan je gehad de afgelopen vier jaar.

Laura, I would like to thank you for the co-operation of the last 4 years. I think we were a perfect team together! And thanks for being my paranimf and to be on stage for the third time in two months!
Mischa, ook jou wil ik bedanken omdat je mijn paranimf wilt zijn. Maar ik wil je vooral bedanken voor alle leuke dingen die we samen gedaan hebben en je vele kaartjes, sms-jes, E-mailtjes en telefoontjes van de afgelopen 4 jaar! Voor mij ben je GOUD waard! Maar… zullen we het ooit leren de lat voor onszelf niet nét iets té hoog te leggen en gewoon te genieten?

Nelke, de afstand Utrecht - Stellenbosch lijkt kleiner dan Enschede - Den Haag! Dat blijf ik vreemd vinden. Maar bedankt voor je begrip en geduld en laten we gewoon afspreken dat we die afstand binnen Nederland vaker gaan overbruggen. Oók met twee overvolle agenda's!

De studenten die ik begeleid heb, wil ik bedanken voor hun werk, inzet en enthousiasme en de meiden + Robert van Onderzoek en Ontwikkeling wil ik bedanken voor de leuke en gezellige tijd op het lab en in het 'kweekhok'. Daarnaast wil ik al mijn andere collega's van de UT (Universiteit Twente) en het MST (Medisch Spectrum Twente) hartelijk bedanken voor de leuke en goede samenwerking, de gezellige koffie-, thee- en lunchpauzes en de verschillende uitjes en feestjes. En MST collega's: ik kijk ontzettend uit naar een goed, leuk en leerzaam vervolg van mijn samenwerking met een ieder van jullie!

Pa en ma: bedankt voor alles wat jullie voor mij doen en gedaan hebben. Er is veel nodig om een promotie onderzoek tot een goed einde te brengen. Onder andere doorzettingsvermogen en geloven in wat je kunt en wat je voor ogen hebt, hebben jullie mij geleerd!
De rest van mijn familie, mijn studiegenootjes en mijn schaats-, fiets- en tennismaatjes wil ik allemaal bedanken voor de belangstelling voor mijn onderzoek, maar vooral voor de broodnodige uurtjes van ontspanning. Deze waren van begin tot het einde van de weg onmisbaar.
Om het dankwoord toch net iets anders dan anders te maken houd ik het hierbij en hoop dat de volgende bladzijde genoeg toevoegt.

Maar tot slot wil ik natuurlijk nog wel mijn 'husband' persoonlijk bedanken. Ik kan bladzijden vol schrijven om dat goed te doen, maar ik kan ook dit kort houden en ervan uitgaan dat de boodschap hoe dan ook wel overkomt:

Lieve Tom, bedankt hè!

Paula


BEDANKT ALLEMAAL !
Laura Buttafoco
Davika Zandwijken
Clemens van Blitterswijk
fam. Engbers
lab bijzonder onderzoek MST
Tom
Istvan Vermes
PBM UT
Trees Schaap
Ada Drost
Cees Schenkeveld
Ellen Kalsbeek
Mischa Coolen
Frank van den Bergh
pa en ma
Marloes Kamphuis
Klaas van den Bergh
Cees Doelman
Mark ten Breteler
Wilburt Pontenagel
Marcel Hengeveld
Lanti Yang
Floor Wolbers
Karin Hendriks
fam. Tibben
Gerard Engbers
Bas Schinck
Wiebe Kruijer
Robert Hulshof
Andre Poot
Bob Geelkerken
zusjes Buijtenhuijs
Clemens Haanen
Hester Blom
Arnold Leemhuis
Sanquin Bloedbank
Hetty ten Hoopen
Lotus Sterk
MST
UT
Cecile de Vos
Kirsten Ampt
Antoinette Heijs
Linda en Edwin Schlosser
Jop van de Palen
Nelke van de Ven
Miranda Wiehink
Jan Feijen
Erwin Nijhuis
Frank Gerritsen
Gert Jan van der Sluijs Veer
cito lab MST
Marcel Wissink
ondersteunende dienst lab MST
Rob de Vos
Bart Willemsen
Bas Siebum
Christine Hiemstra
Judith Olde Wolbers
Piet Dijkstra
Linda Verbeek
Priscilla Lips
Boon Hua Tan
Ralf Triepels
Johan Engbersen
afname lab MST
Zhiyuan Zhong
Arien Bosch
Ronald Poelarends
Sylvie Roke
Barbara van den Hoven
Ingrid Velthoen
Gert-Jan van der Sluijs
Arjen-Kars Boer
Richard Rieksen
Jennita Slomp
Dirk Grijpma
Peter van Os
Henriëtte Weekamp
Zheng Zhang
lab geautomatiseerde analyses MST

Curriculum vitae

De schrijfster van dit proefschrift werd geboren op 4 februari 1977 te Ermelo. Zij behaalde in 1995 haar VWO diploma aan het Rijksscholengemeenschap ‘t Slingerbos te Harderwijk. Hetzelfde jaar startte ze met de studie Scheikunde aan de Universiteit Utrecht. Tijdens het derde en vierde jaar deed ze stage-onderzoeken aan deze Universiteit bij de vakgroepen Biomoleculaire Massaspectrometrie van de faculteit Scheikunde en Haematologie van de faculteit Geneeskunde (in het Academisch Ziekenhuis Utrecht). Na een afstudeeronderzoek bij de vakgroep Biochemie van Lipiden (Centrum voor Biomembranen en Lipid Enzymology, CBLE) onder leiding van Prof. Dr. H. van den Bosch slaagde zij met genoegen voor de studie in april 2000. Aansluitend werkte zij als analist op het Centraal Laboratorium voor de Bloedtransfusiedienst in Amsterdam bij de afdeling Bereiding Immuun Reagentia. In april 2001 begon zij aan een promotie onderzoek aan de Universiteit Twente (faculteit Technische Natuurwetenschappen) bij de vakgroep Polymeerchemie en Biomaterialen onder leiding van Prof. Dr. J. Feijen en Dr. A.A. Poot in samenwerking met het Klinisch Chemisch Laboratorium van het Medisch Spectrum Twente onder leiding van Prof. Dr. I. Vermes. De resultaten van dit onderzoek zijn beschreven in dit proefschrift. In mei 2005 zal zij aan de opleiding tot Klinisch Chemicus beginnen in het Medisch Spectrum Twente te Enschede (opleider: Dr. F.A.J.T.M. van den Bergh).